A systematic analysis of gene expression of human mesenchymal stromal/stem cells derived from acute myeloid leukemia patients identifies potential leukemogenic targets including CD248 and its potential role in MSC adipogenesis

Allolo Aldreiwish

A thesis submitted to the University of Ottawa in partial fulfillment of the requirements for the Ph.D. degree in Microbiology and Immunology

Department of Biochemistry, Microbiology, and Immunology

Faculty of Medicine

University of Ottawa

Abstract

Acute myeloid leukemia (AML), a blood malignancy resulting in abnormal hematopoiesis, is associated with alterations in the bone marrow environment (BME). Current treatments for this heterogeneous disease, mainly targeting the leukemic cells, are largely unsuccessful for the majority of AML subtypes. By better understanding the mechanisms by which the BME contributes to leukemogenesis, it may be possible to introduce more effective treatments for AML. Mesenchymal stromal/stem cells (MSCs) are essential cellular components of the BME/hematopoietic niche and have been shown to support normal hematopoiesis. As a critical component, they may have several roles in altering the BME, thus providing an excellent model for studying the BME *in-vitro*. Several studies have characterized AML-derived MSCs (AML-MSCs). However, their exact role in altering BME remains unclear. Here, we investigated the MSCs' potential role in BME alteration by investigating the genetic profiles of previously characterized AML-MSCs (n=29) and healthy donor MSCs (HD-MSCs) (n=8). We identified that among 7565 common genes, 21 genes were significantly differentially expressed in AML-MSCs. The CD248 gene was identified among these significantly upregulated genes in AML/HD-MSCs (n=29). Focusing on AML-MSCs derived from high-risk patients (HR), CD248 protein was investigated and validated using HR AML-MSCs (n=11) and HD-MSCs (n=4). Interestingly, it was highly abundant in HR samples at the intracellular and cell-surface levels. CD248 is an MSC marker and has a biological significance potentially on their function. To better understand its potential role in MSC, CD248 was knocked down (KD) in HD-MSCs using siRNA (siCD248-MSCs). Functional capacity, the ability of HD-MSCs and siCD248-MSCs to differentiate into cell types that form the BME (adipocytes and osteocytes), and their ability to promote the growth of HL60 human leukemia cell line were assessed. Post-transfection functional assessments showed that siCD248-MSCs had a reduced adipogenic but not osteogenic potential via differentiation assays. Quantitative validation of the adipogenesis pathway by qRT-PCR confirmed the reduction. KD CD248 increased SIRT2 expression and potentially led to adipogenesis inhibition. However, co-culture experiments showed no effect of HD-MSCs or siCD248-MSCs

on HL60 proliferation. Together these data showed that CD248 is a potential player in adipogenesis, essential to MSC's functionality. Thus, it could serve as a prognostic marker and target for AML therapy.

Acknowledgment

"In the name of (God) Allah, the Most Gracious and Merciful."

First and foremost, praise be to Allah for his blessing that enabled me to pursue my education and complete my Ph.D. thesis. I want to thank him for the strength, patience, and guidance given to me, which helped me through all the pleasant and distressing opportunities and experiences that I encountered, at both academic and personal levels, during this challenging 6-year journey away from home, Saudi Arabia. Secondly, I would like to thank Majmaah University and the Saudi Ministry of Higher Education for providing a full scholarship to study abroad. This scholarship enabled me to live and study in Canada without financial hindrances that could have prevented me from continuing my education. Special thanks to Dr. Abdul Aziz Bin Dukhyil for promptly assisting with the official scholarship procedure throughout the journey.

I like to sincerely thank my supervisors at the University of Ottawa and Health Canada: Dr. David Allan, Dr. Michael Rosu-Myles, and Dr. Jessie R. Lavoie, for giving me the opportunity to complete my Ph.D. degree in Canada by accepting me as a graduate student under their supervision, recruiting me into the stem cell-based therapeutics laboratory, Health Canada, and providing me with an interesting project and research funding to conduct the research. I was fortunate to work with these Canadian researchers and learn from their expertise. I want to thank them all for their guidance, encouragement, understanding, and patience.

Thank you, Dr. Michael Rosu-Myles, for your recruiting and mentorship. Your endless support, motivational words, guidance, understanding, stimulating monthly

discussions, and critiques constantly challenged me to push past my limits and improve my research skills.

Thank you, Dr. David Allan, for accepting me as a graduate student and giving me this opportunity to pursue hematology-related research, which is my subject of interest. Your insightful views, questions, and explanation of clinical aspects and encouragements helped me comprehend and shape my project throughout these years.

My deepest gratitude goes to Dr. Jessie. R. Lavoie, the head of the stem cell-based therapeutics laboratory, at Health Canada, for her endless support and research mentorship. She gave me with an exciting opportunity to learn from her and conduct my research independently. Leading my project motivated me to plan, analyze, improve my technical lab skills and enjoy research. Moreover, it helped me develop new research skills. Thank you, (Merci) Dr. Lavoie, for being kind, supportive, understanding, and available to help, explain and guide whenever needed. Thank you for leading our laboratory and research professionally yet inspiringly. Research is exciting yet overwhelming (sometimes); you made complicated issues simple and problematic situations resolvable. Your enthusiasm, attitude, smile, skills, and dedication to research are motivational, inspiring, and contagious. Hopefully, what I have learned from you, Dr. Lavoie, Dr. Allan, and Dr. Rosu-Myles have shaped me into a better researcher for my future career.

I would like to honestly extend my appreciation to my TAC members, Dr. Sean Li and Dr. Marjorie Brand, for their critiques, suggestions, and encouragement. These collectively, along with my supervisors' comments, helped me throughout my study to

stay focused and see the light, which seemed dark sometimes, at the end of the tunnel with the completion of my research project.

Also, I would like to thank the stem cell-based therapeutics laboratory's former and current technologists: Mrs. Carole Westwood, Mrs. Jelica Mehic, and Mrs. Gauri Muradia, for their technical expertise and lab training when needed. Special thanks to Gauri, who was consistently and kindly willing to help whenever I needed her help.

I want to thank my family in Saudi. I want to sincerely thank my forever hero, my father, Mr. Dreiwish. A. Aldreiwish. Without his care, unconditional love, and support throughout my life, I would not have completed my education journey. I want to thank my lovely sisters for their love and prayers. Their strength, care, and love for their children have always inspired me. I also want to thank my brothers, cute nieces, and lovely nephews for all the love that kept me going. I want to send my gratitude to my younger sister Amal (her name means hope in Arabic), to whom I owe much for her tolerance and support. Amal, your love and encouragement, from Saudi to Canada, lifted me and reminded me to stay optimistic. Thank you for being here for me throughout all of these challenging years. I also would like to thank my best friends in Saudi and the USA, who continuously prayed for my success and were willing to help when needed. Lastly, I would like to thank the ABBA band for their inspiring song “I have a dream, “which kept me pushing.

Dedication

"My Lord, have mercy upon them as they brought me up when I was a child" (Quran 17:24).

I dedicate my thesis work and Ph.D. degree to my parents; my late mother and, the most incredible father in the world, my inspiring father.

Contributions of Collaborators

- Research funding for this investigation was provided by the government of Canada through "Genomics Research and Development Initiative" (GRDI) phase VI (2014-2019) and phase VII (2020-2025), which were obtained by Dr. Michael Rosu-Myles and Dr. Jessie R. Lavoie, respectively.
- Supervisors and Thesis committee members:
  - Dr. David Allan
  - Dr. Jessie R. Lavoie
  - Dr. Marjorie Brand
  - Dr. Michael Rosu-Myles
  - Dr. Sean Li.
- AML-MSCs were obtained from Dr. Pablo Menendeza. (Josep Carreras Leukemia Research Institute, Spain)
- Experiments in this study were all designed, performed, and analyzed by myself except for the following:
  - Culturing of AML-MSCs and HD-MSCs and isolating their RNAs prior to RNA sequencing was performed by lab technologist Mrs. Gauri Muradia and myself.
  - RIN determination and RNA sequencing was conducted by Dr. Carole Yolk and her team at Environmental Health Science and Research, HECS at Health Canada (Ottawa, ON, Canada).
  - Running of Flow cytometry samples was performed by the Flow cytometry manager at Health Canada (Ottawa, ON, Canada), Mr. Andrew Stalker, who also assisted in some initial analysis.

Table of Contents

List of Figures

Chapter 1

Chapter 3

Chapter 4

Chapter 5

Chapter 6

List of Tables

Chapter 3

Chapter 4

Chapter 5

Appendix

Supplementary Tables

Supplementary Figures

List of Abbreviation

aa	Amino acid
alloHSCT	Allogenic hematopoietic stem cell transplant
AML	Acute myeloid leukemia
AML-MSCs	MSCs derived from AML patients
Ang-1	Angiopoietin-*1*
BM	Bone marrow
BME	Bone marrow microenvironment
BM-MSCs	Bone marrow mesenchymal stromal/stem cells
BMP	Bone morphogenetic protein
C/EB	CCAAT-enhancer-binding proteins
CCL-5	chemokine (C-C motif) ligand 5
CFU-F	Colony forming unit-fibroblast
CR	Complete remission
CXCL12	C-X-C Motif Chemokine Ligand 12
EGF	Epidermal Growth Factor
End	Endosialin
ETS-1	ETS Proto-Oncogene 1, Transcription Factor
FAB	French-American-British classification of AML
FC	Fold-change
FGF-2	Fibroblast Growth Factor 2
FLT3	FMS-like tyrosine kinase 3
GvHD	Graft versus host disease
HD-MSCs	MSCs derived from healthy donors
HR	High-risk AML subtype
HR AML	AML-MSCs from high risk group
HSC	Hematopoietic stem cell
HSCs	Hematopoietic stem cells
HSPCs	Hematopoietic stem and progenitor cells
IDO	Indoleamine 2,3-dioxygenase
IPA	Ingenuity pathway analysis

IR	Intermediate-risk AML subtype
ISCT	International society for cell therapy
JAG-1	Jagged canonical Notch Ligand 1
KD	knockdown
kDa	kilodalton
LR	Low-risk AML subtype
LSC	Leukemic stem cell
LSCs	Leukemic stem cells
MA	Protein profiler microarray
mAb	Monoclonal Antibody
MCP-1	monocyte chemoattractant protein 1
ME	Microenvironment
MMP-9	Matrix metallopeptidase 9
MRD	Minimal residual disease
MSCs	Mesenchymal stromal/stem cells
NIH	National Institute of health
pAb	Polyclonal Antibody
PPARγ	Peroxisome proliferator- activated receptor gamma
Pre-TF	Before transfection
P-TF	Post-transfection
qRTPCR	Quantitative real-time polymerase chain reaction
RB	RoosterBio
RB CM	RossterBio complete supplemented media
SCT	Stem cell transplant
SDF-1	stromal cell-derived factor 1
SDRGs	Statistically differentially regulated genes
siCD248-MSCs	MSCs transfected/treated with CD248 siRNA
siNegScr-MSCs	MSCs transfected/treated with negative scramble siRNA
SSc-MSCs	MSCs derived from systemic sclerosis patients
TEM-1	Tumor endothelium marker -1
TF	Transfection

TGFβ-1	Transforming growth factor beta
Tie-2	Angiopoietin receptor
UT	Untreated/un-transfected MSCs
VEGF	Vascular endothelial growth factor
WHO	World health organization

CHAPTER 1

Introduction

1.1. Preview of Hematopoiesis

Hematopoiesis is a continuous hierarchical process of forming blood cellular components from hematopoietic stem cells (HSCs) in the bone marrow (BM). HSCs reside in a designated bone marrow microenvironment (BME) known as the HSC niche (1, 2). Each healthy individual is estimated to generate around 4-5 ×1011 hematopoietic cells each day (2). The BM is a multifunctional tissue containing HSCs and several types of immature procurers and mature cells, such as leukocytes, erythrocytes, lymphocytes, and thrombocytes. Those diverse HSC-generated cellular precursors and mature populations have highly designated functionalities. For instance, erythrocytes are responsible for oxygen transport, leukocytes and lymphocytes for immune response and thrombocytes are responsible for blood clotting and hemorrhage ceasing.

Moreover, those HSCs, multipotent precursor cells, have the ability to self-renew and differentiate into lymphoid, erythroid, granulocytic, megakaryocytic, and monocytic cell lineages to produce all mature blood cells of the hematopoietic system (3). Whereas HSCs can self-renew, the committed specified progenitors have limited abilities to self-renew in a healthy physiological state. Having these specific features, self-renewal, and differentiation, HSCs are critical in maintaining the hematopoietic system throughout human life, steady-state, and physiological stress, such as hemorrhage and infections. The hematopoiesis process, HSCs self-renew, differentiation, function, and role are well-regulated and maintained by various mechanisms. In particular, several internal and external factors (4) play multiple parts in regulating and maintaining HSCs and the complex hematopoietic system. Internal factors include, for instance, intracellular molecules, transcriptional

and post-transcriptional regulators, intrinsic signaling pathways, and cell-surface proteins. Nutrients and metabolites also regulate HSCs and the hematopoietic system (5,6,7). For example, mitochondria exhibit multiple roles in providing HSCs nutrients, such as oxidation of essential fatty acids, and impairment of their bioenergetics activities results in HSCs exhaustion.

In addition to internal factors, within BME (8), many extrinsic factors regulate HSCs behaviors, such as interactions between HSCs/ progenitors with niche cellular compartments, like HSC interaction with mesenchymal stromal/stem cells (MSCs) and their differentiated progenies, adipocytes, and osteocytes, which are all critical in HSC pool and function (9,10). MSCs, and several BM cellular comportments, for instance, produce cytokines; cytokine-mediated regulation of the HSC system is a critical extrinsic factor for HSCs proliferation and differentiation toward a specific cell lineage. Interferons, interleukins, thrombopoietin, colony-stimulating factors, and erythropoietin are all examples of cytokines involved in hematopoiesis (11,12,13). These cytokines, for instance, bind, stimulate and activate their designated dimeric or heterodimeric receptors through protein-protein interaction, which consequently leads to various cellular responses and functions. Another example of extrinsic factors that regulate hematopoiesis is neural signals (14). Furthermore, those multiple extrinsic and intrinsic mechanisms and networks work harmoniously to orchestrate and maintain hematopoiesis (15). Dysregulation of these intrinsic, at the HSC level, or extrinsic cellular or molecular components within BME mechanisms could lead to ineffective hematopoiesis (16, 17, and 18). Moreover, alterations of mechanisms that regulate HSCs, either their self-renewal or differentiation by

molecular abnormalities and mutations, could lead to hematological malignancies, leukemia.

1.2 Overview of Acute Myeloid Leukemia

1.2.1 Acute Myeloid Leukemia (AML)

Acute myeloid leukemia is a clonal blood disorder. This aggressive heterogeneous hematological malignancy affects all age groups, mainly older people> 65 years (19, 20). Unfortunately, its incidence is high. According to NIH, there is an estimation of 20,050 new cases of AML in the current year, the year 2022 (20). In AML, an affected HSC gives rise to uncontrolled proliferative blood cell progenitors, and these immature cells, blasts, accumulate in the BM. Infiltration and accumulation of leukemic blasts in the BM are characteristic features of this disease. Consequently, such accumulation negatively impacts and interrupts normal hematopoiesis (21-23). It prevents the production of healthy mature blood cells and eventually leads to blasts released into the circulation and BM failure.

1.2.2 AML heterogeneity and classification

AML is known for its heterogeneity. It is associated with several heterogeneous genetic mutations and cytogenetics abnormalities. Mainly, AML patients are classified based on cytogenetic and molecular profiles (24-29). Furthermore, there are two classification systems for AML. The first classification system is the French-American-British (FAB) system which classifies AML based on microscopic morphology to assess the mature status of leukocytes. The second classification system is the world health organization (WHO) system, which classifies AML based on several factors such as genetic abnormalities and chromosomal alterations (24-27). AML disease heterogeneity impacts/directs its prognosis and therapy outcomes.

Around 50-60% of patients carry clonal chromosomal abnormalities that reflect the chemo-sensitivity of the disease (29).

1.2.3 AML mutations and risk groups

As mentioned above, AML is attributed to various genetic mutations and cytogenetics abnormalities, individual or combined. Genes mutated in AML play partial or central roles in several cellular and molecular functions, implicated in signaling pathways, such as splicing and transcription factors, epigenetic modifiers, and signal transducers. One of the most common genetic mutations in AML is the group of mutations in the FLT3 gene (FMS-like tyrosine kinase 3). Among this FLT3 mutations group is the FLT3-ITD mutation. This mutation is associated, specifically, with both; high risk of relapse and poor prognosis (30-32). There are several available inhibitors against FLT3, such as quizartinib and midostaurin; inhibitors are also classified based on the inhibitor's specificity. Studies found that even though administration of FLT3 inhibitors could clear the AML blasts from blood circulation, some could not clear the blast from the BME and the inhibition effect was not sustainable (33-35). In addition to FLT3, the other most prominent mutation is the NPM1 mutation (29, 36).

Low (LR), intermediate (IR), and high-risk (HR) AML subsets/groups are assigned by cytogenetics features. HR AML is a subset of AML that accounts for a considerable number of disease cases (37-40). HR AML has distinctive cytogenetic characteristics and molecular profiles. FLT3 mutation and KIT, for example, are HR. HR AML patients respond poorly to chemotherapies and have a high rate and risk for relapse (41-42).

1.2.4 AML Treatments

Classic AML treatment is composed of targeted therapy and intensive chemotherapy. Fortunately, following chemotherapy, complete remission (CR) in a high percentage of elderly and adult AML patients, up to 60% and up to 80%, respectively, was attained (43,44). Between 2012 and 2018, the percentage of 5-year survival was estimated to be 30.5% (20). CR in response to chemotherapies is usually evaluated by blasts morphology and percentage and evaluation of blood smears. Simultaneously with leukocytes' count and additional measurements such as signs of lineage-specific processes, erythropoiesis, and megakaryopoiesis. For instance, when the percentage of blasts in BM of AML patients is less than 5%, patients are considered at CR (43,44,46,47).

Stem cell transplant (SCT) is another available AML treatment. After chemotherapy, and depending on each AML patient case, SCT from an allogeneic donor, or what is referred to as allogeneic hematopoietic stem cell transplant (allo-HSCT), could be the cure for some patients, but not all, especially within IR or HR patients. Serval factors could affect the SCT outcome (48). Even though allogeneic SCT has been the option when an undesirable outcome is reached (48, 49), following SCT, induction of GvHD is, unfortunately, still a subsequent challenge.

1.2.5 Minimal residual disease (MRD) and AML Relapse

Even though many AML patients reach CR after chemotherapy, relapse and mortality rates in many AML patients, after CR, are still high (50). Studies have suggested that relapse in AML emerges from not only leukemic stem cells (LSCs) but also MRD. The definition of MRD is that after chemotherapies, some of the LSCs persist/resist the therapies and causing AML patients to relapse (Figure 1.1).

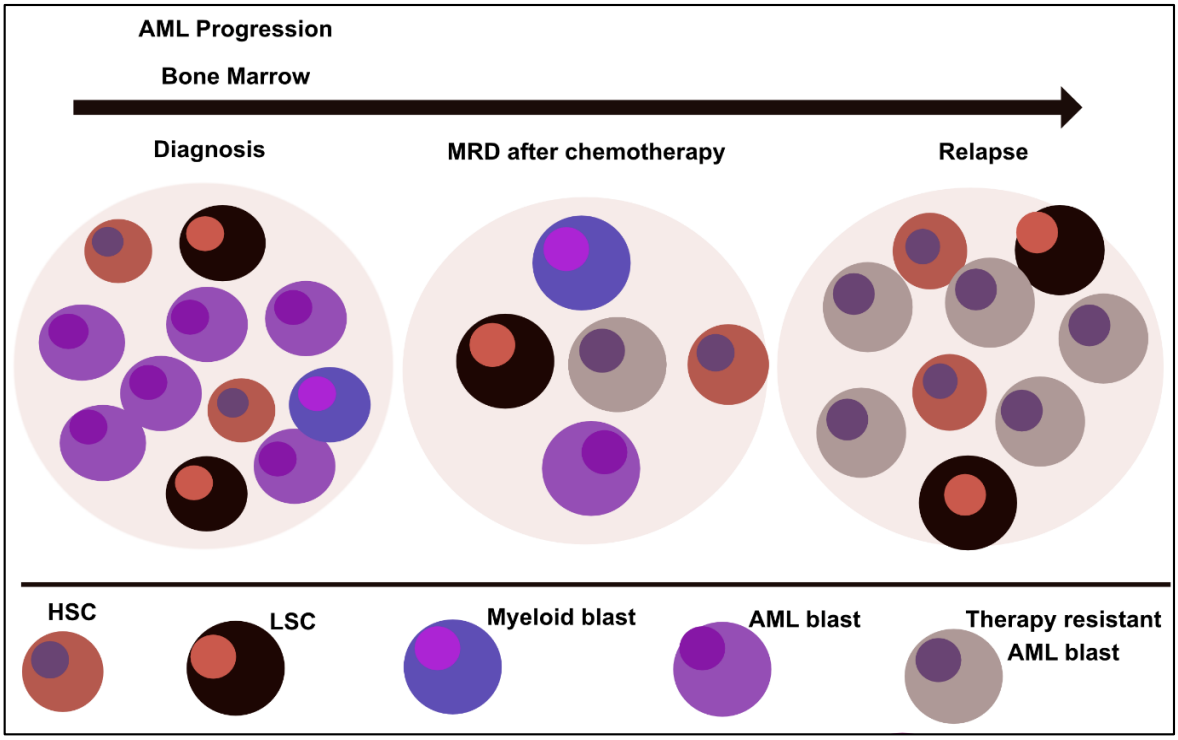

Figure 1.1. Schematic illustration of AML progressing from diagnosis to relapse as a result of MRD after chemotherapy. Representation of the heterogeneous cellular population in the BM of AML patients. This cellular population includes LSCs, HSCs, and therapy-resistant blasts in AML relapse after treatment. Adapted with modification from Ngai, et al. 2021 (51).

With all the challenging heterogeneity of AML, identifying the LSCs, which are considered the cells that initiate the relapse (51, 52), and distinguishing them from other cells within the marrow is another added challenge. LSCs may or may not express an additional altered marker compared to the healthy counterparts, HSCs. There are several cellular and molecular techniques, such as flow cytometry and qPCR, to evaluate MRD. These techniques are either used individually or combined (51) since MRD measuring could help determine treatment directions, pre and post-SCT, prognosis, and risk group (53). Similar to initial AML, AML after relapse is also treated with targeted therapies, and designated therapeutic plans depend on patients' profiles (54). Taken together, available AML treatments, targeted therapies,

and chemotherapies mainly focus on eradicating leukemic cells and do not necessarily cover the need for all AML subtypes. Moreover, despite those available treatments, relapse is still a challenging problem.

1.3. Bone marrow microenvironment, BME, HSC Niche

As mentioned earlier (section 1.1), HSCs reside in BME, the HSC niche. The idea of the niche was initiated in 1978 and suggested maintaining HSCs' behavior and features (55). Presently, the niche concept is accepted and thoroughly investigated in a healthy physiological state. As introduced, hematopoiesis regulation involves numerous complex extrinsic interactions that include cellular and molecular components within the niche. Moreover, the classical function of the niche is to support the HSCs' growth, govern the HSC function, protect and maintain the reservoir, and control the releasing of HSCs, immature and mature blood cells, into the circulatory system (1,56-59) while the mechanisms of hematopoiesis disruption and dysregulation in AML context are yet to be completely understood.

Within the BM, this specialized HSC niche is composed of endosteal and vascular/ perivascular niches (56,58,60).The perivascular niche compartment is a fundamental part of the niche. It mainly contains pericytes and sinusoidal endothelial cells. Furthermore, when sections of murine BM were analyzed, results showed that the majority of HSCs are confined within sinusoidal blood vessels (56,58,61). These findings suggest that this HSC niche compartment has a critical role in regulating HSC. The second compartment of the niche is the endosteal part. It is composed of MSCs, and osteoprogenitors. MSCs are known to be a critical component of the niche and osteoblast progenitors (59,62,63). Osteoblasts are also essential cellular components of the endosteal niche (63). The endosteal niche has also been found

to be critical for HSCs. Although the location of HSCs was found to be dependent on their differentiation stages, HSCs were found to reside near the endosteal part (62,64).The endosteal niche components, osteoblasts, have been found to play a critical role in hematopoiesis (59,60,63). Osteoblasts, for example, participate in hematopoiesis regulation via activation of the Notch signaling pathway (94). Osteoblasts were also found to aid in allogeneic stem cell engraftment (65). Furthermore, balanced interactions between cellular and molecular components of the endosteal and perivascular compartments of the HSC niche are essential. Specifically, essential to orchestrate the endocrine, paracrine and autocrine signaling that maintains the HSC pool, self-renewing HSCs, and quiescent HSCs and, thus, regulate normal hematopoiesis (1,56-58,66). Even though long-term cultures and niche investigation studies showed that the BME is required for maintenance and differentiation of the HSCs progenitors, the complete molecular mechanisms of the effect of an altered BME on hematopoiesis are still to be fully clear.

1.4. Mesenchymal stromal/stem cells (MSCs)

MSCs are non-hematopoietic progenitors with multi-lineage differentiation ability (59,67,68). Earlier in the 1970s, when bone marrow cells were cultured in vitro for several weeks, adherent fibroblast-like cells were produced (69). Those cells were found to support the proliferation of HSC progenitors and have a multi-lineage differentiation potency in which they could differentiate into adipocytes, osteocytes, and chondrocytes in vitro and in vivo (56,67,68,70). Those cells are known as MSCs. There are minimum criteria for characterizing MSCs following the International Society for Cellular Therapy (ISCT) (71) that include 1) under standard

culture conditions, cells are adherent to plastic, 2) they express specific surface molecules, CD73, CD90, CD105, and lack others, HLA-DR, CD14, CD19, CD45, CD34, CD11b, CD79a and 3) they can differentiate into adipocytes, osteocytes, and chondrocytes.

1.4.1. MSC's role in HSCs niche; hematopoiesis

MSCs participate in the HSC niche composition both in vitro and in vivo. As critical constituents of the HSC niche, MSCs are critical players in regulating hematopoiesis (67,72-78). In a physiological state, the balanced harmony amongst HSCs and MSCs, as osteogenic progenitors, provides essential coordination between the marrow and the skeleton to maintain hematopoiesis. HSCs regulation is vigorously reliant on MSCs and the differentiated progenies, demonstrating a critical role for MSCs in the specificity of the stem cell niche and regulation of HSCs within the BME; thus, when altered, MSCs impact the normal process. MSCs are located within proximity to HSCs in the niche. It was shown in vivo that many hematopoietic cells require contact with stromal cells, including MSCs, to proliferate and differentiate (79-82). In vitro, MSCs also have been shown to support hematopoiesis. Directly via cell-to-cell interaction or indirectly by releasing soluble factors (77, 78, 82, 83). Their secretion of several cytokines, such as IL-8, and several growth factors via regulatory signals. It has been shown that when transplanted in mice models, MSCs differentiate in those models' BM into osteoblast and osteocytes, and these cellular components are part of the niche's role in supporting hematopoiesis. Moreover, when co-transplanted with HSCs, MSCs help in HSC homing and engraftment (84-88).

Within the BM, multiple signaling pathways work together through interactions between their cellular and molecular subunits to provide a suitable niche that maintains HSC and progenitors. Many researchers have reviewed a plethora of signaling pathways by which MSCs participate in hematopoiesis and HSC regulation (76,77, 89). Moreover, HSCs surface markers depend on their status.CD34+ cells were found to adhere to MSCs when the latter was used as a feeder layer in culture and suggested that cell-to-cell contact is significant to maintaining HSCs in vitro. Proteins, such as integrin, cadherin, and vascular cell adhesion molecule, in addition to neural cell adhesion molecule 1, are reported to be responsible for such maintenance (83). MSCs regulate HSCs fate through cell-cell interaction via, for instance, adhesion molecule CXCL-12, which is critical for the proliferation and differentiation of HSCs (90). CXCL-12 and CCL-5 are two of the MSCs-produced factors that play a role in STAT signaling pathway activation by activating STAT-5 and STAT-1, respectively (89,90,91). MSCs' role in hematopoiesis is also demonstrated and maintained through ligand-receptor interactions between MSCs and hematopoietic stem and progenitor cells (HSPCs). An example of such protein-protein interaction is the interaction between Ang-1, which is expressed on MSCs, and Tie-2, which is expressed on HSCs. This interaction is essential for maintaining HSCs quiescence (92). Another example demonstrating MSCs' role in supporting HSCs survival and proliferation is via their interaction with HSCs' NOTCH molecule (89, 93).

As mentioned earlier, MSCs produce cytokines that are essential for maintaining the HSC pool and regulating hematopoiesis. While some cytokines promote HSCs quiescence, others support their self-renewal. Besides stromal cell-

derived factor, SDF-1 /CXCL12, (90), MSCs cytokines such as transforming growth factor (TGF), stem cell factor (SCF), bone morphogenetic proteins (BMPs), especially BMP-4, all play critical roles in HSCs regulation (89,95). In addition to their production of cytokines, MSCs are producers of numerous interleukins such as IL- 6, IL-8, IL-1, 1L-14, and IL-15 that are essential in HSCs differentiation, proliferation, and maintenance (78,90,95,96). MSCs subtype, Nestin+ MSCs, (nestin is a protein typical of neural cells), exhibit differentiation abilities, CFU-F, and stemness (self-renewal) and are associated with HSCs in both perivascular and endosteum niches. Moreover, MSCs were found to be important in HSCs homing after transplantation, and MSCs depletion could negatively impact the HSC population in the marrow (74,84).

MSCs were also found to reduce apoptosis via their produced-paracrine factors (Ang1, VEGF, HGF, and FGF-2) through the Akt signaling pathway (97). One critical component of the apoptosis signaling pathway is STAT. Signaling through STAT is critical in the proliferation of HSCs and their progenitors. MSCs were also found to participate indirectly in differentiation blocking via Jagged-1/Notch1: they indirectly block HSCs and progenitors. MSCs produce HGFs, which are critical for HSPCs maturation. MAPK signaling pathway also plays a role in Hematopoiesis regulation, specifically p38 MAPK. Deactivation of MAPK signaling reduces MSC's production of chemokines such as IL-8. IL-6 (91, 98, 99). MSCs play critical roles in HSCs regulation and hematopoiesis, and as seen, some of these roles were demonstrated through several examples. Furthermore, MSCs cellular progenies, through MSCs differentiation into multiple lineages, also play essential roles in HSCs maintenance and hematopoiesis.

1.4.2 Multi-lineage Differentiation potential of MSCs

MSCs support hematopoiesis not only by directly regulating HSPCs within BME but also by providing cellular components for the niche via their differentiation ability. Multi-lineage differentiation potential is a critical characteristic feature of MSCs. MSCs differentiate into osteocytes and adipocytes, which are essential for the structure and function of the HSC niche (60,63,65,71,74,86,96). There are multiple factors and mechanisms that affect and perhaps could determine MSCs' direction toward each lineage. Furthermore, a balanced differentiation is regulated and required within the niche to maintain physiological BME. Several signaling pathways, such as Wnt, Notch, BMP, Hedgehogs, and ECM-integrin pathways, are involved in MSC's differentiation (100-103). Furthermore, within MSC, these pathways are suggested to work collectively to regulate and provide a balanced differentiation process between adipogenesis and osteogenesis as demanded (104). Multiple extracellular and intracellular signaling molecules of each pathway regulate MSCs differentiation. These molecules signal to either activate or inhibit master transcription factors toward a specific lineage. Transcription factors PPARγ and C/EBPα, for example, are major regulators for adipogenesis, while Runx2 and Osterix are osteogenesis master regulators.

Moreover, MSC's differentiation to osteocytes and adipocytes is significant to maintaining HSCs and the HSC niche. Osteocytes and their progenitors are critical in regulating HSC's differentiation and mobilization in the BME. For example, an increased MSC differentiation towards osteogenic cells has been linked to MSCs maintaining the HSCs in their quiescent state (94). Additionally, due to their crucial role in sustaining the osteoprogenitors pool, MSCs, both human and mice, were

found to regulate bone's remodeling process (105-107) and repair bone fractures and injuries. In particular, MSCs migrate to the site of bone injury, differentiate into osteoprogenitors, and repair the bone. Other tissue repair properties have also been attributed to MSCs (105-110).

TGF-β signaling can regulate many cellular contrasting physiological and pathophysiological processes such as cell growth and apoptosis (111), tumor-suppressive, and promotion capabilities. Specifically, TGF-β plays a crucial role in tumor progression, invasion, and metastasis (111-113). BMP signaling belongs to the TGFβ superfamily, which regulates several cellular processes, and is essential for HSCs fate during development and differentiation; furthermore, it participates in the osteogenesis process. BMP signaling participates in MSCs' osteogenesis differentiation (114). When BMPs 2, 4, or 7 bind to their receptors, Type I and type II, they heterodimerize, forming an activated complex triggering signal transduction through SMADs that phosphorylates SMAD proteins. Consequently, the phosphorylated SMADs translate the signals and regulate the transcription of osteoblastic genes (115). The osteogenic differentiation process is regulated by several MSCs molecules such as gremlin-1 (GREM1)(116-118).

GREM1 gene encodes a BMP, bone morphogenetic protein, antagonist. Particularly, it antagonizes BMP2, 4, and 7 and prevents their binding to their receptors. This secreted glycoprotein belongs to the same DAN/Cerberus family as TGF-β and VEGF (119-121). GREM1 protein is mainly disseminated extracellularly and minimally into the endoplasmic reticulum. It plays an essential role in cellular development and differentiation (122,123). As a BMP antagonist, GREM1 has been shown to play a critical role in osteogenesis, and when dysregulated, it negatively

affects MSC osteogenesis differentiation (116-118). In addition to participation in multiple cellular processes, GREM1 has been found to play a critical role as a proangiogenic factor. It activates angiogenic responses via VEGF receptors (121). In addition to GREM1, SCUBE3 is a gene expressed in MSCs. Like BMPs, SCUBE3 is a member of the TGF-β superfamily; members of this family signal through TGFβ and control MSC's differentiation. SCUBE3, Signal peptide-CUB-EGF-like domain-containing protein 3, is a secreted glycoprotein composed of 5 motifs. When cleaved, SCUBE3 releases its N-terminal, EGF-like repeats, and C-terminal, CUB domain. These EGFs participate in protein-to-protein interactions signaling through SMAD canonical pathway, The TGF-β pathway. Dysregulation of SCUBE3 led to pathological conditions in mice (124). Nevertheless, in the AML BME context, when dysregulated, SCUBE3 and GREM1 potential roles in altering MSCs, affecting their differentiation, and thus their function and BM composition role remains unclear.

MSCs differentiate to mature adipocytes through the adipogenesis pathway, where various molecular and transcriptional regulators are involved (Figure 1.2) (125). Adipocytes play an essential part in HSCs homeostasis in BME. Regulated adipocytes are located close to HSCs and work as negative regulators. They prevent the expansion of the progenitors and protect the HSCs pool (126). Both radiation and drug-mediated suppression of these adipocytes were found to boost the expansion of the progenitors and enhance HSC engraftment, respectively. Furthermore, induction or reduction of adipocytes negatively impacts HSC regulation (127,128), suggesting that balanced adipogenesis is required to maintain a healthy niche. Adipocytes' significance relies on the production of multiple secretions and metabolites. They produce several extracellular matrix components or BME, such as

collagen. Adipocytes also secret multiple cytokines, such as IL-6, IL-8, and CCL2 which are essential in BME. In several tissues, adipose tissue alterations were associated with several inflammatory diseases (129). Although the interaction between HSCs and other cellular components within the niche is needed, adipocytes are still critical in maintaining the HSC niche. Moreover, MSC differentiation is essential for tissue hemostasis and affects MSC immunomodulation properties (130). Therefore, impairment of MSC's differentiation could lead to tissue-specific problems, which also emphasizes that a balanced harmony or regulated differentiation is crucial in preventing disruption of tissue hemostasis.

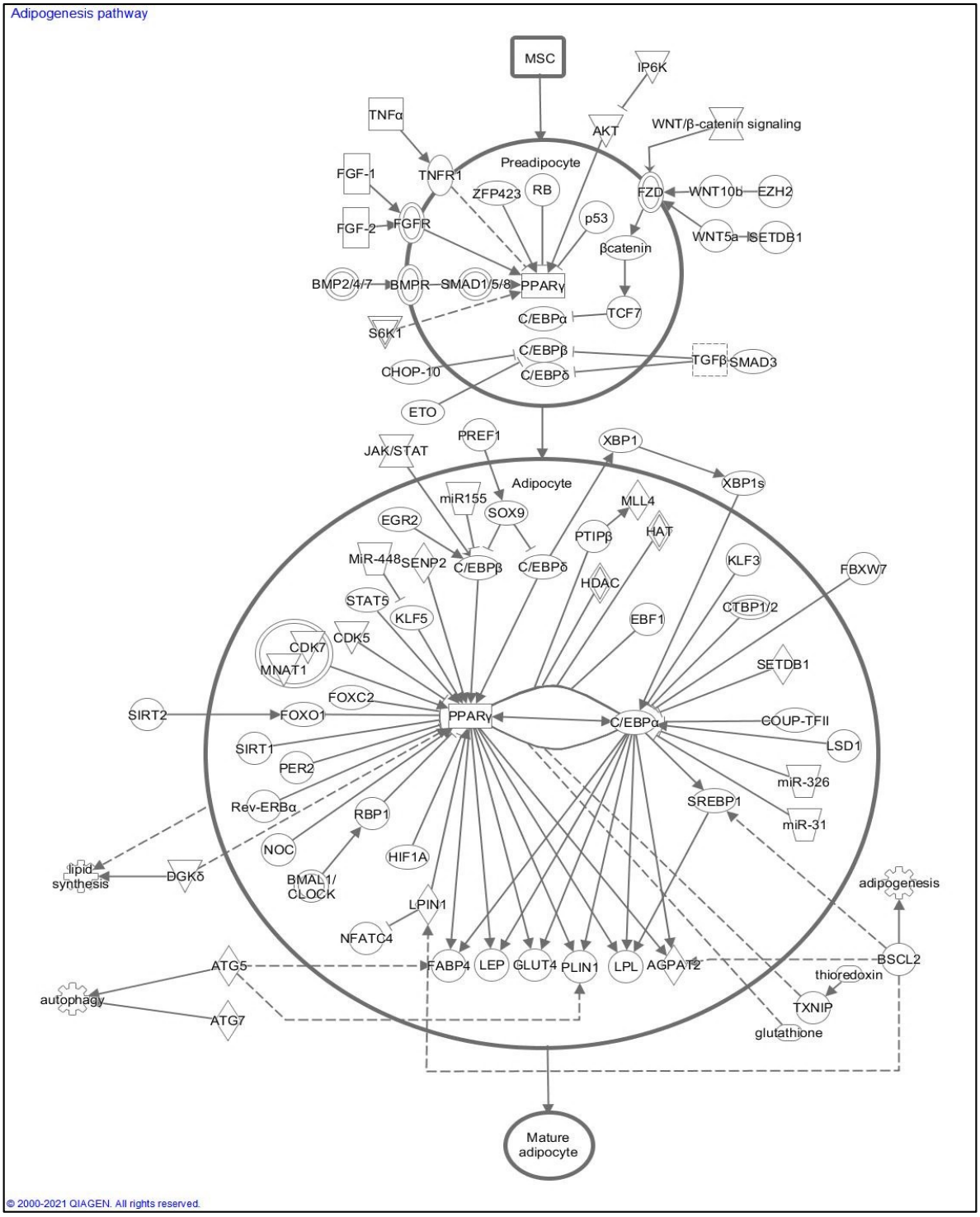

Figure 1.2. MSC's Adipogenesis pathway. C/EBPα and PPARγ are key regulators of MSC's adipogenesis. Taken from IPA 2021(125).

1.4.3. MSC's immunosuppressive properties

In addition to the multi-lineage differentiation ability, MSCs exhibit immunosuppressive properties. MSCs exhibit a dual immunological role; they can act as immunosuppressive or immune-modulators. Mainly, human MSCs use indoleamine 2,3-dioxygenase, IDO, for immunosuppressing function (131,132). Along with IDO, MSCs secrete several immunosuppressive molecules, such as nitric oxide (NO), prostaglandin E2 (PGE2), and transforming growth factor (TGF-β). These factors allow them to modulate immune responses (132-135). It has been suggested that only under the influence of an inflammatory environment MSCs gain their immunosuppressive properties. Studies showed that MSCs interact with several immune cells, such as T cells. They can inhibit T-cell proliferation and the production of pro-inflammatory cytokines (136). Furthermore, they can interact with dendritic and natural killer cells (137,138). MSC's immunoregulatory property enables them to be used in clinical and therapeutic approaches. Having this distinguished ability, MSCs have been used in immunotherapies, especially in allogeneic transplantation and treatments of autoimmune diseases (139-142). In addition, MSCs' ability to inhibit T-cells from recognizing alloantigens was an encouraging character for their utilization in both treatment and prevention of graft versus host disease, GvHD (88,143). Although MSCs could be useful in therapeutic approaches due to their immunosuppressive properties, these properties could, unfortunately, aid MSCs in helping tumors escape the host immune surveillance; for instance, MSCs have been found to support and promote tumors (144-146).

1.5 Leukemic BME

Like HSCs, leukemic cells reside within the BM in the HSC niche. HSCs have been found to home first in the endosteal niche and then in the other compartments (147,148). LSCs were found to have an altered self-renew capacity to generate their heterogeneous population (149). Similar to HSCs' behavior, LSCs rely on niche components and signals for LSCs maintenance. For instance, CXCL12 and SCF, BME factors required for HSC regulation, play a role in LSC's status (150). Using single-cell RNA sequencing, studies of BME showed that both healthy and leukemic environments have a heterogeneous cellular population (151,152). Furthermore, studies have shown that BME cellular components could support disease development. These leukemic cells also interact directly with marrow cells to maintain their pool, such as communicating with vessels endothelium through protein-protein interaction. The interaction between LSCs expressed CXCR4 and endothelium cells expressed SDF-1(153) is an example that demonstrates their designated communication within the niche. Although some of the LSCs' biological features are similar to those of their healthy counterparts, HSCs, LSCs take over the HSCs niche and induce changes to BME to create a favorable environment for their clones' survival (23,47), which also leads to disruption of hematopoiesis.

The disturbance of hematopoiesis caused by those abnormal clones, LSCs clones, during disease initiation includes altering components of BME. Moreover, AML progression and relapse have been associated with BME alterations at cellular and molecular levels. These alterations are suggested to provide a permissive niche that might aid MRD cells to propagate, disrupt normal hematopoiesis, and eventually contribute to disease relapse. Furthermore, this concept emphasizes the need for

further understanding of AML biology in terms of BME. Specifically, understanding the alterations of its components. Several alterations of BME at multiple levels have been reported (23,153-159). For instance, AML was found to induce alterations of the cellular compartment of the BME such as MSCs, and MSCs progenitors toward a committed lineage, toward osteoprogenitors (154,155,158). Alterations in the HSC niche vascular part, specifically endothelium components, were found (153) and associated with myeloproliferative disease. Changes in O2 levels in which LSCs expand hypoxic microenvironment were also found (159). Furthermore, alteration of the cellular composition of BME led to myeloproliferative disorders in mice. In addition, LSCs disrupt hematopoiesis by altering niche neuronal signals to induce LSCs infiltration and proliferation, creating a leukemic environment (157).

1.5.1. MSCs in Leukemic BME

The presence of cross-talk between the niche and leukemic cells, especially in myeloid malignancies, has been suggested. Their cross-talk with stromal cells enables their proliferation and survival and limits HSCs advantaging from BME, suggesting that AML cells compete with their healthy counterparts, HSCs, to benefit from the BME resources (23,156,160). MSCs and MSCs progenitors equip the marrow microenvironment not only for HSCs growth in normal hematopoiesis (as introduced in sections 1.3 and 1.4), but they also support AML cells. Growing evidence suggests that within the HSC niche, MSCs interact and communicate with LSCs; such interactions aid them in surviving and proliferating (Figure 1.3). MSCs also aid blasts within the niche to proliferate through their soluble factors, such as their production of cytokines (160). Furthermore, LSCs in leukemic BME are reprogrammed to utilize high metabolic energy, unlike normal HSCs. In vitro studies

showed that MSCs are among the energy sources that provide LSCs with nutrients for such high-energetic demand through their mitochondrial transfer to LSCs. Although LSCs mainly obtain their energy from mitochondrial oxidative phosphorylation, not glycolysis, the mechanisms behind such reprogramming are not completely clear (161-163). Another tool demonstrating MSC's role in protecting blasts and thus MSCs' participation in AML pathogenesis is MSCs immunosuppressive properties. MSCs produce immunosuppressive factors, such as IDO, that could prevent the immune system from recognizing the leukemic cells (164). These mechanisms collectively could maintain the AML cells and the leukemic environment.

Additionally, some leukemic blasts resist chemotherapy drug-induced apoptosis; such resistance has also been suggested to result from the interaction of these blasts with MSCs in part. MSCs participate in blasts' chemoresistance via their production of several soluble factors. In vivo, AML blasts altered the HSC niche structure to support proliferation and survival. For instance, the murine stromal cell line (MS-5) provided chemo-protection for AML blasts and leukemic cell line HL60 (165). Additionally, interactions between stroma cells and leukemic cells could assist in their metastasis (73,156, 165-170) and prevent them from undergoing apoptosis.

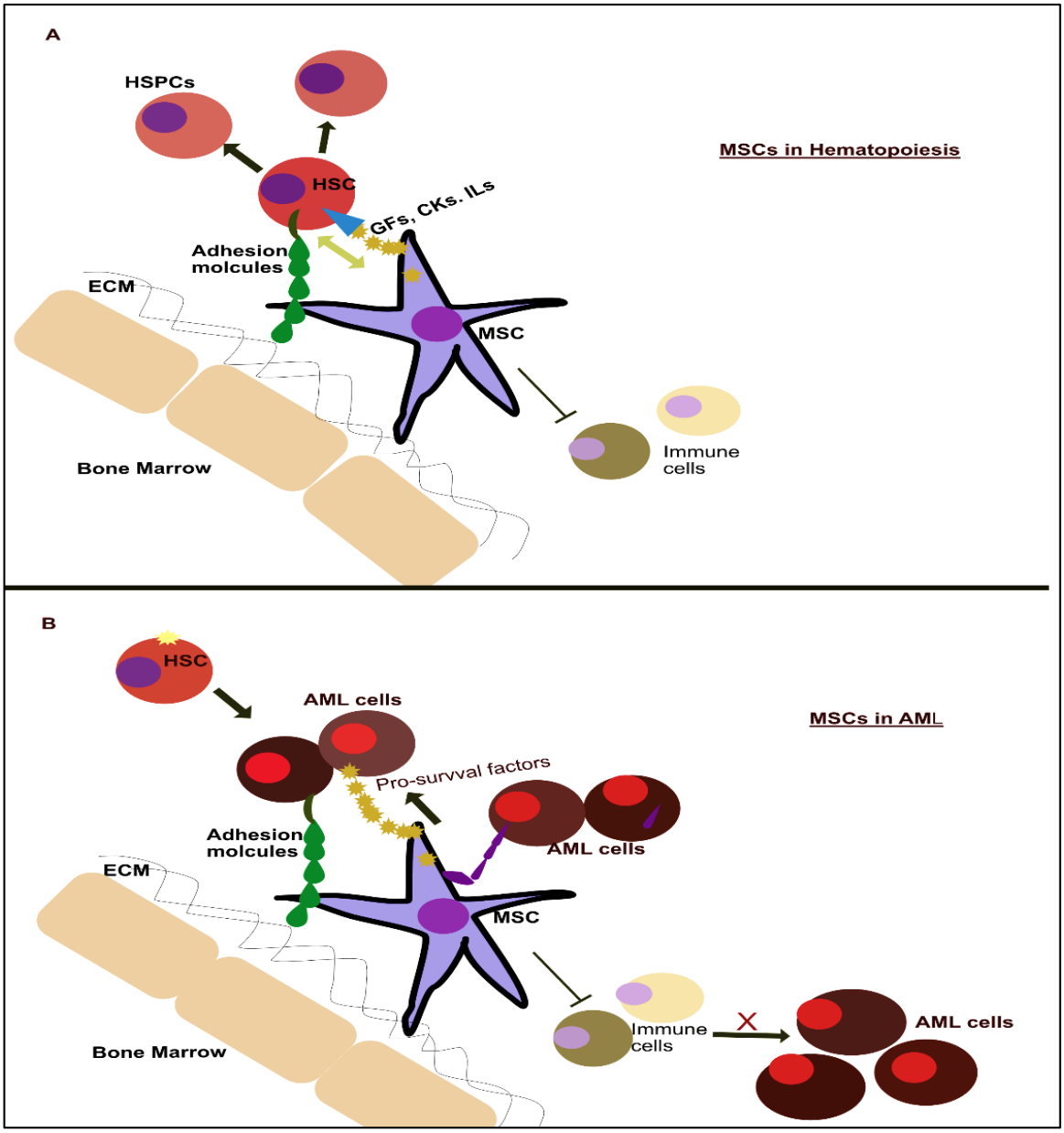

Figure 1.3. MSCs cross-talk with HSCs and AML cells within BME. A) MSCs participate in the regulation of HSCs and HSPCs. They produce several cytokines and express cell-surface proteins essential for the proliferation, homing, and differentiation of these cells. In addition, MSC's immunosuppressive features inhibit the activation of immune cells, which enables their use in preventing GVHD and aiding AML cells to survive. B) MSCs support AML cells within the BM niche; their immunosuppressive properties prevent the recognition of AML cells. Also, provide nutrients and soluble factors that aid those leukemic cells to survive. Such as, MSCs provide nutrients to AML cells through mitochondria. Abbreviations: CKs=cytokines, ECM=extracellular matrix, GFs=growth factors; ILs, interleukins. Adapted from Ciciarello M, et al, 2019 (178).

Differentiated MSCs, osteocytes, and adipocytes, also play a role in the AML environment. Experimental studies in mice models showed that osteoprogenitors play a role in the disease. Genetic mutation of β-catenin of those MSC-derived cells negatively affects HSCs differentiation toward myeloid lineage through activation of HSCs Notch signaling and consequently results in AML development. Additional mutations in MSCs and progenitors were also associated with an increased risk of AML development (155,168,170,171). Moreover, adipocytes are an essential cellular component of the niche. Adipocytes produce and secrete multiple elements; therefore, they participate in hematopoiesis and HSC regulation within BME. Similarly, adipocytes have been found to participate in AML (172-173); they could participate in maintaining leukemic BME and AML pathogenesis. In particular, adipocytes could support AML blasts and maintain the AML environment by providing several molecules (Figure 1.4). Adipocyte production of metabolites, for instance, through lipolysis activation, such as free fatty acids, could be used by AML cells as an energy resource that could help in AML cells' proliferation and survival as shown to contribute to other tumors (174,175). Mainly since a higher fatty acid oxidation rate has been found in AML cells compared to healthy cells. In vitro, adipocyte-AML cell co-culture experiments showed that adipocytes are critical cellular components that support AML survival. Additionally, adipocytes have been found to support AML cells' chemoresistance (176,177). These findings collectively suggest that adipocytes could play a critical role in contributing to AML pathogenesis.

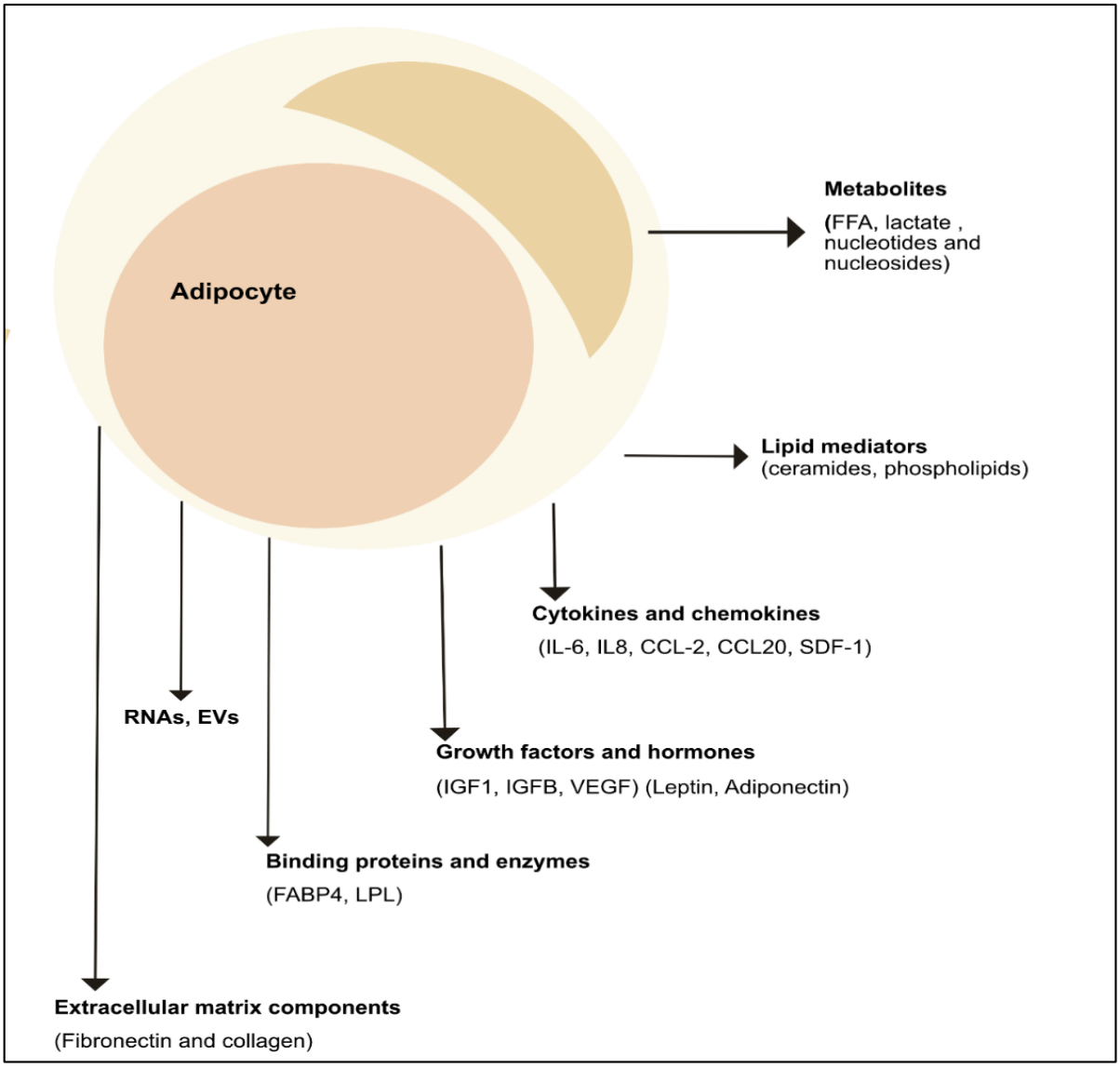

Figure 1.4. Adipocytes have multiple secretions and mechanisms through which they could aid AML cells to survive within BME. Adipocytes participate in BME composition via secretion and production of several molecules and metabolites. Cytokines, chemokines, and enzymes are part of adipocytes' secretions. They also participate in extracellular matrix composition through their fibronectin and collagen products. Abbreviations; FFA: free fatty acids, LPL: leptin, FABP4: Fatty acid-binding protein 4. Adapted from Zinngrebe, J. et al. 2020 (172).

Nevertheless, the molecular differences between MSCs in normal BME and MSCs in leukemic BME and, consequently, their potential roles in BME alterations toward a potential permissive niche are unclear. Thus, investigating the changes of

MSCs and how these stromal cells are different from their healthy counterparts is essential to provide a better understanding of niche biology in AML. Moreover, it could perhaps aid in identifying novel MSCs markers that limit AML progression and prevent its relapse. Therefore, AML-derived MSCs (bone marrow MSCs isolated from BM aspirates of AML patients) known as AML-MSCs are a great model for BME and have been used in the field to study its AML-associated alterations.

1.5.2 MSCs derived from AML patients (AML-MSCs)

Studies that characterize AML-MSCs to investigate their alterations which could aid in understanding the role of MSCs in AML pathogenesis, are limited. Moreover, similarities and differences between these AML-derived MSCs and MSCs from healthy donors were found in these studies (179-190). Impairments and alterations at multiple levels of AML-MSCs, phenotypic properties, and molecular levels have been reported compared to MSCs from healthy donors (HD-MSCs). For instance, while some of these studies found cytogenetic alterations in these MSCs (180,185,186), others showed that AML-MSCs exhibited no cytogenetic aberrations compared to their control HD cells (187). Moreover, molecular alterations were found in some studies to be different from AML blasts cytogenetics aberrations (180).

Functional impairments have also been found in AML-MSCs. For example, an increase in adipogenesis potency of these AML-MSCs was found (182,189). Delayed and impairment of AML-MSCs osteogenic differentiation potential were also reported (181,182). In contrast, another study found that those MSCs exhibit decreased adipogenic and induced osteogenic potentials (188,190). AML-MSCs also were found with reduced CFU and a slow proliferation rate (181,186, 190) in

comparison to their healthy cells. Minor alteration of gene expression was also found between AML-MSCs while their cytokines profile was changed. Alteration of metabolic-related genes of AML-MSCs was found compared to HD-MSCs (183). Interestingly, a recent study found that induction of AML-MSCs adipogenic potential correlated with AML cells survival (189). However, considering AML heterogeneity and subtypes, although some of these studies have characterized AML-MSCs, the exact role of AML-MSCs in impacting the BME and in the disease AML remains unclear. Thus, characterization of a large cohort is needed to confirm and provide additional insights about MSC's role in AML, especially about AML subtypes, with their various molecular and clinical profiles.

A recent study by our group (Guardia et al., 2017(184)) has characterized a large cohort of AML-MSCs. The cohort included 46 AML-MSCs from all AML risk groups/subtypes; IR, LR, and HR AML patients. The study found that AML-MSCs from HR patients exhibited altered functionalities. They have impairments in their differentiation potentials and induction of their immunosuppressive properties. Nonetheless, these studies collectively suggest that understanding MSCs alterations is essential for understanding BME biology and its role in AML pathogenesis and consequently helps prevent its relapse. However, these studies mainly focused on phenotypic and functional characterization of these disease-derived MSCs while limitedly investigating MSCs molecules that could be behind these impairments and; thus provide insights about MSC's role and association with BME alterations. Therefore, in-depth systematic investigation and characterization of AML-MSCs are critical in understanding MSCs' potential function in altering BME.

1.6 Potential role of CD248 in MSCs

1.6.1 CD248 composition and structure

CD248 was initially found in tumor endothelial cells and called tumor endothelium Marker-1 (TEM-1), also called Endosialin, when it was first identified in 1992 (191). The human CD248 gene is located at chromosome 11(11q13). It is composed of 2,274 bp and has no introns. It encodes a 757 amino acid, type-I transmembrane protein. The Endosialin/ CD248 protein is expressed on the cell surface (192,193). CD248 protein is composed of an Intracellular domain, a transmembrane domain, and an extracellular domain (Figure 1.5). The first 685 amino acids compose the extracellular domain. Amino acids 1 - 20 compose the single peptide (leader peptide). The transmembrane domain is composed of a hydrophobic region that includes amino acids 686 to 706. The intracellular domain is composed of only 50 amino acids, amino acids 707 to 757, while the C-terminal domain is composed of many amino acids 60-757. Amino acids 20- 157 compose the lectin-like c-type region. While amino acids 176 -230 compose the sushi domain, and amino acids 235-305 consisting three repeats of EGF (EGF 1; 235-271, EGF 2; 274-311, and the third EGF unit; 316-350) (193). The three EGF repeats are followed by a mucin-like unit. The cytoplasmic tail of this C-type lectin-like protein is highly conserved between several species.

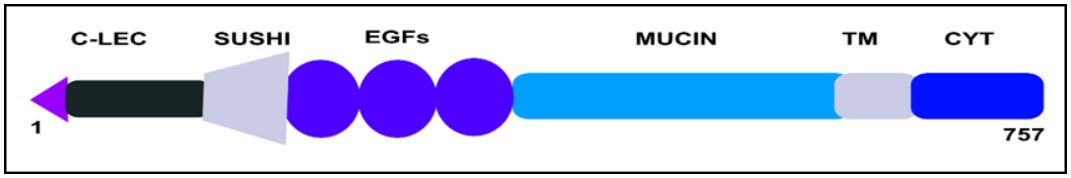

Figure 1.5: Illustration of CD248 protein. Adapted from Christian et al. 2001(193)

CD248 protein is highly glycosylated. The molecular weight of its core protein varied between 80.9 and 95kDa (191,193). CD248 has several potential glycosylation sites, O-glycosylation, and one N-glycosylation; perhaps because of such multiple glycosylation sites, other molecular weights were identified as 95, 120, 165, and 175kDa in several cells types, such as fibroblasts and endothelial cells, and cell lines such as HUVEC, SW872 (191,192). Like the human endosialin, the mouse protein is also a type 1 transmembrane protein (765 aa); however, it varies in its domains' components. It is also highly glycosylated with a core protein 92kDa (194).

CD248 belongs to the CTLD-14 protein family. Structurally, in the human, the length and sequence of its extracellular N-terminal domain (Figure 1.5) include amino acids 30-360, which homologize to other proteins in that same family. It homologizes by 39% to CD141/ thrombomodulin (endothelial cell cell-surface receptor) and by 33% to C1qRp (193). However, homology of its C-terminal domain has not been found with additional proteins. Furthermore, human and mouse End are partially homologized to each other. The former homologized to the latter by 77.5% (195,194).

1.6.2. CD248 expression and physiological role

CD248 expression has been demonstrated on the surface of MSCs (196). Besides its expression on MSCs, CD248 is expressed on fibroblasts as surface glycoprotein, smooth muscle cells, osteoblasts, and especially vascular cells pericytes and myofibroblasts (192,193,195,197). In addition, it has been detected in varieties of cell lines. Physiologically, this single-pass transmembrane protein is temporarily expressed during human development, and its expression decreases

gradually between embryonic to adult life. Human CD248 is not highly expressed in normal tissues (192,193,195,200), and a similar expression pattern was found in mice (197).

CD248 has been shown to serve an essential role in several physiological cellular processes. It has a role in tissue repair, remodeling (198), and cell proliferation. Furthermore, CD248 has a role in embryonic development in cells of mesenchymal origin; it induces stromal cell proliferation; thus was identified as a mesenchymal marker. CD248 is also associated with epithelial structures. Additional to its role in fibroblast and myofibroblasts proliferation (196), CD248 plays a role in cellular adhesion and migration. The inhibition and overexpression of CD248 affect pericytes proliferation (194,197,199), adhesion, and migration through activity of MMP-9, proteinase. CD248 is localized on the cell surface, acting as a receptor for several ligands. In a recent review, a couple of binding partners for CD248 are illustrated (200), although the intracellular mechanisms of CD248 signaling are not precise yet.

Some of the CD248 binding partners, for instance, were components of the extracellular matrix. Mac-2, for example, is a ligand expressed by tumor cells in a tumor environment. Such interaction between these two proteins, CD248 and Mac-2, caused a reduction in tumor cells adhering to myofibroblasts (201). Although the exact mechanism behind the resulted reduction has not been fully demonstrated. Additionally, CD248 has a role in angiogenesis, vessel formation, and maturation. It has been shown that CD248 binds to ColI and ColIV. Such binding promotes cell attachment and migration throughout tumor invasion due to MMP-9 release (196). Studies have demonstrated regulation of CD248 via TGFβ, while others showed a

relation between pro-fibrotic molecules and CD248 in vivo; TGFβ and PDGF BB are examples of these molecules (202,203).

1.6.3 CD248 Pathological role and tumor severity

CD248 has been found in malignancies and varieties of pathological conditions. Furthermore, it was associated with disease and tumor severity. CD248 is expressed on fibroblasts and pericytes in fibrosis. A significant reduction of fibrosis, both renal and hepatic, was observed when CD248 was downregulated (204,205). In cancers, it is expressed in several solid tumors in humans, in sarcomas and carcinoma (206). Upregulation of CD248 mRNA was found in colon cancer. CD248 is found to be highly expressed, specifically in the vascularization of several tumors, such as neurological malignancies. in addition, C248 was found to be highly expressed in some neuroectodermal tumors (207). Furthermore, due to its potential role in cancer and some inflammatory disease, some studies targeted CD248 (207-209).

In murine models, CD248 knockout showed its role in metastasis and progression. For instance, a reduction of the tumor was observed in KO mice compared to WT when xenograft transplantation was performed. In addition to the observed reduced tumor volume, a reduction of metastasis with a higher survival rate was found in CD248 KO mice. Furtherly, while CD248 inhibited CD8+ T-cells proliferation when a CD248 overexpression was performed on a CD248- T-cell, MOLT-4, it induced their proliferation when a knockdown was conducted on naïve T-cells (210). CD248 lack has also been shown to reduce the severity of many other conditions besides hepatic and renal fibrosis, such as inflammatory arthritis and atherosclerosis (208,211). Studies that find reduced tumor volume in CD248/TEM1

knockout mice suggested that the expression of CD248 on host stroma promotes cancer which also suggests the significant role of an increased expression of CD248 in tumor progression. As mentioned above, CD248 has been mainly investigated and demonstrated by its involvement in angiogenesis and near hypoxic environments. CD248 expression has been associated with hypoxia. Its induction resulted from HIF-2-related mechanisms and the involvement of transcription factors ETS-1 and SP1 (212). In MSCs, a recent Investigation of CD248 expression on MSCs from systemic sclerosis (SSc-MSCs) also suggested its involvement in fibrosis through promoting cell proliferation (213). CD248 role in adipocyte function, especially at the metabolic level, was also investigated via multiple in vitro and in vivo experimental approaches of CD248 gene modifications reported by Petrus and colleagues that showed a negative and unfavorable impact of this transmembrane glycoprotein in glucose metabolism (214). It has also been associated with hypoxia-mediated response in adipocytes and vascularization properties.

1.7 Rational

A physiologically balanced BME is essential to support and regulate HSCs growth and differentiation to maintain normal hematopoiesis. Several studies suggested the presence of cross-talk between the niche and leukemic cells in AML. AML relapse has been associated with alterations in the BME, which suggests the potential role of BME in disease pathogenesis. Since multipotent MSCs are a critical component of the BME and play a role in the regulation of HSCs, they may have several roles in the alteration of the BME towards a more permissive niche; thus, leukemogenesis. BM-MSCs can provide an excellent *in vitro* model for studying BME; specifically, MSCs derived from AML patients (AML-MSCs). Since these MSCs were harvested from leukemic marrow where they have been exposed to AML, they could represent BME alterations and greatly aid in better understanding the tumor biology in AML. Therefore, the investigation of AML-MSCs has been the objective of some studies (179-190). Nonetheless, these studies have mainly focused on phenotypical and functional characterizations of AML-MSCs while have limitedly investigated their genetic profiles. Also, most of these studies have examined small sample cohorts of AML-MSCs that did not necessarily represent such a heterogeneous malignancy; moreover, AML-MSCs' exact role in BME is still unclear. Since AML heterogeneity has been a significant challenge in understanding the disease pathogenesis, a large cohort that could represent AML heterogeneity is needed to better understand the disease. A recently published study by our group also has functionally and phenotypically characterized AML-MSCs from 46 AML patients (184). Interestingly those AML-MSCs, specifically HR AML-MSCs, display an impairment in their differentiation potentials, osteogenic and adipogenic, and

exhibit an increased immunosuppressive/anti-inflammatory activity compared to healthy donor MSC (HD-MSCs). Collectively, those findings suggest that these AML-MSCs exhibit significant genetic alterations. Therefore, in-depth transcriptomic characterization of these AML-MSCs was performed in this study to study and discover the possible mechanisms and molecular targets behind the observed alterations. Moreover, further investigation of the identified altered targets was conducted to understand the significance of these discovered effectors in BM-MSCs' function in healthy BME and AML contexts.

1.8. Hypothesis and Objective and Research aims

1.8.1 The overall objective

The overall objective of this study was to determine the potential role of AML-MSCs in the alteration of the bone marrow microenvironment, BME, toward a more permissive niche, in AML through understanding their alterations at the molecular and functional level.

1.8.2 The hypothesis

"Changes in gene expression within AML-MSCs lead to an altered BME which contributes to the pathogenesis of AML."

1.8.3 Research aims

- The first aim of this study was to determine differences in gene expression levels between MSCs derived from healthy donors (HD-MSCs) and patients diagnosed with AML (AML-MSCs) and to perform *in-silico* analyses using the statistically differentially regulated genes (SDRG) dataset to identify critical molecular effectors that could play a role in MSCs altered behavior and consequently in the pathogenesis of AML.
- The second aim was to validate the biological significance of the identified and selected molecular effectors at the HD-MSCs' functional level and their relevance to the leukemic BME.

1.9 Summary of research aims' results and significance

In Chapter 3, RNA sequencing was performed to investigate the differences between the AML-MSCs group, which included AML-MSCs from all AML subtypes IR, LR, and HR (n = 29) and HD-MSCs (n=8). The differences between the two groups of MSCs were determined at mRNA levels. The transcriptomic data analysis showed that AML-MSCs exhibited an altered gene expression profile compared to HD-MSCs. Interestingly, 21 statistically differentially regulated genes (SDRGs) were found in AML-MSCs compared to HD-MSCs. When an in-silico analysis was performed via Ingenuity pathway analysis, IPA, using the SDRGs dataset, several molecular effectors were found to play multiple roles in MSCs processes. No common pathway was identified between these genes; however, several genes play individual roles in multiple MSCs differentiation pathways. Moreover, these dysregulated genes were found to be part of AML signaling. Initially, three molecular effectors were identified, GREM1, SCUBE3, and CD248, due to their potential relevance to MSCs' function, to be with potential roles in MSCs differentiation and BME. Dysregulation of GREM1 and SCUBE3 was confirmed at the mRNA level but could not be confirmed at the protein level. Moreover, dysregulation of CD248 was successfully validated at the protein level, and CD248 was selected among these targets for further investigation and study.

In Chapter 4, CD248 was thoroughly studied. CD248 gene was significantly upregulated in the AML-MSCs group, including AML-MSCs from all AML risk groups. Moreover, its high abundance at the protein level in HR AML-MSCs (n=11) was confirmed after the successful establishment of their cultures. This confirmation enabled further investigation of CD248 as a potential target in AML-MSCs. An

efficient in vitro knockdown model of CD248 in HD-MSCs using siRNA was established, which helped unfold the CD248 role in healthy MSCs. Using AML-MSCs was limited since they exhibited an altered gene profile, and in vitro, AML-MSCs culture establishment and maintenance was challenging, which could have interfered with understanding CD248 role and significance. An efficient knockdown of CD248 total protein and cell-surface receptor was achieved and confirmed by Western blot analysis and flow cytometry. Moreover, additional examination of the established CD248 KD protocol using HR AML-MSCs revealed a high knockdown efficiency. The establishment of such an in vitro model of CD248 in HD-MSCs enabled the determination of its significant role at the HD-MSC's functional level.

In Chapter 5, the significance of CD248 KD in HD-MSCs at a functional level was investigated. The investigation was conducted through three primary functional assessments of (siCD248-MSCs): 1) its effect on HD-MSCs differentiation potentials, 2) its effect on MSCs protein profile, and 3) its effect on HL60 proliferation using co-culture experiments. CD248 KD altered HD-MSCs protein profile, and a relative significance was found primarily on TGF-β1 protein. CD248 KD in siCD248-MSCs did not affect HL60 viability, nor did HD-MSCs. Moreover, while no significant alteration was found in their osteogenic differentiation potential, the adipogenic differentiation potential of siCD248-MSCs was altered. Microscopic reduction in their adipogenesis was observed. Thus, further validation and examination of CD248 biological involvement in the adipogenesis pathway were performed at the gene expression level. Not only master adipogenesis regulators, C/EBPα and PPARγ, were tested but also multiple genes within the adipogenesis pathway. The analysis revealed that adipogenic-differentiated siCD248-MSCs overexpressed SIRT2, a

known adipogenic regulator. In-silico analysis of SIRT2 upregulation enabled the Identification of a potential mechanism by which CD248 KD could alter HD-MSCs' function through its reduction and involvement in their adipogenesis.

The transcriptomic analysis results in chapter 3 will provide significant knowledge and insights about AML-MSCs alterations and their potential participation in altering the niche, especially since the available AML-MSCs studies are limited. Moreover, the analysis could help understand the role of BME in such a heterogeneous hematological malignancy, AML. Since BM-MSCs are a significant component of BME and an altered AML-MSC's functionality could eventually lead to disruption of the balanced HSC niche, these results will provide further knowledge of the AML context. Future studies can use the data of this study to help in the discovery of new prognostic as well as therapeutic targets that could prevent AML relapse. The results of chapters 4 and 5 provide an in vitro CD248 KD model using primary cells, HD-MSCs. This model could also be used in future investigations to explore the exact mechanism behind the role of CD248 in adipogenesis; thus, it would help understand its role in BME. Moreover, the in vitro model of CD248 in this study could be used to investigate intracellular mechanisms through which CD248 signals within MSCs since the intracellular mechanisms are unclear. Thus, the study data add to the MSC's/ISCT community since it aids in understanding CD248 significance on MSC's behavior and functionality.

CHAPTER 2

Materials and Methods

2.1 Sample size and heterogeneity

Twenty-nine AML-MSCs samples were obtained from Dr. Menendez, a collaborator from Joseph Carreras Leukemia Research Institute, School of Medicine University of Barcelona, Spain. Those 29 samples were among the 46 patients' derived MSCs previously used by Guardia et.al (184). MSCs vials were received in dry ice and stored in liquid nitrogen till used for RNA sequencing analysis. These AML-MSCs were previously fully characterized by the collaborator as bone marrow MSCs (BM-MSCs) following ISCT characterization. Samples were obtained from patients of both gender; female (n=12) and male (n=17). Those patients belong to several age groups infant, youth, and old (8 months to 80 years). These AML-MSCs were derived from AML patients cytogenetically varied and clinically characterized in three risk groups/AML subtypes; high HR (n= 11), intermediate IR (n=8), and low LR (n=10) risk. Each subtype displays designated molecular features according to AML characterization systems (LR-AML displaying favorable cytogenetics/ molecular features), (IR-AML exhibit normal karyotype and lack FLT3, C/EBPα, and NPM mutations), and (HR-AML showing unfavorable cytogenetics/ molecular features). For control samples, MSCs from eight healthy donors (HD-MSCs), male (n=7), and female (n=1), previously used and described (215, 216), were used. Complete demographical information of AML-MSCs and HD-MSCs are shown in Table 3.1 and Table 3.2

2.2 Culturing AML-MSCs and HD-MSCs for RNA sequencing

HD-MSCs (n=8) and AML-MSCs (n=29) were thawed, suspended, and cultured in AML complete media. This complete media consisted of advanced DMEM (Cat# 12491-015, Gibco) that contains 20% fetal bovine serum, FBS

(Cat#F1051, Sigma). In addition to FBS, the media was supplemented with L-Glutamine (200Mm) to final concentration of 2mM (Cat#7100, Stem cell), Penicillin/streptomycin final concentration of 1% (Cat#15140122, Gibco), Amphotericin B (250µg/ml) final concentration of 0.20% (Cat# 15290018, Gibco) and plasmocin (2.5 mg/ml) to final concentration of 0.02% (Cat#ant-mmp, InvivoGen). Cells suspension was centrifuged at 1200xg for 8 minutes at room temperature. Cell's pellet was re-suspended in 1mL of AML complete media and counted using Trypan blue stain 0.4 % (Cat#T10282, Invitrogen) and Countess Cell counter. Then MSCs were seeded at 2.5-3 $\times 10^5$ cells/cm2 in T-75 or T-175 cm2 plastic tissue-culture treated flasks and incubated at 37°C and 5%CO2. Cells were checked for growth and confluence every 2-3 days, and media was replaced with fresh AML complete media when needed.

2.3 Harvesting AML-MSCs and HD-MSCs for RNA isolation

When MSCs (AML-MSCs and HD-MSCs) reached 80%-90% confluence, media was removed, and 5mL or 7mL, per T-75,T-175 flask respectively, of 0.25% Trypsin/EDTA (Cat#25200072, Gibco) was added, then cells were incubated for 5 minutes at 37°C, 5% CO2. After five minutes, 5 - 7mL of FBS (Cat#F1051, Sigma) was added to neutralize the trypsin activity. MSCs were then harvested and centrifuged at 1200xg for 8 minutes at room temperature. 1-2mL of ice-cold D-PBS (Cat # 14190-144, Life Technologies) was added to suspend cell pellets. Tubes were placed on ice, and cell viability and count were checked using Trypan blue stain 0.4 % (Cat#T10282, Invitrogen) and Countess Cell counter. After determining their viabilities, cell pellets were stored at -80°C for RNA isolation.

2.4 RNA Extraction and isolation

RNAs from MSCs (AML (n=29) and HD (n=8)) frozen pellets were isolated using mirVana miRNA isolation kit (Cat#, AM1560, ThermoFisher). As per the manufacturer's protocol, frozen cell pellets were taken from - 80°C and quickly placed on ice. Then 600µl of lysis buffer was added to cell pellets, mixed well by pipetting up and down, and cell suspensions were transferred to a new labeled tube. 1:10 volume of miRNA homogenate additive were added to the lysate while on ice, mixed, and incubated on ice for 10 minutes. Then, an equal volume of chloroform (Cat#CX10541, Millipore) was added to the lysate (600µL of lysate + 600µL of chloroform), mixed gently, vortexed for 45 seconds, then centrifuged for 5 minutes at 10,000xg, room temperature, to separate the aqueous from the organic phase. When centrifugation was over, the upper layer was removed carefully (aqueous layer: RNA-containing phase) from the tube without touching and disturbing the bottom layer, and volume was measured and transferred to a new tube. At room temperature, 1.25 volume of 100% ethanol (Cat#P006EAAN, Commercial Alcohols) was added to the RNA-containing layer, mixed, and transferred to a collection tube, centrifuged for 5-10 seconds at 10,000xg. The filtrate was discarded while the filter was washed twice with 500-700µL of washing solutions centrifuged for 5-10 seconds at 10,000xg. Additional centrifugation was performed to remove any remaining liquids bound to the filter and placed into a new collection tube. 100µL of preheated (95°C) elution solution was added to the filter's center, and the tube was spun for 30 seconds at maximum speed. After spinning, the filter was discarded, and elution was collected. Then nucleic acid concentration and purity were measured and assessed by Nanodrop using 1-2µL of each sample.

2.5 TURBO DNase

Isolated RNA was treated to ensure purification and removal of DNA contaminations using a TURBO DNA-free kit (Cat#AM1907, Life Technologies). Samples were placed on ice, 10µL of 10X buffer and 2-3uL of Turbo-DNase were added to each sample, vortexed, transferred to PCR tubes, and incubated for 1 hour in a thermocycler at 37°C. After incubation, a 0.2 volume of inactivation reagent was added to each sample to stop the enzyme activity, and samples were incubated for 5 minutes at room temperature. The tubes were occasionally mixed up and down during incubation, then centrifuged for 1 minute at 10000xg. Supernatants were then collected on ice, and RNA concentration was measured and assessed by Nanodrop using 1-2µL of each sample. 50µL of each sample was used for further purification through ethanol precipitation, while the remaining sample volume was frozen at -80°C for future use.

2.6 Ethanol precipitation

Ethanol precipitation of total RNA samples was carried out overnight to ensure samples purification. In brief, 0.1 volume of 3M Sodium Acetate pH 5.2 (Cat#R1181, Life Technologies) and 2.5-3 volumes of ice-cold 100% ethanol (Cat#P006EAAN, Commercial Alcohols) were added to 50µL of each RNA sample. Samples were then vortexed, mixed thoroughly, and precipitated overnight at -20°C. Samples the next day were centrifuged at 16,435xg for 30 minutes at 4°C. RNA pellets were then washed with 0.5 mL of ice-cold 75% ethanol and spun at 16,435xg for 10 minutes at 4°C. To ensure complete removal of ethanol trace, samples were spun for 10 seconds at room temperature. RNAs were then air-dried for 5-10 minutes at room temperature. Air-dried RNAs were suspended in 50µL of

Nuclease-free water (Cat # 10977015, Life Technologies) and incubated for 15 minutes at room temperature for complete solubilisation. Final assessment of RNA purity, 260/280 ≥1.8 and 260/230 ≥ 2.0, and measuring RNA concentration were performed in Nanodrop using 1-2µL of each RNA sample. All RNA samples were kept at -80°C till used for RNA-sequencing.

2.7 Determination of RNA Integrity Number (RIN)

Checking RNAs purity and measuring RNAs concentrations was performed three times throughout the isolation process, as seen above. Moreover, prior to RNA sequencing, the RNA integrity was assessed using Agilent RNA Screen Tape System (Agilent Technologies, Germany) to determine the RNA integrity number of each sample. The RNA integrity number (RIN) is an algorithmic-based measurement tool that assesses the integrity of RNA based on the electrophoretic ratio of rRNA 28S and 18S. RIN values should range from 1 to 10; the highest the RIN, the less degraded the RNA. Samples for RIN analysis were prepared following the Agilent RNA Screen Tape System manufacturer's instructions. Analysis was performed at the RNA sequencing facility using Tape Station Analysis Software. High-quality RNAs, RIN ≥7.0, were obtained from all samples; therefore, RNAs from all MSCs cultures (AML-MSCs (n=29) and HD-MSCs (n=8)) were used for RNA sequencing.

2.8 RNA-Sequencing

Total RNA samples were 1:5 diluted in RNAse-free H2O. A volume containing 75ng of each sample was brought up to 15µL by RNAse-free H2O for NeoPrep PCR strips. 1.5µl of the diluted sample was used for analysis in bioanalyzer strips prior to RNA sequencing, while 1µg of total RNA was used in 7µl of H2O for small RNA testing. However, RNA samples were not analyzed for miRNAs. All RNA samples

were transferred on ice to the RNA sequencing facility at Dr.Yolk's laboratory in Environmental health Canada, Ottawa, Canada. NeoPrep PCR Illumina RNA-sequencing was performed with an average of 40 million read alignment and the use of a poly-A tail sequencing and 75 base pair, with the reference of human genome version 8.6 by Ensemble Sequence Alignment. Significance in gene expression was determined by adjusted p-value < 0.05 between the two groups, AML/HD.

2.9 *In silico* analysis of statistically differentially regulated genes in AML/HD-MSCs

RNA sequencing data of gene expression profiles of average AML/HD-MSCs was used to perform an in silico analysis. The analysis was carried out using IPA (IPA, Qiagen), which collects and compares the interactions between statistically differentially regulated gene, SDRG, with all available and relative molecules in the ingenuity database. A similar analysis was performed within each AML subtype and HD-MSCs. In brief, Comparison analysis was performed on the dataset to determine significant differences using the comparison analysis tool. Statistically expressed genes were determined by a fold-change parameter of 1.5 in addition to the applied 0.05 adjusted p-value. The findings that were only associated with the human species, and mesenchymal stem/stromal cells were selected. The pathway tool was used to determine the top 5 canonical pathways associated with the SDRGs. The disease and function tool was used to identify associated networks and explore possible connections and interactions between those significantly altered genes. In addition, the bio-profile tool was used to generate and obtain a bio profile of these SDRGs.

2.10 qRT-PCR Validation of SDRGs

RNAs from HR AML-MSCs (n=11) were used to validate GREM1 and SCUBE3 dysregulated expressions using qRT-PCR. IScript Reverse Transcription Supermix (Cat# 1708840, BioRad) was used for cDNA synthesis. As per manufacturer protocol, 1µg of each RNA sample, in a total volume of 5-8µL, was added to 8µL of nuclease-free H2O. Reaction cycles were set as follows: priming for 5 minutes at 25°C, then reverse transcription for 20 minutes at 46°C, followed by 1 minute at 95°C for RT inactivation. After that, SsoAdvanced Universal SYBR Green Supermix (Cat# 1725270, BioRad) was used to perform the PCR reaction following manufacturer protocol. Primer and template of the reference gene, GAPDH (Cat#10025716, Cat#10025636, Bio-Rad), SCUBE3 (Cat#272415539, Cat#229760580, BioRad), and GREM1 (Cat#236264692, Cat#229760581, BioRad) were used to generate standard curves. Reactions were carried out in PCR instrument CFX96 (BioRad), and relative gene expression data were analyzed by CFX Maestro version 1.1(BioRad). Details about the used templates and primers can be seen in table S2.

2.11 Culturing MSCs in RoosterBio complete media

MSCs (AML-MSCs and HD-MSCs) were thawed, and 5-10mL of RoosterBio complete media; Rooster Basal MSC media (Cat# SU-022, RoosterBio) supplemented with RoosterBio supplement (Cat# SU-003, RoosterBio) was added to thawed cells. Cells were centrifuged at 200xg for 8-10 minutes, and pellets were suspended in 1mL of RoosterBio complete media and counted. Viability was determined by Trypan blue stain 0.4 % (Cat#T10282, Invitrogen) using Countess

Cell counter. Cells were then seeded at 2.5 -3×105cells in T-75, or T-175 plastic tissue-culture treated flasks. Cultures were incubated and maintained at 37°C and 5% CO2.

2.12 Generation of MSCs lysates and determination of protein concentration

MSCs lysates were generated for western blot analysis. In brief, cells were cultured in AML or RoosterBio complete media in 6-well plates or T-75 flasks. Cell pellets were washed twice with 5mL of ice-cold D-PBS (Cat # 14190-144, Life Technologies). D-PBS was aspirated, 5-10mL/ flask of ice-cold PBS was added, and cells in flasks were scraped on ice with cells scrapers. Scraped cells were collected and centrifuged for 10 minutes at 800xg and 4°C. After centrifugation, cell pellets were washed with 2-10mL of ice-cold PBS for the second time and centrifuged at 800xg for 8 minutes at 4°C. Then, cells pellets were lysed while on ice in RIPA Buffer (1X) (Cat# PI8990, Pierce) supplemented with protease inhibitor, 10µl/mL of buffer (Cat#1861281, Pierce). For MSCs cultured in 6-well plates, cells were washed twice with ice-cold PBS on ice. RIPA Buffer supplemented with protease inhibiter was added directly to each well (120-250µL/well); cells then were scraped gently on ice with cell scrapers and collected in LoBind protein tubes. Lysates were incubated in a shaker for 30 minutes at 4°C to ensure complete lysing. After incubation, cell lysates were sonicated at an amplitude of 30% for 10 seconds three times with 30 seconds intervals in between using a sonication instrument. Lysates were kept on ice between sonication cycles and cleared by centrifugation for 5 minutes at 14000xg at 4°C. Supernatants were collected in LoBind tubes and kept at -20°C for same or next day use while kept at -80°C for long-term storage. Determination of

protein concentration of cell lysates was performed using the Bicinchoninic acid assay (BCA) kit (Cat#PI23227, Pierce).

2.13 Western Blot

MSCs (HR AML-MSCs and HD-MSCs) lysates generated and stored at -20°C or -80°C were thawed and used for western blot analysis. To prepare these lysates for WB analysis, the required concentration of protein of each Lysate (total volume ≤26µL) was mixed with 4µL of sample reducing reagent (Cat# B0009, Life Technologies) and 10µL of protein loading buffer (Cat#928-40004, Li-Cor) prior to 5 minutes of boiling. Boiled samples were separated by SDS-PAGE (Bolt 4-12% BisTris Plus Gels, 1.00 mm x 12 wells, Invitrogen). The electrophoresis was adjusted to 200V for 30-35 minutes for the separation step. For the transferring step, protein was transferred to the Immboilin-FL membrane for an hour at 20V. After that, the membrane was blocked in iBind Flex solution (Cat# SLF 2019, Invitrogen) for 1 hour, then incubated overnight with a specific primary antibody diluted in iBind solution and fluorochrome-conjugated secondary antibody using the iBind device (ThermoFisher). The next day, the membrane was washed and imaged on Odyssey infra-red instrument (LI-COR Biosciences). Membranes were stripped using stripping buffer (Cat# 928-40032, Li-Cor), washed with PBS, and re-blocked in an iBind solution for 1 hour. Similar to initial staining, incubated overnight with primary antibody against reference gene. For total protein stain, the membrane was stained using revert total protein stain (Cat# 926-11010, Li-Cor). Target band signals were detected in Odyssey infra-red instrument at channel 800, while total protein signals were detected and quantified at channel 700. Antibodies that were used for western blot analysis are listed in table S3.

2.14 CD248 siRNA Knockdown

Healthy MSCs (sample HD2-55RB) were transfected with either CD248 Silencer Select siRNA (Cat#4392420, Ambion) or with scrambled, negative control siRNA (Cat# 4390843, Ambion) to silence the expression of CD248 using TransIT-X2 transfection reagent (Cat#MIR6000, Mirus). The transfection was optimized and carried out in a 6-well plate or T-75 flasks. Cells seeded at $10x10^5$ cells/well, $3.7x10^5$/flask in RoosterBio complete media and incubated at 37°C, 5%CO2, for two days. When cells reached ≤ 80 %, media was removed before transfection, and cells were washed twice with 2-5mL of (Cat # 14190-144, Life Technologies). Then low serum Opti-MEM media (X1)(Gibco) was added, 16mL/flask and 2.5mL/well. Transfection complexes were made in Opti-MEM following TransIT-X2 manufacturer protocol. Cells were transfected with siRNA (10μM stock, final concentration of 25nM) and incubated at 37°C, 5%CO2 for 4 hours. After 4-hour incubation with transfection complexes, the media was replaced with RoosterBio complete media, and cells were maintained for 72 hours at 37°C, 5% CO2 before conducting any downstream analysis. Functional assays were performed after ensuring the high efficiency of the established knockdown protocol.

2.15 Determination of MSCs CD248 expression by Flow Cytometry

To assess the expression of CD248 on HD-MSCs, and AML-MSCs, and validate CD248 knockdown, MSCs, transfected and un-transfected, were harvested and suspended in flow buffer, D-PBS (Cat # 14190-144, Life Technologies) + 2% FBS (ThermoFisher). Cell counts were determined using trypan blue and Countess Cell counter. Prior to staining, cells suspensions were filtered through a 70μm cell strainer. $0.2\ x10^6$ cells/100μL from each condition were stained with either CD248

antibody conjugated to Alexa flour 647 (1µg/µL) (Endosialin/CD248- Mouse Anti-Human, Alexa Fluor 647(Cat#564994, BD Pharmingen) or IgG isotype control (IgG1k Isotype Control-Mouse- AlexaFluor 647, Cat#557714, BD Biosciences). 1mL of Live/dead stain (Cat# L34961) was added to determine live cells. Stained and unstained cells were incubated for 30 minutes at 4°C, washed twice with 1mL of flow buffer, and centrifuged for 6 minutes at 4°C. Washed cells were re-suspended in 300-500µL of flow buffer and kept at 4° C till analysis. Samples were assessed by the flow cytometry facility at Health Canada using the LSRII instrument (BD Bioscience). Then, data were analyzed by FlowJo software version 10 (BD Biosciences).

2.16 MSCs differentiation Assays

siCD248-Treated, siNegScr-Treated, and UT HD-MSCs (HD2-55RB) were assessed for MSCs differentiation potentials, adipogenic and osteogenic differentiation. Cells were seeded in 6-well plates at a seeding density of $1x10^5$/well and cultured for two days in 3mL/well of RoosterBio complete media; Rooster Basal MSC media (Cat#SU-022, RoosterBio) supplemented with RoosterBooster MSC (Cat#SU-003). At 80% confluence, cells were transfected with CD248 siRNA or negative control siRNA as per the CD248 siRNA knockdown protocol. After 4-hour incubation with transfection complexes, RoosterBio complete media was replaced with 2.5mL/well of base differentiation media (StemXVivo Osteogenic/Adipogenic Base Media, Cat#CCM007, R&D), supplemented with adipogenic supplement (StemXVivo Adipogenic Supplement (100X), Cat#CCM011, R&D), to induce MSCs adipogenic differentiation. While media was changed to base media supplemented with osteogenic supplement (StemXVivo Osteogenic Supplement (20X), Cat #

CCM008, R&D) to induce MSCs osteogenesis. After media change, cells were re-incubated and maintained at 37°C, %5 CO2. Media was replaced with fresh base differentiation supplemented media every three days for 14-21 days; throughout the differentiation, cultures were maintained at 37°C. Fixation and chemical staining was used in order to assess MSCs differentiation qualitatively. Differentiated and undifferentiated MSCs were fixed in 1.5-2mL/well of 4% paraformaldehyde (Cat#15710, Electron Microscopy Sciences) and stained with Alizarin S 2% solution(Cat#26206-01, Electron Microscopy Sciences) for mature osteoblast or Oil Red O stain (Cat# 26503-02, Electron Microscopy Sciences) for adipocytes. Fixation and staining were performed following our lab standard staining protocol (LOP #04-009 Chemical Staining for Human Bone Marrow MSC Differentiation Assays) based on manufacturer protocol for MSC's functional Identification Kit (Cat# SC006, R&D). Lipid vacuoles and mineral deposits were examined and visualized by bright field microscopy.

2.17 RNA isolation for Adipogenesis qRT-PCR Assay

Differentiated siCD248-Treated, siNegScr-Treated, and differentiated control UT HD-MSCs (HD2-55RB), were treated with Trizol reagent (Cat#15596026, Invitrogen) 500µL/well to extract their total RNA using phasemaker tubes (Cat#A33248, Invitrogen) as per their manufacturer protocol. DNA digestion (Cat#M0303S, NEB) and ethanol precipitation were performed in RNA samples to ensure high purification of the extracted RNAs. RNA purity and concentration were detected by Nanodrop using 1-2µL of each RNA sample. Only RNA with 260/230 ≥ 1.85 ratios and 260/280 ≥1.8 were used. 1µg of each RNA sample was used for reverse transcription, and reactions were carried out using the IScript Reverse

Transcription Supermix kit (Cat# 1708840, BioRad). RT-PCR was conducted in a 96-well plate using Adipogenesis predesigned PrimePCR assay 96-well plate. (Cat# 14952688, BioRad). Samples for the assay were prepared with SsoAdvanced Universal SYBR Green Supermix kit (Cat# 1725270, BioRad), and the thermocycler was programmed following the kit's manufacturer protocol. Relative gene expression data were analyzed using CFX Maestro software version 1.1(BioRad). Gene expression was calculated by △△Cq. Gene expressions of siNeg-Treated MSCs were used as a control to compare the expression of all amplified adipogenesis genes in siCD248-treated and UT cells.

2.18 In *silico* analysis of adipogenesis pathway

qRT-PCR results of adipogenic-differentiated siCD248-Treated HD-MSCs, HD2-55RB, gene expressions were applied to the adipogenesis pathway through IPA, ingenuity pathway analysis(IPA, Qiagen). The classical adipogenesis pathway was obtained through the pathway analysis tool. Then, siCD248-treated altered gene expression of the SIRT2 gene was added to the pathway through add molecule tool, and the SIRT2 gene was upregulated to modulate its expression in siCD248-treated MSCs. The prediction was turned on to predict the effect of the altered expression of the molecule and explore the relationship between their dysregulated levels in adipogenic-differentiated siCD248-treated MSCs with MSCs adipogenesis pathway in physiological status.

2.19 Protein Profiler Array

Lysates of siCD248-Treated, siNegScr-Treated, and UT MSCs (HD-55RB) were generated, and their protein concentration was determined as described earlier. Proteome Profiler Array (Human Angiogenesis Array kit, Cat#ARY007, R&D)

consisted of 55 specific antibodies against 55 proteins. Each membrane has the 55 antibodies spotted in duplicate. 300µg of protein from each lysate was used in an array membrane. A membrane was used for each sample of the three transfection conditions. Following the manufacturer protocol with modifications, samples were separately incubated with an antibodies cocktail, and membranes were blocked with a blocking buffer. Samples were incubated with antibodies for 30 minutes at room temperature. Membranes were blocked for 1 hour. After 1-hour incubation, samples were added to the membranes and re-incubated in a shaker overnight at 4°C. Prior to staining, membranes were washed three times with washing buffer for 10 minutes the next day. Then, a 1:2000 dilution of Streptavidin (IRDye 800CW Streptavidin, Cat#92632230, LiCor) was prepared and added to each well where the washed membrane was then placed. Membranes were incubated in a rocker for 30 minutes at room temperature. After incubation with Streptavidin, membranes were washed three times with the washing buffer, and images were taken. Images were collected using Odyssey infra-red instrument; a resolution of 84 µm and image quality was set to Medium. Proteins signals were detected at both 700 and 800 channels; a grid analysis was designed for each membrane and applied, and signals at channel 800 were calculated, averaged, and normalized to negative signals at channel 700.

2.20 HL60 co-culture and viability determination

In order to examine the effects of siCD248-Treated and UT HD-MSCs on HL60 proliferation, HL60-MSCs co-culture experiments were conducted. HD-MSCs, HD2-55RB, were seeded at $1x10^5$/well in a 6-well plate and cultured in RoosterBio complete media for two days. At 80% confluence, MSCs were transfected with either siRNA CD248 or negative control siRNA as per established knockdown protocol and

incubated at 37°C, 5%CO2. Prior to co-culture experiments, HL60 (Cat#ATCC-CCL240) were thawed and seeded in T-75 flasks to grow and recover in IMDM (Cat#ATCC30-2005) media supplemented with 20% FBS (Cat#16000044). 24 hours post-transfection, MSCs were used as a feeder layer, HL60 were collected from the flasks, suspended in RoosterBio media, counted, and added to MSCs plates to each well $4x10^4$ /well of each condition of the three transfection condition, transfected and un-transfected HD-MSCs. Cells on the co-cultured plates were maintained with RoosterBio complete media 2.5-3mL/well for five days at 37°C. After 24 hours of co-culturing, HL60 viabilities were determined daily throughout the 5-day co-culture experiment. Each day, HL60 cells were collected from each well, suspended in 1mL of RoosterBio complete media, and counted using trypan blue and Countess Cell counter. Cells' morphology was visualized throughout the 5-day co-culture experiment using bright field microscopy. MSCs from each corresponding plate/day were lysed, and cell lysates were generated.

2. 21 Flow cytometry determination of CD45+

On day 5 of the MSCs-HL60 co-culture experiment, HL60 cells were collected, counted, and stained for Flow cytometry analysis. In brief, cells were washed and suspended in flow buffer (D-PBS + 2% FBS). Prior to staining, suspended cells were filtered through a 70µm cell strainer. HL60 cells from each co-culture condition, and HL60 cultured alone, were stained with either CD45 antibody conjugated to FITC, CD45 Mouse Anti-Human FITC (1µg/µL)(Cat#555482, BD Pharmingen) or Isotype control, IgG1k Isotype - Mouse – FITC, (Cat# 555748, BD Pharmingen). 1mL of Live/dead stain (Cat# L34961, Company) was added to each tube to determine live cells. Stained and unstained cells were incubated for 30

minutes at 4°C, washed twice with 1mL of flow buffer, and centrifuged at X for 6 minutes at 4°C. Cell pellets were then re-suspended in 300-500µL of flow buffer and kept at 4° C till analysis. Samples were assessed by the Health Canada flow cytometry facility using the LSRII instrument (BD Bioscience). Then data were analyzed using FlowJo software version 10 (BD Biosciences).

2. 22 Statistical analysis

Data obtained from replicates within each independent experiment were considered technical replicates of that experiment, and >3 independent experiments were performed unless specified. Data obtained from multiple AML-MSCs samples or HD-MSCs considered biological replicates. For CD248 knockdown, each independent experiment, with 2-3 replicates, was conducted using new cell vials of HD-MSCs (HD2-55RB) to establish new culture and transfection each time. To perform any given experiment and generation of lysates for an assay, new transfection was performed, and lysates were freshly generated and assessed for any given experiment. AML-MSCs expression, gene, and protein were normalized to their healthy counterparts, HD-MSCs expression. Transfected HD-MSCs, were normalized to siRNA negative control-treated HD-MSCs and untreated HD-MSCs. Data of < 2 experiments of a given functional assay were not statistically analyzed. For statistical analysis, GraphPad Prism 7 software (GraphPad Software, LA Jolla, CA, USA) was used, and a p-value of < 0.05 determined the significance of the data. An unpaired T-test was used when two groups with one variable were compared. Grouped analysis using FDR method of Benjamini and Hochberg (Q = 1%) was used for multiple comparisons, for the protein profile analysis of protein microarray data (n=3).

CHAPTER 3

Comparison of MSCs from AML patients and healthy donors

3.1. RNA sequencing of MSCs derived from patients suffering from various AML subtypes (AML-MSC) showed an altered gene expression profile in comparison to those derived from healthy donors (HD-MSCs)

A full transcriptomic analysis was conducted to understand the possible mechanisms and genes behind the previously observed functional impairments of AML-MSCs. Specifically, RNA sequencing was performed to compare the gene expression levels in AML-MSCs against the mean levels of gene expressions from HD-MSC controls.

As AML is a heterogeneous hematological malignancy, its heterogeneity is a key challenge in understanding its pathogenesis. A large cohort was used here to better represent the disease and cover its subtypes. Twenty-nine clinically and cytogenetically varied AML-MSCs samples were used. These samples belonged to AML patients of several age groups and both sex, and they were characterized by AML subtypes (LR (n=10), IR (n=8), HR (n=11)). In addition to AML-MSCs, HD-MSCs (n=8) were used as controls. All of these HD-MSCs and AML-MSCs' samples were previously fully characterized and found to meet the standard ISCT criteria defining human bone-marrow MSCs (hBMMSCs). AML-MSCs were characterized and obtained from Guardia et al. (184), while HD-MSCs were obtained and fully characterized by our stem-cell-based therapeutics laboratory as previously described (215,216). (Demographical information of AML-MSC and HD-MSCs can be found in tables 3.1 and 3.2, respectively).

Sample ID	Age (y)	Sex	Diagnostic	Cytogenetics	Molecular	Blasts (%)	Risk
hBMMSC14004	4	F	AML-M2	46,XX t(8;21) AML1-ETO	FLT3-ITD	40	H
hBMMSC-14008	10	M	AML	46,XY	Ø	92	I
hBMMSC-14009	20	M	AML-M4	46,XY, inv(16)	46,XY, inv(16)	56	L
hBMMSC-14011	8 mo	M	AML-M5	46, XY, inv(16) (p13.1q22)	Cbfb-MYH11	50	L
hBMMSC-14012	48	F	AML-M5	46,XX,t(11;19) (q23;p13)	MLL-ENL	77	H
hBMMSC-14013	44	F	AML-M4	46,XX	FLT3WT, NPM1WT, MLLWT, cEBPaWT	65	I
hBMMSC-14016	35	M	AML	89-92,XY	Ø	80	H
hBMMSC-14018	61	M	AML	46,XY	FLT3WT, NPM1WT, MLLWT, cEBPaWT	1	I
hBMMSC-14022	20	F	AML	46,XX	NPM1MUT, IDH1MUT	92	L
hBMMSC-14030	18	M	AML	46,XY	NPM1MUT	32	L
hBMMSC-14031	52	F	AML	46,XX	FLT3WT, NPM1WT, MLLWT, cEBPaWT	79	I
hBMMSC-14032	80	M	AML	46,XY	NPM1MUT	49	L
hBMMSC-14043	37	F	AML-M4	46,XX	NPM1MUT	80	L
hBMMSC-14048	63	F	AML-M4	46,XX	MLL-AF9	90	H
hBMMSC-14056	77	M	AML-M5	46,XY	NPM1MUT, FLT3del	80	H
hBMMSC-14057	65	F	AML-M5	46,XX	NPM1MUT, FLT3-ITD	90	H
hBMMSC-14059	81	M	AML	46,XY	FLT3WT, NPM1WT, MLLWT, cEBPaWT	35	I
hBMMSC-14067	27	M	AML-M3	46,XY,t(15;17) (q22;q12)[20]	PML-RARa (bcr1)	92	L
hBMMSC-14070	77	F	AML-M1	46,XX	MLL-AF9	80	H
hBMMSC-14074	69	M	AML	46,XY,del(7)(q 22) [13]	Ø	22	H
hBMMSC-14078	53	M	AML	46,XY,-7q	FLT3WT, NPM1WT, MLLWT, cEBPaWT	56	H
hBMMSC-14085	42	M	AML-M4	46,XY	BAALCMUT, WT1MUT, NPM1MUT,FLT3MUT	99	H
hBMMSC-14086	78	F	AML	46,XX	NPM1MUT	67	L
hBMMSC-14088	61	F	AML	47,XX,+8/46,XX	FLT3WT, NPM1WT,	71	I

					MLLWT, cEBPaWT		
hBMMSC-14089	77	M	AML	46,XY	cEBPaMUT	45	I
hBMMSC-14096	25	M	AML-M3	46,XY,t(15;17)	PML-RARa	90	L
hBMMSC-14097	27	M	AML-M3	46,XY,inv(16)	Cbfb-MYH11	40	L
hBMMSC-14101	8	F	AML	46,XX	FLT3MUT	95	H
hBMMSC-14113	56	M	AML	46,XY	FLT3WT, NPM1WT, MLLWT, cEBPaWT	40	I

Table 3.1. Demographics and clinical features of AML patients. AML-MSCs (n=29) information according to their source (184). Abbreviation hBMMSC= human bone-marrow mesenchymal stromal/stem cells, AML=acute myeloid leukemia. M1-M5 AML classification system. Molecular/genetic risk group/AML subtype; H= High, I= Intermediate, and L= low risk according to the genetics classification.

Sample ID	Age (y)	Sex	Diagnostic
hBMMSC-10A	24	M	N/A
hBMMSC-18A	34	F	N/A
hBMMSC-19A	34	M	N/A
hBMMSC-37RB	31-45	M	N/A
hBMMSC-49RB	18-30	M	N/A
hBMMSC-55RB	18-30	M	N/A
hBMMSC-81RB	18-30	M	N/A
hBMMSC-84RB	31-45	M	N/A

Table 3.2. Demographics of healthy donors. HD-MSCs (n=8) information. Abbreviation hBMMSC= human bone-marrow mesenchymal stromal/stem cells, N/A= not applicable. HD-MSCs were purchased and obtained by stem-cell-based therapeutics, Health Canada. When the donor exact age could not be determined, age range was used and confirmed by the source. RB=RoosterBio cells.

Frozen cell vials of these MSCs, from both groups HD and AML, were thawed and cultured in AML complete media to ensure consistency and eliminate variabilities between culture conditions. Cultures were maintained in AML complete media till confluence. Unlike MSCs from healthy donors (HD-MSCs), AML-MSCs grew slower and required more days in culture to reach a relatively high confluence. Similar morphology of spindle-shaped fibroblast was observed for both groups. Then, cultured MSCs were harvested for RNA isolation and total RNA extraction. Isolated RNAs' purity and integrity were assessed prior to RNA sequencing as described in sections 2.4-2.7 of chapter 2. Since RNA sequencing requires high-quality RNAs and high-quality RNAs with RIN ≥ 7.0 were successfully obtained from all cultured AML-MSCs (n=29) and HD-MSCs (n=8) (Table 3.3), all samples were used in the sequencing. Then, gene profiles of AML-MSCs from all subtypes were compared to HD-MSCs (Figure 3.1).

Results of this unbiased transcriptomic analysis of AML-MSCs and HD-MSCs showed that AML-MSCs have an altered gene expression profile. In particular, when a cut-off adjusted p-value of ≤ 0.05 was applied, among 7565 common genes between the two groups, 30 genes were found to be dysregulated in AML-MSCs compared to HD-MSCs. Out of these 30 dysregulated genes, 18 genes were upregulated, and 12 genes were downregulated in AML/HD. These 30 genes are shown in the heat map (Figure 3.2). This hierarchal cluster was generated to show expression values as a raw-scaled log of fragments per kilobase. Additionally, when the transcriptomic analysis was performed between AML subtypes HR, IR and LR no significant differences were found within AML groups. Moreover, no significant

differences within age groups nor between sexes, male versus female were found in AML-MSCs /HD-MSCs. As seen above, our transcriptomic analysis showed that the AML-MSCs group (including MSCs from all AML subtypes IL, LR, and HR) had an altered genetic profile compared to HD-MSCs. Availabilities of healthy donor samples derived from other age groups (children and old) was a limitation of the transcriptomic analysis between AML-MSCs and HD-MSCs based on age.

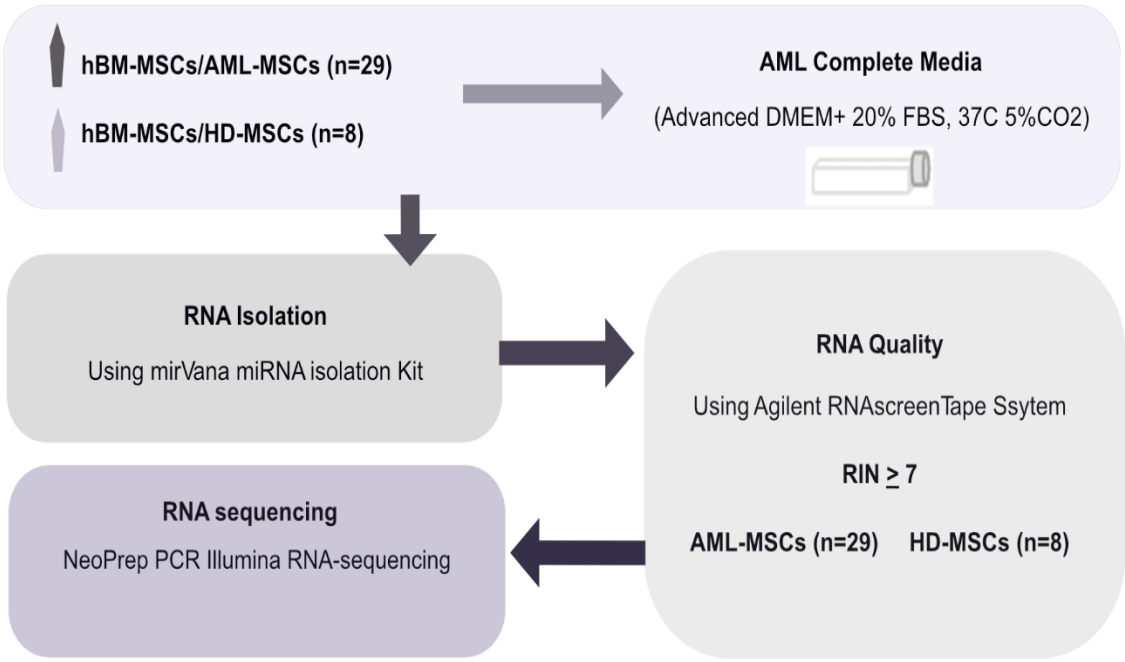

Figure 3.1. Schematic workflow outline for transcriptomic analysis of AML-MSCs in comparison to HD-MSCs. Process for sample preparation prior to performing the RNA-sequencing. Frozen MSCs from 29 AML patients' bone marrow aspirates ((AML-MSCs (n=29)) were obtained from Guardia et al. (Joseph Carreras Leukemia Research Institute, Spain) and kept in liquid nitrogen till used. HD-MSCs (n=8) were characterized in the stem cell-based therapeutics laboratory (Health Canada). All MSCs then were cultured (passage 2-5) in AML complete media till confluent. Cells were then harvested for RNA isolation using the mirVana kit. RNAs quality was checked. Samples with RIN ≥ 7 were used for RNA-sequencing analysis to identify significant gene differences between AML-MSCs and HD-MSCs. Abbreviations: hBM-MSCs: human bone-marrow mesenchymal stromal/stem cells. AML: acute myeloid leukemia, HD: healthy donor. A detailed description of the procedures of these experiments is available in chapter 2.

	Sample ID	RIN		Sample ID	RIN
AML-MSCs	hBMMSC-14004	7.4	AML-MSCs	hBMMSC-14074	8.3
	hBMMSC-14008	8.1		hBMMSC-14078	7.7
	hBMMSC-14009	8.2		hBMMSC-14085	7.8
	hBMMSC-14011	7.9		hBMMSC-14086	7.6
	hBMMSC-14012	7.6		hBMMSC-14088	7.4
	hBMMSC-14013	8		hBMMSC-14089	7.9
	hBMMSC-14016	7.2		hBMMSC-14096	7.6
	hBMMSC-14018	7.9		hBMMSC-14097	7.6
	hBMMSC-14022	8.1		hBMMSC-14101	7.2
	hBMMSC-14030	7.9		hBMMSC-14113	8
	hBMMSC-14031	7.5	HD-MSCs	hBMMSC-10A	8.3
	hBMMSC-14032	8.3		hBMMSC-18A	7.8
	hBMMSC-14043	7.5		hBMMSC-19A	8.3
	hBMMSC-14048	7.9		hBMMSC-37RB	8.1
	hBMMSC-14056	7.8		hBMMSC-49RB	7.4
	hBMMSC-14057	7.6		hBMMSC-55RB	8.3
	hBMMSC-14059	7.9		hBMMSC-81RB	8.2
	hBMMSC-14067	8		hBMMSC-84RB	7.2
	hBMMSC-14070	8			

Table 3.3. RNA integrity number (RIN) for AML-MSCs (n=29) and HD-MSCs'(n=8) RNAs samples. Assessment of RNA integrity prior to RNA sequencing by determining the RNA integrity numbers (RINs) was performed using Agilent RNA ScreenTape System (Agilent Technologies, Germany)(RNA assessment details are described in chapter 2). All AML-MSCs (n=29) and HD-MSCs (n=8) were used in RNA-sequencing.

Original ID	Simplified ID	Original ID	Simplified ID
hBMMSC-14089	AML-IR1	hBMMSC-14048	HR -AML1
hBMMSC-14088	AML-IR2	hBMMSC-14085	HR-AML2
hBMMSC-14113	AML-IR3	hBMMSC-14056	HR-AML 3
hBMMSC-14031	AML-IR4	hBMMSC-14078	HR -AML4
hBMMSC-14059	AML-IR5	hBMMSC-14074	HR-AML5
hBMMSC-14018	AML-IR6	hBMMSC-14016	HR-AML 6
hBMMSC-14013	AML-IR7	hBMMSC-14057	HR-AML 7
hBMMSC-14008	AML-IR8	hBMMSC-14070	HR-AML 8
hBMMSC-14043	AML-LR1	hBMMSC-14012	HR -AML9
hBMMSC-14022	AML-LR2	hBMMSC-14004	HR-AML 10
hBMMSC-14030	AML-LR3	hBMMSC-14101	HR-AML 11
hBMMSC-14097	AML-LR4	hBMMSC-84RB	HD1-84RB
hBMMSC-14096	AML-LR5	hBMMSC-55RB	HD2-55RB
hBMMSC-14086	AML-LR6	hBMMSC-49RB	HD3-49RB
hBMMSC-14009	AML-LR7	hBMMSC-81RB	HD4-81RB
hBMMSC-14067	AML-LR8	hBMMSC-37RB	HD5-37RB
hBMMSC-14032	AML-LR9	hBMMSC-19A	HD6-19A
hBMMSC-14011	AML-LR10	hBMMSC-10A	HD7-10A
		hBMMSC-18A	HD8-18A

Table 3.4. Simplified IDs of the used AML-MSCs and HD-MSCs as appeared in figure 3.2. Original information is found in Tables 3.1 and 3.2. AML: MSCs derived from AML patients. Risk group; HR, IL. LR. HD: healthy donor.

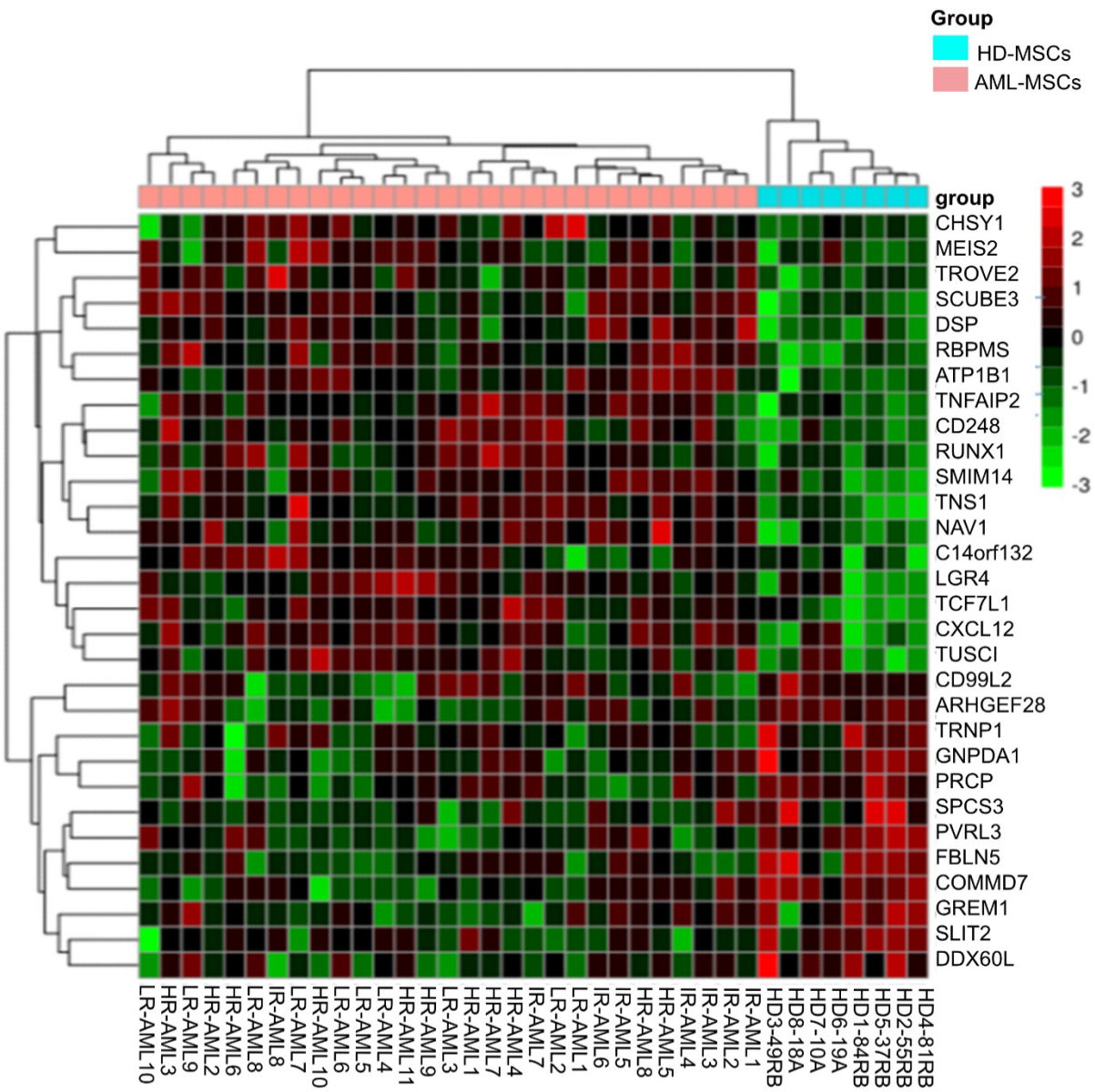

Figure 3.2. Hierarchal cluster analysis of all 30 dysregulated genes in AML-MSCs/HD-MSCs. The heat map shows RNA-seq gene profile data of the 30 (adj.p-value of ≤ 0.05) altered genes between AML-MSCs (group 2 in pink) and HD-MSCs (group 1, in blue). From top to bottom, 18 upregulated genes and 12 downregulated genes. The increase in color intensity represents the degree of upregulation/downregulation on gene expression levels. Sample abbreviation, AML=AML-MSCs, LR=Low risk (n=10), HR=High Risk (n=11), IR=Intermediate risk (n=8), HD=HD-MSCs= control sample (n=8). RB and A represent the hBMMSCs sample suppliers. Original details about samples are found in Table 3.1 and 3.2.

3.2. Twenty-one statistically differentially regulated genes (SDRGs) between AML-MSCs and HD-MSCs

As seen above in section 3.1, the primary analysis of the RNA-seq data that compares the genetic profile of AML-MSCs with HD-MSCs, showed that 30 genes were dysregulated in AML-MSCs (adj p-value < 0.05). An additional restriction was applied using a fold-change (FC) difference to investigate the significance of these 30 genes that were dysregulated in AML-MSCs compared to HD-MSCs. When a cut-off value for a FC difference in gene expression level in AML/HD MSCs of (≤ -1.50 or ≥ 1.50) was applied, a total of 21 genes of the 30 genes (adj p-value of < 0.05) met these cutoff values, and were significantly dysregulated in AML/HD. Therefore, 21 genes were identified as statistically differentially regulated genes (SDRGs) between AML and HD-MSCs (Figure 3.3A). Of the 21 SDRGs, 13 genes were up-regulated in AML-MSCs, while eight were down-regulated in AML/HD-MSCs.

Upregulated genes included TNS1, SCUBE3, ATP1B1, MEIS2, CXCL-12, DSP, TNFAIP2, LGR4, TUSC1, CD248, C14orf132, TCF7L1, and RUNX1 (Figure 3.3B). The change in expression of these 13 upregulated genes ranged from 1.5 to 3.9 FC. RUNX1 was the gene with the lowest significantly upregulated expression level in AML-MSCs with a 1.54 FC which is equal to 0.62 Log2FC with an adj. p-value of 0.002, while SCUBE3 was the gene with the most upregulated expression level in AML-MSCs, it was up-regulated by 3.9 FC which is equal to 1.96 Log2FC with an adj p-value of 0.0007. The expression value of each upregulated gene is shown and described in (Table 3.5/Top).

The downregulated genes included SPCS3, DDX60L, PVRL3, SLIT2, TRNP1, ARHGEF28, FBLN5, and GREM1 (Figure 3.3C). The change in expression of these eight downregulated genes ranged from -1.6 to -4.8 FC. SPCS3 was the gene with the lowest significantly downregulated expression level in AML-MSCs. It was downregulated by 1.6 FC, which is equal to 0.69 Log2FC with an adj. p-value of 0.042, while GREM1 was the gene with the most significant downregulated expression in AML-MSCs; it was down-regulated by 4.89 FC (2.29 Log2FC) with an adj p-value of 0.043. The downregulated expression values of all eight statistically differentially regulated genes in AML-MSCs are shown in (Table 3.5/bottom) (Figure 3.3C).

3.3 In-silico analysis of the SDRGs in AML-MSCs versus HD-MSCs

An in-silico analysis was performed using several analysis tools of the ingenuity pathway analysis system (IPA) on the dataset to gain a better knowledge and understanding of the identified 21-SDRGs in AML/HD. First, a bio-profile for all 21 genes was generated (Table 3.6). The analysis showed that these genes were located in various intracellular and extracellular locations (nucleus, cytoplasm, plasma membrane, and extracellular space), and they were functionally varied and included transcription regulator, transporter, transmembrane receptors, and cytokines (Table 3.6) and (Figure 3.3D).

Secondly, to determine whether these dysregulated genes in AML/HD play a part in a physiological signaling pathway or play a part in a pathological signaling pathway, IPA canonical pathway tool was explicitly used to analyze the dataset. The analysis predicted that those 21 SDRGs were involved in several canonical signaling

pathways. Interestingly, the AML signaling pathway was among the top five canonical pathways (Figure 3.3E); these genes were associated with AML signaling.

Then, the network analysis tool was used to perform network analysis on the transcriptomic dataset to assess the relationship and interactions between the 21 genes that were found and identified as SDRGs in AML/HD-MSCs and to explore any possible link between these 21 genes. The analysis showed that several genes of these 21 SDRGs in AML-MSCs were involved in two main networks of interactions where they indirectly interact with each other (Figure 3.4A and B). Further analysis of these genes using the function tool showed that these genes were involved in many critical cellular processes. Some genes of the 21 SDRGs play a significant role in cellular movement, cell-mediated immune response, hematological system development and function, cell-to-cell signaling, cell interaction, and cellular assembly and organization. Moreover, although some genes were associated separately with differentiation pathways, performing additional analysis using IPA pathway and overlay tools revealed no common MSCs differentiation or metabolic pathway between these altered genes within MSCs.

In addition, The IPA analysis predicted three common miRNA to be possibly associated with many of the dysregulated genes. However, the type/ direction of effect or association is not known. Findings in sections 3.1 and 3.2 of this chapter suggest that the designated alterations in AML-MSCs genetic profiles may be behind the altered AML-MSCs' previously observed functionalities. Furthermore, these genetic alterations could lead to an altered MSCs role and function in BME and consequently result in alterations of BME through which they could contribute to

AML relapse. Additionally, these findings confirmed the available knowledge that AML-MSCs exhibit their unique alterations rather than retaining AML blast mutations.

Upregulated Genes			
Gene Symbol	**Fold-Change (FC)**	**Adjusted p-value**	**Log2 FC**
SCUBE3	3.912063	0.0007801	1.967929604
CXCL12	3.004718	0.0068605	1.587229597
C14orf132	2.271148	0.043066485	1.183421723
TNS1	2.253484	0.000231268	1.172157207
DSP	2.032755	0.009806922	1.023436343
TNFAIP2	2.006981	0.023066416	1.005026959
TCF7L1	1.911159	0.047018994	0.934447809
TUSC1	1.899027	0.036972087	0.925260418
CD248	1.897716	0.037827945	0.924264104
ATP1B1	1.784947	0.001234213	0.835881237
LGR4	1.741113	0.028777353	0.800009838
MEIS2	1.724862	0.005445646	0.786480942
RUNX1	1.544966	0.002581002	0.627575679
Downregulated Genes			
SPCS3	-1.61851	0.042066328	0.694666279
DDX60L	-1.67605	0.02810287	0.745065188
PVRL3	-1.69976	0.043591937	0.765331057
SLIT2	-1.73748	0.03972451	0.796996371
TRNP1	-1.78222	0.043591937	0.833675436
ARHGEF28	-2.19495	0.005611879	1.134188076
FBLN5	-2.70416	2.24E-06	1.435180516
GREM1	-4.89815	0.043591937	2.29223

Table 3.5. Gene expression values of the 21 SDRGs in AML-MSCs/HD-MSCs. Transcriptomic data of the 21 dysregulated genes in AML/HD. Top: 13 significantly upregulated genes in AML/HD-MSCs (adjusted p-value <0.05) and (≥ 1.5 fold-change, FC). Bottom: 8 significantly down-regulated genes in AML/HD-MSCs (adjusted p-value <0.05) and (FC ≤ -1.5).

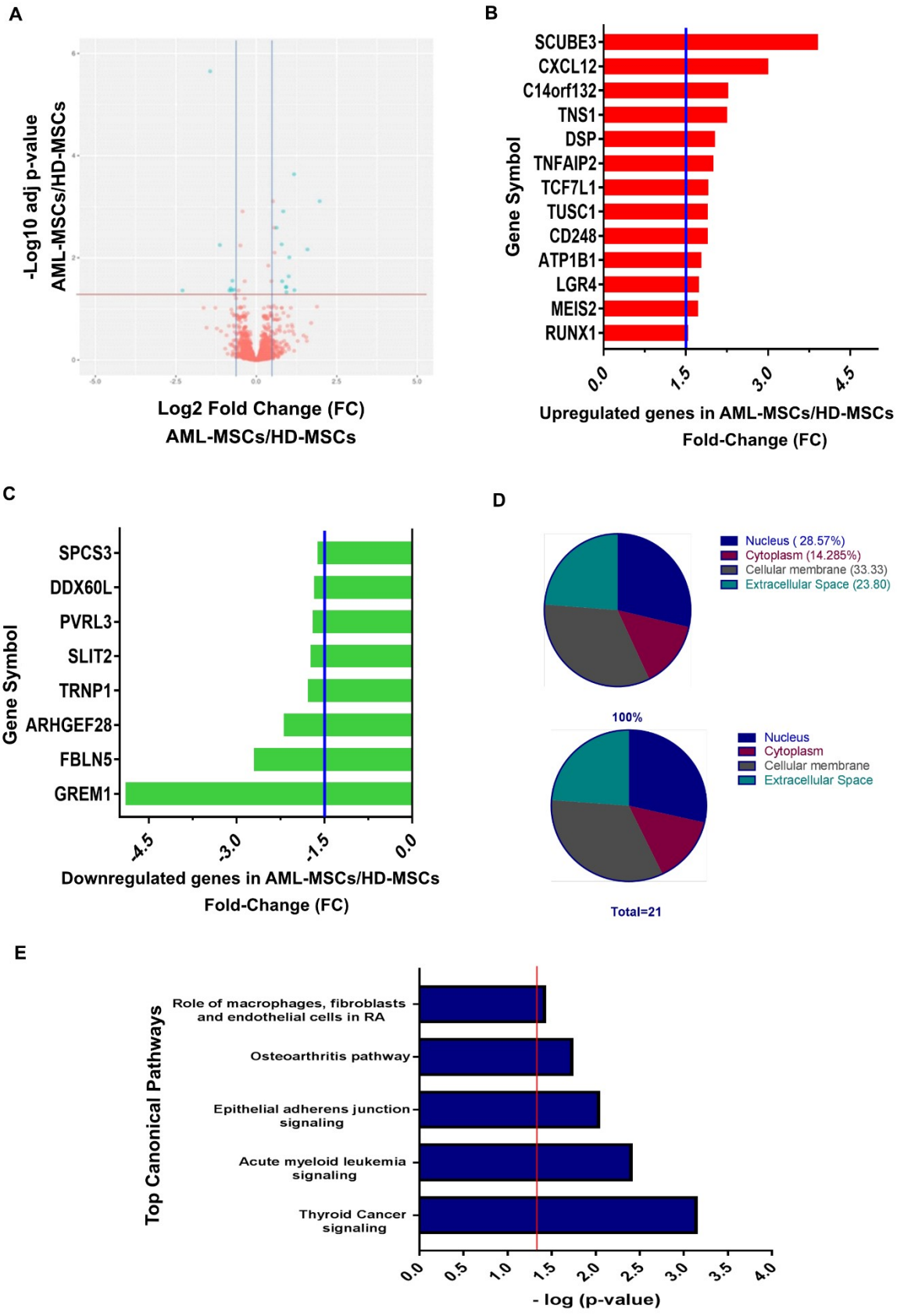
A
-Log10 adj p-value
AML-MSCs/HD-MSCs
Log2 Fold Change (FC)
AML-MSCs/HD-MSCs
B
SCUBE3
CXCL12
C14orf132
TNS1
DSP
TNFAIP2
TCF7L1
TUSC1
CD248
ATP1B1
LGR4
MEIS2
RUNX1
Gene Symbol
0.0
1.5
3.0
4.5
Upregulated genes in AML-MSCs/HD-MSCs
Fold-Change (FC)
C
SPCS3
DDX60L
PVRL3
SLIT2
TRNP1
ARHGEF28
FBLN5
GREM1
Gene Symbol
-4.5
-3.0
-1.5
0.0
Downregulated genes in AML-MSCs/HD-MSCs
Fold-Change (FC)
D
Nucleus (28.57%)
Cytoplasm (14.285%)
Cellular membrane (33.33)
Extracellular Space (23.80)
100%
Nucleus
Cytoplasm
Cellular membrane
Extracellular Space
Total=21
E
Top Canonical Pathways
Role of macrophages, fibroblasts and endothelial cells in RA
Osteoarthritis pathway
Epithelial adherens junction signaling
Acute myeloid leukemia signaling
Thyroid Cancer signaling
0.0
0.5
1.0
1.5
2.0
2.5
3.0
3.5
4.0
- log (p-value)

Figure 3.3. Twenty-one statistically differentially regulated genes (SDRGs) in AML/HD. A) Volcano plot showing the significantly dysregulated 21 genes between AML-MSCs and HD-MSCs out of the 7565 common genes. The blue lines indicate the statistical significance of 1.5 fold-change (=0.584 Log2 FC), and the red line indicates the significant adjusted p-value. Blue dots represent genes with $p < 0.05$ and significant FC < -1.5 or > 1.5 AML/HD. Red dots represent statistically insignificant genes. B) Demonstration of the13 upregulated genes out of the 21 SDRGs in AML/HD by FC (> 1.5 FC) (red). C) Demonstration of the 8 downregulated genes out of the 21 SDRGs in AML/HD (< -1.5 FC) (green). D) Pie charts show the location and distribution of the 21 SDRG within MSCs cellular level. E) Involvement of the 21 SDRGs AML/HD in canonical pathways using the ingenuity pathway analysis (IPA) tool for top canonical pathways.

Symbol	Gene Name	Location	Type
ARHGEF28	Rho guanine nucleotide exchange factor 28	Cytoplasm	other
ATP1B1	ATPase Na+/K+ transporting subunit beta 1	Plasma Membrane	transporter
C14orf132	Chromosome 14 open reading frame 132	Other	other
CD248	CD248 molecule	Plasma Membrane	other
CXCL12	C-X-C motif chemokine ligand 12	Extracellular Space	cytokine
DDX60L	DExD/H-box 60 like	Other	other
DSP	Desmoplakin	Plasma Membrane	other
FBLN5	Fibulin 5	Extracellular Space	other
GREM1	Gremlin 1, DAN family BMP antagonist	Extracellular Space	other
LGR4	Leucine rich repeat containing G protein-coupled receptor 4	Plasma Membrane	transmembrane receptor
MEIS2	Meis homeobox 2	Nucleus	transcription regulator
NECTIN3/PVRL3	Nectin cell adhesion molecule 3	Plasma Membrane	other
RUNX1	Runt related transcription factor 1	Nucleus	transcription regulator
SCUBE3	Signal peptide, CUB domain and EGF like domain containing 3	Plasma Membrane	other
SLIT2	Slit guidance ligand 2	Extracellular Space	other
SPCS3	Signal peptidase complex subunit 3	Cytoplasm	peptidase
TCF7L1	Transcription factor 7 like 1	Nucleus	transcription regulator
TNFAIP2	TNF alpha induced protein 2	Extracellular Space	other
TNS1	Tensin 1	Plasma Membrane	other
TRNP1	TMF1-regulated nuclear protein 1	Nucleus	other
TUSC1	Tumor suppressor candidate 1	Other	other

Table 3.6. Bio-profile of the 21 SDRGs in AML-MSCs/HD-MSCs. IPA bio-profile tool was used on the 21 SDRGs in AML/HD-MSCs to analyze the gene dataset and obtain detailed information about the function and location of these 21 dysregulated genes in AML/HD.

A

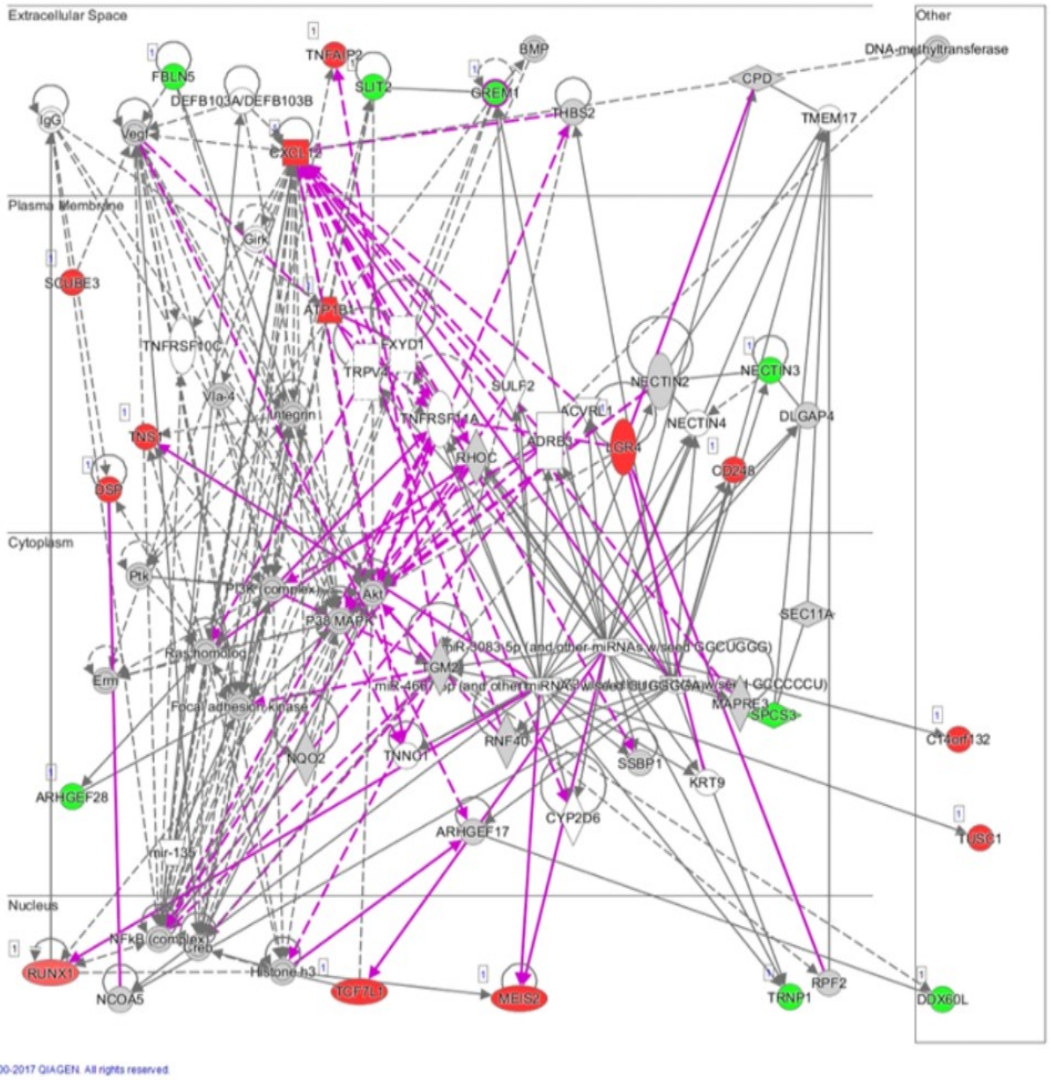

B

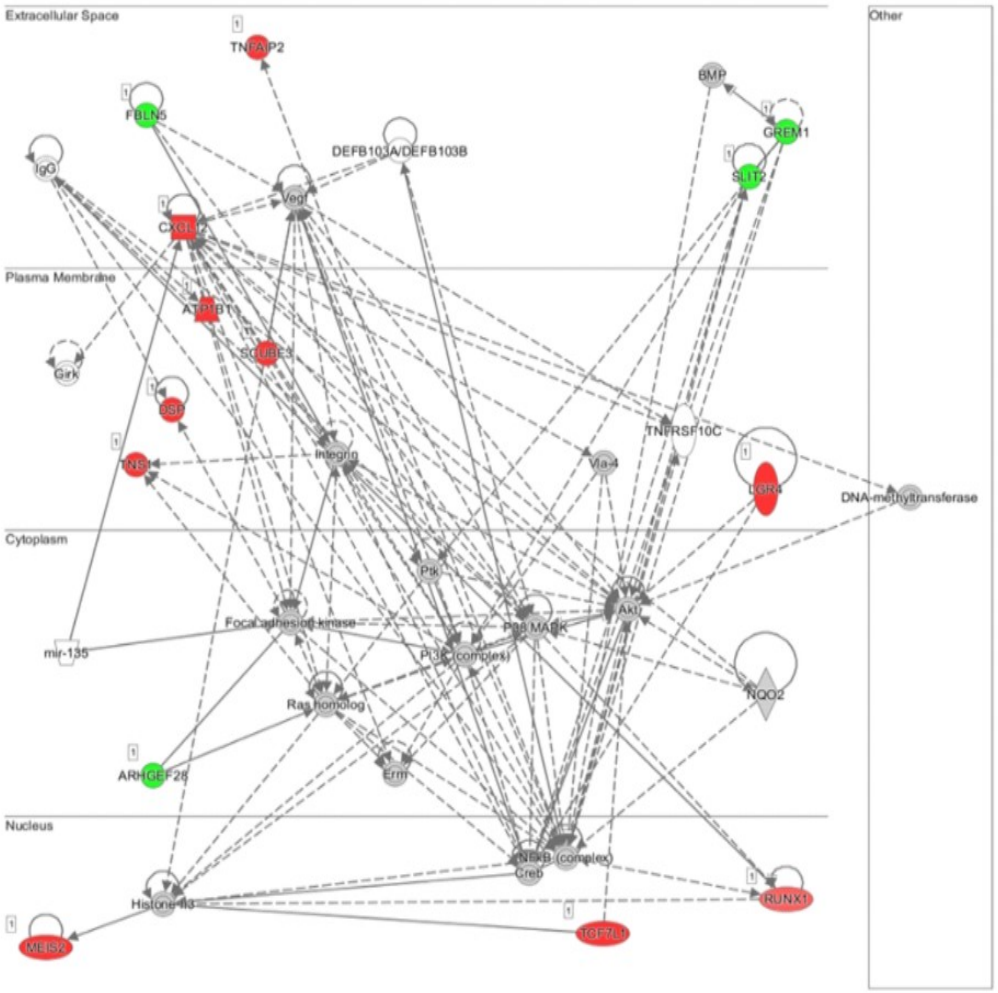

Figure 3.4. IPA Network analysis of the 21 SDRGs in AML-MSCs/HD-MSCs. The possible link and interactions between the 21 SDRGs in AML/HD-MSCs were explored and analyzed by Ingenuity pathway analysis (IPA) using the network tool and the dataset of AML/HD-MSCs. Two networks (A and B) were predicted for the interactions, association, and link between some downregulated and overexpressed genes in AML/HD-MSCs. Green represents downregulated genes, while a red represents upregulated genes. The gray/purple dotted lines represent indirect relations between molecules. The gray/purple solid lines represent a direct association between the molecules, while the effect was not predicted or unknown.

3.4. Evaluation of GREM1 and SCUBE3 as potential targets in MSCs

SCUBE-3 and GREM-1 were among the 21 SDRG-list. Both GREM1 and SCUBE3 have critical roles in proliferation, angiogenesis, and MSCs differentiation potentials. Specifically, GREM1 plays a role in osteogenic differentiation as BMP-antagonist, as introduced earlier in section 1.4 of chapter 1. However, their potential roles in AML-MSCs' alterations and HR AML-MSCs observed functional impairments are still to be cleared. In particular, the impact of GREM-1 downregulation and SCUBE3 upregulation on AML-MSC remains elusive. Therefore, due to their role in MSCs and thus their potential relevance in the alterations of AML-MSCs' function, which could consequently alter MSC's physiological role in BME, SCUBE3, and GREM1 were initially identified and selected for further study as potential molecules that might be correlated with the reported alteration in HR AML-MSCs.

3.4.1. Downregulation of GREM1 gene in all AML subtypes, AML/HD

The transcriptomic data analysis, as shown in section 3.2 (Table 3.3), showed that in the AML-MSCs group, GREM1 gene expression is significantly downregulated by approximately 5 FC (2.29 Log2FC) (adj p-value = 0.04). Moreover, among other AML subtypes, HR AML-MSCs showed impairment in their osteogenic differentiation (184). Considering that GREM1 is involved in osteogenesis as a BMP-antagonist, further analysis of these HR samples was performed. Precisely, to determine if GREM-1 downregulation mainly was attributed to its downregulation in a specific AML risk group particularly the HR group, the transcriptomic dataset of each subtype of AML, HR (n=11), LR (n= 10), and IR (n=8)

was analyzed and compared separately to HD-MSCs. The results showed that GREM1 was downregulated in AML-MSCs of all three AML risk groups. In LR, its expression was reduced by 4.22FC; in IR, it was downregulated by 4.08FC; in HR, GREM1 expression was downregulated by 7.3FC (Table 3.7).

AML Risk Group	Fold-Change ((FC)	Log2 FC	P-adjusted
*AML-MSCs	- 4.89	- 2.29	0.043
HR AML-MSCs	**- 7.3**	**- 2.88**	**0.08**
LR AML-MSCs	- 4.22	- 2.08	0.16
IR AML-MSCs	- 4.08	- 2.03	0.673

Table 3.7. GREM-1 gene expression in AML risk groups. RNA-seq data of GREM1 expression values represented by fold-change, log2FC and P-adjusted in MSCs from all AML groups (AML-MSCs/HD-MSCs). The high-risk group (HR) demonstrated the most downregulated expression among other AML-MSCs groups with a Log2FC of -2.88. *AML-MSCs= (IL+LR+HR). The cut-off value of 1.5 FC in comparison to HD-MSCs.

3.4.2 qRT-PCR Validation of GREM1 dysregulation in HR AML-MSCs

As mentioned earlier, the initial study of these AML-MSCs samples by Guardia et al. and our group found that HR AML-MSCs had an impairment in their differentiation. In section 4.1.1. GREM1 downregulated expression was slightly higher in HR-AML-MSCs compared to its expression in the IR and LR samples. Before the investigation of GREM1 potential role in the alteration of MSC's functionalities, confirmation of its dysregulation in HR AML-MSCs (n=11) was performed using HD-MSCs (n=8) as controls and qRT-PCR. Similar to RNA-seq, qRT-PCR results showed a significant decrease in GREM1 ($P^* = 0.0374$) expression in these HR samples compared to their normal counterparts (Figure 3.5). These results validated its dysregulation in HR AML-MSCs/HD-MSCs.

3.4.3 Detection of GREM1 protein in HD-MSCs.

Prior to performing any gene modification studies on HD-MSCs to modulate its downregulation, GREM1 protein was verified in HD-MSCs using Western blot analysis. Both previously and freshly prepared cell lysates of 5 HD-MSCs (five biological replicates) were tested for GREM1 protein. Moreover, those HD-MSCs differed from the primary controls used in RNA-seq. The western blot results confirmed the presence of GREM1 bands at ~28kDa in all 5 used HD-MSCs samples (Figure 3.6). GREM1 protein was successfully detected on HD-MSCs, which validated and enabled the use of these HD-MSCs for GREM1 gene modification. Furthermore, no investigation of GREM1 protein was conducted using AML-MSCs.

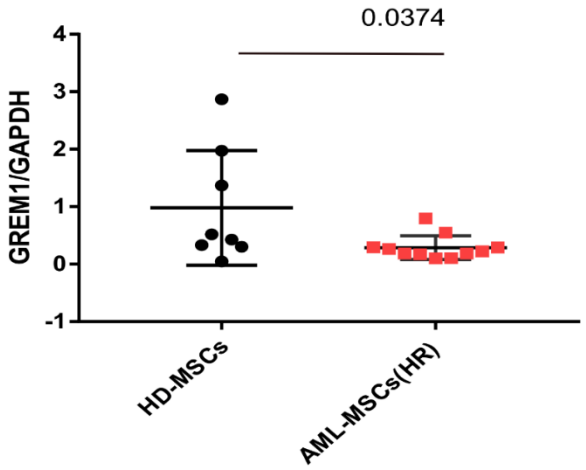

Figure 3.5. qRT-PCR Validation of GREM1 significant downregulation in HR AML-MSCs. qRTPCR analysis of mRNA expression of GREM1 using the extracted RNA samples used for RNA sequencing. cDNAs were synthesized from each RNA sample, and qRTPCR was performed. Results showed that GREM1 was significantly downregulated in HR AML-MSCs (n=11) in comparison to HD-MSCs (n=8) (p* = 0.0374). GAPDH served as a control. Black dots represent HD-MSCs, and red symbols represent HR AML-MSCs. Every single symbol represents the mean of >3 independent experiments. An unpaired T-test was used to compare the expression between the two groups, and ($P < 0.05$) was used to calculate the significance through graph prism software.

Figure 3.6. Validation of GREM1 protein in HD-MSCs (n=5). Western blot confirmation of physiological level of GREM1 protein in 20µg of cell lysates from five biological samples of HD-MSCs different than the HD samples used in RNA sequencing. (Details about the donors can be found in the appendix). Left: MSCs lysates from 4 biological donors 10C, 11C, 12 and 13C. Right: MSCs lysates from the same donor (TC7078-2) lysed with several concentration of RIPA lysing buffer. GREM-1 protein was detected at 28kDa using GREM1 primary antibody; Rabbit pAb Anti-GREM1 (1:500) and a secondary pAb, IRDye800CW Goat Anti-rabbit IgG (1/2000). Odyssey Li Core imaging system was used for imaging.

3.4.4 SCUBE3 upregulation in all AML subtypes

The RNA-seq data showed that in AML-MSCs SCUBE3 gene expression was significantly upregulated by 3.9 FC (adj.P-value < 0.001) as shown in section 3.2 and 3.4. To determine whether SCUBE3 gene increased expression was specifically attributed to AML-subtype, the transcriptomic dataset of each subtype of AML, HR, LR, and IR MSCs compared to HD-MSCs were analyzed for SCUBE3 expression. Interestingly, transcriptomic data analysis revealed that SCUBE3 gene expression was upregulated in AML-MSCs of all three AML risk groups. In LR it was increased significantly by 2.04 Log2FC (P-value of 3.3E-06, P-adj of 0.0038), in IR it was significantly upregulated by 2.0 log2FC (P-value of 4.03E-5, P-adj 0.06), and by 1.75 Log2FC (P-value of 0.0007 and adj.p-value of 0.144) in HR-AML-MSCs (Table 3.8). Suggesting that the upregulation of SCUBE3 in AML-MSCs is not accounted for its upregulation in HR AML-MSCs rather, it is significant in all AML-MSCs and could be used as a potential target in BME of all AML subtypes.

3.4.5 qRT-PCR Validation of SCUBE3 dysregulation in HR AML-MSCs

To validate SCUBE3 upregulation in HR AML-MSCs and confirm the primary transcriptomic data, SCUBE3 upregulation in HR samples (n=11) was examined by qRT-PCR using HD-MSCs (n=8) as controls. qRT-PCR results did not confirm the upregulation of SCUBE3 gene expression in these HR samples compared to its expression in their normal counterparts (P =0.209) (Figure 3.7).

AML Risk Group	Fold-Change (FC)	Log2 FC	P-adjusted
*AML-MSCs	+ 3.91	1.96	0.0007
HR AML-MSCs	+ 3.0	1.75	0.144
LR AML-MSCs	+ 4.1	2.04	0.0038
IR AML-MSCs	+ 4	2	0.06

Table 3.8. SCUBE3 gene expression in AML risk groups. RNA-seq data of SCUBE3 expression in AML-MSCs/HD-MSCs. The high-risk group (HR) demonstrated the least upregulated expression among the other AML groups with a Log2FC of 1.75.

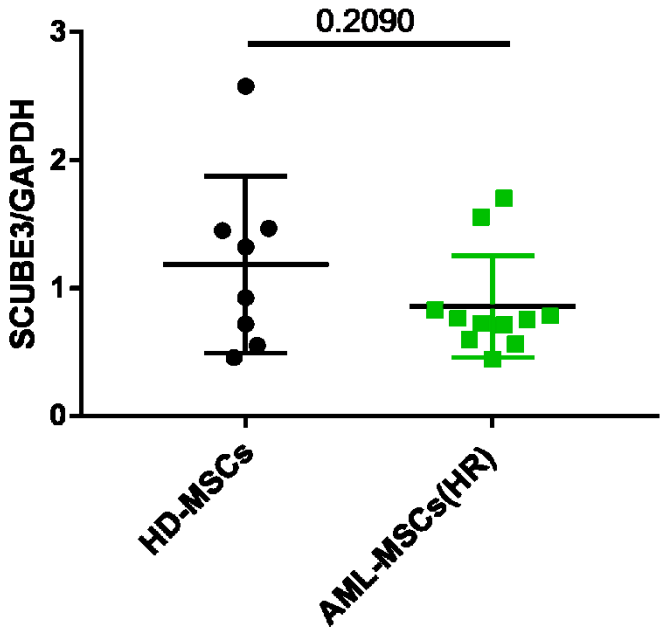

Figure 3.7. qRT-PCR Validation of SCUBE3 expression in HR AML-MSCs. qRTPCR analysis results of mRNA expression of SCUBE3 using the extracted RNAs samples that were used for RNA sequencing to synthesize cDNAs. SCUBE3 dysregulation was not confirmed in HR AML-MSCs (n=11) in comparison to HD-MSCs (n=8) (ns. p = 0.209). GAPDH served as a control. Black dots represent HD-MSCs, Green symbols represent HR AML-MSCs. Each single symbol represents the mean of >3 independent experiments. ($P < 0.05$) used to calculate the significance.

3.4.6. In vitro gene-modification approach for GREM-1 silencing and SCUBE-3 overexpression in HD-MSCs

To validate the significance of GREM-1 dysregulation and to understand its potential role in altering MSC's functionality, HD-MSCs (hBMMSC-TC7078-2) were used as *in-vitro* model to perform GREM1 knockdown since their physiological level of GREM1 protein was successfully confirmed (Figure 3.5). Using four targeted siRNAs, against GREM-1.siGREM-1(1), siGREM-1(2), siGREM-1(3), and siGREM-1(4), GREM1 KD was conducted on HD-MSCs. Negative scramble siRNA and untreated HD-MSCs were used as controls. Following the KD, high viabilities of transfected cells were observed and then cells, transfected and un-transfected, were collected and lysed. Western blot analysis was used to assess the KD efficiency using 20µg of protein from each cell lysate. Results showed no KD effect on GREM-1 protein abundance level on all transfection conditions compared to siRNA-Negative scrambled, and untreated cells. Although, initially, siGREM-1(1) showed some KD effect compared to the other three utilized siRNAs, when tested separately (n=2) and compared to negative siRNA control, similar bands were found; no significant difference was found between all conditions. Moreover, the both tested 24 and 72 hours post transfection assessment showed similar effect; no KD effect was observed. Even when siRNA cocktail was generated using these 4 siRNAs combined, no KD was seen. Furthermore, SCUBE3 protein detection in HD-MSCs was unsuccessful which limited the completion of several initial optimization approaches to modify its expression using overexpression plasmids. Therefore, no further investigation of GREM1 and SCUBE3 was performed.

CHAPTER 4

Evaluating CD248 as a Potential Target in AML-MSCs

4.1 CD248 Expression in AML subtypes

The transcriptomic analysis showed that the CD248 gene is among the 21 SDRG in AML-MSCs/HD-MSCs. Specifically, its expression level was significantly upregulated by 1.89 FC (0.924 Log2FC) (adj.p-value = 0.036) in AML-MSCs (n=29) in comparison to HD-MSCs (n=8) as shown in chapter 3. To determine CD248 expression profiles in AML-MSCs from each AML risk group, CD248 expression values in IR (n=8), LR (n=10), and HR (n= 11) were compared using the raw transcriptomic dataset of each subtype. In comparison to HD-MSCs, CD248 gene expression level was increased in IR AML-MSCs by 1.66 FC (adj.p-value = 0.7), and in LR AML-MSCs by 1.9FC (adj.p-value = 0.064). Moreover, it was significantly upregulated in HR AML-MSCs by approximately 2.4 FC (1.249 Log2FC) with a p-value of 0.000006 (adj. p-value of 0.034) (Figure 4.1 and Table 4.1). These results showed that HR AML-MSCs exhibited the most upregulated profile of CD248 at the gene level among the other two subtypes, IR and LR, which suggested that CD248 could be involved in the previously observed functional alterations in these HR samples that have been investigated by Guardia and colleagues (184).

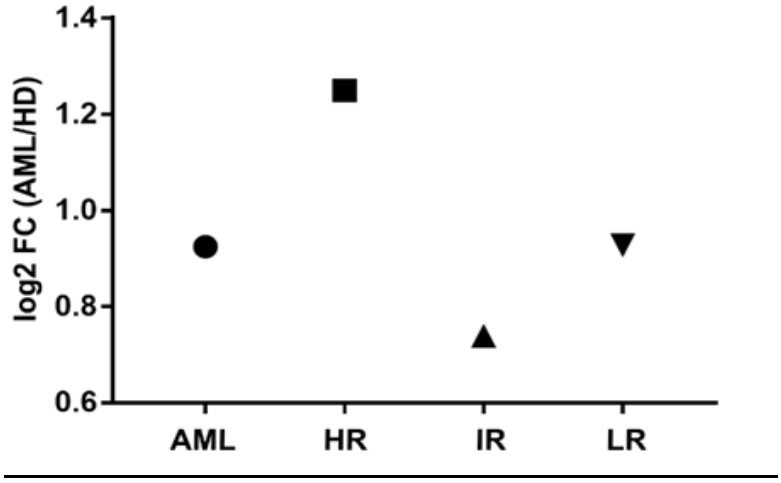

Figure 4.1. CD248 gene Expression was significantly higher in HR AML-MSCs. RNA-seq data of CD248 expression in AML-MSCs/HD-MSCs from all AML risk groups graphed using the Log2Fold-change (FC) values. CD248 gene expression was higher in HR than its expression in the other AML risk groups. (Details of the expression values are shown in the corresponding table below).

AML Risk Group	Fold-Change	Log2 FC	P-value	Adjusted P-value
*AML-MSCs	1.89	0.9242	0.00011	0.0369
HR AML-MSCs	**2.37**	**1.249**	**6.1E-06**	**0.034**
IR AML-MSCs	1.66	0.739	0.01115	0.738
LR AML-MSCs	1.9	0.928	0.00042	0.064

Table 4.1. CD248 gene expression in AML subtypes. The HR AML-MSCs demonstrated the highest upregulated expression of CD248 among other AML-MSCs groups with a Log2FC of 1.249 (equal to 2.37FC).The cut off value is >1.5FC in comparison to HD-MSCs. (Log2 (1.5FC = 0.58). *AML-MSCs=AML-MSCs from all AML subtypes (IR+LR+HR).

HR AML-MSCs Upregulated Genes			
Gene Symbol	**Fold-Change (FC)**	**Log2 FC**	**Adjusted p-value**
NOTCH3	3.0674	1.617004119	0.004153792
COL5A3	6.984	2.804066291	0.013449111
CXCL12	3.863	1.949777767	0.026598805
CD248	2.378	1.249712737	0.034465283
TNFAIP2	2.424	1.277444988	0.041398807

Table 4.2. Significantly upregulated genes in HR AML-MSCs/HD-MSCs. RNA-seq data of significantly upregulated genes in HR AML-MSCs/HD-MSCs.

4.2 Culturing HR AML-MSCs (n=11) for CD248 validation

As shown above, in section 4.1, transcriptomic data showed a significant increase in CD248 gene expression in HR AML-MSCs compared to HD-MSCs. Furthermore, as mentioned in chapter 1, those MSCs samples from HR patients exhibited impairment in their differentiation potentials. To determine whether or not upregulated CD248 gene expression was involved in their reported altered functionality, HR samples, in particular, were selected and used for further investigation and understanding of CD248 dysregulation.

Cell cultures of these 11 HR samples were prepared from frozen MSCs vials and maintained until confluence. In addition, 4 HD-MSCs frozen samples were thawed, cultured, and used as controls (Table.4.3). HD-MSCs (RoosterBio cells) manufacturer document recommends using RoosterBio media, which contains special supplements without adding FBS. However, to minimize variations and ensure similar culturing conditions for HD and AML-MSCs cultures, HD-MSCs were cultured in AML complete media that contains 20%FBS after conditions were tested and validated. Especially that AML complete media was used for cell culture and generation of RNAs for the RNA sequencing (section 3.1) from all of these MSCs. MSCs from both groups grew well in AML complete media despite the variation of the required days to achieve the highest possible confluences. In contrast to MSCs from healthy donors, which grew faster, the AML-MSCs from HR patients needed more days in culture to reach ≥ 75 % confluence (Table. 4.4). Performing microscopic evaluation of cells morphology using bright field microscopy, similar morphology of fibroblast-like / spindle-shaped was observed in both MSCs from HD and HR AML patients (Figure 4.2).

HR AML-MSCs	Diagnostic	Cytogenetics	Molecular	Age (y)	Sex
HR -AML1	M4	46,XX	MLL-AF9	63	F
HR-AML2	M4	46,XY	BAALCMUT, WT1MUT, NPM1MUT,FLT3MUT	42	M
HR-AML 3	M5	46,XY	NPM1MUT, FLT3del	77	M
HR -AML4	AML	46,XY,-7q	FLT3WT, NPM1WT, MLLWT, cEBPaWT	53	M
HR-AML5	AML	46,XY,del(7)(q22) [13]	Ø	69	M
HR-AML 6	AML	89-92,XY	Ø	35	M
HR-AML 7	M5	46,XX	NPM1MUT, FLT3-ITD	65	F
HR-AML 8	M1	46,XX	MLL-AF9	77	F
HR -AML9	M5	46,XX,t(11;19)(q23;p13)	MLL-ENL	48	F
HR-AML 10	M2	46,XX t(8;21) AML1-ETO	FLT3-ITD	4	F
HR-AML 11	AML	46,XX	FLT3MUT	8	F
HD-MSCs	**Age (Y)**	**Gender**			
HD1-84RB	31-45	M			
HD2-55RB	18-30	M			
HD3-49RB	18-30	M			
HD4-81RB	18-30	M			

Table 4.3. Demography of HR AML-MSCs (n=11) and control HD-MSCs (n=4) that were used for CD248 evaluation. Adapted from Table 3.1.

High-Risk (HR) AML-MSCs	% Confluence when harvested	Culture establishment
HR -AML1	65%	✓
HR-AML2	60%	✓
HR-AML 3	85%	✓
HR -AML4	95%	✓
HR-AML5	55%	✓
HR-AML 6	80%	✓
HR-AML 7	80%	✓
HR-AML 8	75%	✓
HR -AML9	80%	✓
HR-AML 10	75%	✓
HR-AML 11	80%	✓
HD-MSCs	**% Confluence when harvested**	**Culture establishment**
HD1-84RB	95%	✓
HD2-55RB	95%	✓
HD3-49RB	95%	✓
HD4-81RB	95%	✓

Table 4.4. Successful culturing of HR AML-MSCs and HD-MSCs for CD248 protein assessment. (Details about AML-MSCs and HD-MSCs culture conditions were described in chapter 2).

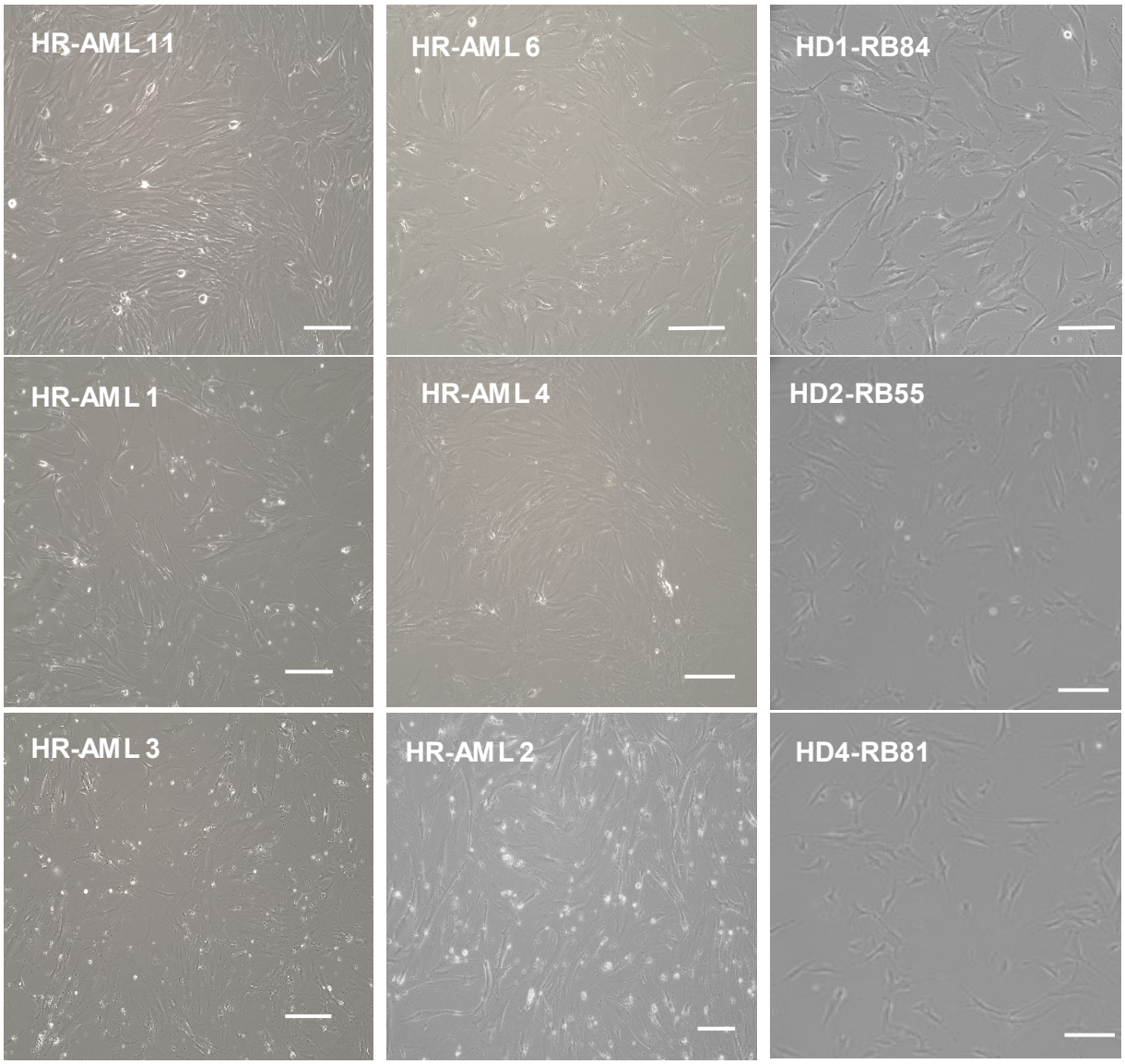

Figure.4.2. HR AML-MSCs and HD-MSCs cultures. HR AML-MSCs, and HD-MSCs, MSCs were cultured in AML complete media (20% FBS, in advanced DMEM media) for 4-10 days. Representative images of HR AML-MSCs (left and middle panel) and HD-MSCs (right panel). Images were taken using bright-field microscopy. Magnification X10, Scale bar 100µm.

4.3. Determination of CD248 protein abundance level in both HD and HR AML-MSCs

As introduced in chapter 1, section 1.6, the CD248 gene encodes a transmembrane protein normally expressed in human MSCs. As shown in chapter 3 and section 4.1, the CD248 gene was upregulated in MSCs from all AML risk groups, AML-MSCs/HD-MSCs. To be able to determine the CD248 protein abundance level in HR AML-MSCs and to investigate if upregulated CD248 gene expression was also translated to a higher level of CD248 protein, cell lysates were generated from the HR AML-MSCs cultures (n=11), and HD-MSCs (n=4) as described in section 4.2.

After lysing MSCs to generate lysates from these 15 MSCs samples (11 AML and 4 HD), western blot analysis was performed using 20µg of protein from each lysate. The 11 HR AML-MSCs' lysates were randomly divided into two sets, and each set was run separately. This dividing approach was carried out after determining several limitations that prevented the run of 15 lysates on the same gel. These limitations were identified through initial optimization experiments. They included the minimum required protein concentration to detect CD248 on these HR lysates, which was ≥ 20µg with the utilized CD248 pAb (TEM1 rabbit polyclonal Antibody). In addition to the required protein concentration, other technical factors, such as the total volume of the sample per well and the number of samples per gel. Thus samples were run in two sets separately to ensure accuracy. Set 1 included HR-AML1-6, while set 2 included HR-AML7-11 (Table 4.3). Moreover, the same HD-MSCs (n=4) lysates were used with each set of HR samples to minimize variations between technical and biological replicates.

Western blot analysis showed that the CD248 protein abundance level was upregulated in HR AML-MSCs compared to its level in HD-MSCs (Figure 4.3 and Figure 4.4). Among several primary mAbs and pAbs tested to detect CD248 (Supplementary Table), only one pAb showed reactivity to CD248 protein in both AML-MSCs and HD-MSCs. It detected CD248 bands at ~90kDa at both healthy and AML groups, while other antibodies did not react to either group. To accurately normalize the CD248 signals of these HR samples, two normalization measurements were used; normalization to housekeeping genes GAPDH and β-actin and normalization using total protein stain (TPS). The β-actin bands were smeared and not consistent between the samples and, therefore, could not be used to normalize CD248 signals. Furthermore, GAPDH signals showed slight variations within HR samples (Figure 4.3A) (Figure 4.4A). When GAPDH was used to normalize CD248 signals, the protein abundance level of CD248 was upregulated with a p-value of 0.14 (Figure 4.3 B and C) in set 1 of HR samples (HR-AML1-6), while when these CD248 signals were normalized to TPS, the protein abundance level of CD248 was significantly higher in HR AML-MSCs (HR-AML1 - 6) with a p-value of 0.0065 (Figure 4.3D and E) compared to HD-MSCs (n=4). CD248 protein was also significantly highly abundant in set 2 of HR AML-MSCs (HR-AML7 - HR-AML11) with a p-value of 0.039 (Figure 4.4B and C) relative to GAPDH and a p-value of 0.027 (Figure. 4.4D and E) when normalized to TPS compared to HD-MSCs (n=4).

GAPDH showed some variation, not as TPS, between these 15 biological samples within each group, HR AML-MSCs group and HD-MSCs group. GAPDH (37kDa) high abundance in 20µg of protein from cell lysates possibly overlaid the

low detected level of CD248 (90kDa). Additionally, proteins with lower molecular weight could transfer and provide better signals. Therefore, although normalization of CD248 to GAPDH showed upregulated results in HR AML-MSCs, using TPS to normalize was more reliable to ensure the accuracy of western blot results. Particularly since TPS would not be affected by biological conditions, it reflected the actual protein transferred to the membrane during the transferring step as reported. Technical replicates of each set were performed to ensure the reproducibility of data. Figure 4.3 and Figure 4.4 demonstrate and represent the average of 2 technical replicates for each set. Moreover, although there was some variation in CD248 expression level between HR AML-MSCs samples, all samples exhibited a relatively higher level than their healthy counterparts and showed a trend toward an increased abundance of CD248 protein. An increase of >2 FC was observed in the HR AML-MSCs group compared to the HD-MSCs group (Figure 4.5). Additionally, HD-MSCs, HD2-55RB, showed a higher level of CD248 than the other three control samples.

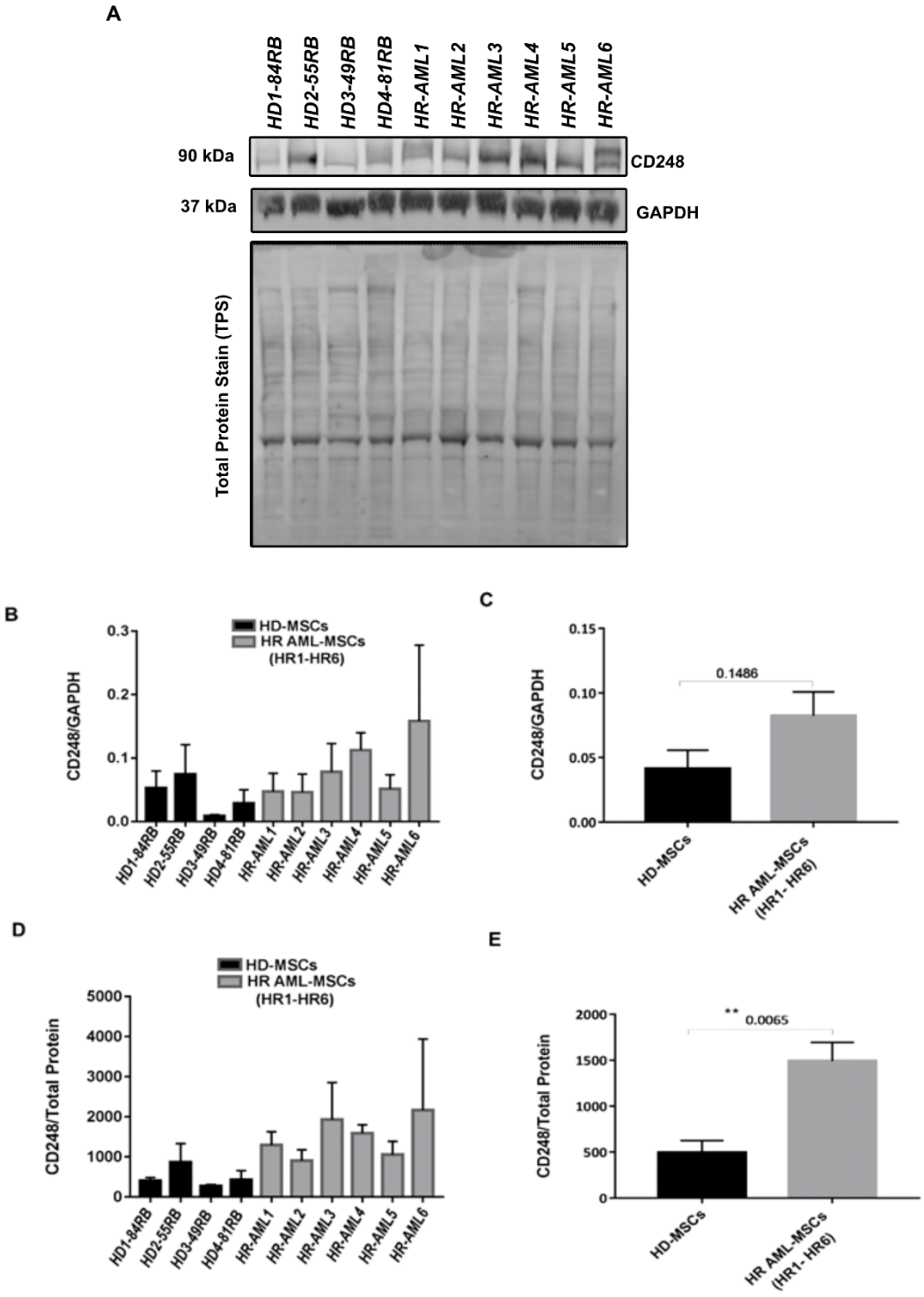
A
HD1-84RB
HD2-55RB
HD3-49RB
HD4-81RB
HR-AML1
HR-AML2
HR-AML3
HR-AML4
HR-AML5
HR-AML6
90 kDa
CD248
37 kDa
GAPDH
Total Protein Stain (TPS)
B
HD-MSCs
HR AML-MSCs
(HR1-HR6)
CD248/GAPDH
C
0.1486
CD248/GAPDH
HD-MSCs
HR AML-MSCs
(HR1- HR6)
D
HD-MSCs
HR AML-MSCs
(HR1-HR6)
CD248/Total Protein
E
**
0.0065
CD248/Total Protein
HD-MSCs
HR AML-MSCs
(HR1- HR6)

Figure 4.3. CD248 Protein abundance level was significantly higher in HR AML-MSCs (n=6) in comparison to HD-MSCs (n=4). Western blot was used to detect CD248 in HR AML (1-6) cell lysates. 20ug of each MSCs lysates HR (n=5) vs. HD-MSCs (n=4) were used for WB. First, blots were incubated with pAb-CD248 (1:500), then was stripped and incubated with GAPDH and βactin separately. Secondary conjugated antibodies were used to detect the signals. Total protein stain was performed on each blot. Images were taken by the Li core Odyssey instrument at channel 800 for CD248 and channel 700 for total protein signals. A) Representative blot showing CD248, GAPDH bands, and TPS for the same blot. B) CD248 signals from each sample were normalized to GAPDH and graphed individually (average of 2 replicates). C) CD248/GAPDH signals from (B) were grouped and averaged for statistical significance. Then total protein was used to normalize CD248 signals. D) CD248/TPS signals of each sample individually. E) CD248/TPS signals from (D) were grouped and averaged. Results were graphed by graphprism.7. SEM and unpaired T-test were used for comparison of the two groups.

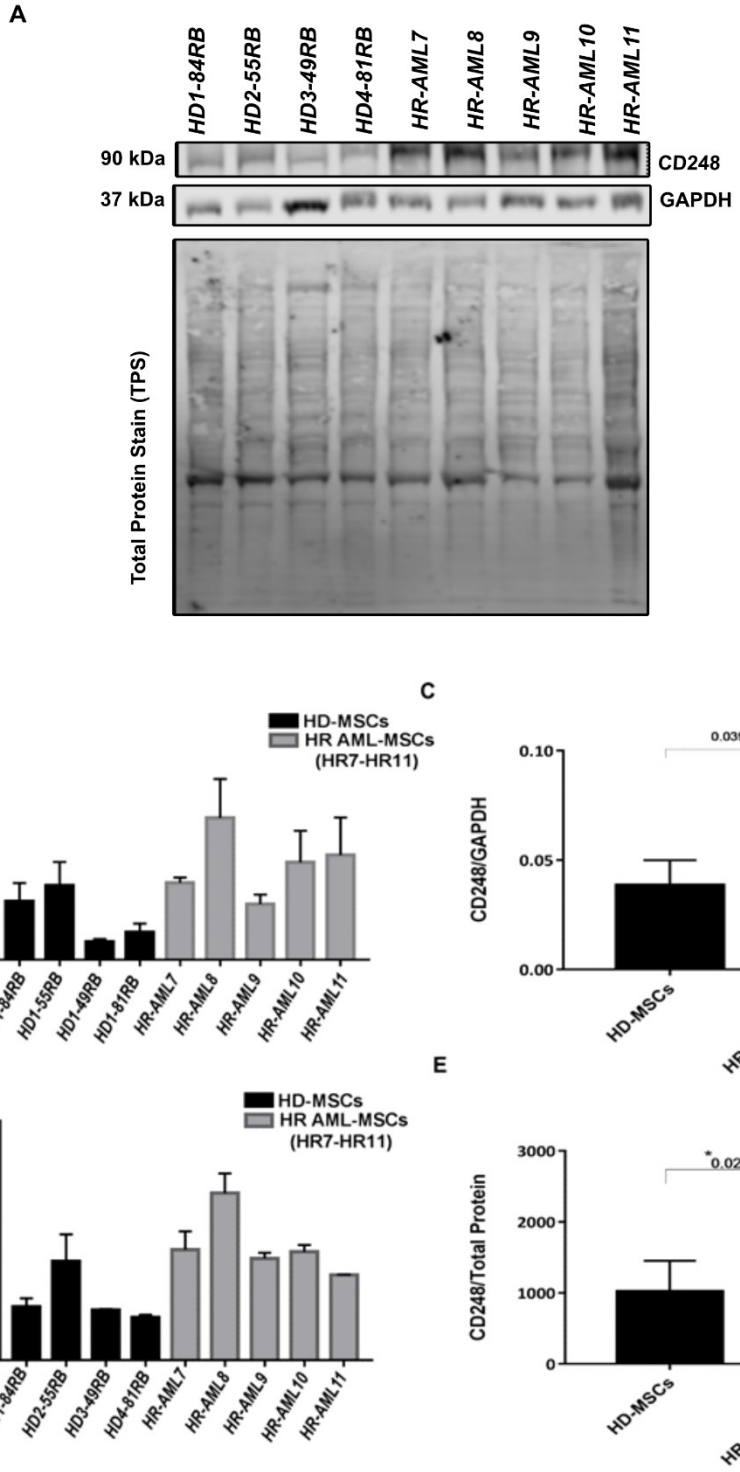
A
HD1-84RB
HD2-55RB
HD3-49RB
HD4-81RB
HR-AML7
HR-AML8
HR-AML9
HR-AML10
HR-AML11
90 kDa
CD248
37 kDa
GAPDH
Total Protein Stain (TPS)
B
HD-MSCs
HR AML-MSCs (HR7-HR11)
CD248/GAPDH
0.20
0.15
0.10
0.05
0.00
HD1-84RB
HD1-55RB
HD1-49RB
HD1-81RB
HR-AML7
HR-AML8
HR-AML9
HR-AML10
HR-AML11
C
0.0391
0.10
0.05
0.00
CD248/GAPDH
HD-MSCs
HR AML-MSCs (HR7- HR11)
D
HD-MSCs
HR AML-MSCs (HR7-HR11)
CD248/Total Protein
4000
3000
2000
1000
0
HD1-84RB
HD2-55RB
HD3-49RB
HD4-81RB
HR-AML7
HR-AML8
HR-AML9
HR-AML10
HR-AML11
E
*0.0279
3000
2000
1000
0
CD248/Total Protein
HD-MSCs
HR AML-MSCs (HR7- HR11)

Figure 4.4. CD248 Protein abundance level was significantly higher in HR AML-MSCs (n=5) in comparison to HD-MSCs (n=4). Western blot was used to detect CD248 in HR AML (7-11) cell lysates. 20ug of each MSCs lysates HR (n=5) vs. HD-MSCs (n=4) were used for WB. First blots were incubated with pAb-CD248 (1:500), then was stripped and incubated with GAPDH and βactin separately. Secondary conjugated antibodies were used to detect the signals. Total protein stain was performed on each blot. Images were taken by the Li core Odyssey instrument at channel 800 for CD248 and channel 700 for total protein signals. A) Representative blot showing the CD248, GAPDH, and TPS for the same blot. B) CD248 signals from each sample were normalized to GAPDH and graphed individually (average of 2 replicates). C) CD248/GAPDH signals from (B) were grouped and averaged for statistical significance. Then total protein was used to normalize CD248 signals. D) CD248/TPS signals of each sample individually. E) CD248/TPS signals from (D) were grouped and averaged. Results were graphed by graphprism.7. SEM and unpaired T-test was used for comparison of the two groups.

Collectively, the upregulated gene expression of CD248 in HR AML-MSCs (n=11) in comparison to HD-MSCs (n=4) was validated at protein abundance level by western blot analysis using cell lysates from all 15 samples. A significant upregulation in CD248 protein abundance level was found in HR AML-MSCs (HR-AML1 – HR-AML11) with p-values of 0.053 and 0.0038, relative to GAPDH and TPS, respectively, in comparison to their healthy counterparts (4.5A and B)(Figure 4.5C and D). Additionally, a similar pattern of upregulation between transcriptomic and protein data of CD248 level among HR AML-MSCs was found (Figure 4.6). CD248 was upregulated at the gene level and also at the protein abundance level. These results suggest that dysregulation of CD248 at both gene and protein levels is associated with AML-MSC and supports further investigation of the potential role of this molecule in the altered functional properties previously attributed to these cells.

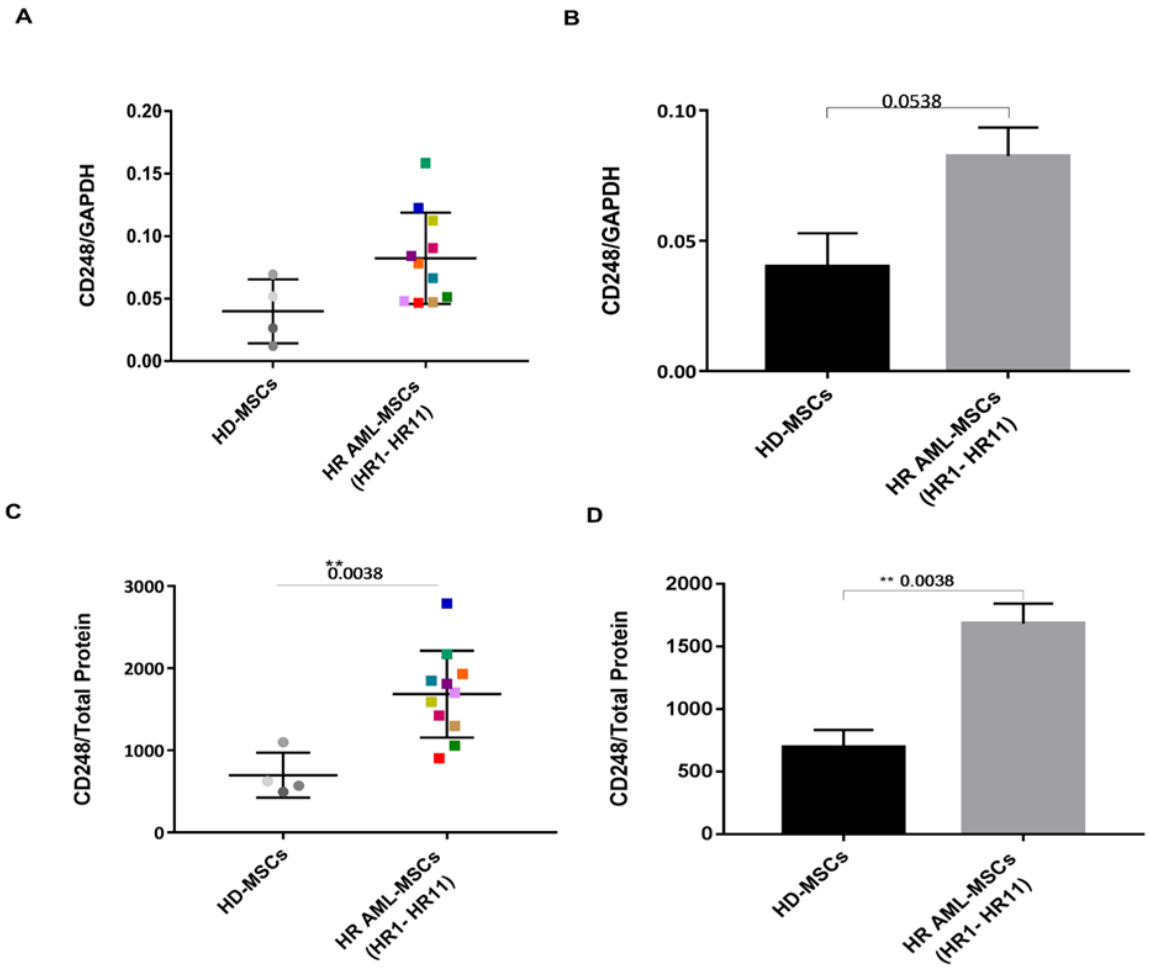

Figure 4.5. CD248 protein abundance level was significantly higher in HR AML-MSCs (n=11) than its level in HD-MSCs (n=4). The western blot analysis and results in Figure 4.3 and Figure 4.4 of AML-MSCs HR were grouped and averaged. A) and B) CD248/GAPDH signals of all HR and HD AML-MSCs. Each symbol represents a mean of 2 replicates of each sample. C) and D) CD248/TPS of all 11 HR samples compared to HD-MSCs (n=4). Error bar represents SEM. An unpaired T-test was used for the comparison of the two groups. Graph prism 7 was used to perform the analysis.

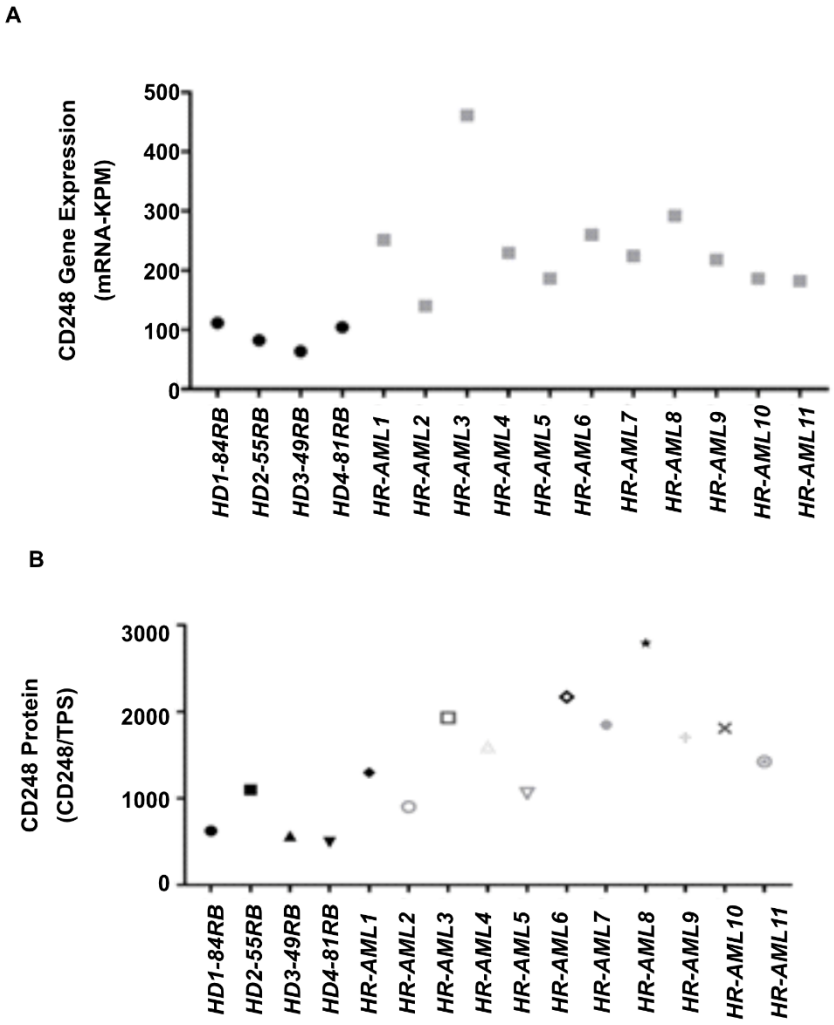

Figure 4.6. Similar increase pattern of CD248 among HR AML-MSCs at gene expression level and protein abundance level. HR AML-MSCs samples demonstrated similar CD248 upregulated pattern at A)mRNA and protein level B) (CD248/TPS) and C) CD248/GAPDH.

4.4 Cell surface expression level of CD248 is altered in HR AML-MSCs

Western blot results in section 4.3 showed that CD248 is significantly upregulated at the protein level in HR AML-MSCs. To identify whether it was also overexpressed at the cell-surface level of HR AML-MSCs, CD248 surface protein was investigated using flow cytometry analysis. Mainly, its level was determined on HD-MSCs (HD2-55RB) and HR AML-MSCs (HR-AML8), respectively, by utilizing a different clone of CD248-pAb (Endosialin/CD248 - Mouse Anti-Human conjugated to Alexa Fluor 647) than the pAb used for Western blot analysis in the previous sections to determine total CD248 protein.

Interestingly, using IgG isotype as a negative control (IgG1k Isotype - Mouse - Alexa Fluor 647), CD248 was found to be expressed at the cell-surface level on both HD-MSCs and HR AML-MSCs (Figure 4.7A). CD248 MFI results showed that cell surface CD248 was significantly higher on HR AML-MSCs with a > 2-fold increase compared to HD-MSCs, and a higher percentage of CD248+ cells was found in HR AML-MSCs than HD-MSCs (Figure 4.7B). Around 40% of HR AML-MSCs were CD248+ while only 20% of MSCs were CD248+ within the HD sample. Furthermore, the antibody's titration of 10µl was the optimal concentration (Figure 4.7C). These findings confirmed that overexpression of CD248 in HR AML-MSCs was not only limited to gene and total protein levels, but also cell-surface CD248 was upregulated on the tested HR sample. Suggesting that overexpression of surface CD248 on HR AML-MSCs might play a part in AML-MSCs altered functionality and potentially impact MSCs-to-cell interactions with other cellular components of the HSCs niche compared to healthy MSCs.

A

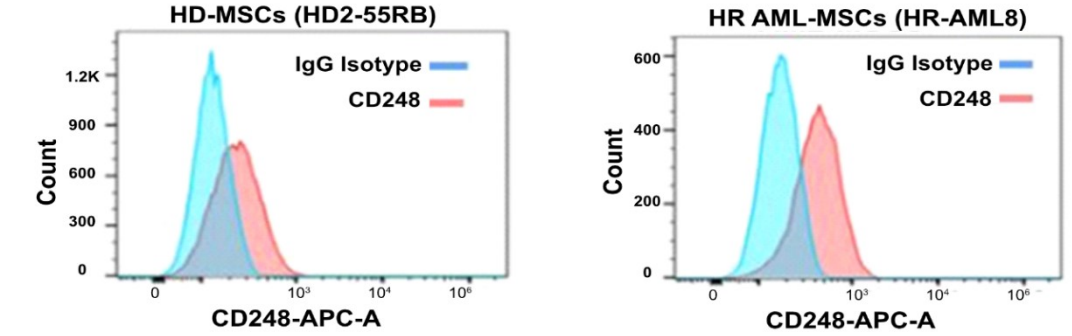

B

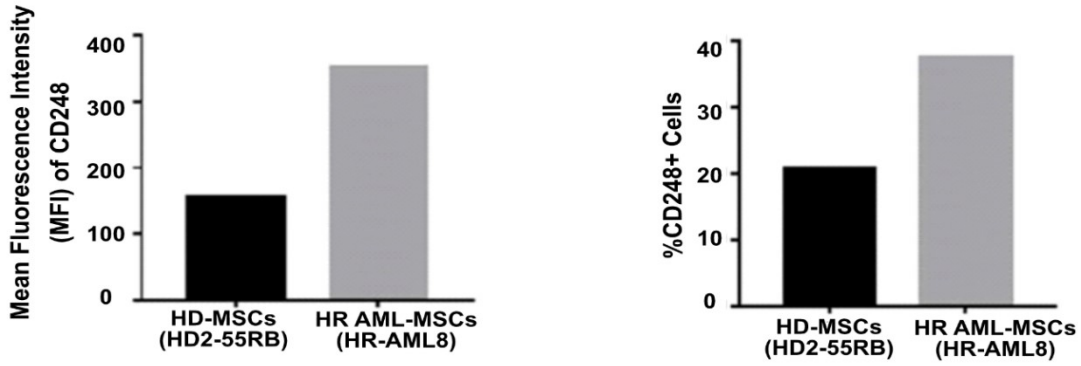

C

	Antibody Titration (10µL)	Ab Type	%CD248⁺ Cells	%Live	MFI
Sample	HR AML-MSCs (HD2-55RB)	CD248	20.7	ND	328
		IgG	0.26	ND	173
	HR AML-MSCs (HR-AML8)	CD248	37.5	99.9	578
		IgG	0.094	99.9	225

Figure 4.7. AML-MSCs sample (HR-AML8) from the HR group showed a higher level of surface marker CD248 in comparison to HD-MSCs sample (HD2-55RB). CD248 was determined by flow cytometry analysis on a) HD-MSCs (hBM55RB) (left), and AML-MSCs (AML8=14070) (right). Cells were incubated with anti-CD248 antibody conjugated with Alexa Fluor 647 (pink) or negative IgG isotype (blue). Data for antibody titration 10µl is graphed (b). Three titrations of the antibodies were performed, as shown in the table (1µl=1µg/µl) for both CD248 and isotype control(C). Data were analyzed by FlowJo software. MFI of HD-MSCs and AML-MSCs were determined. The figures above represent a single experiment of each sample. Negative Isotype control was used to set experiments bars.

4.5. HD-MSCs as an in-vitro model to study CD248 effect on MSCs functionality

As shown in section 3.2 of chapter 3 and sections 4.3 and 4.4 of this chapter, CD248 was identified as a novel potential target in AML-MSCs (MSCs from all AML risk groups) and HR AML-MSCs by RNA sequencing and selected for further investigation. Its high abundance level was validated and confirmed at total protein and cell-surface levels using HR AML-MSCs. In the following sections of this chapter, gene modification studies were conducted using HD-MSCs, rather than HR AML-MSCs, as an in-vitro model to precisely investigate CD248's novel potentiality and understand its role in MSC's functional level.

HR AML-MSCs were harvested from unhealthy BME, exposed to a leukemic environment, and exhibited several defects at both gene and functional levels as seen. These defects might interfere with the modification-resulted alteration in MSCs' function, and thus, it would be difficult to distinguish between the modification effect and the primary alterations of these HR samples. Additionally, several technical limitations limited the use of AML-MSCs in the optimization protocols that were essential for establishing a stable in-vitro model for CD248 gene modification studies. Therefore, HD-MSCs, not AML-MSCs, were used as a model to study CD248 dysregulation's impact on healthy-derived MSCs and enabled the understanding of their altered function when dysregulated. Nonetheless, further verification of the efficiency of the established KD protocol, after the successful confirmation in HD-MSCs as seen above, was performed in HR AML-MSCs (n=1), which could serve future AML-MSCs studies.

4.6 CD248 Gene modification studies

Although CD248 is well-known to be expressed on BM-MSCs, little is known about its functional role in these therapeutically relevant cells. Therefore, to understand the potential role of CD248 in MSC's functionality, both knockdown and overexpression protocols had to be established since no validated protocols were available. Initial in-vitro optimization experiments were conducted simultaneously to establish these protocols. Several overexpression plasmids were tested for the overexpression study, while single silencing siRNA was utilized for the CD248 knockdown study. These CD248 gene modification studies were performed on primary cells, HD-MSCs, specifically (HD2-55RB), due to their relatively higher abundance of CD248 compared to the other 3 HD-MSCs as shown in sections 4.3 and 4.4.

Unfortunately, initial attempts of CD248 overexpression in HD-MSCs using three purchased various plasmids were unsuccessful. Results showed that increased CD248 expression levels could not be achieved. The high level of toxicity could explain such observation for the plasmids in MSC. Thus, further overexpression experiments could not be pursued.

4.7. siRNA Knockdown of CD248

4.7.1 Efficient siRNA CD248 knockdown in HD-MSCs confirmed by Western blot analysis

As seen in previous sections of this chapter, determination and validation of CD248 at total protein and cell-surface levels were conducted using Western blot and Flow cytometry analyses. Similarly, these two analytical methods were used in the following sections to determine and confirm the efficiency of CD248 siRNA knockdown (KD) in HD-MSCs.

When MSCs were > 80% confluent, they were transfected with either CD248 siRNA (siCD248-Treated) or a negative scramble siRNA (NegScr-Treated). Untreated HD-MSCs (UT-Cells) were used as an additional control. After 4 hours of transfection, the cells were rescued by changing the media to complete RoosterBio media. 72-hour post-transfection (P-TF)), cells were collected and assessed for KD efficiency by Western blot analysis (Figure 4.8A).

Microscopic evaluation of MSCs' morphology under all transfection conditions; siCD248-Treated, siNegScr-Treated, and UT-cells showed normal fibroblast-like/ spindle-shaped morphology and high viabilities (Figure 4.8B). Western blot analysis was performed using 40µg of protein from each lysate, and blots were incubated with CD248 pAb (TEM1 Rabbit Polyclonal Antibody). Interestingly, results showed that siCD248-Treated, siNegScr-Treated, and UT-cells showed an absence of CD248 protein at 90kDa on siCD248-Treated compared to siNegScr-Treated and UT-cells. GAPDH was used as a reference gene, and additionally, a total protein stain was used to validate the accuracy of the visualized KD band (Figure 4.8C). CD248 was knocked down efficiently in siCD248-Treated

HD2-55RB compared to siNegScr-Treated and un-transfected MSCs, UT-cells (by >70%)(Figure S). Interestingly, it efficiently knocked down the 90kDa form of CD248 protein, possibly the core protein (Figure 4.8C and D left panel). The KD was mainly shown in the 90kDa band when the pAb was used. Further, the analysis showed that a partial KD was seen at ~55-60 kDa bands (Figure 4.8D). Discontinuing the above-used pAb from the manufacturer prevented additional assessment with the same CD248-pAb to obtain sufficient technical replicates for statistical significance and enforce the need to optimize and use new CD248 Ab. Out of three additional antibodies tested (one pAb, and two mAb), only one mAb showed reactivity to CD248 (antibodies used can be found in the appendix section).

Additional confirmation of the KD efficiency was seen with the used CD248-mAb. Using the CD248-mAb, Western blot analysis of KD lysates showed partial knockdown of CD248 at 150kDa and an additional knockdown at 55-60kDa in siCD248-Treated lysate in comparison to siNegScr-Treated and UT-Cells (Figure 4.8E) (Figure 4.8F). While the pAb-CD248 showed the most reactivity to CD248 at 90kDa, in transfected and untransfected MSCs, the mAb-CD248 showed no reactivity to CD248 at 90kDa neither in UT-cells nor in siNegScr-Treated (Figure 4.8E). Moreover, the 90kDa band of CD248 was the band of interest since it was initially observed to be the overexpressed band in HR AML-MSCs (Figure 4.3A, 4.4A)(Figure 4.8D, right panel). Following these Western blot initial confirmation of efficient CD248 KD, Flow cytometry was used with a varied clone of CD248-pAb to furtherly assess and determine the KD efficiency.

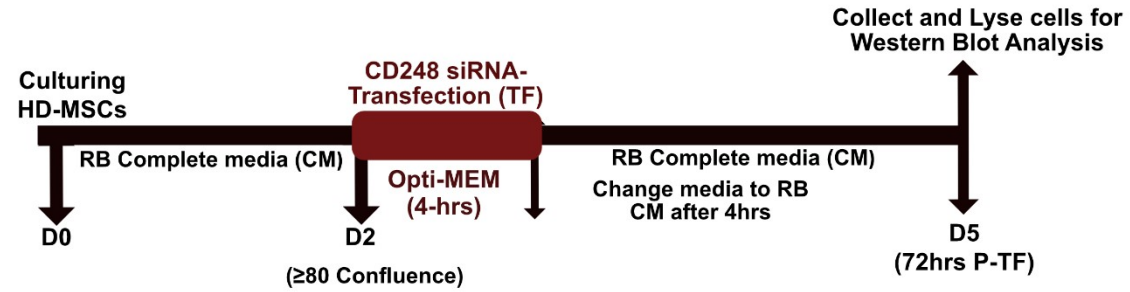
Collect and Lyse cells for Western Blot Analysis
Culturing HD-MSCs
CD248 siRNA-Transfection (TF)
RB Complete media (CM)
Opti-MEM (4-hrs)
RB Complete media (CM)
Change media to RB CM after 4hrs
D0
D2
(≥80 Confluence)
D5
(72hrs P-TF)

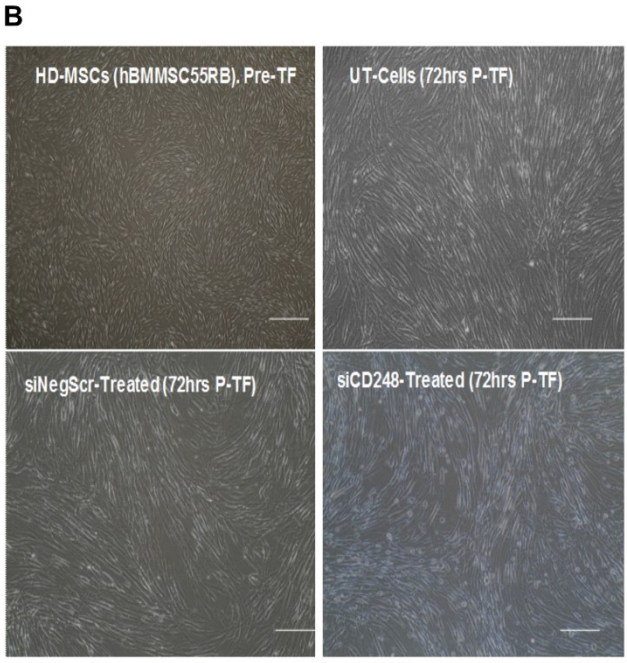
B
HD-MSCs (hBMMSC55RB). Pre-TF
UT-Cells (72hrs P-TF)
siNegScr-Treated (72hrs P-TF)
siCD248-Treated (72hrs P-TF)

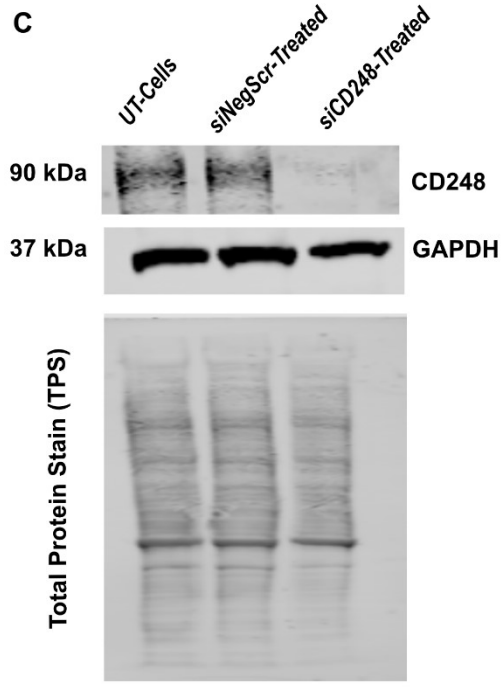
C
UT-Cells
siNegScr-Treated
siCD248-Treated
90 kDa
CD248
37 kDa
GAPDH
Total Protein Stain (TPS)

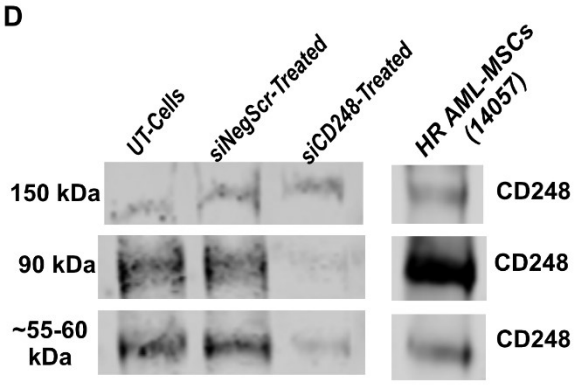
D
UT-Cells
siNegScr-Treated
siCD248-Treated
HR AML-MSCs (14057)
150 kDa
CD248
90 kDa
CD248
~55-60 kDa
CD248

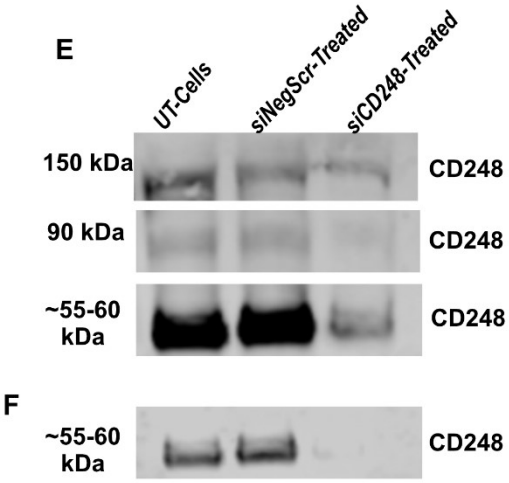
E
UT-Cells
siNegScr-Treated
siCD248-Treated
150 kDa
CD248
90 kDa
CD248
~55-60 kDa
CD248
F
~55-60 kDa
CD248

Figure.4.8. Efficient siRNA CD248 knockdown in HD-MSCs confirmed by Western blot analysis. siCD248-Treated MSCs have a significant decrease in CD248 protein level compared with siNegScr-Treated and untreated UT-cells. A) Transfection (TF) timeline: HD-MSCs seeded at 3.7x10 in T75 flasks. After 2 days (80% confluence), media was changed to Opti-MEM low serum media, and transfection complexes were added to each condition. After 4 hours of TF, media was replaced by complete media, and cells were incubated for three days at 37OC. Then cells were harvested, lysed, and cell lysates were used for Western blot analysis to confirm KD using protein concentration of 40ug of siCD248-Treated, siNegScr-Treated, and un-transfected cells lysates. B) Microscopic images were taken 72-hours post-TF and before analysis, showing normal morphology and high viability of transfected and un-transfected cells. c) A representative blot of western blot analyses was performed using pAb-CD248 and a secondary conjugated Ab. GAPDH was used as a control. The KD was initially observed at 90kDa; then, the blot was stripped and stained with TPS. Images were taken by Li core Odyssey instrument at channel 800 for CD248, GAPDH, and channel 700 for total protein signals. D) Western blot analysis shows additional bands of CD248 using the pAb as in (B) and representative bands of HR AML-MSCs. E and F) Western blots incubated with CD248-mAb showing most reactivity to CD248 at ~55-60kDa bands.

4.7.2 Efficient siRNA CD248 Knockdown on HD-MSCs confirmed by Flow cytometry

Prior to Flow cytometry staining, the viability of transfected and un-transfected MSCs 72-hour P-TF was determined. MSCs were harvested and counted in Trypan blue using a cell counter to determine the percentage of viable cells in each condition. Normal fibroblast-like morphology was observed for transfected and un-transfected MSCs (Figure 4.9B). Interestingly, all transfected; siCD248-Treated, siNegScr-Treated, and un-transfected MSCs exhibited high viabilities. The viability of these CD248 KD MSCs was comparable to the viabilities of un-transfected control cells, UT-cells, and siNeg-transfected cells. Specifically, viabilities results showed that an average of 91.5% of siCD248-Treated cells were viable, 92.6% of siNegScr-Treated cells were viable, and 94% UT-cells were viable (Figure 4.9C) (n=5).

Utilizing a varied clone of CD248-pAB (CD248 Ab-conjugated to Alexa flour 647), consistent with the western blot results, Flow cytometry results of five independent experiments with ≥ 2 technical replicates of each experiment showed a significant KD of CD248 on siCD248-Treated HD-MSCs. CD248 was significantly KD with a p-value of (0.0007) and a p-value of (0.0008) in comparison to siNegScr-Treated and UT-Cells, respectively (Figure 4.9D and E). A consistent and similar pattern of KD was observed in each experiment individually between the three conditions, transfected (siCD248-Treated, siNegScr-Treated) and un-transfected UT-Cells. (Figure 4.9D). These results collectively confirmed a successful siRNA KD of CD248 in HD2-55RB. Therefore, the established siRNA CD248 KD protocol was used to perform additional verification of CD248 KD in HR AML-MSCs (n=1).

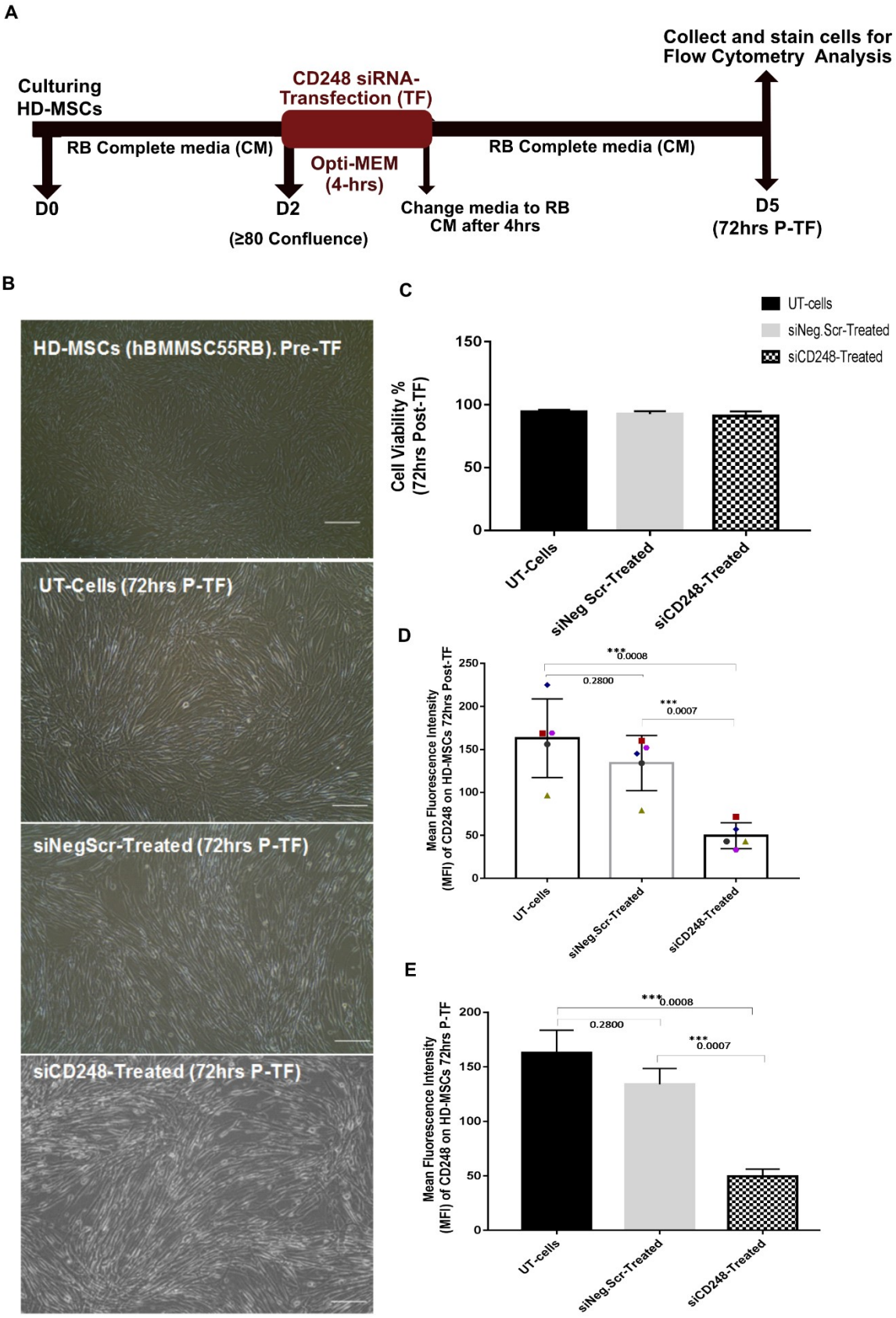
A
Collect and stain cells for Flow Cytometry Analysis
Culturing HD-MSCs
CD248 siRNA-Transfection (TF)
RB Complete media (CM)
Opti-MEM (4-hrs)
RB Complete media (CM)
D0
D2
(≥80 Confluence)
Change media to RB CM after 4hrs
D5
(72hrs P-TF)
B
HD-MSCs (hBMMSC55RB). Pre-TF
UT-Cells (72hrs P-TF)
siNegScr-Treated (72hrs P-TF)
siCD248-Treated (72hrs P-TF)
C
UT-cells
siNeg.Scr-Treated
siCD248-Treated
Cell Viability % (72hrs Post-TF)
150
100
50
0
UT-Cells
siNeg Scr-Treated
siCD248-Treated
D
Mean Fluorescence Intensity (MFI) of CD248 on HD-MSCs 72hrs Post-TF
250
200
150
100
50
0
***0.0008
0.2800
***0.0007
UT-cells
siNeg.Scr-Treated
siCD248-Treated
E
Mean Fluorescence Intensity (MFI) of CD248 on HD-MSCs 72hrs P-TF
200
150
100
50
0
***0.0008
0.2800
***0.0007
UT-cells
siNeg.Scr-Treated
siCD248-Treated

Figure.4.9. Efficient siRNA CD248 knockdown on HD-MSCs validated by Flow cytometry. siCD248 treated MSCs have a significant decrease in CD248 protein level compared with siNeg-Scr and untreated UT-cells. A) Transfection (TF) outline: HD-MSCs seeded at 3.7x10 in T75 flasks. After 2 days (80% confluence), media was changed to Opti-MEM low serum media, and transfection complexes were added to each condition. After 4 hours of TF, media was replaced by complete media, and cells were incubated for three days at 37OC. Then cells were harvested, stained, and analyzed by Flow cytometry B) Normal morphology and C) High viability of transfected and un-transfected cells were observed. C) Flow cytometry results of CD248 MFI normalized to IgG isotype 72-hrs pot-transfection. Five independent experiments were performed. Each colored symbol in the figure represents the mean of >2 technical replicates of each experiment. CD248 was KD with a *** $p = 0.0007$ in comparison to siNeg-Scr-treated cells, and *** $p = 0.0008$ compared to UT-cells.

4.7.3 Efficient siRNA KD of CD248 on HR AML-MSCs (HR-AML4)

CD248 was upregulated in HR AML-MSCs at the gene and protein levels, as determined by the transcriptomic analysis and western blot validation in sections and X, respectively. CD248 KD was efficient on HD-MSCs (HD2-55RB), as seen in sections 4.7.1 and 4.7.2 of this chapter. To validate and confirm the KD protocol efficiency on HR AML-MSCs, siRNA KD of CD248 was performed on HR AML-MSCs (HR AML-4). HR-AML4 were cultured in RoosterBio complete media. Following the establishment and maintenance of their culture, transfection was performed using the established protocol in section 4.7.1. Then, the cell-surface CD248 level was determined by Flow cytometry (Figure 4.10A). (Three technical replicates were performed).

Similar to HD-MSCs, both transfected and un-transfected HR AML-MSCs exhibited high viability (Figure 4.10B). Interestingly, an efficient KD of CD248 in siCD248- Treated HR AML-MSCs was found compared to siNegScr-Treated, and UT-cells HR AML-MSCs. CD248 was KD by 73.0% in siCD248-Treated HR AML-MSCs compared to siNegScr and by 78.9% compared to UT-MSCs.The knockdown was significant, with a p-value of 0.0075 compared to siNegScr-Treated cells and a p-value of <0.0001 compared to untreated AML-MSCs (Figure 4.10C).

As seen, the efficiency of the established KD protocol using TransIT-X2 was validated and confirmed by the consistent results of Western blot and flow cytometry analyses using three various Abs clones against CD248 in both HD-MSCs and HR AML-MSCs. Both efficient KD and high and comparable viabilities of transfected (siCD248-Treated and siNegScr-Treated) and UT-MSCs were obtained.

These results collectively validated the efficiency of CD248 KD and confirmed the establishment of siCD248-MSCs as an in vitro KD model using (HD2-55RB) which enabled the further investigation of CD248 significance at MSC's functional level. Furthermore, as seen in sections 4.7.1, 4.7.2, and 4.7.2, only western blot and flow cytometry analyses were used to determine the KD efficiency, and no additional technique was used to estimate the KD efficiency further.

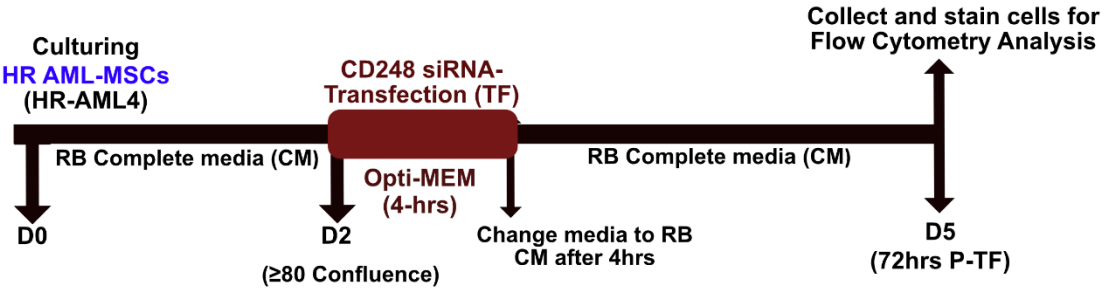
Culturing
HR AML-MSCs
(HR-AML4)
CD248 siRNA-
Transfection (TF)
Collect and stain cells for
Flow Cytometry Analysis
RB Complete media (CM)
Opti-MEM
(4-hrs)
RB Complete media (CM)
D0
D2
(≥80 Confluence)
Change media to RB
CM after 4hrs
D5
(72hrs P-TF)

B

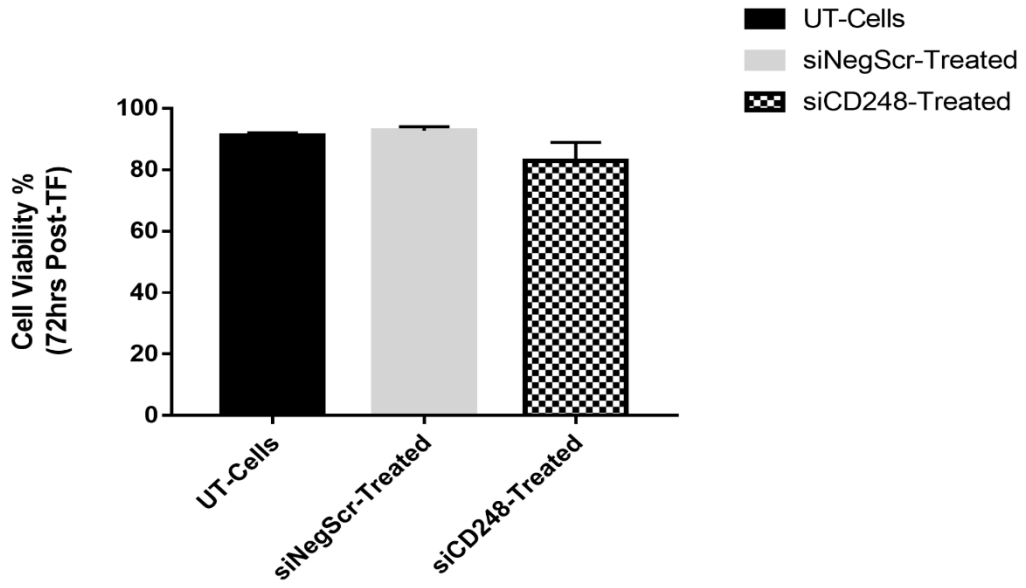
UT-Cells
siNegScr-Treated
siCD248-Treated
Cell Viability %
(72hrs Post-TF)
100
80
60
40
20
0
UT-Cells
siNegScr-Treated
siCD248-Treated

C

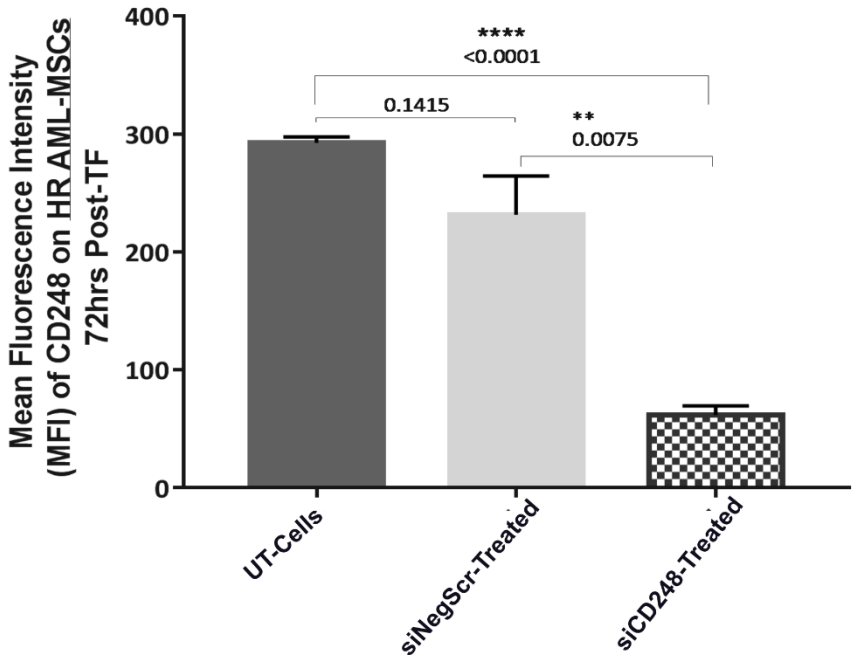
Mean Fluorescence Intensity
(MFI) of CD248 on HR AML-MSCs
72hrs Post-TF
400
300
200
100
0
****
<0.0001
0.1415
**
0.0075
UT-Cells
siNegScr-Treated
siCD248-Treated

Figure.4.10. Successful Knockdown of CD248 on HR AML-MSCs (HR-AML4) validated by Flow cytometry. siCD248 treated MSCs have a significant decrease in CD248 protein level compared with siNeg-Scr and untreated cells (UT-cells). A) Transfection (TF) outline: HR AML-MSCs (HR-AML4) seeded at $3.7x10^5$ in T75 flasks. After 2 days (80% confluence), media was changed to Opti-MEM low serum media, and transfection complexes were added to each condition. After 4 hours of TF, media was replaced by complete media, and cells were incubated for 3 days at 37OC. Then cells were analyzed by Flow cytometry. B) HR AML-4 viabilities 27hrs Post-TF (n=3) were determined by trypan blue and a cell counter. C) Flow cytometry results of CD248 MFI normalized to IgG isotype 72-hrs pot-transfection. Results of one experiment with three technical replicates are shown. CD248 was KD efficiently with a ** $p = 0.0075$ in comparison to siNeg-Scr-treated cells, and *** $p = 0.0001$ compared to UT-cells. An unpaired t-test was used for determining the significant p-value.

CHAPTER 5

Potential role of CD248 in HD-MSCs Function (siCD248-MSCs Functional Assessments)

5.1. CD248 Knockdown effect on HD-MSCs Differentiation

As introduced in chapter 1, section 1.4, one of MSC's characteristic features is the ability to differentiate into adipocytes and osteocytes, two cell types that are essential components of BME, in vivo as well as in vitro. As observed previously by Guardia and colleagues (184), HR AML MSCs exhibited an impairment of their differentiation potentials, particularly reduction in both adipogenesis and osteogenesis. Interestingly, significant upregulation of CD248 at both gene and protein levels on these HR samples was found (as seen in chapters 3 and 4). Considering these observations, to understand the potential involvement of CD248 in HD-MSCs' function, an investigation of the impact of CD248 KD in HD-MSCs was conducted through in vitro differentiation assays, including adipogenesis and osteogenesis.

5.1.1 siCD248-MSCs osteogenic differentiation

The osteogenic potential of healthy untreated MSCs and siCD248-MSCs was tested using a well-accepted in vitro MSCs osteogenic differentiation assay. Using the previously described CD248 KD protocol (chapter 4), HD-MSCs (HD2-55RB) were transfected for 4 hours, and then MSC's osteogenic differentiation was induced. The normal and siRNA-treated cells, KD MSCs, were treated and maintained in differentiation media supplemented with an osteogenic supplement that contains essential growth factors to drive MSC osteogenesis, which was driven over a 2-week culture period. Following the first osteogenic induction, media was changed to fresh base differentiation media supplemented with osteogenic supplement every three days for 13-14 days. Following the entire induction/ culture

period, osteocyte formation was detected using Alizarin Red staining, which binds directly to calcium deposits produced by mature osteoblasts. All MSCs, transfected; siCD248-Treated and siNegScr-Treated, and un-transfected control MSCs, UT-Cells, were stained with Alizarin Red stain to assess their osteogenic differentiation qualitatively. Also, undifferentiated cells of each transfection condition were stained and used as negative controls (Figure 5.1A and B).

Microscopic evaluation was performed using bright field microscopy. Results showed that all stained undifferentiated transfected and untransfected cells, siCD248-Treated, siNegScr-Treated, and UT-MSCs, UT-Cells, (Figure 5.1B Right panel) were confluent and exhibited normal morphology. Furthermore, all differentiated siCD248-Treated, siNegScr-Treated, and un-transfected MSCs, UT-Cells, could differentiate to osteogenic lineage. Mature osteoblasts were observed under all transfection conditions. (Figure 5.1B, Left and middle panel). Moreover, no significant difference in HD-MSCs' ability to form calcium deposits between siCD248-Treated, siNegScr-Treated, and control un-transfected HD-MSCs, UT-Cells, was observed (n=4). As seen above, osteogenic differentiation results showed no effect of CD248 KD on siCD248-Treated HD-MSCs when differentiated toward osteogenic lineage compared to un-transfected control cells UT-Cells, and siNegSCr-Treated HD-MSCs (four independent experiments were performed, n=4). These results suggested that a reduced level of CD248 protein in HD-MSCs had no significant effect on their osteogenic differentiation potency.

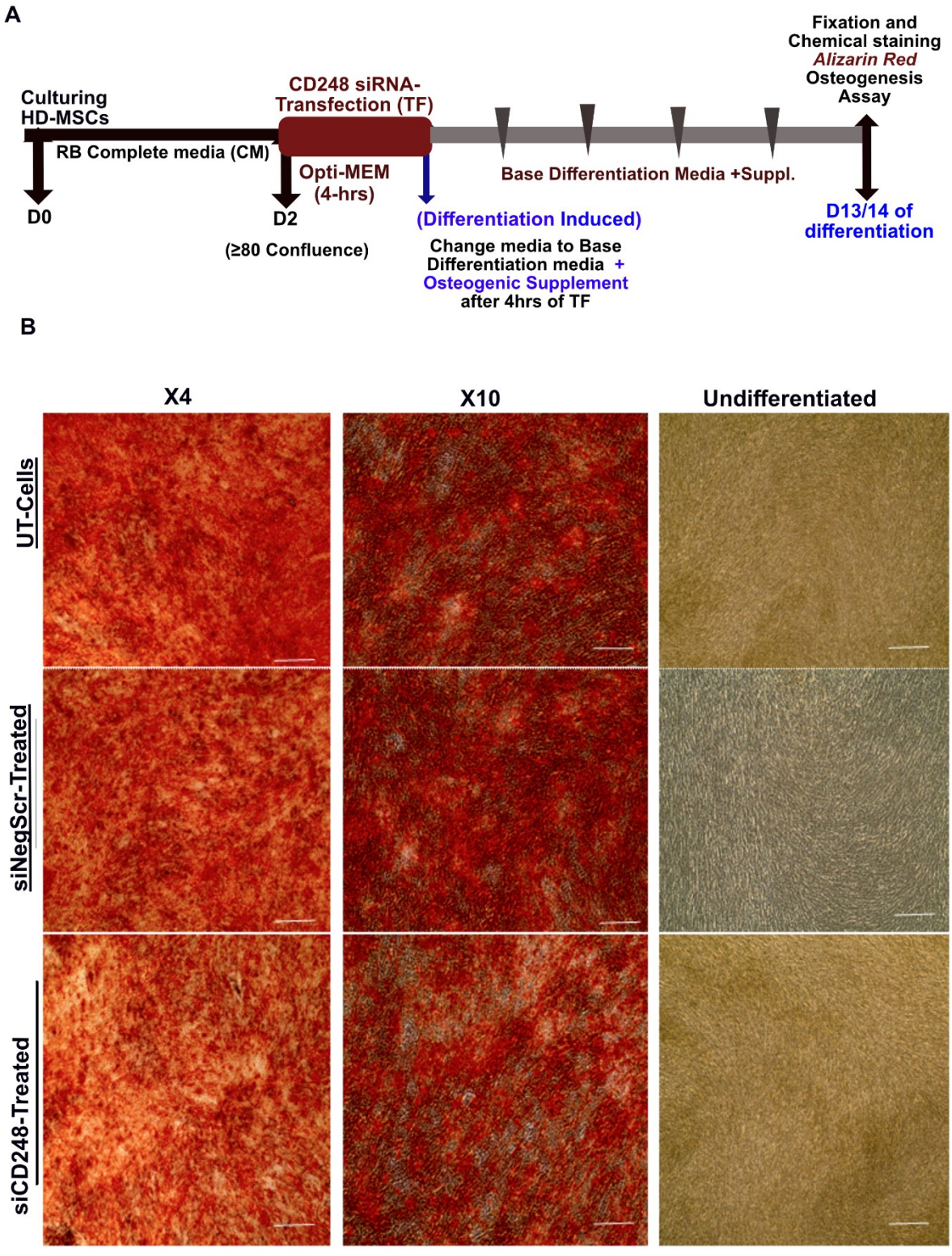
A
Culturing
HD-MSCs
RB Complete media (CM)
D0
CD248 siRNA-
Transfection (TF)
Opti-MEM
(4-hrs)
D2
(≥80 Confluence)
(Differentiation Induced)
Change media to Base
Differentiation media +
Osteogenic Supplement
after 4hrs of TF
Base Differentiation Media +Suppl.
Fixation and
Chemical staining
Alizarin Red
Osteogenesis
Assay
D13/14 of
differentiation
B
X4
X10
Undifferentiated
UT-Cells
siNegScr-Treated
siCD248-Treated

Figure.5.1. siCD248-MSCs Osteogenic differentiation. siCD248 transfected, and un-transfected cells were induced after 4 hours of transfection. Representative images of transfected and un-transfected MSCs following three-four rounds of induction with osteogenic-supplemented media throughout 14 days of culture. Alizarin red staining (left and middle panel) showed no significant difference between transfected and un-transfected cells. (n = 4). A) Transfection and differentiation timeline. B) Differentiated and undifferentiated cells HD-MSCs (HD2-55RB). All cells have the same osteogenic differentiation ability. Top panel: UT-cells, middle panel: siNeg-Scr treated, and bottom: siCD248 treated cell. Undifferentiated cells of each condition (right panel) were stained and used as negative controls for differentiation. Images were taken using bright field microscopy. Magnification X10, Scale bar 100µm.

5.1.2. siCD248-MSCs exhibited a reduced adipogenic differentiation potential

The adipogenic potential of healthy untreated MSCs and siCD248-MSCs was tested using a well-accepted in vitro MSCs adipogenic differentiation assay. HD-MSCs (HD2-55RB) were transfected for 4 hours per the established KD protocol. Then the normal (un-transfected control cells, UT-Cells) and KD MSCs (siCD248-Treated and siNegScr-Treated) were treated with base differentiation media supplemented with the adipogenic supplement that contains essential growth factors to drive MSC's adipogenesis. Cells were maintained under differentiation conditions for 14 days. Following the entire induction period, formed lipid vacuoles were detected using Oil Red O staining to assess MSCs adipogenic differentiation. All MSCs, transfected (siCD248-Treated and siNegScr-Treated) and un-transfected control MSCs, were stained with Oil Red O (Figure 5.2A).

Microscopic evaluation was performed to examine the stained cells using bright field microscopy. siCD248-Treated, siNegScr-Treated, and un-transfected UT-Cells, HD-MSCs were all able to differentiate to adipocytes (Figure 5.2B left and middle). Moreover, although transfected (siCD248-Treated, siNegScr-Treated) and un-transfected cells all differentiated toward adipocytes (represented by the formation of lipid vacuoles), a reduced amount of Oil Red O stained lipid vacuoles was consistently observed in siCD248-treated MSCs compared to the control cells Four independent experiments were performed however, no image software was used to quantify the adipocytes which could limit the current analysis. Moreover, these observations suggested that decreased level of CD248 negatively impacted HD-MSCs adipogenic differentiation capacity.

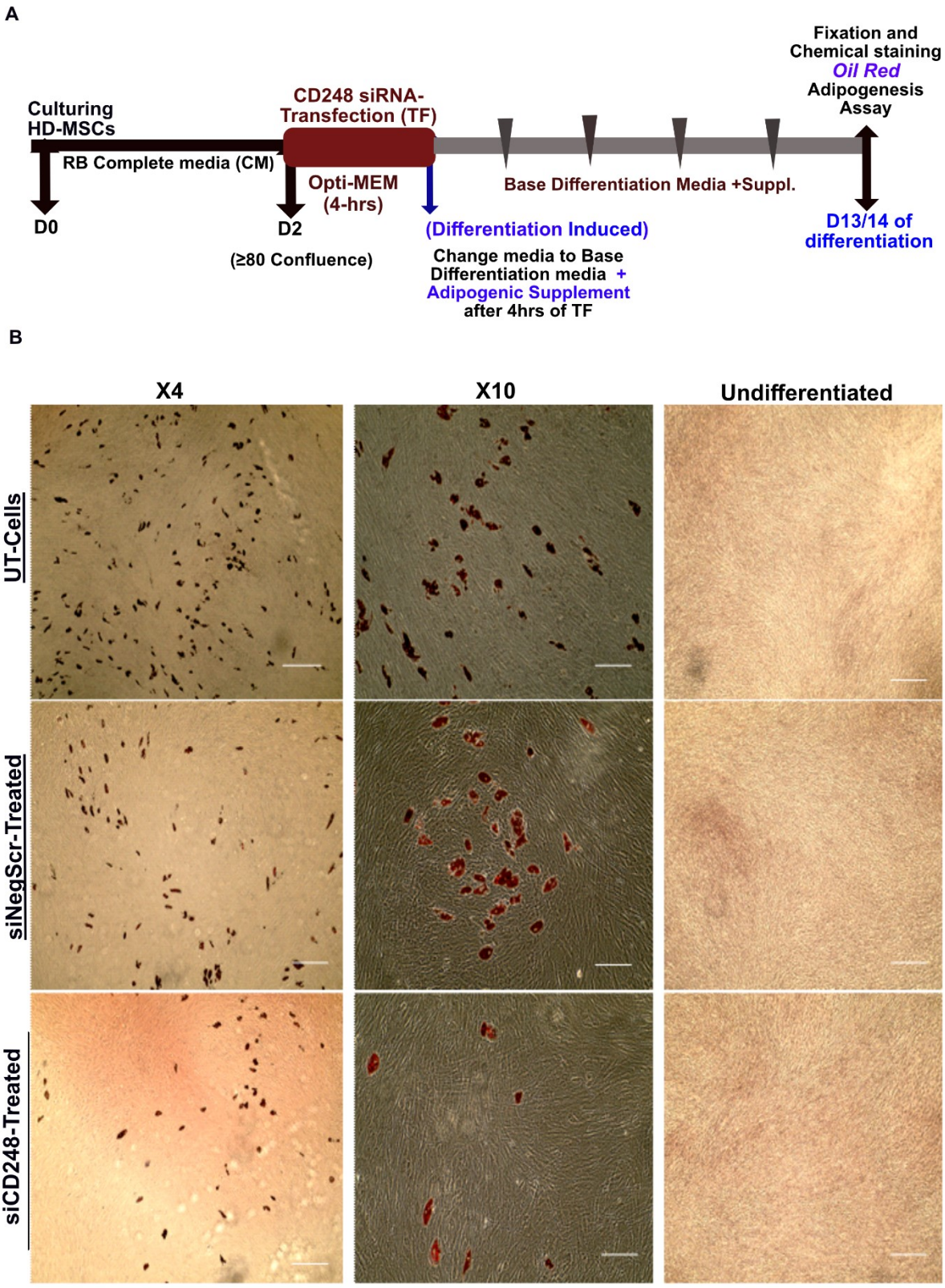
A
Culturing HD-MSCs
RB Complete media (CM)
D0
CD248 siRNA-Transfection (TF)
Opti-MEM (4-hrs)
D2
(≥80 Confluence)
(Differentiation Induced)
Change media to Base Differentiation media + Adipogenic Supplement after 4hrs of TF
Base Differentiation Media +Suppl.
Fixation and Chemical staining Oil Red Adipogenesis Assay
D13/14 of differentiation
B
X4
X10
Undifferentiated
UT-Cells
siNegScr-Treated
siCD248-Treated

Figure.5.2. CD248 knocked down HD-MSCs (siCD248-HD-MSCs) have reduced adipogenic differentiation potential. siCD248 transfected, and un-transfected cells were induced after 4 hours of transfection. Representative images of transfected and untransfected MSCs following three-four rounds of induction with adipogenic-supplemented media throughout 14 days of culture. A) Transfection and differentiation outline. B) Oil red staining (left and middle panel) showed a reduced capacity for forming lipid vacuoles between siCD248-transfected (bottom, and control cells (top and middle) (n = 4). Undifferentiated cells of each condition (right panel) were stained and used as negative controls for differentiation. Images were taken using bright field microscopy. Magnification X10, Scale bar 100µm.

5.1.3 qRT-PCR Validation of siCD248-MSCs reduced adipogenesis

In section 5.1.2, microscopic evaluation of the effect of CD248 KD in HD-MSCs adipogenic differentiation using adipocytes staining, Oil Red O Stain, showed that although positive staining was observed in all transfection conditions, siCD248-Treated HD-MSCs showed a reduced adipogenic potential. They formed fewer adipocytes and lipid vacuoles than the controls; NegScr-Treated and UT-Cells.

A targeted quantitative gene expression analysis was conducted using qRT-PCR (n=1) to evaluate expression levels of genes involved in adipogenesis to confirm and quantify the observed reduced adipogenic potential of CD248 KD HD-MSCs. The pathway analysis included key adipogenesis markers and multiple adipogenesis-associated genes (Table 5.1). HD-MSCs were transfected using the established CD248 KD protocol. Transfected and untransfected HD-MSCs were then differentiated with adipogenic supplemented media as described in section 5.1.2. After that, total RNA was extracted and isolated from these transfected and un-transfected differentiated cells and then used in the predesigned prime PCR assay (Figure 5.3A).

A heat map was generated using qRT-PCR results (n=1) of gene expressions. Expressions of all amplified adipogenesis-associated genes were included and graphed. The results demonstrated dysregulation in some genes' expressions between the KD conditions (Figure 5.3B). Although no significant change in the gene expression levels of adipogenesis key markers, CEBP (CEBPβ, CEBPδ) and PPARγ (PPARα, PPARδ) was found between siCD248-Treated and untreated MSCs; interestingly, CEBPα expression was slightly increased in

siCD248-MSCs compared to its level in siNegScr-Treated and UT-MSCs (Figure 5.3C) (Figure 3.5D). Additionally, the assay showed some alteration in other adipogenesis-associated genes. While some genes were upregulated, others were downregulated in siCD248-Treated MSCs (Figure 3.5E). Interestingly, among some slightly altered adipogenesis genes, ADIPOQ and SIRT2 were highly dysregulated in siCD248-Treated MSCs. The expression levels of these genes were increased in siCD248-MSCs by approximately 13 FC compared to their levels in siNegScr-Treated and UT-Cells. Due to the limitation of regenerating high-quality RNAs from these differentiated KD cells, obtaining the gene expression data using the exact qRT-PCR approach from two additional independent experiments was unsuccessful. Therefore, additional validation of these primary qRTPCR results (n=1) could be required in future studies to confirm the expression of adipogenesis master genes and the SIRT2 gene.

Gene	Gene	Gene	Gene
ADIG	BMP4	LRP5	SLC2A4
ADIPOQ	BMP7	MAPK14	SRC
ADRB2	CCND1	NCOA2	SREBF1
AGT	CDK4	NCOR2	TAZ
ANGPT2	CDKN1A	NR0B2	TCF7L2
AXIN1	CDKN1B	NR1H3	TSC22D3
B2M	CEBPA	NRF1	TWIST1
BMP2	CEBPB	PPARA	UCP1
CEBPD	ACTB	PPARG	WNT1
CFD	EGR2	PPARGC1A	WNT10B
CREB1	FABP4	PPARGC1B	WNT3A
DDIT3	FASN	PRDM16	WNT5A
DIO2	FGF1	RB1	WNT5B
DKK1	FGF10	RETN	TBP
DLK1	FGF2	RPLP0	GAPDH
E2F1	FOXC2	RUNX1T1	IRS2
GATA2	FOXO1	RXRA	JUN
GATA3	KLF15	SFRP1	LIPE
GUSB	KLF2	SFRP5	LMNA
HES1	KLF3	SHH	LPL
HPRT1	CACB	PPARD	VDR
INSR	KLF4	SIRT1	SIRT3
IRS1	LEP	SIRT2	

Table 5.1. List of the adipogenesis genes tested in the prime PCR assay. PrimePCR adipogenesis (predesigned 96-well) assay was used to validate the significance of siCD248-MSCs adipogenesis reduction

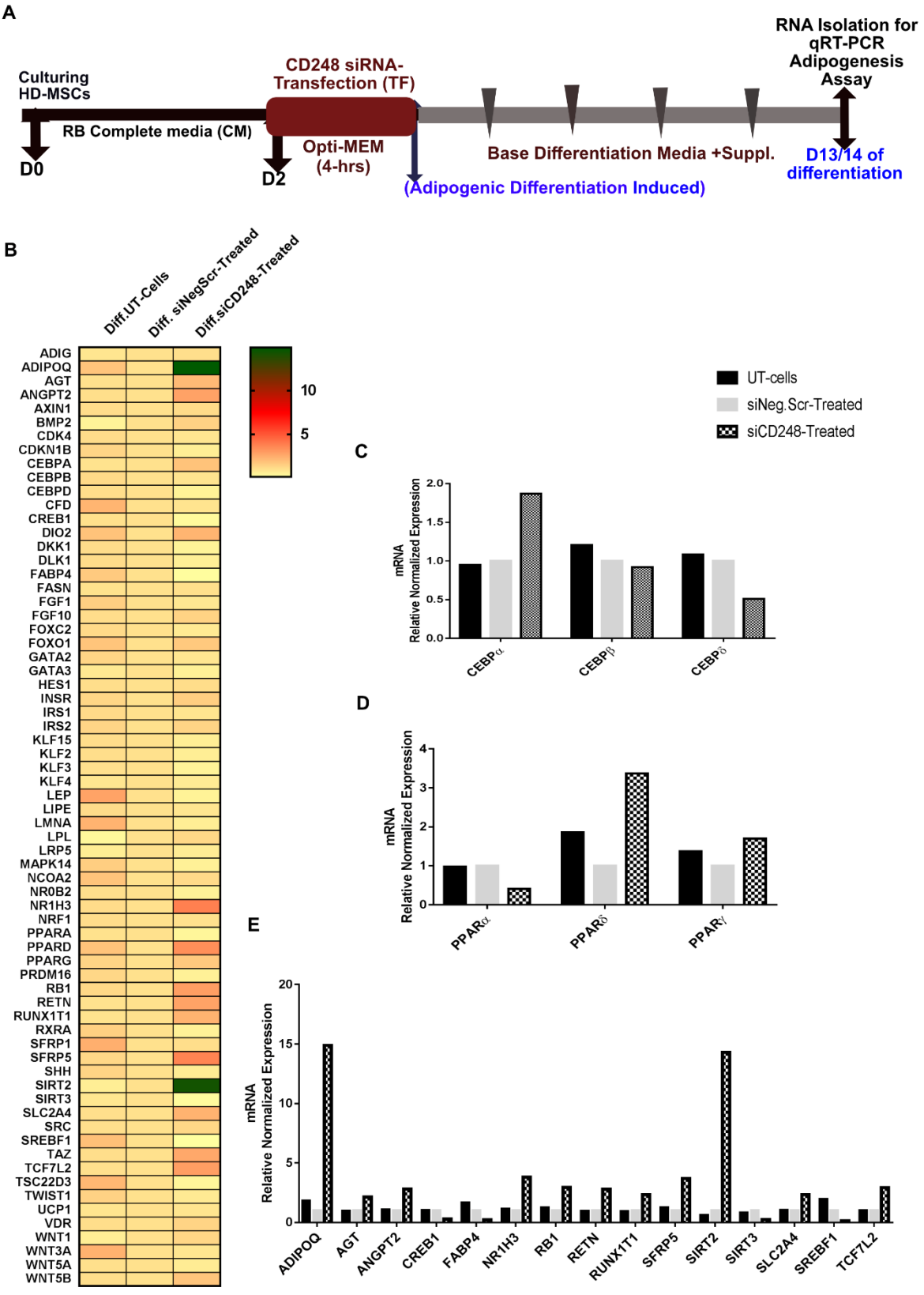
A
Culturing HD-MSCs
RB Complete media (CM)
D0
CD248 siRNA-Transfection (TF)
Opti-MEM (4-hrs)
D2
(Adipogenic Differentiation Induced)
Base Differentiation Media +Suppl.
RNA Isolation for qRT-PCR Adipogenesis Assay
D13/14 of differentiation
B
Diff.UT-Cells
Diff. siNegScr-Treated
Diff.siCD248-Treated
ADIG
ADIPOQ
AGT
ANGPT2
AXIN1
BMP2
CDK4
CDKN1B
CEBPA
CEBPB
CEBPD
CFD
CREB1
DIO2
DKK1
DLK1
FABP4
FASN
FGF1
FGF10
FOXC2
FOXO1
GATA2
GATA3
HES1
INSR
IRS1
IRS2
KLF15
KLF2
KLF3
KLF4
LEP
LIPE
LMNA
LPL
LRP5
MAPK14
NCOA2
NR0B2
NR1H3
NRF1
PPARA
PPARD
PPARG
PRDM16
RB1
RETN
RUNX1T1
RXRA
SFRP1
SFRP5
SHH
SIRT2
SIRT3
SLC2A4
SRC
SREBF1
TAZ
TCF7L2
TSC22D3
TWIST1
UCP1
VDR
WNT1
WNT3A
WNT5A
WNT5B
10
5
C
UT-cells
siNeg.Scr-Treated
siCD248-Treated
mRNA Relative Normalized Expression
2.0
1.5
1.0
0.5
0.0
CEBPα
CEBPβ
CEBPδ
D
mRNA Relative Normalized Expression
4
3
2
1
0
PPARα
PPARδ
PPARγ
E
mRNA Relative Normalized Expression
20
15
10
5
0
ADIPOQ
AGT
ANGPT2
CREB1
FABP4
NR1H3
RB1
RETN
RUNX1T1
SFRP5
SIRT2
SIRT3
SLC2A4
SREBF1
TCF7L2

Figure 5.3. **qRT-PCR confirmation of CD248 knockdown effect on adipogenesis genes.** A) Transfection and differentiation outline to generate RNAs from transfected differentiated MSCs. Isolated RNAs were then used to synthesize cDNAs and used in the Adipogenesis prime PCR assay. B) Heat map generated from PCR gene expressions results (n=1) of amplified and expressed genes in at least one of the three transfection conditions, siCD248-treated, siNeg-Scr-treated, and UT-cells. C and D) Adipogenesis master markers expressions were graphed from the heat map. siNegScr-treated MSCs expressions were set as a control in CFX maestro Bio-Rad PCR software to normalize the values of both UT- and siCD248-treated in the graphed expressions. E) Adipogenesis genes with relatively increased expression or decreased expression compared to the two controls. SIRT2 showed an upregulated expression in siCD248-MSCs.

5.1.4. Reduction of siCD248-MSCs adipogenesis potentially attributed to SIRT2

To further explore the possible mechanism by which CD248 KD-resulted gene alterations were involved in adipogenesis reduction, an in-silico analysis using the above findings (section 5.1.3) (Figure 5.4 E) was performed. When an upregulation of SIRT2 was applied to the canonical adipogenesis pathway using IPA overlay and prediction tools, the analysis predicted inhibition of MSCs adipogenesis pathway (Figure 5.5). It showed that upregulation of SIRT2 gene directly affects FoxO1 gene and leads to its inhibition. Inhibition of FoxO1 directly inhibited MSCs differentiation toward mature adipocytes. Particularly, it inhibited both adipogenesis key markers CEBPα and PPARγ and consequently inhibited the expression of their downstream targets. These initial results showed that CD248 KD on HD-MSCs impacted their adipogenesis gene profile toward a reduction of adipogenesis and validated the microscopic observation of siCD248-MSCs' reduced ability to form adipocytes. Although, slight increase was observed in CEBPα while no change was seen in FoxO1 (Figure 3.5), the predicted mechanism validated the observed microscopic reduction. Considering the limitation of PCR predesigned assay, additional validation of SIRT2, CEBPα genes using specific primers could be required to ensure the effect of CD248 KD on MSCs and the validity of the predicted mechanism. Taken together, the reduced potential was predicted to be attributed to SIRT2 upregulation in CD248 KD cells. These *in silico* predictions suggest that loss of CD248 in HD-MSC results in increased SIRT2 gene expression, which in turn could lead to inhibition of mature adipocyte formation through inhibiting the FoxO1 gene.

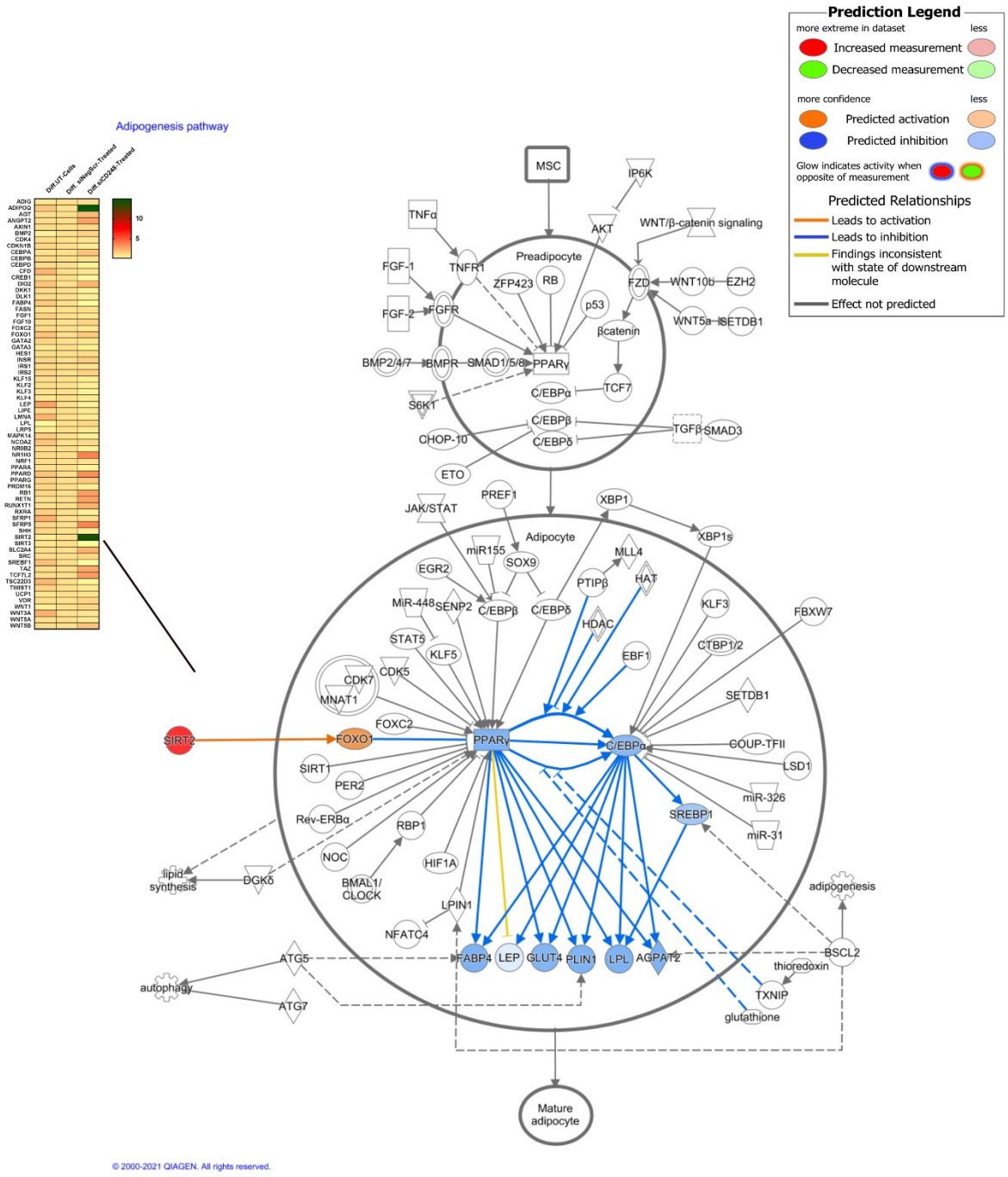

Figure 5.4. IPA analysis of SIRT2 upregulation in siCD248-MSCs showed inhibition of MSCs adipogenesis pathway. Red=applying SIRT2 upregulation,

blue predicted inhibition. The solid line represents the direct effect, while the dotted line represents the indirect effect.

5.2 Profiling of siCD248-MSCs proteins using protein microarray (MA)

As introduced in chapter 1, MSCs are significant players in BME, providing cellular components through differentiation and producing multiple proteins with critical autocrine and paracrine activities. These proteins define several functions of MSCs, such as their role in HSCs regulation, immunomodulation, and angiogenesis. In section 5.1, knocking down CD248 negatively impacted HD-MSCs adipogenic differentiation. Differentiated siCD248-MSCs showed a reduced adipogenic differentiation potential. To gain more insights into the CD248 KD effect on HD-MSCs from a proteomic aspect, the effect of CD248 KD was examined on HD-MSCs protein profile using protein microarray (human angiogenesis array). This membrane-based specific-antibody microarray was used to simultaneously compare the relative expression level of 55 proteins (Table 5.2) in siCD248-Treated MSCs with control MSCs. This approach could identify potential correlations between CD248 and other MSCs proteins. Mostly MSCs proteins with angiogenic roles such as VEGF, Ang-1, and TGF-β, mainly since CD248 role in angiogenesis is thoroughly investigated.

As per the transfection protocol in chapter 4, HD-MSCs (HD2-55RB) were transfected. 72 hours post-transfection, cells were harvested, and lysates were generated from all transfection conditions. Then, using a protein concentration of 300µg from each lysate, protein microarray (MA) was performed (Figure 5.5A). A lysate of each transfection condition was incubated in a single microarray membrane.

Confirmation of KD on siCD248-Treated MSCs lysate in comparison to lysates from the two controls, siNegScr-Treated and UT- cells, was assessed by Western blot analysis (Figure 5.5B). Positive and negative control signals were detected on the three MA membranes. Signals of all 55 proteins were observed in each membrane (n=3); fluorescent signals were detected in all three conditions (Figure 5.5C). The average signal intensity of two signals for each protein was determined and calculated in each membrane. Signals were then normalized to the average signal of five negative controls in that same membrane, and intensities were analyzed.

A heat map was generated using the mean of the normalized signals of each protein in each condition from three independent experiments (Figure 5.5D). As shown in the heat map, alterations in signals of multiple proteins were found between siCD248-Treated MSCs, siNegScr-Treated MSCs, and UT-Cells. Some proteins were highly abundant in siCD248-Treated MSCs, while others showed lower abundance levels in siCD248-MSCs. Furthermore, as expected, levels of several proteins were not changed between conditions. Their abundance level was comparable between the two conditions, siCD248-Treated and siNegScr-Treated MSCs, such as Endoglin/CD105 protein, a phenotypic marker of MSCs. It was among the unchanged proteins.

Moreover, grouped analysis using multiple t-tests through the FDR approach (Benjamini and Hochberg Q = 1%) was performed on these normalized signals (n=3) to precisely determine the significant difference in protein abundance levels between the two conditions; siCD248-Treated and siNegScr-Treated MSCs. Results

showed that among all of these proteins (p-value > 0.05) (Tables 5.3 and 5.4) growth factors HB-EGF (heparin-binding EGF-like) and EG-VEGF (endocrine-gland-derived vascular endothelial factor) were abundant in siCD248-MSCs (p-values of 0.012 and 0.006, respectively) in comparison to their levels in siNegScr-Treated MSCs. Further, when the grouped analysis was performed using UT-Cells as control, HB-EGF and EG-VEGF were also increased in siCD248-MSCs with a significant raw p-value (0.004 and 0.003), respectively. At the same time, PLGF increase was not significant in siCD248/UT-Cells (0.850, data not shown). However, the differences in these proteins' expression levels between the KD MSCs and siNegScr-Treated were with q-value > 0.05 (Table 5.3 and Table 5.4). Therefore, further validation of the increased levels of these two proteins using Western blot might be required to provide a definitive result. These results showed that knocking down CD248 insignificantly altered the MSC's protein profile; nonetheless, considering the complexity and nature of proteins, the results here provided an initial proteomic and signaling aspects of in vitro CD248 KD effect concerning HD-MSCs proteins. Further validation of the protein abundance levels of these two proteins (HB-EGF and EG-VEGF) in siCD248-MSCs using ELISA could confirm these findings and add additional insights into MSC's proteomic aspects.

Protein symbol	Protein symbol	Protein symbol
Activin A	FGF-7/KGF	PD-ECGF
ADAMTS-1	GDNF	PDGF-AA
Angiogenin	GM-CSF	PDGF-AB/PDGF-BB
Angiopoietin-1	HB-EGF	Persephin
Angiopoietin-2	HGF	CXCL4/PF4
Angiostatin/Plasminogen	IGFBP-1	PlGF
Amphiregulin	IGFBP-2	Prolactin
Artemin	IGFBP-3	Serpin B5/Maspin
Tissue Factor/Factor III	IL-1 beta	Serpin E1/PAI-1
CXCL16	CXCL8/IL-8	Serpin F1/PEDF
DPPIV/CD26	LAP (TGF-beta 1)	TIMP-1
EGF	Leptin	TIMP-4
EG-VEGF	CCL2/MCP-1	Thrombospondin-1
Endoglin/CD105	CCL3/MIP-1 alpha	Thrombospondin-2
Endostatin/Collagen XVIII	MMP-8	uPA
Endothelin-1	MMP-9	Vasohibin
FGF acidic	NRG1-beta 1	VEGF
FGF basic	Pentraxin 3	VEGF-C
FGF-4		

Table 5.2. Protein-list of all tested proteins in the protein profiler array. (Details about the assay can be found in chapter 2).

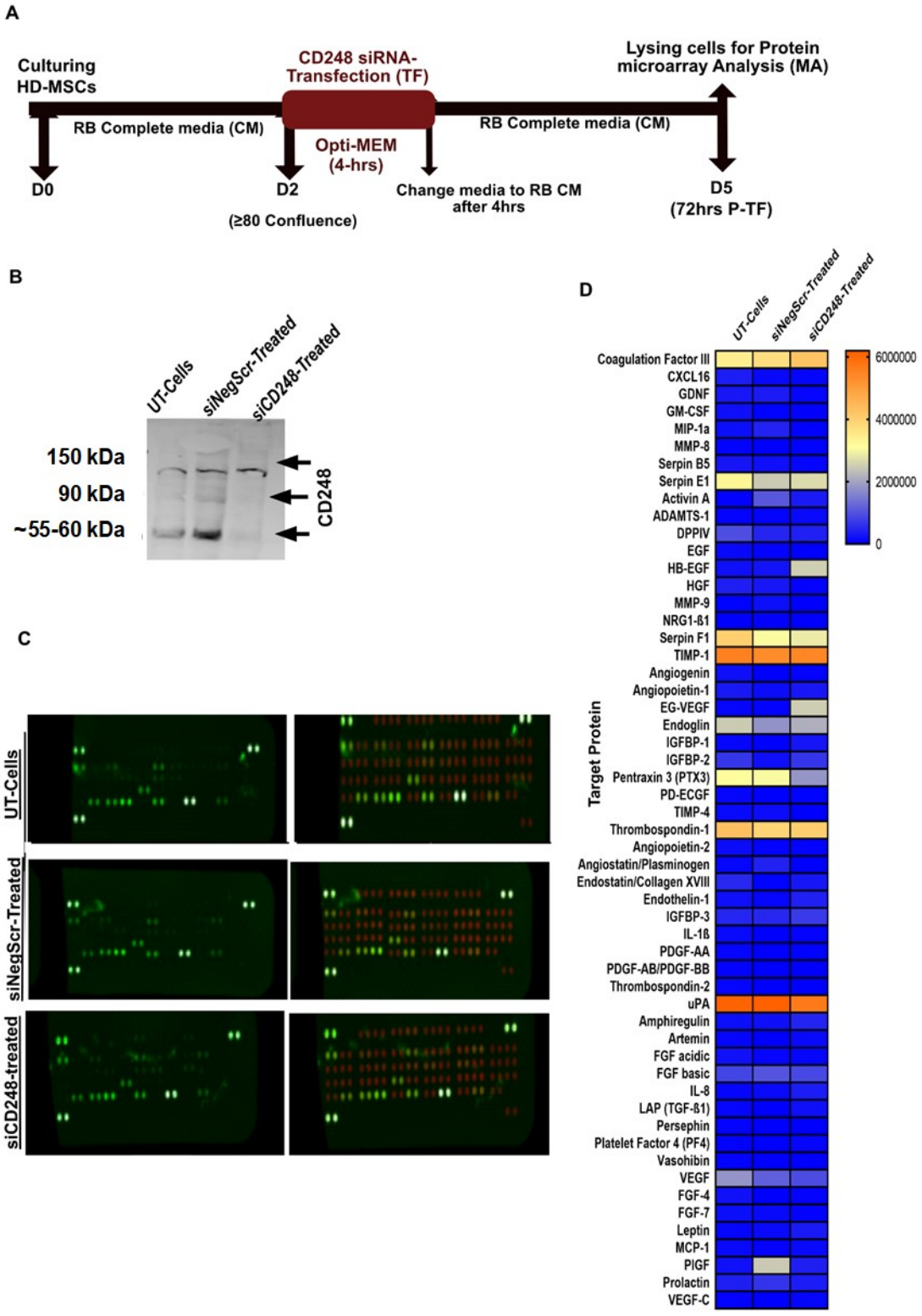
A
Culturing HD-MSCs
CD248 siRNA-Transfection (TF)
Lysing cells for Protein microarray Analysis (MA)
RB Complete media (CM)
Opti-MEM (4-hrs)
RB Complete media (CM)
D0
D2
(≥80 Confluence)
Change media to RB CM after 4hrs
D5
(72hrs P-TF)
B
UT-Cells
siNegScr-Treated
siCD248-Treated
150 kDa
90 kDa
~55-60 kDa
CD248
C
UT-Cells
siNegScr-Treated
siCD248-treated
D
UT-Cells
siNegScr-Treated
siCD248-Treated
Target Protein
Coagulation Factor III
CXCL16
GDNF
GM-CSF
MIP-1a
MMP-8
Serpin B5
Serpin E1
Activin A
ADAMTS-1
DPPIV
EGF
HB-EGF
HGF
MMP-9
NRG1-ß1
Serpin F1
TIMP-1
Angiogenin
Angiopoietin-1
EG-VEGF
Endoglin
IGFBP-1
IGFBP-2
Pentraxin 3 (PTX3)
PD-ECGF
TIMP-4
Thrombospondin-1
Angiopoietin-2
Angiostatin/Plasminogen
Endostatin/Collagen XVIII
Endothelin-1
IGFBP-3
IL-1ß
PDGF-AA
PDGF-AB/PDGF-BB
Thrombospondin-2
uPA
Amphiregulin
Artemin
FGF acidic
FGF basic
IL-8
LAP (TGF-ß1)
Persephin
Platelet Factor 4 (PF4)
Vasohibin
VEGF
FGF-4
FGF-7
Leptin
MCP-1
PlGF
Prolactin
VEGF-C
6000000
4000000
2000000
0

Figure 5.5. Profiling of siCD248-MSCs' proteins using protein microarray (MA). A) Transfection outline to generate lysates. B) KD confirmation on 55-60kDa CD248 protein band using cell lysates and mAb-CD248. C) Microarray membranes were activated, incubated with cell lysates, then stained with streptavidin-800-conjugated infrared secondary Ab and imaged. Images were taken by Li-Core system using 800 (green) and 700 (red) channels. The signal of each spot for the 55 proteins in replicates (110 spots) was detected. Then, an average signal was calculated for each protein and normalized to signals of negative controls (spots at the lower right corner of each membrane indicate negative control). D) A heat map of all proteins tested and expressed in all three transfection conditions, siCD248-treated, siNeg-Scr-treated, and UT-cells, using the mean signals (n=3). Color scaling represents the normalized and averaged signals against the background and negative controls signals. For statistical significance, grouped analysis using multiple t-tests through the FDR approach (Benjamini and Hochberg Q = 1%) was performed using the normalized signals of three MA independent experiments (n=3).

Proteins in siCD248-MSCs/siNegScr-MSCs					
Target Protein	**Discovery?**	**Raw P-value**	**Mean (siNeg-T)**	**Mean (siCD248-T)**	**q-value**
Coagulation Factor III	No	0.561586	3723795	4242994	>0.99
CXCL16	No	0.947626	132891	74160	>0.99
GDNF	No	0.788744	328865	89286	>0.99
GM-CSF	No	0.963766	27516	68132	>0.99
MIP-1a	No	0.666973	414244	29437	>0.99
MMP-8	No	0.987721	11033	24792	>0.99
Serpin B5	No	0.909058	187924	85795	>0.99
Serpin E1	No	0.815184	2445080	2654077	>0.99
Activin A	No	0.40836	1065728	325945	>0.99
ADAMTS-1	No	0.957177	62875	110883	>0.99
DPPIV	No	0.955929	439689	390280	>0.99
EGF	No	0.945964	60597	0	>0.99
HB-EGF	**No**	**0.012076**	**249987**	**2510242**	**0.33**
HGF	No	0.8051	281917	61286	>0.99
MMP-9	No	0.848173	176968	5790	>0.99
NRG1-ß1	No	0.939521	67836	0	>0.99
Serpin F1	No	0.841076	3046869	2867583	>0.99
TIMP-1	No	0.915814	5330780	5425293	>0.99
Angiogenin	No	0.982085	18430	38506	>0.99
Angiopoietin-1	No	0.864554	148774	301290	>0.99
EG-VEGF	**No**	**0.006584**	**40912**	**2490852**	**0.332**
Endoglin	No	0.689157	1780869	2138564	>0.99
IGFBP-1	No	0.766753	0	265232	>0.99
IGFBP-2	No	0.61579	195528	644327	>0.99
Pentraxin 3 (PTX3)	No	0.168827	3032600	1799712	>0.99
PD-ECGF	No	0.97402	2090	31207	>0.99
TIMP-4	No	0.861828	161386	5768	>0.99

Table 5.3.Proteins in siCD248/siNegScr-MSCs. Results of the protein profiler microarray (n=3) of siCD248-MSCs/siNegScr-MSCs proteins signals using grouped analysis: multiple t-tests through the FDR approach (Benjamini and Hochberg Q = 1%).Statistical analysis was performed using Graphprism.

Proteins in siCD248-MSCs/siNegScr-MSCs (Continued)					
Target Protein	**Discovery?**	**Raw P-value**	**Mean (siNeg-T)**	**Mean (siCD248-T)**	**q-value**
Thrombospondin-1	No	0.890711	3907336	4030189	>0.99
Angiopoietin-2	No	0.98632	39089	54419	>0.99
Angiostatin/Plasminogen	No	0.653829	408907	7867	>0.99
Endostatin/Collagen XVIII	No	0.781496	36413	284425	>0.99
Endothelin-1	No	0.733588	91243	395588	>0.99
IGFBP-3	No	0.801856	475758	700138	>0.99
IL-1ß	No	0.96782	24033	60102	>0.99
PDGF-AA	No	0.970333	0	33251	>0.99
PDGF-AB/PDGF-BB	No	>0.9999	0	0	>0.99
Thrombospondin-2	No	0.996299	4148	0	>0.99
uPA	No	0.544657	6198252	5656407	>0.99
Amphiregulin	No	0.80017	200930	427261	>0.99
Artemin	No	0.89385	0	119303	>0.99
FGF acidic	No	0.990342	86728	75905	>0.99
FGF basic	No	0.865021	1019793	867808	>0.99
IL-8	No	0.797967	118392	347274	>0.99
LAP (TGF-ß1)	No	0.83165	0	190078	>0.99
Persephin	No	0.985949	361.9	16107	>0.99
Platelet Factor 4 (PF4)	No	0.93869	12774	81544	>0.99
Vasohibin	No	>0.9999	0	0	>0.99
VEGF	No	0.798951	1160533	932791	>0.99
FGF-4	No	0.963895	16715	57186	>0.99
FGF-7	No	0.908	143482	40159	>0.99
Leptin	No	0.822153	120520	321499	>0.99
MCP-1	No	0.928191	39500	120075	>0.99
PlGF	No	0.021183	2454525	381414	0.388
Prolactin	No	0.74191	640230	345753	>0.99
VEGF-C	No	0.91975	11539	101617	>0.99

Table 5.4.Proteins in siCD248/siNegScr-MSCs. Results of the protein profiler microarray (n=3) of siCD248-MSCs/siNegScr-MSCs protein signals using grouped analysis: multiple t-tests through the FDR approach (Benjamini and Hochberg Q = 1%). Statistical analysis was performed using Graphprism.

5.3. Investigating the effect of reduced CD248 level on the ability of MSCs to support leukemic cells viability

One of the mechanisms through which MSCs participate in hematopoiesis and regulate HSCs is via cell-to-cell interactions and receptor-ligand interaction through several molecules. However, MSCs' exact role in leukemic cell viability, whether they increase or decrease leukemic cells' viability, is not well-understood since contradicting results were reported and suggested to be influenced and dependable on experimental conditions. Focusing on the effect of MSCs-surface CD248 and its potential in altering MSCs' function in AML-context, the role of MSCs and siCD248-MSCs in the leukemic cell line HL60 viability was investigated in this study. Such investigation was performed to gain insights into CD248 role in HD-MSCs' possible communication with the leukemic blast in vitro.

After 24 hours of knocking down CD248 on HD-MSCs, HL60 co-culture experiments were conducted using siCD248-Treated MSCs, siNegScr-Treated, and UT MSCs as feeder layers. These co-culture experiments (n=3) were carried on for five days. Performing microscopic evaluation using bright-field microscopy throughout the five-day experiment, normal morphology and high confluence of HD-MSCs and HL60 were observed. HL6O showed rounded-shaped cells, and MSCs showed a spindle-fibroblast shape (Figure 5.6). siCD248-treated, siNegScr-Treated, and UT MSCs were collected and lysed on a daily basis from each co-culture plate to assess the lasting of CD248 KD throughout the five days (D1-D5) of the co-culture experiments using Western blot analysis(Figure 5.7A).

Western blot analysis showed that CD248 KD persisted for four days (D1-D4) of the co-culture experiment. Compared to its expression in siNegScr-Treated MSCs, a partial KD of CD248 was seen in siCD248-Treated MSCs at ~150kDa, and a higher KD effect was observed at ~55-60kDa, bands of perhaps the incompletely modified CD248 protein, while at D5, both siCD248-Treated and siNegScr-Treated cells showed similar CD248 abundance pattern (Figure 5.7B). GAPDH and total protein stain were both used to ensure proper analysis.

Further, to determine HL60 viability in each co-culture condition, HL60 cell counts were performed using a trypan blue viability test every day for five days. Viability results showed no difference in HL60 viabilities between the three co-culture conditions from D1-D4 (Figure 5.7C). Although viability was observed to be slightly higher at D5, between HL60 co-cultured with siCD248 and siNegScr-Treated MSCs, the difference was insignificant (Figure 5.7 D). Additionally, an apoptosis assay was performed to test if HD-MSCs or siCD249-MSCs induce HL60 apoptosis at D5. Results of apoptosis assay (n=1) showed that all transfected, siCD248-Treated, siNegScr-Treated, and un-transfected HD-MSCs exhibited no observable apoptotic effect on HL60. Additionally, to investigate whether the presence of HD-MSC impacted HL60 expression of CD45, flow cytometry analysis was performed in the co-cultured HL60 cells at D5 to determine the CD45+ population (n=2). Flow cytometry results showed a comparable level of CD45+ between all co-cultured conditioned and HL60 cultured alone (Figure 5.7 E and F). These results showed that under the co-culture conditions of this study, HD-MSCs and siCD248-MSCs did

not affect HL60 viability. Furthermore, CD248 had no significant effect on MSC's interactions with HL60; it neither affected HL60 viability nor their apoptosis.

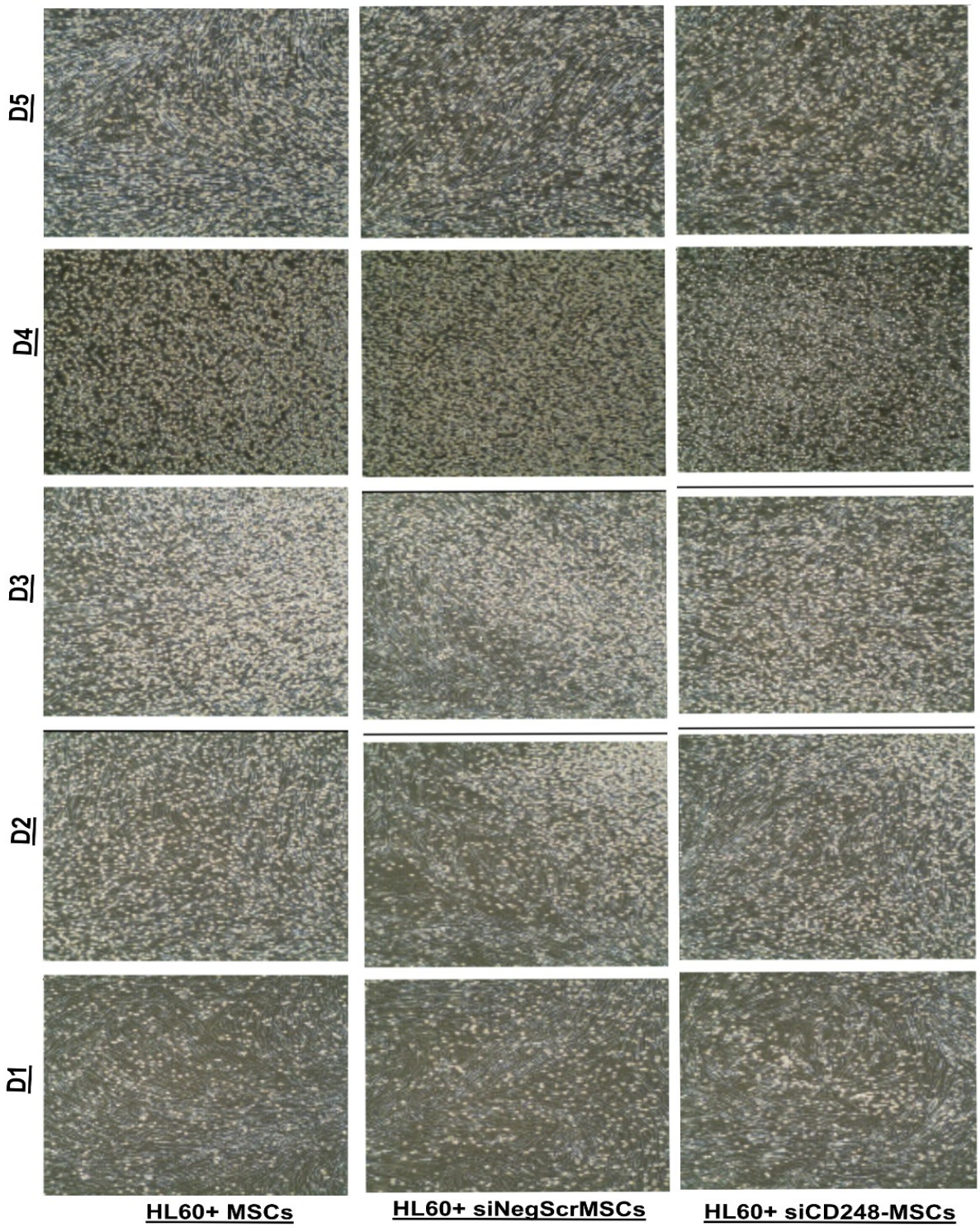

Figure 5.6. HL60 co-cultured with HD-MSCs and siCD248-MSCs. HL-60 cells were added to transfected and un-transfected MSCs plates after 24 hours of siCD248 transfection. Throughout the five days of co-culture (D1-D5), images were taken before collecting HL60 and lysing the feeder layer, HD-MSCs from all conditions. Bright-field microscopy images (magnification X10) representing each of the co-culture conditions in each co-culture plate.

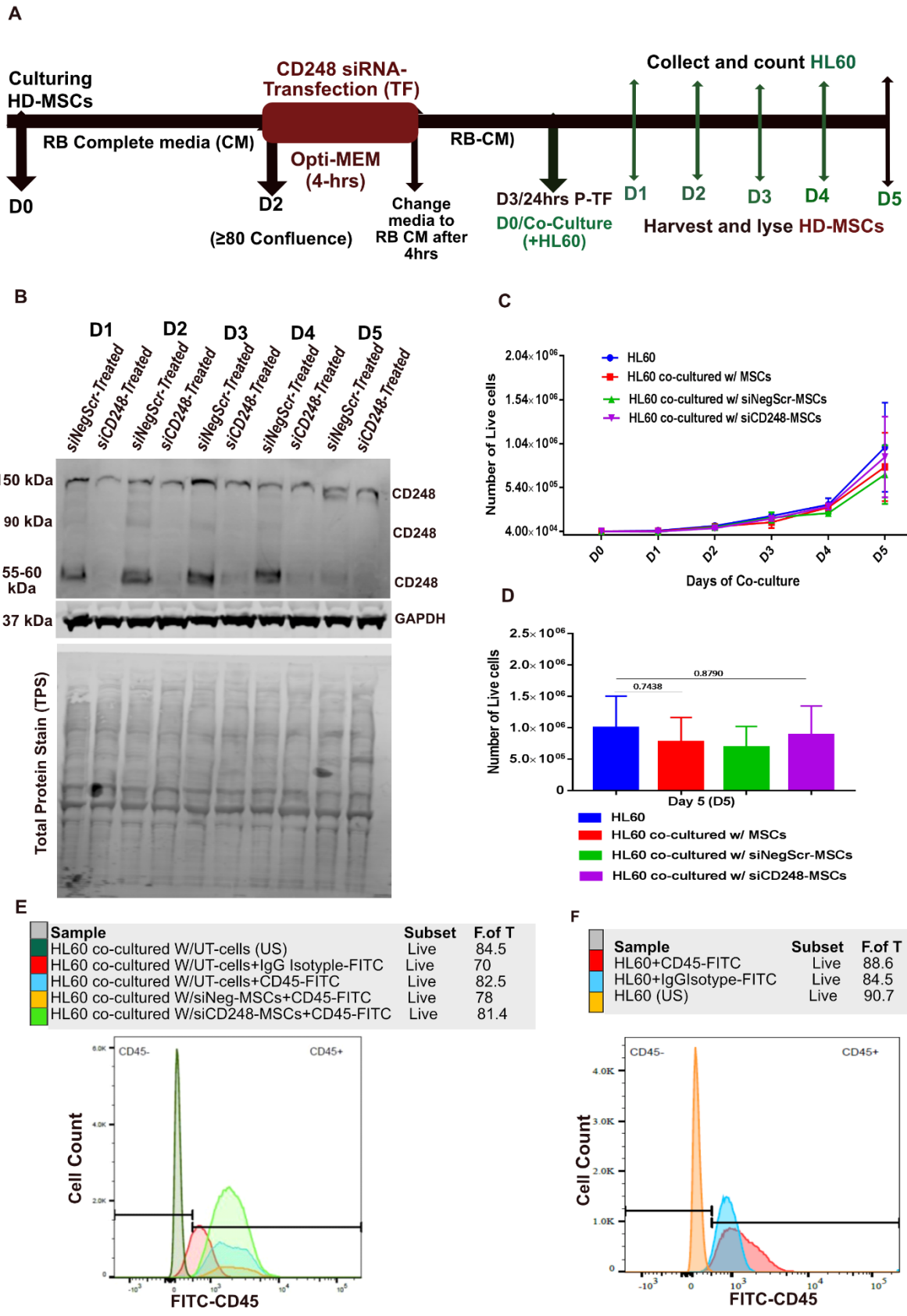
A
Culturing HD-MSCs
RB Complete media (CM)
D0
CD248 siRNA-Transfection (TF)
Opti-MEM (4-hrs)
D2
(≥80 Confluence)
Change media to RB CM after 4hrs
RB-CM)
D3/24hrs P-TF
D0/Co-Culture (+HL60)
Collect and count HL60
D1
D2
D3
D4
D5
Harvest and lyse HD-MSCs
B
D1
D2
D3
D4
D5
siNegScr-Treated
siCD248-Treated
150 kDa
90 kDa
55-60 kDa
37 kDa
CD248
CD248
CD248
GAPDH
Total Protein Stain (TPS)
C
HL60
HL60 co-cultured w/ MSCs
HL60 co-cultured w/ siNegScr-MSCs
HL60 co-cultured w/ siCD248-MSCs
Number of Live cells
Days of Co-culture
D
Number of Live cells
0.7438
0.8790
Day 5 (D5)
HL60
HL60 co-cultured w/ MSCs
HL60 co-cultured w/ siNegScr-MSCs
HL60 co-cultured w/ siCD248-MSCs
E
Sample
Subset
F.of T
HL60 co-cultured W/UT-cells (US)
Live
84.5
HL60 co-cultured W/UT-cells+IgG Isotyple-FITC
Live
70
HL60 co-cultured W/UT-cells+CD45-FITC
Live
82.5
HL60 co-cultured W/siNeg-MSCs+CD45-FITC
Live
78
HL60 co-cultured W/siCD248-MSCs+CD45-FITC
Live
81.4
CD45-
CD45+
Cell Count
FITC-CD45
F
Sample
Subset
F.of T
HL60+CD45-FITC
Live
88.6
HL60+IgGIsotype-FITC
Live
84.5
HL60 (US)
Live
90.7
CD45-
CD45+
Cell Count
FITC-CD45

Figure.5.7. HL60 co-culture with HD-MSCs and siCD248-MSCs. A) Co-culture outline. HL-60 cells were added to transfected and un-transfected MSCs plates after 24 hours of siCD248 transfection. HL60 viabilities and cell counts were determined every day after 24 hours of co-culturing for five days. B) After each day count, MSCs from the same co-cultured plates were harvested and lysed for CD248 expression assessment to ensure the KD throughout the 5- day co-culturing experiment (n=3).CD248 KD lasted from 4 days (55kDa) in siCD248-treated vs. siNeg-treated MSCs lysates from the co-culture plates. GAPDH and total protein were used to ensure KD results.mAb-CD248 was used in this Western blot. C and D) No significant difference was found in viabilities between co-culturing conditions. E) On day 5, after HL60 cell counts, the level of HL60 marker, CD45, was measured by flow cytometry. HL60 were stained with either CD45-FITC Ab or IgG-isotype. Unstained cells were used to set the histograms. Results (n=2) showed no significant difference between the percentage of CD45+ cells in each condition, HL60 co-cultured conditions, F) HL60 alone.

CHAPTER 6

Discussion

Balanced physiological cellular and molecular compositions of the niche are critical in maintaining normal hematopoiesis. Multiple experimental studies suggest a negative impact of an altered BME in hematopoiesis. Although the exact role of an altered BME in the hematological malignancy AML is not fully understood, pathogenesis and relapse of AML, where abnormal hematopoiesis is the case, have been associated with BME alterations (23,47,73,159,160,170). This association emphasizes that an altered niche plays a critical role in AML progression. Simultaneously, such association stresses the importance of the niche and its components in maintaining normal hematopoiesis, subsequently preventing AML relapse. Therefore, an in-depth investigation and understanding of possible mechanisms and molecules that could contribute to alterations in the BME and consequently aid AML relapse is needed.

Playing a significant role in regulating hematopoiesis (67,72-79-82) and composing the niche, human bone marrow MSCs (hBM-MSCs) may provide an excellent in vitro model for studying BME alterations which could aid in the understanding of leukemogenesis, especially since a comprehensive and a well-established in vitro model investigating possible BME alterations and effects on the HSC niche is limited. Moreover, MSCs exhibit several characteristics that enable their use as a model; 1) being able to differentiate into several lineages, multipotent, 2) they can be successfully expanded in vitro, 3) expressing several receptors and producing pro and anti-inflammatory factors that modulate the immune response. Thus, AML-derived MSCs (AML-MSCs) have been objective for investigations. Some studies have investigated and characterized AML-MSCs (179-190). These AML-derived MSCs displayed impairments of their phenotypic, genetic

characteristics, or/and differentiation potentials compared to their healthy counterparts (HD-MSCs).

Nonetheless, since AML heterogeneity is still a significant challenge that limits the complete understanding of its pathogenesis, additional investigations of AML-MSCs are still required to gain more insights into the disease biology. Therefore, a recently published study by our group has characterized AML-MSCs from a large cohort of 46 AML patients (184). The cohort included AML-MSCs from all AML subtypes HR, IR, and LR. Interestingly the study found that in comparison to HD-MSCs, AML-MSCs, particularly HR AML-MSCs, displayed a defect in their differentiation potentials and exhibited increased immunosuppressive properties.

In this thesis, an in-depth characterization of 29 AML-MSCs, previously fully characterized as BM-MSCs by Guardia et al. (184), was performed to understand the possible mechanisms and molecules behind the observed alterations in HR AML-MSCs. Moreover, these identified novel molecules could also play a significant role and provide new insights into the normal biological functions of HD-MSCs. Although previous studies have investigated AML-MSCs, only a few studies have performed genome-wide sequencing (182,183,188,190). Moreover, the majority of these studies have investigated small cohorts (such as n=3 and n=5) of AML-MSCs samples (182,183,188), while only a few studies of these conducted have investigated large sample cohorts (190). Here, a high throughput analysis: RNA sequencing was used to ensure high sensitivity and reliability while assessing and investigating a large and heterogeneous cohort of AML-MSCs samples (n=29) to represent AML heterogeneity competently. The large cohort of AML-MSCs samples used here covered both sexes, male and female, several age groups, and the three

AML subtypes. In particular, RNA sequencing was performed to directly compare the transcriptomic profiles of these 29 AML-MSCs to HD-MSCs (n=8).

In vitro, AML-MSCs culture establishment and maintenance are challenging. The initial study by Guardia et al. reported that 40 of the 46 AML-MSCs used samples were successfully expanded, and cultures were established. These reported findings were also confirmed by other investigations (179,187) that the establishment and maintenance of AML-MSCs in vitro is challenging. AML-MSCs cultured in this study exhibited slow growth and low confluences. In particular, AML-MSCs grew slower than HD-MSCs and thus required more days to achieve confluences. These observations were similar to some previous studies (181). Even though low confluences were observed, cultures of all 29 AML-MSCs samples were successfully maintained. Importantly, sufficient confluences were achieved for RNA isolation, and the RNA content of all cultured 29 AML-MSC was efficiently isolated and purified. However, some samples required additional isolation experiments to achieve high-quality RNAs. For AML-MSCs morphology, some studies found that AML-MSCs have similar morphology to HD-MSCs (182,187,189), while others reported large/irregular-shaped cells (181). Here, confirming previous findings, AML-MSCs displayed a normal morphological appearance compared to HD-MSCs. MSCs from both groups, AML and HD, showed spindle-shaped fibroblast-like; slight to no irregularity was observed in AML-MSCs cultures.

Interestingly, our transcriptomic analysis of the AML-MSCs group, which included AML-MSCs from all three risk groups, showed an altered gene expression profile compared to HD-MSCs. There were 30 dysregulated genes in AML-MSCs/HD-MSCs. Additional analysis showed no significant differences within AML

groups LR, IR, HR, age groups nor between sexes in AML-MSCs /HD-MSCs. Studies that included samples from AML patients of both sexes (such as (181,182,187)) have not mentioned whether a sex-based analysis was performed, but their findings showed no specification based on sex.

Moreover, applying a cut-off value (FC of 1.5)to determine genes with statistical significance in the AML-MSCs group compared to the HD-MSCs group, out of the 30 genes, 21 genes were identified as SDRGs in AML/HD. These 21 in AML/HD were disseminated at several cellular and nuclear levels, variously located between the nucleus, cytoplasm, extracellular space, and plasma membrane, and with various functions; transcription factors, transmembrane receptors, cytokines, and peptidases. However, further *in silico* analysis revealed no common pathway through which those altered genes could exhibit an effect on MSCs-altered functions. However, some of these molecules were individually part of MSCs differentiation signaling pathways.

Whereas 13 genes of the 21 SDRGs (TNS1, SCUBE3, ATP1B1, MEIS2, CXCL-12, DSP, TNFAIP2, LGR4, TUSC1, CD248, C14orf132, TCF7L1, and RUNX1) were upregulated, eight genes (SPCS3, DDX60L, PVRL3, SLIT2, TRNP1, ARHGEF28, FBLN5, and GREM1) were downregulated in AML-MSCs compared to their expression levels in HD-MSCs. The 13 significantly overexpressed genes play several physiological and pathological roles. Specifically, some are associated with cancer. ATP1B1, which is involved in the cellular metabolic and ATP-binding processes, has been associated with AML. Interestingly, it has been previously found to be upregulated in MSCs after co-cultured with murine AML cells (217). TCF7L1, a transcription factor that regulates cell viability and survival, DNA-binding

proteins, and β-catenin, was upregulated in our AML/HD and has also been associated with AML. DSP and TNS1, involved in cellular adhesion, migration, and structural protein signaling pathways, were upregulated in our SDRG dataset. TNFAIP2, tumor necrosis factor-α induced protein-2, which plays an essential role in MSCs modifications, immunomodulatory functions, and angiogenesis, was overexpressed in AML-MSCs/HD-MSCs. In addition, LGR4, which is critical in MSCs' activation of Wnt signaling and required in MSCs functional role within BME, was upregulated in our AML/HD-MSCs dataset. Interestingly, LGR4 was previously found to impact MSCs' proliferation when downregulated (218). The second group of the 21 SDRGs in average AML/HD is the group of 8 downregulated genes (SPCS3, DDX60L, PVRL3, SLIT2, TRNP1, ARHGEF28, FBLN5, and GREM1). The significant downregulation ranged from 1.6 to 4.8 FC, where GREM1 was the gene with the lowest expression in AML-MSCs compared to HD-MSCs. SPCS3, DDX60L, and ARHGEF28 are involved in protein binding, ATP-binding, and cell differentiation processes. ARHGEF28 is also involved in cellular migration and development, along with SLT2 and FBLN5, while TRNP1 is involved in cell proliferation and self-renewal and altered levels of these genes were associated with cancers.

Few genes from the 21-gene list were previously found and reported to be dysregulated in AML-MSCs (183,188,190). The dysregulated expressions of these genes were mainly similar to the dysregulation found in this study. Specifically, similar to our finding, a study that investigated AML-MSCs (n=5) compared to HD-MSCs (n=6) also found that CD248 is significantly overexpressed in the AML-MSCs group (183). CD248 was among their differentially regulated genes. However, no further investigation of CD248 upregulation was conducted in that study. C14orf132

and ARGHGEF28 were among the 13 upregulated genes in our 21-SDRG list in AML/HD, MSCs from all AML subtypes. A significant upregulation of other isoforms of these two genes, C14orf28 and ARHGEF26, was previously found in AML/HD-MSCs (183). Another study that investigated AML-MSCs (n=3) compared to HD-MSCs (n=3) also found a significant upregulation of another isoform of ARHGEF, ARHGEF40, (188). Other studies investigated and reported dysregulation of adipogenic and osteogenic specific genes within a small AML-MSCs sample cohort (n≤11) (182,189). Furthermore, SCUBE3, LGR4, and GREM1 were all previously reported to be dysregulated in AML/HD-MSCs (188). While similar dysregulation was previously reported for SCUBE3 and LGR4 expression, both were upregulated in AML/HD-MSCs; unlike the current study's finding, GREM1 was previously found to be upregulated in AML/HD-MSCs (188).

Interestingly, in the current AML-MSCs investigation, CXCL12 was among the 21 SDRGs in AML/HD. It was significantly overexpressed in AML-MSCs by 3 FC. CXCL12, also known as SDF1, is remarkably reported to be associated with AML and has been investigated in the disease context. MSCs, osteoblasts, and osteoprogenitors are all producers of this cross-talk molecule in BME. Specifically, CXCL12 attaches to its receptor (CXCR-4) and helps leukemic blasts survive in the BM niche, similar to its role in HSC homing in the niche. (60,150,219). Moreover, this cross-talk molecule has also been shown to bind to Jagged-1, suppress normal hematopoiesis, and favor the leukemic environment. Therefore, overexpression of SDF-1/CXCl12 by AML-MSCs could aid in LSCs homing to the niche and relapse. Similar to the finding of this study, CXCl12 was also reported in a previous in vivo investigation of AML-MSCs (190). The study transplanted AML cells in a murine

model and then investigated the effect of AML on MSCs gene expression through gene microarray and found that CXCL12 was significantly overexpressed in these AML-derived cells. Another critical gene is RUNX-1, which was upregulated in AML-MSCs/HD-MSCs. RUNX-1 is a critical transcription factor in hematopoiesis and physiological tissue development. It is also essential for proper MSCs proliferation and differentiation (220). Additionally, MEIS2 was found to be upregulated in AML/HD-MSCs. This gene belongs to the MEIS family genes, which are essential in HSCs activity, and HSCs' proteins were found in BME and have been associated with AML (221, 222). Suggesting that those altered AML-MSCs could negatively alter the balanced BME, thus could impact hematopoiesis.

Although few genes from our 21-list of SDRGs were previously reported to be dysregulated in AML-MSCs/HD-MSCs, limited knowledge was available about their role in altering MSC's functions. Upregulation of SCUBE3, CD248, and downregulation of GREM1 gene expression could be involved in AML-MSC's altered functionality (184) in the AML context, mainly since they are physiologically expressed in HD-MSCs and significant in MSCs function. GREM1 plays a critical role in osteogenesis as a BMP antagonist (116-118). BMP signaling regulates MSCs' osteogenesis differentiation. When BMPs 2, 4, or 7 bind to their receptors on MSCs surface, type I and type II, they heterodimerize, forming an active complex. Triggering signal transduction through SMADs that phosphorylates SMAD proteins. Then, the phosphorylated SMADs translate the signals and regulate the transcription of osteoblastic genes. As a BMP antagonist, GREM1 has been suggested to impact MSC osteogenesis differentiation when overexpressed negatively. For instance, the Lack of GREM1 in mice led to skeletal deformities (223). On the contrary, GREM1

overexpression on MSCs has been shown to have an advantageous effect on ischemia treatment (224-225). When dysregulated, GREM1 has also been found to affect tissue homeostasis and promote intestinal tumorigenesis and was implicated in lung, ovary, and other cancers. SCUBE3 encodes a secreted glycoprotein. When cleaved, SCUBE3 releases its N-terminal, EGF-like repeats, and C-terminal, CUB domain (124,226,227). These two fragments participate in protein-to-protein interactions. It signals through SMAD canonical pathway, the TGFβ pathway. SCUBE3 binds to TGFβR-II through the C-terminal of the CUB domain and, subsequently, activates the canonical TGFβ pathway. When SCUBE3 triggers the single transduction through SMAD, the transcriptional activity of SMADs regulates the transcriptions of downstream targets such as VEGF, tumor angiogenic factor, and TGFβ-1. SCUBE3 is involved in cardiac hypertrophy in mice and tissue development. SCUBE3 upregulated expression was found in metastatic lung cancers. Moreover, these two signaling pathways, BMP and TGFβ, are critical in MSCs' function within the BME and their differentiation potentials (104).

Since SCUBE3 and GREM1 are implicated in MSCs differentiation, their dysregulated levels in AML/HD-MSCs could impact MSC's physiological function and differentiation. Thus, these two genes might serve as potential targets in AML BME. In this study, an initial validation of SCUBE3 and GREM1 dysregulated levels was performed using HR AML-MSCs since those MSCs exhibited differentiation impairments (184). Although GREM1 and SCUBE3 could not be genetically modified in the current investigation due to multiple limitations, SCUBE3 and GREM1's potential relevance to AML-MSCs alterations and MSC's differentiation nominates them as potential targets for future investigations primarily since their dysregulation

was also reported in previous AML-MSCs investigations (183,188,190) irrespective to AML subtype, cohort size or gender.

This study generated a list of 21 SDRG from the transcriptome analysis of AML-MSCs compared to HD-MSCs. The current findings showed that compared to HD-MSCs, AML-MSCs were altered at the genetic level. The genetic alterations of AML-MSCs suggest an altered behavior and function at both internal, MSCs, and external levels, at BME compared to healthy MSCs' role in the niche. Possibly, these alterations impact MSCs' critical role in hematopoiesis maintenance and niche composition. The consistency of some of these findings with previous findings of other AML-MSCs investigations (183,188,190) validates and strengthens the currently presented data. Furthermore, the data of this study adds new insights to the accumulative knowledge of the critical role of AML-MSCs alteration with the altered genetic profile in understanding the biology of BME and its alteration in AML pathogenesis. Moreover, the transcriptomic analysis enabled identifying a potential novel target at the MSC's functional level: CD248, which could play a part in the altered AML-MSCs observed functionality and exhibits a critical role in MSC's functionality.

MSC marker CD248 (196) has been suggested with an essential role in several physiological cellular processes, such as tissue repair and remodeling, and stromal cell proliferation, with a role in human tumors, mainly through its involvement in tumor vascularization and angiogenesis (191-192,196,197). Furthermore, CD248 was among the 13 upregulated genes in the SDRG list in AML-MSCs/HD-MSCs. CD248 was significantly overexpressed in MSCs from all AML subtypes (HR, IL, and LR). Furthermore, the most overexpression of the CD248 gene was found in AML-

MSCs samples from HR patients (as shown in chapters 3 and 4). Because HR AML-MSCs showed impairments in their differentiation potentials in the initial study by Guardia et al. (184), a CD248 investigation at the protein level was conducted using these HR AML-MSCs. Interestingly, consistent with the transcriptomic data, CD248 protein level was also significantly abundant in HR AML-MSCs/HD-MSCs. Specifically, HR AML-MSCs showed a tend-toward increase pattern in their CD248 protein abundance level compared to HD-MSCs. These protein results validated the significant upregulation in CD248 gene expression found earlier by RNA-Sequencing.

Interestingly, investigating CD248 protein in HR AML-MSCs revealed that the overexpression of the CD248 gene was also translated to higher protein levels in these HR samples. These results validated and confirmed the overexpression of CD248 at both mRNA and protein levels in HR samples and suggested CD248's possible critical role in MSC's function and that CD248 contributed to the previously observed altered functionality in AML-MSCs (184). Investigation of CD248 expression on the cell surface of HR AML-MSCs (HR-AML8) revealed a higher abundance level of surface marker CD248 on these HR AML-MSCs compared to HD-MSCs. More than a 2-fold increase in expression was found. Before staining MSCs for flow cytometry determination of CD248 protein on MSCs surface, Trypsin was used to detach MSCs from the culture vessels and harvest them for flow cytometry analysis. Although the proteolytic activity of Trypsin, when used to harvest primary cells, could induce alteration of protein levels (228), and thus, CD248 protein level could be affected by the trypsinization step, in this study MSCs from both group HD and AML were treated and processed similarly; therefore, the

comparison between CD248 protein abundance levels between HD and AML-MSCs is still valid. Together, CD248 increased level was not limited to gene expression and intracellular protein levels. Nonetheless, the exact role and effect of dysregulated CD248 in healthy MSC's function have not been investigated, and the molecular mechanisms, interactions, and intracellular signaling behind CD248 regulation and expression are still limited.

Given the importance of MSCs in hematopoiesis and their role in composing the HSCs niche BME, understanding the molecules and mechanisms behind their altered functionality is critical to gaining more insights into their possible contribution to AML. Since CD248 is an MSC marker and is also expressed on the MSC surface (196), it could play a critical role in their functionality and interactions with cellular components within the niche. Therefore, when dysregulated. CD248 overexpression on HR AML-MSCs at both gene and protein levels suggests that MSCs' physiological role and interactions within the BME level could be affected. Similar findings of an increased level of CD248 were found in several tumors and have been suggested and associated with impacting tumor severity when increased (204-207) and decreased (208,211). A high level of CD248 was also found in MSCs from systemic sclerosis (SSc-MSCs) (213). The overexpression of CD248 protein in other tumors was explicitly associated with the induction of vascularization (196,199,201) in the tumor microenvironment via its binding and interaction with angiogenic receptors. The perivascular niche is a critical compartment of the HSC niche. Expressing a high level of CD248 in BME through AML-MSCs could impact the niche physiological balanced and hemostasis by affecting BME vascularization, similar to CD248's reported effect on other tumor vascularization.

Furthermore, CD248 protein properties, belonging to the CTLD-14 family (200), and its homology to thrombomodulin, its three EGFs repeats on its extracellular domain, have been suggested to play a role in protein-protein interactions. Since CD248 is a cell-surface receptor, its overexpression on HR AML-MSCs could impact their interactions within BME, suggesting that CD248 could be part of MSCs interactions with other cellular components in the HSCs niche. In addition, based on the current analysis and findings, CD248 overexpression on HR AML-MSCs was unrelated to a specific HR mutation. It was overexpressed on MSCs samples from 11 patients with various mutations and normal and abnormal karyotypes. These results confirmed and add to the available knowledge that AML-MSCs exhibit alterations in their genetic profiles (182,183,188,190). Thus, understanding AML-MSCs alterations and perhaps normalization of these alterations could aid in the limitation of BME alterations' role in AML pathogenesis and consequently aid in AML subtypes and relapse prevention.

Identification of CD248 gene dysregulation in AML-MSCs, and HR AML-MSCs through RNA sequencing and then the determination of CD248 protein overexpression levels in HR samples enabled exploring its potential role in HD-MSC's functionality through gene modification studies, siRNA knockdown. Up to date, a well-established in vitro model to study CD248 in HD-MSCs is limited (213). Here, HD-MSCs were used as a competent and adequate in vitro model to establish CD248 KD. As observed in this study and previous studies, AML-MSCs culture maintenance is challenging. Moreover, their altered genetic profile could interfere with the assessment and investigation of CD248 dysregulation in MSC's functionality. Confirmation of the physiological expression of CD248 endogenous

protein in MSCs at several forms was achieved; perhaps these were unmodified and highly glycosylated forms as previously observed in MSCs (90kDa in human MSCs (213) and other cell types (191,192,193,213).

Following extensive optimization of the optimal conditions for in vitro approach to knockdown CD248, this study provides an efficient and well-established siRNA KD protocol of total and cell-surface CD248 in primary cells HD-MSCs. Moreover, the KD efficiency was reproducible when tested on the cell-surface level of HR AML-MSCs, resulting in an efficient cell-surface CD248 KD under the same culture conditions between the two groups AML-MSCs and HD-MSCs. The high efficiency of this transit siRNA KD (~70%), partial KD with high viabilities of the siCD248-treated HD-MSCs enabled further investigation of its role in MSCs at a functional level.

Within BME, MSCs contribute to HSCs regulation, and their niche through multiple proteins with autocrine, paracrine, and endocrine activates, some with pro-angiogenic properties and others with immunomodulation properties. These properties collectively define MSCs and enable their use in regenerative medicine (139-143), such as paracrine factors (141). Protein profiling of HD-MSCs using 55 essential cellular proteins with a known role in angiogenesis was performed to gain a proteomic perspective of its KD effect on HD-MSCs profile. Expression of previously known MSCs angiogenic proteins TGF-β, Angiopoietin-1, Ang-1, FGF, and MCP-1 were all detected and confirmed in control untreated HD-MSCs. Profiling of siCD248-treated HD-MSCs provided insights into the CD248 KD effect on HD-MSCs, including the angiogenic factors. Knocking down CD248 insignificantly altered HD-MSCs protein profile. While interestingly, several protein levels were

unchanged in siCD248-MSCs compared to UT-Cells, such as uPA and MMP-9. These two protein levels were directly correlated in MSCs (229). In silico analysis showed that some of these proteins participate in other processes besides angiogenesis. For instance, CXCL8, EGF, PROK1, and HGF proteins which were slightly dysregulated in CD248 KD cells, were associated with tumor microenvironments. While EGF, CXCL-8, and PROK1 proteins were shown to participate in IL-8 signaling and participants in PRAR (adipogenesis key marker) activation. LEP, leptin, is also a downstream target of PPAR in the MSCs adipogenesis pathway.

While the abundance levels of most of the 55 proteins in the CD248 KD model were insignificantly altered, HB-EGF and EG-VEGF were proteins with a significantly increased level (raw p-value <0.05) in siCD248-Treated HD-MSCs compared to their levels siNegScr-treated cells (p-value of 0.012, and 0.009, FDR >0.05). Their level was also increased in siCD248-MSCs/UT-Cells with a significant raw p-value. EG-VEGF and HB-EGF have critical roles in MSC's functionality, especially their interactions with endothelium cells for angiogenesis, cell-cell communication within the BME, and extracellular matrix formation. Herein, downregulation of CD248 by siRNA knockdown induced endogenous HB-EGF and EG-VEGF proteins in HD-MSCs. Notably, in our transcriptomic data where the CD248 gene was highly overexpressed on HR AML-MSCs, the HB-EGF gene was limitedly expressed (0.3 Log2F) on these HR MSCs with no statistical significance relative to our cut-off values, and no expression data for EG-VEGF was found. Although a correlation between mRNA expression and protein level is not strongly supported, these transcriptomic and proteomic findings suggest a potential reverse

correlation between these two angiogenic proteins, HB-EGF, EG-VEGF, and CD248, perhaps through a common signaling pathway within MSCs. A primary in silico analysis using the IPA connection tool showed that STAT5, a transcription factor, and KLF10, a protein-coding gene, could be associated with CD248 and some alterations. However, the possible intracellular signaling mechanisms behind CD248 through STAT are yet to be understood. Further validation could be required to examine whether the increased level of these two proteins affects MSCs differentiation, and could help unfold a common signaling differentiation pathway primarily since exogenous HB-EGF protein was found to impact MSCs adipogenesis (230) negatively. These initial proteomic findings support the knowledge about the known role of CD248 in angiogenesis as an angiogenic protein. Furthermore, it could aid in normalizing the alterations of these proteins since MSC's physiological protein levels are required for proper MSCs function, which nominates them initially and is critical to their use in therapeutic approaches.

HSCs require direct contact with stromal cells, MSCs, to proliferate and differentiate similarly; direct contact between AML cells and MSCs is essential for AML cell maintenance. MSCs participate in the HSCs regulation and niche composition both in vitro and in vivo ,67,72,74), demonstrating a critical role for MSCs in the niche within the BME. Nevertheless, currently no definitive in vitro co-culture effect of MSCs on leukemic blast proliferation. Studies showed contradicting results (187) and suggested that the effect depends on each experimental approach and in vitro culture conditions. For instance, AML-MSCs were found to have a limited ability to support HSPCs compared to HD-MSCs (179).

Since AML-MSCs exhibited slow growth and low confluences could inhibit the precise observations of CD248 role in such cellular interaction. HD-MSCs provided a better understanding of the MSC's cell-surface CD248 significance in cellular communication with AML cells. Through co-culture experiments, the investigation in this study examined the direct effect of untreated HD-MSCs and CD248 KD HD-MSCs, siCD248-Treated, on HL60 viability. This approach was used to 1) exclude any effect of exogenous treatments, growth factors, or drug-induced inhibition from cultural conditions, which helped to observe the role of untreated MSCs, and 2) to identify whether MSCs CD248 play a part in MSCs-leukemic cells interaction. Neither untreated HD-MSCs nor CD248 KD MSCs exhibited an effect on HL60 viability. Both HL60 co-cultured with HD-MSCs and HL60 cultured alone showed comparable viabilities. Moreover, there was no significant impact of CD248 KD MSCs on HL60 compared to healthy counterparts, UT-Cells.

These results suggested that CD248 expressed by MSCs plays no significant part in MSCs cell-cell interaction under the experimental designs of this study. However, examining the CD248 KD effect on alternative leukemic cell lines before defining the exact role of its protein in the cross-talk between AML cells and MSCs in vitro and in vivo is needed. Moreover, the no proliferative /anti-proliferative effect also suggested that the indirect effect of MSCs soluble factor/ secreted proteins of both HD-MSCs and siCD248-MSCs (such as increased HB-EGF) in cell culture had no impact on HL60 proliferation and thus, testing conditioned media was not conducted. The limitation of the HL60 cell line could describe the insignificance. For instance, since HL60 express and produce HB-EGF (231), perhaps the increased level of siCD248-MSCs' HB-EGF has no additional effect on their proliferation. Also,

although TGF-β has been found to play a critical role in inhibiting leukemic blasts proliferation (232,233), HD-MSCs and siCD248-MSCs showed TGF-β1 in their protein profile, but no significant effect on HL60 proliferation was found. The insignificant effect could also be due to the low expression of TGFB receptors since HL60 expression of TGFBR was reported to be limited (234).

Collectively, these results suggested that CD248 expressed by MSCs plays no significant part in MSC-cell interaction under the in vitro conditions of this study. Although KD CD248 did not affect HL60 viability and suggested that CD248 cell surface plays no role in HD-MSCs communication with the used promyelocytic leukemic cell line HL60, it remains unclear the effect of these KD cells on HSCs. The effect of HD-MSCs on HSCs was not investigated in this study. However, in a previous investigation of the direct effect of HD-MSCs on HSCs, HD-MSCs (grown and cultured under similar culture conditions to the currently used HD-MSCs) were found to support the expansion and differentiation of CD34+ cells in an in-vitro co-culture system (179). Therefore, an investigation of the CD248 KD effect (siCD248-MSCs) on HSCs could provide insights into CD248 role in MSC-HSC potential communication and interaction. Considering that as an MSC marker, CD248 could participate in MSC-HSC receptor-ligand interactions. However, multiple factors should be considered when examining the effect of siCD248-MSCs on HSCs in co-culture experiments since the age of these hematopoietic cells could impact their interaction with other cells (235).

Several studies have emphasized BME compartments' roles in HSCs pool maintenance (56, 59,60,63). The HSCs' location in the niche, close to the perivascular or endosteal niche, is essential for their proliferation status and, thus,

maintaining normal hematopoiesis. This evidence stresses the importance of a well-maintained and balanced niche, cellular and molecular compositions of both main compartments; the endosteal and perivascular parts. As a critical component and regulator of the niche, MSCs differentiation to mature adipocytes and osteocytes is one of the fundamental features that define their role in BME and hematopoiesis regulation. Unbalanced niche, MSC's differentiation toward one lineage more than the other could disturb the niche physiological environment. Alteration of osteogenic niche components has been associated with AML pathogenesis (73). The involvement of adipogenic niche was also reported in several tumors. Specifically, within BME, adipocytes promote tumor colonization and growth. Similarly, in AML, the adipogenic niche was found to aid blast survival by providing them with fatty acids via induction of lipolysis and preventing their apoptosis (161-163).

Herein, knocking down of CD248 on HD-MSCs diminished their adipogenesis differentiation. Differentiated siCD248-treated HD-MSCs showed a reduced ability toward adipogenesis and mature adipocyte formation. In vitro examination of the effect of CD248 KD on adipogenesis pathway genes using qRT-PCR enabled confirmation and identification of possible mechanisms behind the observed reduction. It revealed dysregulation in the expression levels of multiple adipogenesis genes. Although knocking down CD248 on HD-MSCs did not result in significant dysregulation of master adipogenic regulators, only a slight increase in C/EBP was found; interestingly, it resulted in upregulation of the expression level SIRT2 and ADIPQ genes. When further in-silico analysis was performed to investigate the effect of SIRT2 upregulation on the adipogenesis pathway, it identified a mechanism by which upregulation of SIRT2 could lead to adipogenesis reduction and inhibition of

formation of mature adipocytes. It predicted that upregulation of SIRT2 expression inhibits the adipogenesis pathway through upregulation of the FoXO1 gene, which inhibits MSCs adipogenesis pathway via inhibiting both C/EBP and PPAR. A similar correlation between SIRT2 and FoXO1 was found previously in mouse fibroblast cell line 3TL3I. In particular, the study found a reversed effect between these two genes, the downregulated expression level of SIRT2 was found to enhance adipogenesis through its effect on the FoXO1 gene (236), which could add additional validation to the predicted mechanism in CD248 KD HD-MSCs. Under physiological conditions, both C/EBP and SIRT2 expressions are downregulated in adipogenesis. SIRT2 can inhibit FOXo1 by inhibiting its phosphorylation and acetylation, leading to its accumulation in the nucleus. Consequently, accumulated FOXo1 can suppress PPARγ. Such inhibition of adipogenesis, key regulator, PPARγ, causes inhibition of several downstream targets and thus inhibits the pathway. SIRT2 caused deacetylation of FoxO1 found to inhibit MSCs adipogenesis and adipocytes formation through PPARγ gene repressing (236,237).

An AML study showed a correlation between SIRT2, AML mutations, and overall survival by examining BM samples. The study suggested that upregulated expression level of SIRT2 has a negative impact on AML prognosis (238). CD248 could also be used as a prognostic tool to indicate AML prognosis. Mainly since AML cells were found to benefit from adipocytes metabolites (161-163) for their proliferation and survival, and CD248 KD on adipocytes affected their metabolic activity (214). CD248 has no direct effect on key regulators of adipogenesis since their expression levels were not changing in siCD248-treated differentiated HD-MSCs. Instead, CD248 is potentially involved in the MSCs adipogenesis pathway

through its direct effect on SRT2 expression, which directly impacts the FoXO1 gene. The mechanisms and interaction between CD248 and SIRT2 are unclear; therefore, further validation of SIRT2 upregulation is needed for a definitive conclusion. CD248 is essential in HD-MSCs adipogenesis differentiation. When knocked down, it reduced their in-vitro differentiation. The effect of MSCs dysregulated CD248 at the BME level could be similar. Overexpression of CD248 on AML-MSCs might lead to an altered cellular composition of the BME and unbalanced adipocytes composition. Thus, the dysregulated level of CD248 in AML-MSCs could affect MSC's ability to provide a healthy niche for maintaining normal hematopoiesis and contribute to AML progression.

Additional to the limitation of some of the used assays (as seen in the results sections), the validation of only three potential targets (GREM-1, SCUBE3, and CD248) out of the 21-gene list could also be considered a limitation of this investigation, and further validation of other targets in the future could add to the understanding of the AML-MSCs in AML biology. In addition, the use of HR AML-MSCs to validate the CD248 significance, which was the focus of this study due to the previously observed functional impairments of these MSCs, could also limit the presented work. Furthermore, future confirmation of the predicted mechanism by which KD CD248 leads to reduced MSCs adipogenesis potential through validation of the SIRT2 level at both gene and protein validation would be required to ensure these findings.

Conclusion

Data in this study provided an extensive systematic analysis of a large cohort of MSCs derived from AML patients (AML-MSCs) and compared them to their healthy counterparts (HD-MSCs). Based on the transcriptomic analysis of their gene expression profile, AML-MSCs have a unique transcriptomic signature, an altered gene profile with 21 SDRGs (Figure 6.1). These altered genes were found to be critical in several cellular and molecular processes; hence their dysregulation could provide new insights into MSC's role in BME alterations and their contribution to a more permissive BME and thus contribute to AML pathogenesis. Furthermore, the 21-gene list helped in the identification of novel potential targets. Investigation of CD248 specifically in HR AML-MSCs enabled the selection of CD248 as a potential target in MSCs' function.

An in-vitro knockdown model of CD248 was successfully established in HD-MSCs. CD248 knockdown (KD) had no significant effect on HD-MSCs osteogenesis, HL60 proliferation, or MSCs protein profile. Interestingly, CD248 KD on HD-MSCs affected their adipogenesis differentiation. Knocking down CD248 increased their SIRT2 expression, which was predicted to cause inhibition of the adipogenesis pathway. Results collectively suggest that the physiological level of CD248 at both gene and protein levels is necessary and required to maintain MSCs' function, especially their adipogenesis differentiation. Both overexpression and down-regulation of CD248 on HR AML-MSCs and HD-MSCs correlated with MSCs altered differentiation. The impairments on HR AML-MSCs adipogenesis could have resulted from MSCs compensation mechanism since several genes were

dysregulated on these AML-MSCs. Since CD248 overexpression in AML-MSCs was not related to a specific mutation or AML risk group (CD248 was overexpressed in hMSCs samples from 11 AML patients with various mutations and normal and abnormal karyotypes), it would be interesting to investigate its potential as a prognostic or diagnostic marker for AML. Moreover, the investigation of CD248 using HD-MSCs provided a significant role of CD248 in MSCs differentiation; their adipogenic differentiation, which is critical in their physiological role and function in BME, HSC niche, composition, and hematopoiesis regulation.

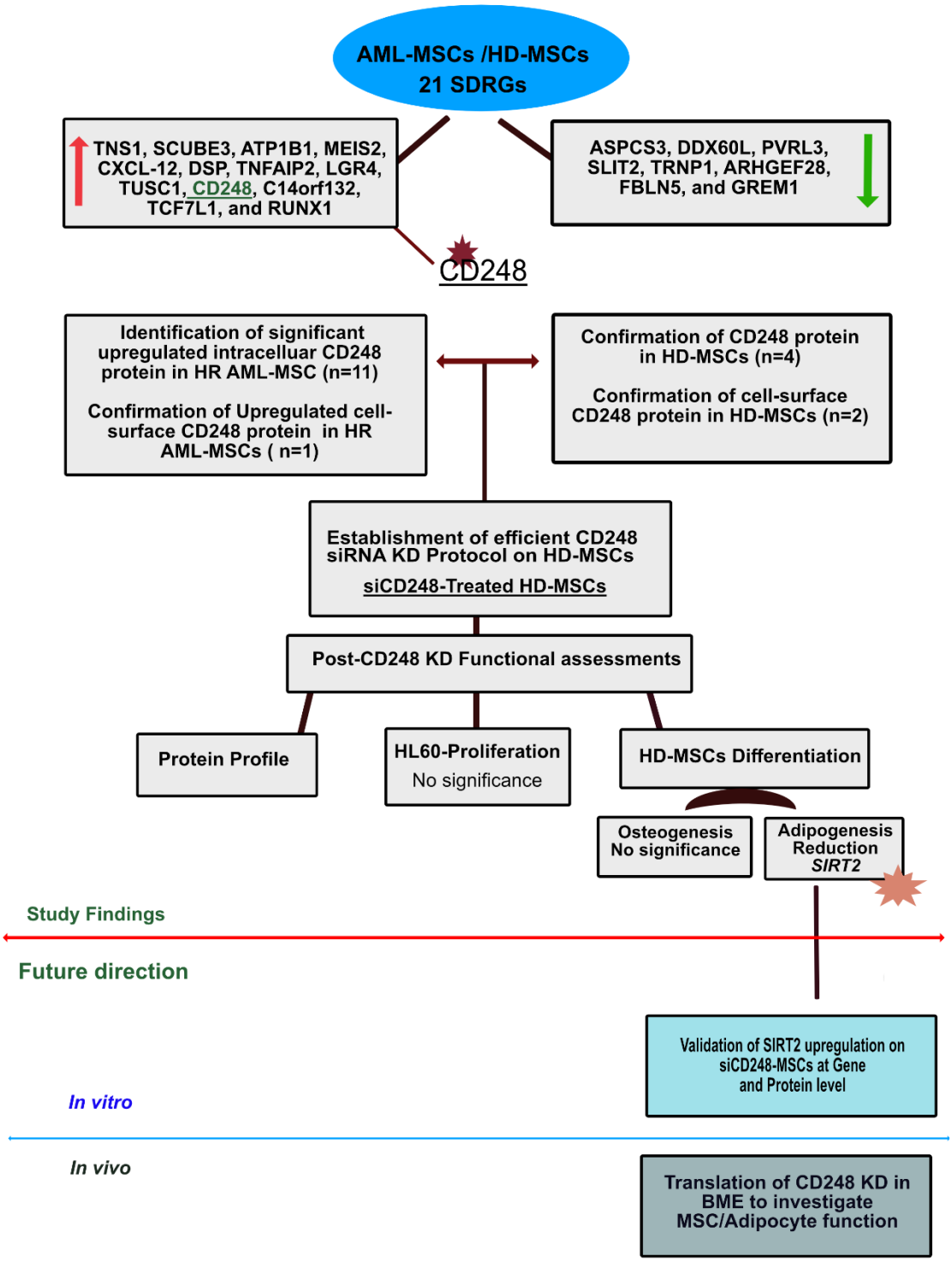

Figure 6.1. Summary of main study findings and future direction.

References

References

1. Scadden, D. T. (2006). The stem-cell niche as an entity of action. Nature, 441(7097), 1075-1079.
2. Jagannathan-Bogdan, M., & Zon, L. I. (2013). Hematopoiesis. Development, 140(12), 2463-2467.
3. Seita, J., & Weissman, I. L. (2010). Hematopoietic stem cell: self-renewal versus differentiation. Wiley Interdisciplinary Reviews: Systems Biology and Medicine, 2(6), 640-653.
4. Zon, L. I. (2008). Intrinsic and extrinsic control of haematopoietic stem-cell self-renewal. Nature, 453(7193), 306-313.
5. Filippi, M. D., & Ghaffari, S. (2019). Mitochondria in the maintenance of hematopoietic stem cells: new perspectives and opportunities. Blood, The Journal of the American Society of Hematology, 133(18), 1943-1952.
6. Snoeck, H. W. (2017). Mitochondrial regulation of hematopoietic stem cells. Current opinion in cell biology, 49, 91-98.
7. Nakada, D., Saunders, T. L., & Morrison, S. J. (2010). Lkb1 regulates cell cycle and energy metabolism in haematopoietic stem cells. Nature, 468(7324), 653-658.
8. Balderman, S. R., & Calvi, L. M. (2014). Biology of BM failure syndromes: role of microenvironment and niches. Hematology 2014, the American Society of Hematology Education Program Book, 2014(1), 71-76.
9. Anthony, B. A., & Link, D. C. (2014). Regulation of hematopoietic stem cells by bone marrow stromal cells. Trends in immunology, 35(1), 32-37.
10. Kollet, O., Dar, A., Shivtiel, S., Kalinkovich, A., Lapid, K., Sztainberg, Y., ... & Lapidot, T. (2006). Osteoclasts degrade endosteal components and promote mobilization of hematopoietic progenitor cells. Nature medicine, 12(6), 657-664.
11. Solar, G. P., Kerr, W. G., Zeigler, F. C., Hess, D., Donahue, C., de Sauvage, F. J., & Eaton, D. L. (1998). Role of c-mpl in early hematopoiesis. Blood, The Journal of the American Society of Hematology, 92(1), 4-10.
12. Robb, L. (2007). Cytokine receptors and hematopoietic differentiation. Oncogene, 26(47), 6715-6723.
13. Metcalf, D. (2008). Hematopoietic cytokines. Blood, The Journal of the American Society of Hematology, 111(2), 485-491.
14. Hanoun, M., Maryanovich, M., Arnal-Estapé, A., & Frenette, P. S. (2015). Neural regulation of hematopoiesis, inflammation, and cancer. Neuron, 86(2), 360-373.
15. Mendelson, A., & Frenette, P. S. (2014). Hematopoietic stem cell niche maintenance during homeostasis and regeneration. Nature medicine, 20(8), 833-846.
16. Rigaud, S., & Sauer, K. (2015). IP3 3-kinase B prevents bone marrow failure. Oncotarget, 6(18), 15706.
17. Desterke, C., Bennaceur-Griscelli, A., & Turhan, A. G. (2021). EGR1 dysregulation defines an inflammatory and leukemic program in cell trajectory of human-aged hematopoietic stem cells (HSC). Stem cell research & therapy, 12(1), 1-20.
18. Wang, Q., Stacy, T., Binder, M., Marin-Padilla, M., Sharpe, A. H., & Speck, N. A. (1996). Disruption of the Cbfa2 gene causes necrosis and hemorrhaging in the

central nervous system and blocks definitive hematopoiesis. Proceedings of the National Academy of Sciences, 93(8), 3444-3449.
19. Risk factors for acute myelogenous leukemia (AML). (n.d.). Retrieved 2022.Canadain Cancer society. https://cancer.ca/en/cancer-information/cancer-types/acute-myelogenous-leukemia-aml/risks
20. Cancer Stat Facts: Leukemia — Acute Myeloid Leukemia (AML). (n.d.). Retrieved 2022. National cancer institute. https://seer.cancer.gov/statfacts/html/amyl.html
21. Steffen, B., Müller-Tidow, C., Schwäble, J., Berdel, W. E., & Serve, H. (2005). The molecular pathogenesis of acute myeloid leukemia. Critical reviews in oncology/hematology, 56(2), 195-221.
22. Estey, E., & Döhner, H. (2006). Acute myeloid leukaemia. The Lancet, 368(9550), 1894-1907.
23. Colmone, A., Amorim, M., Pontier, A. L., Wang, S., Jablonski, E., & Sipkins, D. A. (2008). Leukemic cells create bone marrow niches that disrupt the behavior of normal hematopoietic progenitor cells. Science, 322(5909), 1861-1865.
24. Hwang, S. M. (2020). Classification of acute myeloid leukemia. Blood research, 55(S1), S1-S4.
25. Arber, D. A., Orazi, A., Hasserjian, R., Thiele, J., Borowitz, M. J., & Michelle, M. Le Beau, Clara D. Bloomfield, Mario Cazzola, et James W. Vardiman. 2016.«The 2016 Revision to the World Health Organization Classification of Myeloid Neoplasms and Acute Leukemia». Blood, 127(20), 2391-2405.
26. Acute myeloid leukemia.(n.d).Retrieved 2021. American Cancer society https://www.cancer.org/cancer/acutemyeloidleukemia/detection-diagnosis-staging/how-classified.html
27. Abdul-Hamid, G. (2011). Classification of Acute Leukemia. In (Ed.), Acute Leukemia - The Scientist's Perspective and Challenge. IntechOpen. https://doi.org/10.5772/19848
28. Deschler, B., & Lübbert, M. (2008). Acute myeloid leukemia: epidemiology and etiology. Acute Leukemias, 47-56.
29. Papaemmanuil, E., Gerstung, M., Bullinger, L., Gaidzik, V. I., Paschka, P., Roberts, N. D., ... & Campbell, P. J. (2016). Genomic classification and prognosis in acute myeloid leukemia. New England Journal of Medicine, 374(23), 2209-2221.
30. Kottaridis, P. D., Gale, R. E., Frew, M. E., Harrison, G., Langabeer, S. E., Belton, A. A., ... & Linch, D. C. (2001). The presence of a FLT3 internal tandem duplication in patients with acute myeloid leukemia (AML) adds important prognostic information to cytogenetic risk group and response to the first cycle of chemotherapy: analysis of 854 patients from the United Kingdom Medical Research Council AML 10 and 12 trials. Blood, The Journal of the American Society of Hematology, 98(6), 1752-1759.
31. Nakao, M., Yokota, S., Iwai, T., Kaneko, H., Horiike, S., Kashima, K., ... & Misawa, S. (1996). Internal tandem duplication of the flt3 gene found in acute myeloid leukemia. Leukemia, 10(12), 1911-1918.
32. Daver, N., Schlenk, R. F., Russell, N. H., & Levis, M. J. (2019). Targeting FLT3 mutations in AML: review of current knowledge and evidence. Leukemia, 33(2), 299-312.

33. Majothi, S., Adams, D., Loke, J., Stevens, S. P., Wheatley, K., & Wilson, J. S. (2020). FLT3 inhibitors in acute myeloid leukaemia: assessment of clinical effectiveness, adverse events and future research—a systematic review and meta-analysis. Systematic reviews, 9(1), 1-14.
34. Pratz, K. W., Cortes, J., Roboz, G. J., Rao, N., Arowojolu, O., Stine, A., ... & Levis, M. (2009). A pharmacodynamic study of the FLT3 inhibitor KW-2449 yields insight into the basis for clinical response. Blood, The Journal of the American Society of Hematology, 113(17), 3938-3946.
35. Levis, M., Brown, P., Smith, B. D., Stine, A., Pham, R., Stone, R., ... & Small, D. (2006). Plasma inhibitory activity (PIA): a pharmacodynamic assay reveals insights into the basis for cytotoxic response to FLT3 inhibitors. Blood, 108(10), 3477-3483.
36. Falini, B., Martelli, M. P., Bolli, N., Sportoletti, P., Liso, A., Tiacci, E., & Haferlach, T. (2011). Acute myeloid leukemia with mutated nucleophosmin (NPM1): is it a distinct entity?. Blood, The Journal of the American Society of Hematology, 117(4), 1109-1120.
37. Estey, E. H. (2012). How to manage high-risk acute myeloid leukemia. Leukemia, 26(5), 861-869.
38. Estey, E. (2010). High cytogenetic or molecular genetic risk acute myeloid leukemia. Hematology 2010, the American Society of Hematology Education Program Book, 2010(1), 474-480.
39. Schiller, G. J. (2013). High-risk acute myelogenous leukemia: treatment today and tomorrow. Hematology 2013, the American Society of Hematology Education Program Book, 2013(1), 201-208.
40. Paschka, P., Marcucci, G., Ruppert, A. S., Mrózek, K., Chen, H., Kittles, R. A., ... & Bloomfield, C. D. (2006). Adverse prognostic significance of KIT mutations in adult acute myeloid leukemia with inv (16) and t (8; 21): a Cancer and Leukemia Group B Study. Journal of Clinical Oncology, 24(24), 3904-3911.
41. Tsirigotis, P., Byrne, M., Schmid, C., Baron, F., Ciceri, F., Esteve, J., ... & Nagler, A. (2016). Relapse of AML after hematopoietic stem cell transplantation: methods of monitoring and preventive strategies. A review from the ALWP of the EBMT. Bone marrow transplantation, 51(11), 1431-1438.
42. Ossenkoppele, G. J., Janssen, J. J., & van de Loosdrecht, A. A. (2016). Risk factors for relapse after allogeneic transplantation in acute myeloid leukemia. Haematologica, 101(1), 20.
43. Döhner, H., Estey, E. H., Amadori, S., Appelbaum, F. R., Büchner, T., Burnett, A. K., ... & Bloomfield, C. D. (2010). Diagnosis and management of acute myeloid leukemia in adults: recommendations from an international expert panel, on behalf of the European LeukemiaNet. Blood, The Journal of the American Society of Hematology, 115(3), 453-474.
44. De Greef, G. E., Van Putten, W. L., Boogaerts, M., Huijgens, P. C., Verdonck, L. F., Vellenga, E., ... & Swiss Group for Clinical Cancer Research SAKK. (2005). Criteria for defining a complete remission in acute myeloid leukaemia revisited. An analysis of patients treated in HOVON-SAKK co-operative group studies. British journal of haematology, 128(2), 184-191.
45. Vainstein, V., Buckley, S. A., Shukron, O., Estey, E. H., Abkowitz, J. L., Wood, B. L., & Walter, R. B. (2014). Rapid rate of peripheral blood blast clearance

accurately predicts complete remission in acute myeloid leukemia. Leukemia, 28(3), 713-716.
46. Cheson, B. D., Bennett, J. M., Kopecky, K. J., Büchner, T., Willman, C. L., Estey, E. H., ... & Bloomfield, C. D. (2003). Revised recommendations of the international working group for diagnosis, standardization of response criteria, treatment outcomes, and reporting standards for therapeutic trials in acute myeloid leukemia. Journal of clinical oncology, 21(24), 4642-4649.
47. Zeijlemaker, W., & Schuurhuis, G. J. (2013). Minimal residual disease and leukemic stem cells in acute myeloid leukemia. Leukemia.
48. Sakamaki, H., Miyawaki, S., Ohtake, S., Emi, N., Yagasaki, F., Mitani, K., ... & Ohno, R. (2010). Allogeneic stem cell transplantation versus chemotherapy as post-remission therapy for intermediate or poor risk adult acute myeloid leukemia: results of the JALSG AML97 study. International journal of hematology, 91(2), 284-292.
49. Hospital, M. A., Thomas, X., Castaigne, S., Raffoux, E., Pautas, C., Gardin, C., ... & Dombret, H. (2012). Evaluation of allogeneic hematopoietic SCT in younger adults with adverse karyotype AML. Bone marrow transplantation, 47(11), 1436-1441.
50. Patel, A., Agha, M., Raptis, A., Hou, J. Z., Farah, R., Redner, R. L., ... & Boyiadzis, M. (2021). Outcomes of patients with acute myeloid leukemia who relapse after 5 years of complete remission. Oncology Research Featuring Preclinical and Clinical Cancer Therapeutics, 28(78), 811-814.
51. Ngai, L. L., Kelder, A., Janssen, J. J., Ossenkoppele, G. J., & Cloos, J. (2021). MRD tailored therapy in AML: what we have learned so far. Frontiers in Oncology, 10, 603636.
52. Van Rhenen, A., Feller, N., Kelder, A., Westra, A. H., Rombouts, E., Zweegman, S., ... & Schuurhuis, G. J. (2005). High stem cell frequency in acute myeloid leukemia at diagnosis predicts high minimal residual disease and poor survival. Clinical cancer research, 11(18), 6520-6527.
53. Estey, E. (2016). Acute myeloid leukemia: 2016 Update on risk-stratification and management. American journal of hematology, 91(8), 824-846.
54. Thol, F., & Ganser, A. (2020). Treatment of relapsed acute myeloid leukemia. Current Treatment Options in Oncology, 21(8), 1-11.
55. Schofield, R. (1978). The relationship between the spleen colony-forming cell and the haemopoietic stem cell. Blood cells, 4(1-2), 7-25.
56. Morrison, S. J., & Scadden, D. T. (2014). The bone marrow niche for haematopoietic stem cells. Nature, 505(7483), 327-334.
57. Boulais, P. E., & Frenette, P. S. (2015). Making sense of hematopoietic stem cell niches. Blood, The Journal of the American Society of Hematology, 125(17), 2621-2629.
58. Ellis, S. L., & Nilsson, S. K. (2012). The location and cellular composition of the hemopoietic stem cell niche. Cytotherapy, 14(2), 135-143.
59. Calvi, L. M., & Link, D. C. (2014). Cellular complexity of the bone marrow hematopoietic stem cell niche. Calcified tissue international, 94(1), 112-124.
60. Gong, J. K. (1978). Endosteal marrow: a rich source of hematopoietic stem cells. Science, 199(4336), 1443-1445.

61. Kiel, M. J., Yilmaz, Ö. H., Iwashita, T., Yilmaz, O. H., Terhorst, C., & Morrison, S. J. (2005). SLAM family receptors distinguish hematopoietic stem and progenitor cells and reveal endothelial niches for stem cells. cell, 121(7), 1109-1121.
62. Lévesque, J. P., Helwani, F. M., & Winkler, I. (2010). The endosteal 'osteoblastic'niche and its role in hematopoietic stem cell homing and mobilization. Leukemia, 24(12), 1979-1992.
63. Galán-Díez, M., & Kousteni, S. (2017). The osteoblastic niche in hematopoiesis and hematological myeloid malignancies. Current molecular biology reports, 3(2), 53-62.
64. Lo Celso, C., Fleming, H. E., Wu, J. W., Zhao, C. X., Miake-Lye, S., Fujisaki, J., ... & Scadden, D. T. (2009). Live-animal tracking of individual haematopoietic stem/progenitor cells in their niche. Nature, 457(7225), 92-96.
65. El-Badri, N. S., Wang, B. Y., & Good, R. A. (1998). Osteoblasts promote engraftment of allogeneic hematopoietic stem cells. Experimental hematology, 26(2), 110-116.
66. Ding, L., & Morrison, S. J. (2013). Haematopoietic stem cells and early lymphoid progenitors occupy distinct bone marrow niches. Nature, 495(7440), 231-235.
67. Matsuoka, Y., Nakatsuka, R., Sumide, K., Kawamura, H., Takahashi, M., Fujioka, T., ... & Sonoda, Y. (2015). Prospectively isolated human bone marrow cell-derived MSCs support primitive human CD34-negative hematopoietic stem cells. Stem Cells, 33(5), 1554-1565.
68. Pittenger, M. F., Mackay, A. M., Beck, S. C., Jaiswal, R. K., Douglas, R., Mosca, J. D., ... & Marshak, D. R. (1999). Multilineage potential of adult human mesenchymal stem cells. science, 284(5411), 143-147.
69. Friedenstein, A. J., Chailakhjan, R. K., & Lalykina, K. (1970). The development of fibroblast colonies in monolayer cultures of guinea-pig bone marrow and spleen cells. Cell Proliferation, 3(4), 393-403.
70. Prockop, D. J. (1997). Marrow stromal cells as stem cells for nonhematopoietic tissues. Science, 276(5309), 71-74.
71. Viswanathan, S., Shi, Y., Galipeau, J., Krampera, M., Leblanc, K., Martin, I., ... & Sensebe, L. (2019). Mesenchymal stem versus stromal cells: International Society for Cell & Gene Therapy (ISCT®) Mesenchymal Stromal Cell committee position statement on nomenclature. Cytotherapy, 21(10), 1019-1024.
72. Anthony, B. A., & Link, D. C. (2014). Regulation of hematopoietic stem cells by bone marrow stromal cells. Trends in immunology, 35(1), 32-37.
73. Raaijmakers, M. H., Mukherjee, S., Guo, S., Zhang, S., Kobayashi, T., Schoonmaker, J. A., ... & Scadden, D. (2010). Bone progenitor dysfunction induces myelodysplasia and secondary leukaemia. Nature, 464(7290), 852-857.
74. Méndez-Ferrer, S., Michurina, T. V., Ferraro, F., Mazloom, A. R., MacArthur, B. D., Lira, S. A., ... & Frenette, P. S. (2010). Mesenchymal and haematopoietic stem cells form a unique bone marrow niche. nature, 466(7308), 829-834.

75. Geyh, S., Rodriguez-Paredes, M., Jäger, P., Khandanpour, C., Cadeddu, R. P., Gutekunst, J., ... & Schroeder, T. (2016). Functional inhibition of mesenchymal stromal cells in acute myeloid leukemia. Leukemia, 30(3), 683-691.
76. Crippa, S., & Bernardo, M. E. (2018). Mesenchymal stromal cells: role in the BM niche and in the support of hematopoietic stem cell transplantation. Hemasphere, 2(6).
77. Saleh, M., Movassaghpourakbari, A., Akbarzadehlaleh, P., & Molaeipour, Z. (2015). The impact of mesenchymal stem cells on differentiation of hematopoietic stem cells. Advanced pharmaceutical bulletin, 5(3), 299.
78. Dazzi, F., Ramasamy, R., Glennie, S., Jones, S. P., & Roberts, I. (2006). The role of mesenchymal stem cells in haemopoiesis. Blood reviews, 20(3), 161-171.
79. Dexter, T. M., & Spooncer, E. (1987). Growth and differentiation in the hemopoietic system. Annual review of cell biology, 3, 423-441.
80. Bianco, P. (2011). Minireview: the stem cell next door: skeletal and hematopoietic stem cell “niches” in bone. Endocrinology, 152(8), 2957-2962.
81. Dorshkind, K. (1990). Regulation of hemopoiesis by bone marrow stromal cells and their products. Annual review of immunology, 8, 111-137.
82. Koller, M. R., Oxender, M., Jensen, T. C., Goltry, K. L., & Smith, A. K. (1999). Direct contact between CD34+ lin− cells and stroma induces a soluble activity that specifically increases primitive hematopoietic cell production. Experimental hematology, 27(4), 734-741.
83. Wagner, W., Roderburg, C., Wein, F., Diehlmann, A., Frankhauser, M., Schubert, R., ... & Ho, A. D. (2007). Molecular and secretory profiles of human mesenchymal stromal cells and their abilities to maintain primitive hematopoietic progenitors. Stem cells, 25(10), 2638-2647.
84. Bensidhoum, M., Chapel, A., Francois, S., Demarquay, C., Mazurier, C., Fouillard, L., ... & Lopez, M. (2004). Homing of in vitro expanded Stro-1-or Stro-1+ human mesenchymal stem cells into the NOD/SCID mouse and their role in supporting human CD34 cell engraftment. Blood, 103(9), 3313-3319.
85. Devine, S. M., Bartholomew, A. M., Mahmud, N., Nelson, M., Patil, S., Hardy, W., ... & Hoffman, R. (2001). Mesenchymal stem cells are capable of homing to the bone marrow of non-human primates following systemic infusion. Experimental hematology, 29(2), 244-255.
86. Muguruma, Y., Yahata, T., Miyatake, H., Sato, T., Uno, T., Itoh, J., ... & Ando, K. (2006). Reconstitution of the functional human hematopoietic microenvironment derived from human mesenchymal stem cells in the murine bone marrow compartment. Blood, 107(5), 1878-1887.
87. Koç, O. N., Gerson, S. L., Cooper, B. W., Dyhouse, S. M., Haynesworth, S. E., Caplan, A. I., & Lazarus, H. M. (2000). Rapid hematopoietic recovery after coinfusion of autologous-blood stem cells and culture-expanded marrow mesenchymal stem cells in advanced breast cancer patients receiving high-dose chemotherapy. Journal of clinical oncology, 18(2), 307-307.
88. Lazarus, H. M., Koc, O. N., Devine, S. M., Curtin, P., Maziarz, R. T., Holland, H. K., ... & Bacigalupo, A. (2005). Cotransplantation of HLA-identical sibling culture-expanded mesenchymal stem cells and hematopoietic stem cells in hematologic malignancy patients. Biology of blood and marrow transplantation, 11(5), 389-398.

89. Aqmasheh, S., Akbarzadehlaleh, P., Sarvar, D. P., & Timari, H. (2017). Effects of mesenchymal stem cell derivatives on hematopoiesis and hematopoietic stem cells. Advanced pharmaceutical bulletin, 7(2), 165.
90. Sugiyama, T., Kohara, H., Noda, M., & Nagasawa, T. (2006). Maintenance of the hematopoietic stem cell pool by CXCL12-CXCR4 chemokine signaling in bone marrow stromal cell niches. Immunity, 25(6), 977-988.
91. Feng, L., Xue, D., Chen, E., Zhang, W., Gao, X., Yu, J., ... & Pan, Z. (2016). HMGB1 promotes the secretion of multiple cytokines and potentiates the osteogenic differentiation of mesenchymal stem cells through the Ras/MAPK signaling pathway. Experimental and therapeutic medicine, 12(6), 3941-3947.
92. Arai, F., Hirao, A., Ohmura, M., Sato, H., Matsuoka, S., Takubo, K., ... & Suda, T. (2004). Tie2/angiopoietin-1 signaling regulates hematopoietic stem cell quiescence in the bone marrow niche. Cell, 118(2), 149-161.
93. Weber, J. M., & Calvi, L. M. (2010). Notch signaling and the bone marrow hematopoietic stem cell niche. Bone, 46(2), 281-285.
94. Calvi, L. M., Adams, G. B., Weibrecht, K. W., Weber, J. M., Olson, D. P., Knight, M. C., ... & Scadden, D. T. (2003). Osteoblastic cells regulate the haematopoietic stem cell niche. Nature, 425(6960), 841-846.
95. Han, J. Y., Goh, R. Y., Seo, S. Y., Hwang, T. H., Kwon, H. C., Kim, S. H., ... & Lee, Y. H. (2007). Cotransplantation of cord blood hematopoietic stem cells and culture-expanded and GM-CSF-/SCF-transfected mesenchymal stem cells in SCID mice. Journal of Korean medical science, 22(2), 242-247.
96. Mishima, S., Nagai, A., Abdullah, S., Matsuda, C., Taketani, T., Kumakura, S., ... & Masuda, J. (2010). Effective ex vivo expansion of hematopoietic stem cells using osteoblast-differentiated mesenchymal stem cells is CXCL12 dependent. European journal of haematology, 84(6), 538-546.
97. Gnecchi, M., He, H., Noiseux, N., Liang, O. D., Zhang, L., Morello, F., ... & Dzau, V. J. (2006). Evidence supporting paracrine hypothesis for Akt-modified mesenchymal stem cell-mediated cardiac protection and functional improvement. The FASEB Journal, 20(6), 661-669.
98. Wang, L., Li, Y., Zhang, X., Liu, N., Shen, S., Sun, S., ... & Shen, L. (2021). Paracrine interleukin-8 affects mesenchymal stem cells through the Akt pathway and enhances human umbilical vein endothelial cell proliferation and migration. Bioscience Reports, 41(5).
99. Dumitru, C. A., Hemeda, H., Jakob, M., Lang, S., & Brandau, S. (2014). Stimulation of mesenchymal stromal cells (MSCs) via TLR3 reveals a novel mechanism of autocrine priming. The FASEB Journal, 28(9), 3856-3866.
100. Yuan, Z., Li, Q., Luo, S., Liu, Z., Luo, D., Zhang, B., ... & Xiao, J. (2016). PPARγ and Wnt signaling in adipogenic and osteogenic differentiation of mesenchymal stem cells. Current stem cell research & therapy, 11(3), 216-225.
101. Song, B. Q., Chi, Y., Li, X., Du, W. J., Han, Z. B., Tian, J. J., ... & Han, Z. C. (2015). Inhibition of Notch signaling promotes the adipogenic differentiation of mesenchymal stem cells through autophagy activation and PTEN-PI3K/AKT/mTOR pathway. Cellular Physiology and Biochemistry, 36(5), 1991-2002.

102. Chen, G., Deng, C., & Li, Y. P. (2012). TGF-β and BMP signaling in osteoblast differentiation and bone formation. International journal of biological sciences, 8(2), 272.
103. Fontaine, C., Cousin, W., Plaisant, M., Dani, C., & Peraldi, P. (2008). Hedgehog signaling alters adipocyte maturation of human mesenchymal stem cells. Stem cells, 26(4), 1037-1046.
104. Chen, Q., Shou, P., Zheng, C., Jiang, M., Cao, G., Yang, Q., ... & Shi, Y. (2016). Fate decision of mesenchymal stem cells: adipocytes or osteoblasts?. Cell Death & Differentiation, 23(7), 1128-1139.
105. Bianco, P., Robey, P. G., Saggio, I., & Riminucci, M. (2010). "Mesenchymal" stem cells in human bone marrow (skeletal stem cells): a critical discussion of their nature, identity, and significance in incurable skeletal disease. Human gene therapy, 21(9), 1057-1066.
106. Manolagas, S. C., & Jilka, R. L. (1995). Bone marrow, cytokines, and bone remodeling—emerging insights into the pathophysiology of osteoporosis. New England journal of medicine, 332(5), 305-311.
107. Bianco, P., Cao, X., Frenette, P. S., Mao, J. J., Robey, P. G., Simmons, P. J., & Wang, C. Y. (2013). The meaning, the sense and the significance: translating the science of mesenchymal stem cells into medicine. Nature medicine, 19(1), 35-42.
108. Chen, L., Tredget, E. E., Wu, P. Y., & Wu, Y. (2008). Paracrine factors of mesenchymal stem cells recruit macrophages and endothelial lineage cells and enhance wound healing. PloS one, 3(4), e1886.
109. Lee, R. H., Pulin, A. A., Seo, M. J., Kota, D. J., Ylostalo, J., Larson, B. L., ... & Prockop, D. J. (2009). Intravenous hMSCs improve myocardial infarction in mice because cells embolized in lung are activated to secrete the anti-inflammatory protein TSG-6. Cell stem cell, 5(1), 54-63.
110. Wang, G., Bunnell, B. A., Painter, R. G., Quiniones, B. C., Tom, S., Lanson Jr, N. A., ... & Kolls, J. K. (2005). Adult stem cells from bone marrow stroma differentiate into airway epithelial cells: potential therapy for cystic fibrosis. Proceedings of the National Academy of Sciences, 102(1), 186-191.
111. Siegel, P. M., & Massagué, J. (2003). Cytostatic and apoptotic actions of TGF-β in homeostasis and cancer. Nature Reviews Cancer, 3(11), 807-820.
112. de Araújo Farias, V., Carrillo-Gálvez, A. B., Martin, F., & Anderson, P. (2018). TGF-β and mesenchymal stromal cells in regenerative medicine, autoimmunity and cancer. Cytokine & Growth Factor Reviews, 43, 25-37.
113. Grafe, I., Alexander, S., Peterson, J. R., Snider, T. N., Levi, B., Lee, B., & Mishina, Y. (2018). TGF-β family signaling in mesenchymal differentiation. Cold Spring Harbor perspectives in biology, 10(5), a022202.
114. Kang, Q., Sun, M. H., Cheng, H., Peng, Y., Montag, A. G., Deyrup, A. T., ... & He, T. C. (2004). Characterization of the distinct orthotopic bone-forming activity of 14 BMPs using recombinant adenovirus-mediated gene delivery. Gene therapy, 11(17), 1312-1320.
115. Wu, M., Chen, G., & Li, Y. P. (2016). TGF-β and BMP signaling in osteoblast, skeletal development, and bone formation, homeostasis and disease. Bone research, 4(1), 1-21.

116. Ali, I. H., & Brazil, D. P. (2014). Bone morphogenetic proteins and their antagonists: current and emerging clinical uses. British journal of pharmacology, 171(15), 3620-3632.
117. Dean, D. B., Watson, J. T., Moed, B. R., & Zhang, Z. (2009). Role of bone morphogenetic proteins and their antagonists in healing of bone fracture. Frontiers in Bioscience-Landmark, 14(8), 2878-2888.
118. Hu, K., Sun, H., Gui, B., & Sui, C. (2017). Gremlin-1 suppression increases BMP-2-induced osteogenesis of human mesenchymal stem cells. Molecular medicine reports, 15(4), 2186-2194.
119. Hsu, D. R., Economides, A. N., Wang, X., Eimon, P. M., & Harland, R. M. (1998). The Xenopus dorsalizing factor Gremlin identifies a novel family of secreted proteins that antagonize BMP activities. Molecular cell, 1(5), 673-683.
120. Topol, L. Z., Bardot, B., Zhang, Q., Resau, J., Huillard, E., Marx, M., ... & Blair, D. G. (2000). Biosynthesis, post-translation modification, and functional characterization of Drm/Gremlin. Journal of Biological Chemistry, 275(12), 8785-8793.
121. Mitola, S., Ravelli, C., Moroni, E., Salvi, V., Leali, D., Ballmer-Hofer, K., ... & Presta, M. (2010). Gremlin is a novel agonist of the major proangiogenic receptor VEGFR2. Blood, The Journal of the American Society of Hematology, 116(18), 3677-3680.
122. Xiang, Q., Hong, D., Liao, Y., Cao, Y., Liu, M., Pang, J., ... & Xiang, A. P. (2017). Overexpression of gremlin1 in mesenchymal stem cells improves hindlimb ischemia in mice by enhancing cell survival. Journal of Cellular Physiology, 232(5), 996-1007.
123. Michos, O., Panman, L., Vintersten, K., Beier, K., Zeller, R., & Zuniga, A. (2004). Gremlin-mediated BMP antagonism induces the epithelial-mesenchymal feedback signaling controlling metanephric kidney and limb organogenesis.
124. Yang, H. Y., Cheng, C. F., Djoko, B., Lian, W. S., Tu, C. F., Tsai, M. T., ... & Yang, R. B. (2007). Transgenic overexpression of the secreted, extracellular EGF-CUB domain-containing protein SCUBE3 induces cardiac hypertrophy in mice. Cardiovascular research, 75(1), 139-147.
125. Adipogenesis Pathway. (2021). Ingenuity pathway analysis, Qiagen.
126. Naveiras, O., Nardi, V., Wenzel, P. L., Hauschka, P. V., Fahey, F., & Daley, G. Q. (2009). Bone-marrow adipocytes as negative regulators of the haematopoietic microenvironment. Nature, 460(7252), 259-263.
127. Bajaj, M. S., Ghode, S. S., Kulkarni, R. S., Limaye, L. S., & Kale, V. P. (2015). Simvastatin improves hematopoietic stem cell engraftment by preventing irradiation-induced marrow adipogenesis and radio-protecting the niche cells. Haematologica, 100(8), e323.
128. Wilson, A., Fu, H., Schiffrin, M., Winkler, C., Koufany, M., Jouzeau, J. Y., ... & Desvergne, B. (2018). Lack of adipocytes alters hematopoiesis in lipodystrophic mice. Frontiers in immunology, 9, 2573.
129. Desreumaux, P., Ernst, O., Geboes, K., Gambiez, L., Berrebi, D., Müller-Alouf, H., ... & Colombel, J. F. (1999). Inflammatory alterations in mesenteric adipose tissue in Crohn's disease. Gastroenterology, 117(1), 73-81.
130. Munir, H., Ward, L. S., Sheriff, L., Kemble, S., Nayar, S., Barone, F., ... & McGettrick, H. M. (2017). Adipogenic differentiation of mesenchymal stem cells

alters their immunomodulatory properties in a tissue-specific manner. Stem Cells, 35(6), 1636-1646.
131. Ling, W., Zhang, J., Yuan, Z., Ren, G., Zhang, L., Chen, X., Rabson, A. B., Roberts, A. I., Wang, Y., & Shi, Y. (2014). Mesenchymal stem cells use IDO to regulate immunity in tumor microenvironment. Cancer research, 74(5), 1576–1587.
132. Ren, G., Su, J., Zhang, L., Zhao, X., Ling, W., L'huillie, A., ... & Shi, Y. (2009). Species variation in the mechanisms of mesenchymal stem cell-mediated immunosuppression. Stem cells, 27(8), 1954-1962.
133. Herrero, C., & Pérez-Simón, J. A. (2010). Immunomodulatory effect of mesenchymal stem cells. Brazilian Journal of Medical and Biological Research, 43, 425-430.
134. Németh, K., Leelahavanichkul, A., Yuen, P. S., Mayer, B., Parmelee, A., Robey, P. G., ... & Mezey, É. (2009). Bone marrow stromal cells attenuate sepsis via prostaglandin E2–dependent reprogramming of host macrophages to increase their interleukin-10 production. Nature medicine, 15(1), 42-49.
135. Nemeth, K., Keane-Myers, A., Brown, J. M., Metcalfe, D. D., Gorham, J. D., Bundoc, V. G., ... & Mezey, E. (2010). Bone marrow stromal cells use TGF-β to suppress allergic responses in a mouse model of ragweed-induced asthma. Proceedings of the National Academy of Sciences, 107(12), 5652-5657.
136. Di Nicola, M., Carlo-Stella, C., Magni, M., Milanesi, M., Longoni, P. D., Matteucci, P., ... & Gianni, A. M. (2002). Human bone marrow stromal cells suppress T-lymphocyte proliferation induced by cellular or nonspecific mitogenic stimuli. Blood, The Journal of the American Society of Hematology, 99(10), 3838-3843.
137. Nauta, A. J., Lurvink, E., Kruisselbrink, A. B., Willemze, R., & Fibbe, W. E. (2005). Mesenchymal Stem Cells Inhibit Generation and Function of Both Monocyte-Derived and CD34-Derived Dendritic Cells. Blood, 106(11), 593.
138. Prigione, I., Benvenuto, F., Bocca, P., Battistini, L., Uccelli, A., & Pistoia, V. (2009). Reciprocal interactions between human mesenchymal stem cells and γδ T cells or invariant natural killer T cells. Stem cells, 27(3), 693-702.
139. Reinders, M. E., de Fijter, J. W., Roelofs, H., Bajema, I. M., de Vries, D. K., Schaapherder, A. F., ... & Rabelink, T. J. (2013). Autologous bone marrow-derived mesenchymal stromal cells for the treatment of allograft rejection after renal transplantation: results of a phase I study. Stem cells translational medicine, 2(2), 107-111.
140. Batten, P., Sarathchandra, P., Antoniw, J. W., Tay, S. S., Lowdell, M. W., Taylor, P. M., & Yacoub, M. H. (2006). Human mesenchymal stem cells induce T cell anergy and downregulate T cell allo-responses via the TH2 pathway: relevance to tissue engineering human heart valves. Tissue engineering, 12(8), 2263-2273.
141. Chen, L., Tredget, E. E., Wu, P. Y., & Wu, Y. (2008). Paracrine factors of mesenchymal stem cells recruit macrophages and endothelial lineage cells and enhance wound healing. PloS one, 3(4), e1886.
142. Lee, R. H., Seo, M. J., Reger, R. L., Spees, J. L., Pulin, A. A., Olson, S. D., & Prockop, D. J. (2006). Multipotent stromal cells from human marrow home to and promote repair of pancreatic islets and renal glomeruli in diabetic NOD/scid mice. Proceedings of the National Academy of Sciences, 103(46), 17438-17443.

143. Klyushnenkova, E., Mosca, J. D., Zernetkina, V., Majumdar, M. K., Beggs, K. J., Simonetti, D. W., Deans, R. J., & McIntosh, K. R. (2005). T cell responses to allogeneic human mesenchymal stem cells: immunogenicity, tolerance, and suppression. Journal of biomedical science, 12(1), 47–57.
144. Zhu, W., Xu, W., Jiang, R., Qian, H., Chen, M., Hu, J., ... & Chen, Y. (2006). Mesenchymal stem cells derived from bone marrow favor tumor cell growth in vivo. Experimental and molecular pathology, 80(3), 267-274.
145. Karnoub, A. E., Dash, A. B., Vo, A. P., Sullivan, A., Brooks, M. W., Bell, G. W., ... & Weinberg, R. A. (2007). Mesenchymal stem cells within tumour stroma promote breast cancer metastasis. Nature, 449(7162), 557-563.
146. Han, Z., Jing, Y., Zhang, S., Liu, Y., Shi, Y., & Wei, L. (2012). The role of immunosuppression of mesenchymal stem cells in tissue repair and tumor growth. Cell & bioscience, 2(1), 1-8.
147. Ishikawa, F., Yoshida, S., Saito, Y., Hijikata, A., Kitamura, H., Tanaka, S., ... & Shultz, L. D. (2007). Chemotherapy-resistant human AML stem cells home to and engraft within the bone-marrow endosteal region. Nature biotechnology, 25(11), 1315-1321.
148. Ninomiya, M., Abe, A., Katsumi, A., Xu, J., Ito, M., Arai, F., ... & Naoe, T. (2007). Homing, proliferation and survival sites of human leukemia cells in vivo in immunodeficient mice. Leukemia, 21(1), 136-142.
149. Hope, K. J., Jin, L., & Dick, J. E. (2004). Acute myeloid leukemia originates from a hierarchy of leukemic stem cell classes that differ in self-renewal capacity. Nature immunology, 5(7), 738-743.
150. Agarwal, P., Isringhausen, S., Li, H., Paterson, A. J., He, J., Gomariz, Á., ... & Bhatia, R. (2019). Mesenchymal niche-specific expression of Cxcl12 controls quiescence of treatment-resistant leukemia stem cells. Cell Stem Cell, 24(5), 769-784.
151. Tikhonova, A. N., Dolgalev, I., Hu, H., Sivaraj, K. K., Hoxha, E., Cuesta-Domínguez, Á., ... & Aifantis, I. (2019). The bone marrow microenvironment at single-cell resolution. Nature, 569(7755), 222-228.
152. Baryawno, N., Przybylski, D., Kowalczyk, M. S., Kfoury, Y., Severe, N., Gustafsson, K., ... & Scadden, D. T. (2019). A cellular taxonomy of the bone marrow stroma in homeostasis and leukemia. Cell, 177(7), 1915-1932.
153. Sipkins, D. A., Wei, X., Wu, J. W., Runnels, J. M., Côté, D., Means, T. K., ... & Lin, C. P. (2005). In vivo imaging of specialized bone marrow endothelial microdomains for tumour engraftment. Nature, 435(7044), 969-973.
154. Frisch, B. J., Ashton, J. M., Xing, L., Becker, M. W., Jordan, C. T., & Calvi, L. M. (2012). Functional inhibition of osteoblastic cells in an in vivo mouse model of myeloid leukemia. Blood, The Journal of the American Society of Hematology, 119(2), 540-550.
155. Kode, A., Manavalan, J. S., Mosialou, I., Bhagat, G., Rathinam, C. V., Luo, N., ... & Kousteni, S. (2014). Leukaemogenesis induced by an activating β-catenin mutation in osteoblasts. Nature, 506(7487), 240-244.
156. Krause, D. S., Fulzele, K., Catic, A., Hurley, M., Lezeau, S., Attar, E. C., ... & Scadden, D. T. (2012). Differential Regulation of Myeloid Leukemias by the Bone Marrow Microenvironment.

157. Hanoun, M., Zhang, D., Mizoguchi, T., Pinho, S., Pierce, H., Kunisaki, Y., ... & Frenette, P. S. (2014). Acute myelogenous leukemia-induced sympathetic neuropathy promotes malignancy in an altered hematopoietic stem cell niche. Cell stem cell, 15(3), 365-375.
158. Schepers, K., Pietras, E. M., Reynaud, D., Flach, J., Binnewies, M., Garg, T., ... & Passegué, E. (2013). Myeloproliferative neoplasia remodels the endosteal bone marrow niche into a self-reinforcing leukemic niche. Cell stem cell, 13(3), 285-299.
159. Bruno, S., Mancini, M., De Santis, S., Monaldi, C., Cavo, M., & Soverini, S. (2021). The role of hypoxic bone marrow microenvironment in acute myeloid leukemia and future therapeutic opportunities. International Journal of Molecular Sciences, 22(13), 6857.
160. Reikvam, H., Brenner, A. K., Hagen, K. M., Liseth, K., Skrede, S., Hatfield, K. J., & Bruserud, Ø. (2015). The cytokine-mediated crosstalk between primary human acute myeloid cells and mesenchymal stem cells alters the local cytokine network and the global gene expression profile of the mesenchymal cells. Stem cell research, 15(3), 530-541.
161. Yang, S., Lu, W., Zhao, C., Zhai, Y., Wei, Y., Liu, J., ... & Shi, J. (2020). Leukemia cells remodel marrow adipocytes via TRPV4-dependent lipolysis. Haematologica, 105(11), 2572.
162. Rashkovan, M., & Ferrando, A. (2019). Metabolic dependencies and vulnerabilities in leukemia. Genes & development, 33(21-22), 1460-1474.
163. Ye, H., Adane, B., Khan, N., Sullivan, T., Minhajuddin, M., Gasparetto, M., ... & Jordan, C. T. (2016). Leukemic stem cells evade chemotherapy by metabolic adaptation to an adipose tissue niche. Cell stem cell, 19(1), 23-37.
164. Mansour, I., Zayed, R. A., Said, F., & Latif, L. A. (2016). Indoleamine 2, 3-dioxygenase and regulatory T cells in acute myeloid leukemia. Hematology, 21(8), 447-453.
165. Konopleva, M., Konoplev, S., Hu, W., Zaritskey, A. Y., Afanasiev, B. V., & Andreeff, M. (2002). Stromal cells prevent apoptosis of AML cells by up-regulation of anti-apoptotic proteins. Leukemia, 16(9), 1713-1724.
166. Forte, D., García-Fernández, M., Sánchez-Aguilera, A., Stavropoulou, V., Fielding, C., Martín-Pérez, D., ... & Méndez-Ferrer, S. (2020). Bone marrow mesenchymal stem cells support acute myeloid leukemia bioenergetics and enhance antioxidant defense and escape from chemotherapy. Cell metabolism, 32(5), 829-843.
167. Schajnovitz, A., & Scadden, D. T. (2014). Bone's dark side: mutated osteoblasts implicated in leukemia. Cell Research, 24(4), 383-384.
168. Dong, L., Yu, W. M., Zheng, H., Loh, M. L., Bunting, S. T., Pauly, M., ... & Qu, C. K. (2016). Leukaemogenic effects of Ptpn11 activating mutations in the stem cell microenvironment. Nature, 539(7628), 304-308.
169. Lopatina, T., Gai, C., Deregibus, M. C., Kholia, S., & Camussi, G. (2016). Cross talk between cancer and mesenchymal stem cells through extracellular vesicles carrying nucleic acids. Frontiers in oncology, 6, 125.
170. Xiao, P., Sandhow, L., Heshmati, Y., Kondo, M., Bouderlique, T., Dolinska, M., ... & Qian, H. (2018). Distinct roles of mesenchymal stem and progenitor cells

during the development of acute myeloid leukemia in mice. Blood advances, 2(12), 1480-1494.
171. Kode, A., Mosialou, I., Manavalan, S. J., Rathinam, C. V., Friedman, R. A., Teruya-Feldstein, J., ... & Kousteni, S. (2016). FoxO1-dependent induction of acute myeloid leukemia by osteoblasts in mice. Leukemia, 30(1), 1-13.
172. Zinngrebe, J., Debatin, K. M., & Fischer-Posovszky, P. (2020). Adipocytes in hematopoiesis and acute leukemia: friends, enemies, or innocent bystanders?. Leukemia, 34(9), 2305-2316.
173. Lu, W., Weng, W., Zhu, Q., Zhai, Y., Wan, Y., Liu, H., ... & Shi, J. (2018). Small bone marrow adipocytes predict poor prognosis in acute myeloid leukemia. Haematologica, 103(1), e21.
174. Röhrig, F., & Schulze, A. (2016). The multifaceted roles of fatty acid synthesis in cancer. Nature Reviews Cancer, 16(11), 732-749.
175. Shafat, M. S., Oellerich, T., Mohr, S., Robinson, S. D., Edwards, D. R., Marlein, C. R., ... & Rushworth, S. A. (2017). Leukemic blasts program bone marrow adipocytes to generate a protumoral microenvironment. Blood, The Journal of the American Society of Hematology, 129(10), 1320-1332.
176. Yan, F., Shen, N., Pang, J. X., Zhang, Y. W., Rao, E. Y., Bode, A. M., ... & Liu, S. J. (2017). Fatty acid-binding protein FABP4 mechanistically links obesity with aggressive AML by enhancing aberrant DNA methylation in AML cells. Leukemia, 31(6), 1434-1442.
177. Tabe, Y., Sekihara, K., Yang, H., Saito, K., Ruvolo, V., Taka, H., ... & Konopleva, M. (2017). Inhibition of FAO in AML Co-Cultured with BM Adipocytes: Mechanisms of Survival and Chemosensitization to Cytarabine. Blood, 130, 3832.
178. Ciciarello, M., Corradi, G., Loscocco, F., Visani, G., Monaco, F., Cavo, M., ... & Isidori, A. (2019). The Yin and Yang of the bone marrow microenvironment: pros and cons of mesenchymal stromal cells in acute myeloid leukemia. Frontiers in oncology, 9, 1135.
179. Chandran, P., Le, Y., Li, Y., Sabloff, M., Mehic, J., Rosu-Myles, M., & Allan, D. S. (2015). Mesenchymal stromal cells from patients with acute myeloid leukemia have altered capacity to expand differentiated hematopoietic progenitors. Leukemia research, 39(4), 486-493.
180. Blau, O., Baldus, C. D., Hofmann, W. K., Thiel, G., Nolte, F., Burmeister, T., ... & Blau, I. W. (2011). Mesenchymal stromal cells of myelodysplastic syndrome and acute myeloid leukemia patients have distinct genetic abnormalities compared with leukemic blasts. Blood, The Journal of the American Society of Hematology, 118(20), 5583-5592.
181. Geyh, S., Rodriguez-Paredes, M., Jäger, P., Khandanpour, C., Cadeddu, R. P., Gutekunst, J., ... & Schroeder, T. (2016). Functional inhibition of mesenchymal stromal cells in acute myeloid leukemia. Leukemia, 30(3), 683-691.
182. Le, Y., Fraineau, S., Chandran, P., Sabloff, M., Brand, M., Lavoie, J. R., ... & Allan, D. S. (2016). Adipogenic mesenchymal stromal cells from bone marrow and their hematopoietic supportive role: towards understanding the permissive marrow microenvironment in acute myeloid leukemia. Stem Cell Reviews and Reports, 12(2), 235-244.
183. Von der Heide, E. K., Neumann, M., Vosberg, S., James, A. R., Schroeder, M. P., Ortiz-Tanchez, J., ... & Baldus, C. D. (2017). Molecular alterations in bone

marrow mesenchymal stromal cells derived from acute myeloid leukemia patients. Leukemia, 31(5), 1069-1078.
184. de la Guardia, R. D., Lopez-Millan, B., Lavoie, J. R., Bueno, C., Castaño, J., Gómez-Casares, M., ... & Menéndez, P. (2017). Detailed characterization of mesenchymal stem/stromal cells from a large cohort of AML patients demonstrates a definitive link to treatment outcomes. Stem Cell Reports, 8(6), 1573-1586.
185. Blau, O., Hofmann, W. K., Baldus, C. D., Thiel, G., Serbent, V., Schümann, E., ... & Blau, I. W. (2007). Chromosomal aberrations in bone marrow mesenchymal stroma cells from patients with myelodysplastic syndrome and acute myeloblastic leukemia. Experimental hematology, 35(2), 221-229.
186. Villar, O. L., García, J. L., Guijo, F. M. S., Robledo, C., Campo, P. H., Campelo, M. D., ... & Cañizo, M. C. D. (2008). Both Expanded and Uncultured Mesenchymal Stem Cells from MDS Patients Are Genomically Abnormal, Showing a Specific Genetic Profile for the 5q-Syndrome.
187. Corradi, G., Baldazzi, C., Očadlíková, D., Marconi, G., Parisi, S., Testoni, N., ... & Ciciarello, M. (2018). Mesenchymal stromal cells from myelodysplastic and acute myeloid leukemia patients display in vitro reduced proliferative potential and similar capacity to support leukemia cell survival. Stem cell research & therapy, 9(1), 1-15.
188. Zhang, L., Chi, Y., Wei, Y., Zhang, W., Wang, F., Zhang, L., ... & Han, Z. (2021). Bone marrow-derived mesenchymal stem/stromal cells in patients with acute myeloid leukemia reveal transcriptome alterations and deficiency in cellular vitality. Stem Cell Research & Therapy, 12(1), 1-13.
189. Azadniv, M., Myers, J. R., McMurray, H. R., Guo, N., Rock, P., Coppage, M. L., ... & Liesveld, J. L. (2020). Bone marrow mesenchymal stromal cells from acute myelogenous leukemia patients demonstrate adipogenic differentiation propensity with implications for leukemia cell support. Leukemia, 34(2), 391-403.
190. Battula, V. L., Le, P. M., Sun, J. C., Nguyen, K., Yuan, B., Zhou, X., ... & Andreeff, M. (2017). AML-induced osteogenic differentiation in mesenchymal stromal cells supports leukemia growth. JCI insight, 2(13).
191. Rettig, W. J., Garin-Chesa, P., Healey, J. H., Su, S. L., Jaffe, E. A., & Old, L. J. (1992). Identification of endosialin, a cell surface glycoprotein of vascular endothelial cells in human cancer. Proceedings of the National Academy of Sciences, 89(22), 10832-10836.
192. MacFadyen, J. R., Haworth, O., Roberston, D., Hardie, D., Webster, M. T., Morris, H. R., ... & Isacke, C. M. (2005). Endosialin (TEM1, CD248) is a marker of stromal fibroblasts and is not selectively expressed on tumour endothelium. FEBS letters, 579(12), 2569-2575.
193. Christian, S., Ahorn, H., Koehler, A., Eisenhaber, F., Rodi, H. P., Garin-Chesa, P., ... & Lenter, M. C. (2001). Molecular cloning and characterization of endosialin, a C-type lectin-like cell surface receptor of tumor endothelium. Journal of Biological Chemistry, 276(10), 7408-7414.
194. Opavsky, R., Haviernik, P., Jurkovicova, D., Garin, M. T., Copeland, N. G., Gilbert, D. J., ... & Wolff, L. (2001). Molecular Characterization of the MouseTem1/endosialin Gene Regulated by Cell Density in Vitro and Expressed in Normal Tissues in Vivo. Journal of Biological Chemistry, 276(42), 38795-38807.

195. Carson-Walter, E. B., Watkins, D. N., Nanda, A., Vogelstein, B., Kinzler, K. W., & St. Croix, B. (2001). Cell surface tumor endothelial markers are conserved in mice and humans. Cancer research, 61(18), 6649-6655.
196. Christian, S., Winkler, R., Helfrich, I., Boos, A. M., Besemfelder, E., Schadendorf, D., & Augustin, H. G. (2008). Endosialin (Tem1) is a marker of tumor-associated myofibroblasts and tumor vessel-associated mural cells. The American journal of pathology, 172(2), 486-494.
197. Tomkowicz, B., Rybinski, K., Sebeck, D., Sass, P., Nicolaides, N. C., Grasso, L., & Zhou, Y. (2010). Endosialin/TEM-1/CD248 regulates pericyte proliferation through PDGF receptor signaling. Cancer biology & therapy, 9(11), 908-915.
198. Lax, S., Hardie, D. L., Wilson, A., Douglas, M. R., Anderson, G., Huso, D., ... & Buckley, C. D. (2010). The pericyte and stromal cell marker CD248 (endosialin) is required for efficient lymph node expansion. European journal of immunology, 40(7), 1884-1889.
199. Bagley, R. G., Honma, N., Weber, W., Boutin, P., Rouleau, C., Shankara, S., ... & Teicher, B. A. (2008). Endosialin/TEM 1/CD248 is a pericyte marker of embryonic and tumor neovascularization. Microvascular research, 76(3), 180-188.
200. Khan, K. A., McMurray, J. L., Mohammed, F., & Bicknell, R. (2019). C-type lectin domain group 14 proteins in vascular biology, cancer and inflammation. The FEBS journal, 286(17), 3299-3332.
201. Becker, R., Lenter, M. C., Vollkommer, T., Boos, A. M., Pfaff, D., Augustin, H. G., & Christian, S. (2008). Tumor stroma marker endosialin (Tem1) is a binding partner of metastasis-related protein Mac-2 BP/90K. The FASEB Journal, 22(8), 3059-3067.
202. Suresh Babu, S., Valdez, Y., Xu, A., O'Byrne, A. M., Calvo, F., Lei, V., & Conway, E. M. (2014). TGFβ-mediated suppression of CD248 in non-cancer cells via canonical Smad-dependent signaling pathways is uncoupled in cancer cells. BMc cancer, 14(1), 1-11.
203. Wilhelm, A., Aldridge, V., Haldar, D., Naylor, A. J., Weston, C. J., Hedegaard, D., ... & Newsome, P. N. (2016). CD248/endosialin critically regulates hepatic stellate cell proliferation during chronic liver injury via a PDGF-regulated mechanism. Gut, 65(7), 1175-1185.
204. Mogler, C., Wieland, M., König, C., Hu, J., Runge, A., Korn, C., ... & Augustin, H. G. (2015). Hepatic stellate cell-expressed endosialin balances fibrogenesis and hepatocyte proliferation during liver damage. EMBO molecular medicine, 7(3), 332-338.
205. Chang-Panesso, M., & Humphreys, B. D. (2015). CD248/endosialin: a novel pericyte target in renal fibrosis. Nephron, 131(4), 262-264.
206. Rouleau, C., Curiel, M., Weber, W., Smale, R., Kurtzberg, L., Mascarello, J., ... & Teicher, B. A. (2008). Endosialin protein expression and therapeutic target potential in human solid tumors: sarcoma versus carcinoma. Clinical cancer research, 14(22), 7223-7236.
207. Brady, J., Neal, J., Sadakar, N., & Gasque, P. (2004). Human endosialin (tumor endothelial marker 1) is abundantly expressed in highly malignant and invasive brain tumors. Journal of Neuropathology & Experimental Neurology, 63(12), 1274-1283.

208. Maia, M., de Vriese, A., Janssens, T., Moons, M., Van Landuyt, K., Tavernier, J., ... & Conway, E. M. (2010). CD248 and its cytoplasmic domain: a therapeutic target for arthritis. Arthritis & Rheumatism, 62(12), 3595-3606.
209. Teicher, B. A. (2019). CD248: A therapeutic target in cancer and fibrotic diseases. Oncotarget, 10(9), 993.
210. Hardie, D. L., Baldwin, M. J., Naylor, A., Haworth, O. J., Hou, T. Z., Lax, S., ... & Buckley, C. D. (2011). The stromal cell antigen CD248 (endosialin) is expressed on naive CD8+ human T cells and regulates proliferation. Immunology, 133(3), 288-295.
211. Hasanov, Z., Ruckdeschel, T., König, C., Mogler, C., Kapel, S. S., Korn, C., ... & Augustin, H. G. (2017). Endosialin promotes atherosclerosis through phenotypic remodeling of vascular smooth muscle cells. Arteriosclerosis, thrombosis, and vascular biology, 37(3), 495-505.
212. Ohradanova, A., Gradin, K., Barathova, M., Zatovicova, M., Holotnakova, T., Kopacek, J., ... & Pastorek, J. (2008). Hypoxia upregulates expression of human endosialin gene via hypoxia-inducible factor 2. British journal of cancer, 99(8), 1348-1356.
213. Di Benedetto, P., Liakouli, V., Ruscitti, P., Berardicurti, O., Carubbi, F., Panzera, N., ... & Giacomelli, R. (2018). Blocking CD248 molecules in perivascular stromal cells of patients with systemic sclerosis strongly inhibits their differentiation toward myofibroblasts and proliferation: a new potential target for antifibrotic therapy. Arthritis research & therapy, 20(1), 1-12.
214. Petrus, P., Fernandez, T. L., Kwon, M. M., Huang, J. L., Lei, V., Safikhan, N. S., ... & Conway, E. M. (2019). Specific loss of adipocyte CD248 improves metabolic health via reduced white adipose tissue hypoxia, fibrosis and inflammation. EBioMedicine, 44, 489-501.
215. Cheung, W. Y., Hovey, O., Gobin, J. M., Muradia, G., Mehic, J., Westwood, C., & Lavoie, J. R. (2018). Efficient nonviral transfection of human bone marrow mesenchymal stromal cells shown using placental growth factor overexpression. Stem cells international, 2018.
216. Gobin, J., Muradia, G., Mehic, J., Westwood, C., Couvrette, L., Stalker, A., ... & Lavoie, J. R. (2021). Hollow-fiber bioreactor production of extracellular vesicles from human bone marrow mesenchymal stromal cells yields nanovesicles that mirrors the immuno-modulatory antigenic signature of the producer cell. Stem cell research & therapy, 12(1), 1-20.
217. Ling, X., Chen, Y., Ruvolo, P. P., Ruvolo, V., Wang, Z., Zhang, M., ... & Andreeff, M. (2012). Unique Effects of p53−/− Leukemic Cells on Mesenchymal Stromal Cell Gene Expression Profile in Vitro. Blood, 120(21), 3468.
218. Sun, P., Jia, K., Zheng, C., Zhu, X., Li, J., He, L., ... & Luo, J. (2019). Loss of Lgr4 inhibits differentiation, migration and apoptosis, and promotes proliferation in bone mesenchymal stem cells. Journal of Cellular Physiology, 234(7), 10855-10867.
219. Cho, B. S., Kim, H. J., & Konopleva, M. (2017). Targeting the CXCL12/CXCR4 axis in acute myeloid leukemia: from bench to bedside. The Korean journal of internal medicine, 32(2), 248.
220. Kim, W., Barron, D. A., San Martin, R., Chan, K. S., Tran, L. L., Yang, F., ... & Rowley, D. R. (2014). RUNX1 is essential for mesenchymal stem cell proliferation

and myofibroblast differentiation. Proceedings of the National Academy of Sciences, 111(46), 16389-16394.
221. Argiropoulos, B., Yung, E., & Humphries, R. K. (2007). Unraveling the crucial roles of Meis1 in leukemogenesis and normal hematopoiesis. Genes & development, 21(22), 2845-2849.
222. Turan, R. D., Albayrak, E., Uslu, M., Siyah, P., Alyazici, L. Y., Kalkan, B. M., ... & Kocabas, F. (2020). Development of Small Molecule MEIS Inhibitors that modulate HSC activity. Scientific reports, 10(1), 1-17.
223. Khokha, M. K., Hsu, D., Brunet, L. J., Dionne, M. S., & Harland, R. M. (2003). Gremlin is the BMP antagonist required for maintenance of Shh and Fgf signals during limb patterning. Nature genetics, 34(3), 303-307.
224. Michos, O., Panman, L., Vintersten, K., Beier, K., Zeller, R., & Zuniga, A. (2004). Gremlin-mediated BMP antagonism induces the epithelial-mesenchymal feedback signaling controlling metanephric kidney and limb organogenesis.
225. Xiang, Q., Hong, D., Liao, Y., Cao, Y., Liu, M., Pang, J., ... & Xiang, A. P. (2017). Overexpression of gremlin1 in mesenchymal stem cells improves hindlimb ischemia in mice by enhancing cell survival. Journal of Cellular Physiology, 232(5), 996-1007.
226. Chou, C. H., Cheng, Y. F., Siow, T. Y., Kumar, A., Peck, K., & Chang, C. (2013). SCUBE3 regulation of early lung cancer angiogenesis and metastatic progression. Clinical & experimental metastasis, 30(6), 741-752.
227. Wu, Y. Y., Peck, K. O. N. A. N., Chang, Y. L., Pan, S. H., Cheng, Y. F., Lin, J. C., ... & Yang, P. C. (2011). SCUBE3 is an endogenous TGF-β receptor ligand and regulates the epithelial-mesenchymal transition in lung cancer. Oncogene, 30(34), 3682-3693.
228. Huang, H. L., Hsing, H. W., Lai, T. C., Chen, Y. W., Lee, T. R., Chan, H. T., ... & Chan, H. L. (2010). Trypsin-induced proteome alteration during cell subculture in mammalian cells. Journal of biomedical science, 17(1), 1-10.
229. Breznik, B., Motaln, H., Vittori, M., Rotter, A., & Turnšek, T. L. (2017). Mesenchymal stem cells differentially affect the invasion of distinct glioblastoma cell lines. Oncotarget, 8(15), 25482.
230. Krampera, M., Pasini, A., Rigo, A., Scupoli, M. T., Tecchio, C., Malpeli, G., ... & Vinante, F. (2005). HB-EGF/HER-1 signaling in bone marrow mesenchymal stem cells: inducing cell expansion and reversibly preventing multilineage differentiation. Blood, 106(1), 59-66.
231. Vinante, F., & Rigo, A. (2013). Heparin-binding epidermal growth factor-like growth factor/diphtheria toxin receptor in normal and neoplastic hematopoiesis. Toxins, 5(6), 1180-1201.
232. Kim, S. J., & Letterio, J. (2003). Transforming growth factor-β signaling in normal and malignant hematopoiesis. Leukemia, 17(9), 1731-1737.
233. Lin, H. K., Bergmann, S., & Pandolfi, P. P. (2005). Deregulated TGF-β signaling in leukemogenesis. Oncogene, 24(37), 5693-5700.
234. Wu Y, Chen P, Huang H, Huang M, Chen Y. Reduction of transforming growth factor-β1 expression in leukemia and its possible role in leukemia development. Leuk Lymphoma. 2(012)

235. de Haan, G., & Van Zant, G. (1999). Dynamic changes in mouse hematopoietic stem cell numbers during aging. Blood, The Journal of the American Society of Hematology, 93(10), 3294-3301.
236. Jing, E., Gesta, S., & Kahn, C. R. (2007). SIRT2 regulates adipocyte differentiation through FoxO1 acetylation/deacetylation. Cell metabolism, 6(2), 105-114.
237. Wang, F., & Tong, Q. (2009). SIRT2 suppresses adipocyte differentiation by deacetylating FOXO1 and enhancing FOXO1's repressive interaction with PPARγ. Molecular biology of the cell, 20(3), 801-808.
238. Deng, A., Ning, Q., Zhou, L., & Liang, Y. (2016). SIRT2 is an unfavorable prognostic biomarker in patients with acute myeloid leukemia. Scientific reports, 6(1), 1-8.

Appendix

Supplementary Table S1. Primers and templates utilized in qRT-PCR validation of two genes of the SDRGs, GRE1M and SCUBE3.

Target Gene	Type	Application	Cat#	Manufacturer
GAPDH	Template	qRT-PCR	10025716	Bio Rad
GAPDH	Primer	qRT-PCR	232183854	Bio Rad
β-actin	Primer	qRT-PCR	10025636	Bio rad
GREM1	Primer	qRT-PCR	229760581	Bio Rad
GREM1	Template	qRT-PCR	236264692	Bio Rad
SCUBE3	Template	qRT-PCR	272415539	Bio Rad
SCUBE3	Primer	qRT-PCR	229760580	Bio Rad

Supplementary Table S2. Genes in the 21-SDRGs that were previously reported in AML-MSCs/HD-MSCs

Gene name	Current study	Previous studies	Reference
LGR4	Upregulated	Upregulated	188
GREM1	Downregulated	Upregulated	188
SCUBE3	Upregulated	Upregulated	188
CD248	Upregulated	Upregulated	183
CXCL12	Upregulated	Upregulated	190

Supplementary Table S3. Recombinant proteins used in Western blot validation.

Recombinant Proteins	Cat#	Manufacturer
GREM1 Recombinant Protein	MBS691636	myBioSource
Recombinant Human SCUBE3	7730-SC	R&D Systems
Recombinant Human End/CD248	7855-CD	R&D Systems

Supplementary Table S4. Antibodies utilized in Western Blot analysis

Western Blot Antibody	Target	Cat#	Manufacturer
CD248 Mouse mAb	CD248	MyBioSource	MBS6183207
CD248 Mouse anti Human mAb	CD248	MyBioSource	MBS2542325
Endosialin-Human	CD248	BD Biosciences	564994
TEM1 (CD248) mAb	CD248	Invitrogen	MA-526838
TEM1/CD248 Antibody	CD248	LS Bio	LS-C170323
TEM1 Mouse mAb	CD248	Proteintech	60170-1-Ig
TEM1 Rabbit anti-human pAb	CD248	Proteintech	18160-1-AP
Rabbit pAb Anti-GREM1	GREM1	Csb pa168659	CusaBio
Anti-SCUBE3 pAB	SCUBE3	NBP2-41122	Novus
GAPDH (GT239) mAb	GAPDH	GTX627408	GeneTex
Anti-SCUBE3 mAb	SCUBE3	H00222663-M07	Novus
IRDye 800CW Goat anti-Mouse IgG	2°	926-32210	LI-COR
IRDye 800CW Goat anti-Rabbit IgG	2°	925-32211	LI-COR

Supplementary Table S5. Antibodies utilized in Flow cytometry analysis

Antibody	Target	Cat#	Manufacturer
Endosialin (CD248) - Mouse Anti-Human, Alexa Fluor 647	CD248	564994	BD Pharmingen
IgG1k Isotype Control - Mouse - Alexa Fluor 647	Isotype Control	557714	BD Biosciences
CD45 Mouse Anti-Human FITC	CD45	555482	BD Pharmingen
IgG1k Isotype - Mouse - FITC	Isotype Control	555748	BD Biosciences

Supplementary Table S6. siRNA and overexpression plasmids for *in vitro* gene modifications in HD-MSCs. Top Tested, validated and utilized in this study. Bottom, initially tested and invalidated (no further optimization was performed).

Validated	Target	Type	Cat#	Manufacturer
Silencer Select CD248 siRNA	CD248	siRNA	4392420	Ambion
siRNA Negative Control	Negative	siRNA	4390843	Ambion
Tested/not validated				
GREM1 siRNA	GREM1	siRNA	1027416	Qiagen
pCMV6-XL5-SCUBE3	SCUBE3	Overexpression plasmid	SC126481	OriGene
pCMV6-XL5-EV	Empty Vector	Overexpression plasmid		OriGene
pCMV6-XL4-CD248 (untagged)	CD248	Overexpression plasmid	SC113126 NM-020404	OriGene
pCMV6-XL4-EV	Empty Vector	Overexpression plasmid	pCMV6-XL4	OriGene
CD248-GFP tagged	CD248	Overexpression plasmid	RG208576	Origene
CD248-GFPSpark	CD248	Overexpression plasmid	HG13403-ACG	Sino Biological
pCMV3-C-GFPSpark Control Vector	Empty vector	Overexpression plasmid	CV026	Sino Biological

Supplementary Table S7. 91 Genes in Adiogenesis PrimePCR assay.

Gene	Gene	Gene	Gene
ADIG	BMP4	LRP5	SLC2A4
ADIPOQ	BMP7	MAPK14	SRC
ADRB2	CCND1	NCOA2	SREBF1
AGT	CDK4	NCOR2	TAZ
ANGPT2	CDKN1A	NR0B2	TCF7L2
AXIN1	CDKN1B	NR1H3	TSC22D3
B2M	CEBPA	NRF1	TWIST1
BMP2	CEBPB	PPARA	UCP1
CEBPD	ACTB	PPARG	WNT1
CFD	EGR2	PPARGC1A	WNT10B
CREB1	FABP4	PPARGC1B	WNT3A
DDIT3	FASN	PRDM16	WNT5A
DIO2	FGF1	RB1	WNT5B
DKK1	FGF10	RETN	TBP
DLK1	FGF2	RPLP0	GAPDH
E2F1	FOXC2	RUNX1T1	IRS2
GATA2	FOXO1	RXRA	JUN
GATA3	KLF15	SFRP1	LIPE
GUSB	KLF2	SFRP5	LMNA
HES1	KLF3	SHH	LPL
HPRT1	CACB	PPARD	VDR
INSR	KLF4	SIRT1	SIRT3
IRS1	LEP	SIRT2	

Supplementary figure S1. Heat map of the 21-SDRGs in AML/HD-MSCs. RNA-sequencing results.

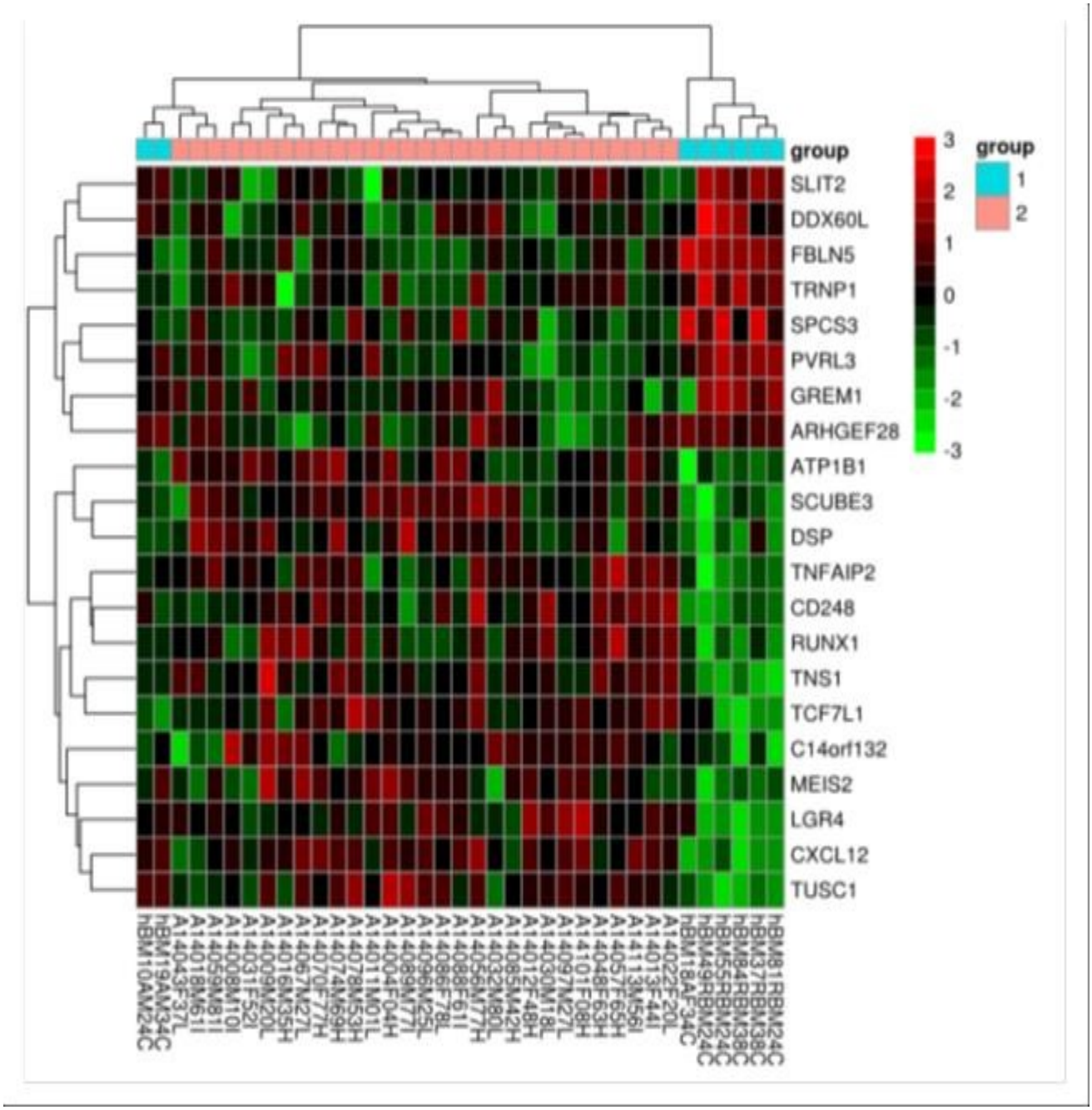

Supplementary Table S8. Participation of the 21 SDRGs in two networks. The table shows the genes of each predicted IPA two common networks.

Symbol	Entrez Gene Name	Expr Log Ratio	p-value	Networks
GREM1	gremlin 1, DAN family BMP antagonist	-2.292	0.0436	1,2
FBLN5	fibulin 5	-1.435	0.00000224	1
ARHGEF28	Rho guanine nucleotide exchange factor 28	-1.134	0.00561	1
TRNP1	TMF1-regulated nuclear protein 1	-0.834	0.0436	2
SLIT2	slit guidance ligand 2	-0.797	0.0397	1
NECTIN3	nectin cell adhesion molecule 3	-0.765	0.0436	2
DDX60L	DExD/H-box 60 like	-0.745	0.0281	2
SPCS3	signal peptidase complex subunit 3	-0.695	0.0421	2
RUNX1	runt related transcription factor 1	0.628	0.00258	1
MEIS2	Meis homeobox 2	0.786	0.00545	1
LGR4	leucine rich repeat containing G protein-coupled receptor 4	0.8	0.0288	1
ATP1B1	ATPase Na+/K+ transporting subunit beta 1	0.836	0.00123	1
CD248	CD248 molecule	0.924	0.0378	2
TUSC1	tumor suppressor candidate 1	0.925	0.037	2
TCF7L1	transcription factor 7 like 1	0.934	0.047	1
TNFAIP2	TNF alpha induced protein 2	1.005	0.0231	1
DSP	desmoplakin	1.023	0.00981	1
TNS1	tensin 1	1.172	0.000231	1
C14orf132	chromosome 14 open reading frame 132	1.183	0.0431	2
CXCL12	C-X-C motif chemokine ligand 12	1.587	0.00686	1
SCUBE3	signal peptide, CUB domain and EGF like domain containing 3	1.968	0.00078	1

Supplementary Figure S2. Main miRNA control the most dysregulated genes using upstream analysis tool in IPA. IPA analysis predicted three common miRNA to be possibly associated with many of the dysregulated genes, however, the type/ direction of effect or association is not known.miR-3072 target genes in data set are CD248, CXCL12, NECTIN3.

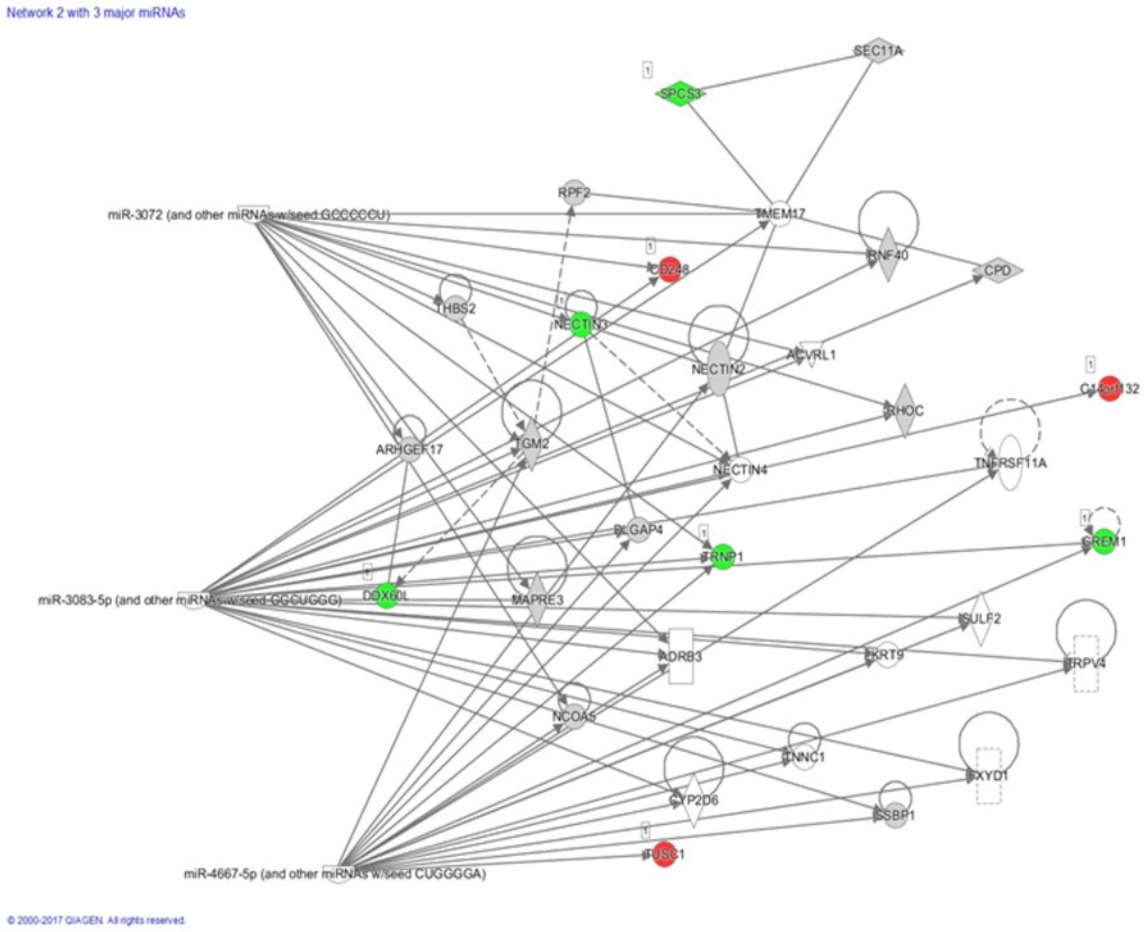

Supplementary Table S9: Information of healthy donor samples that were used to generate the used lysates in GREM1 protein validation.

hBM Aspirate Sample ID	Donor	Sex	Age
10C	Healthy	Male	24
11C	Healthy	Female	23
12C	Healthy	Male	21
13C	Healthy	Male	41

Supplementary Figure S3. GREM1 siRNA knockdown using four siRNAs.

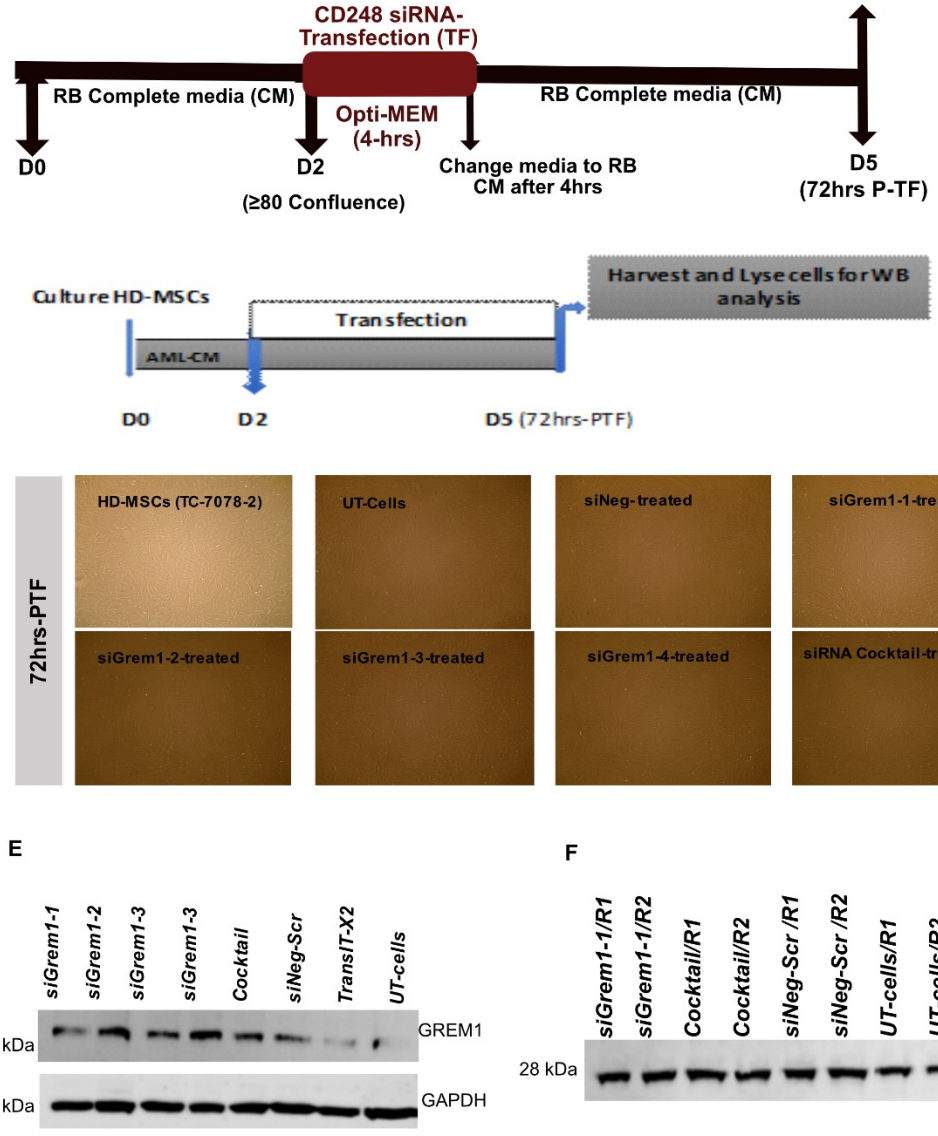

Supplementary Figure S4. Ingenuity Pathway Analysis. Common regulators connected to CD248 using common pathway tool. Using the disease and function tool to determine major pathway network of the some dysregulated proteins.

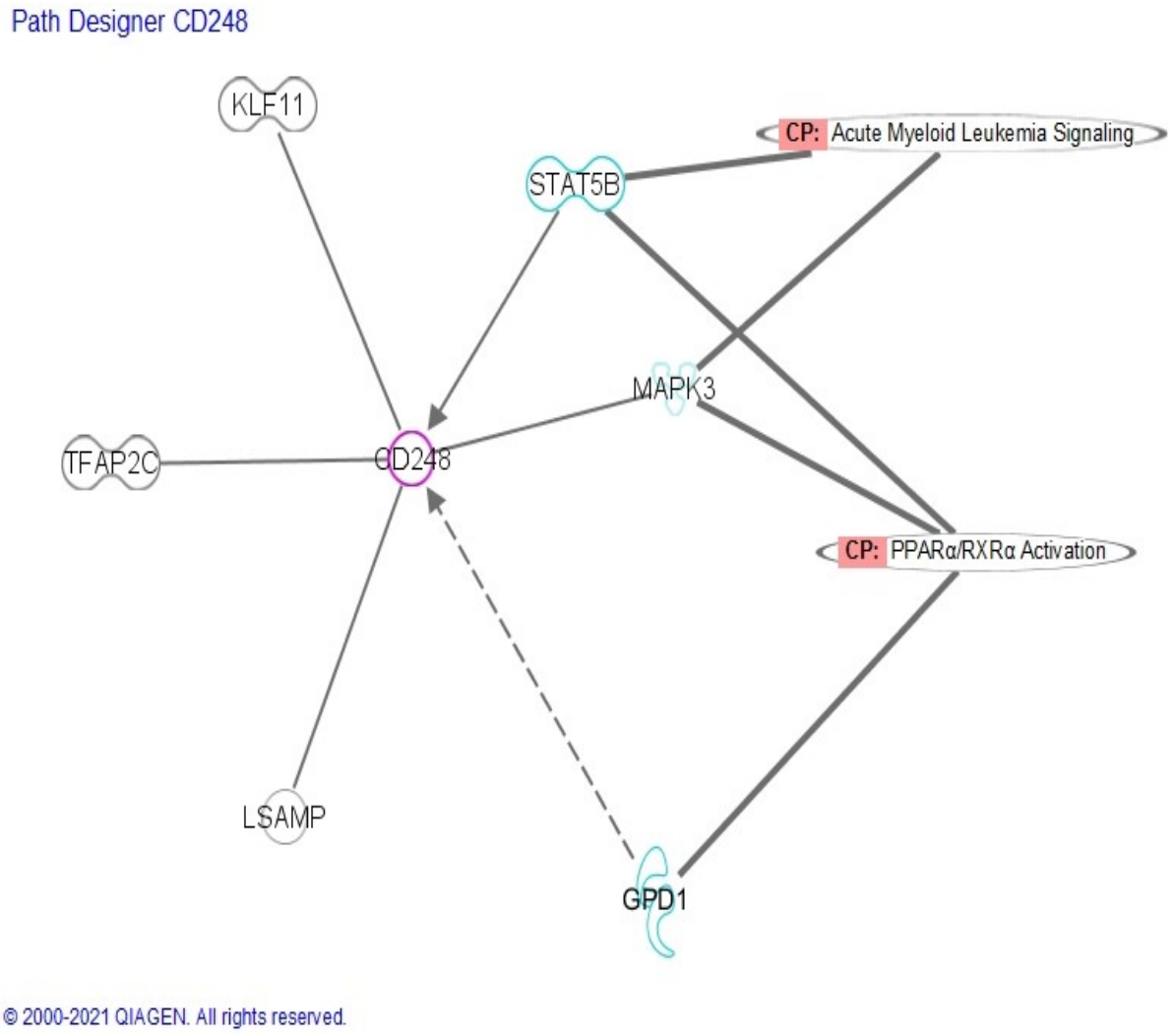

Supplementary Figure S5. Ingenuity Pathway Analysis of microarray protein profile of siCD248-treated HD-MSCs. Using the disease and function tool to determine major common pathway of the some dysregulated proteins.

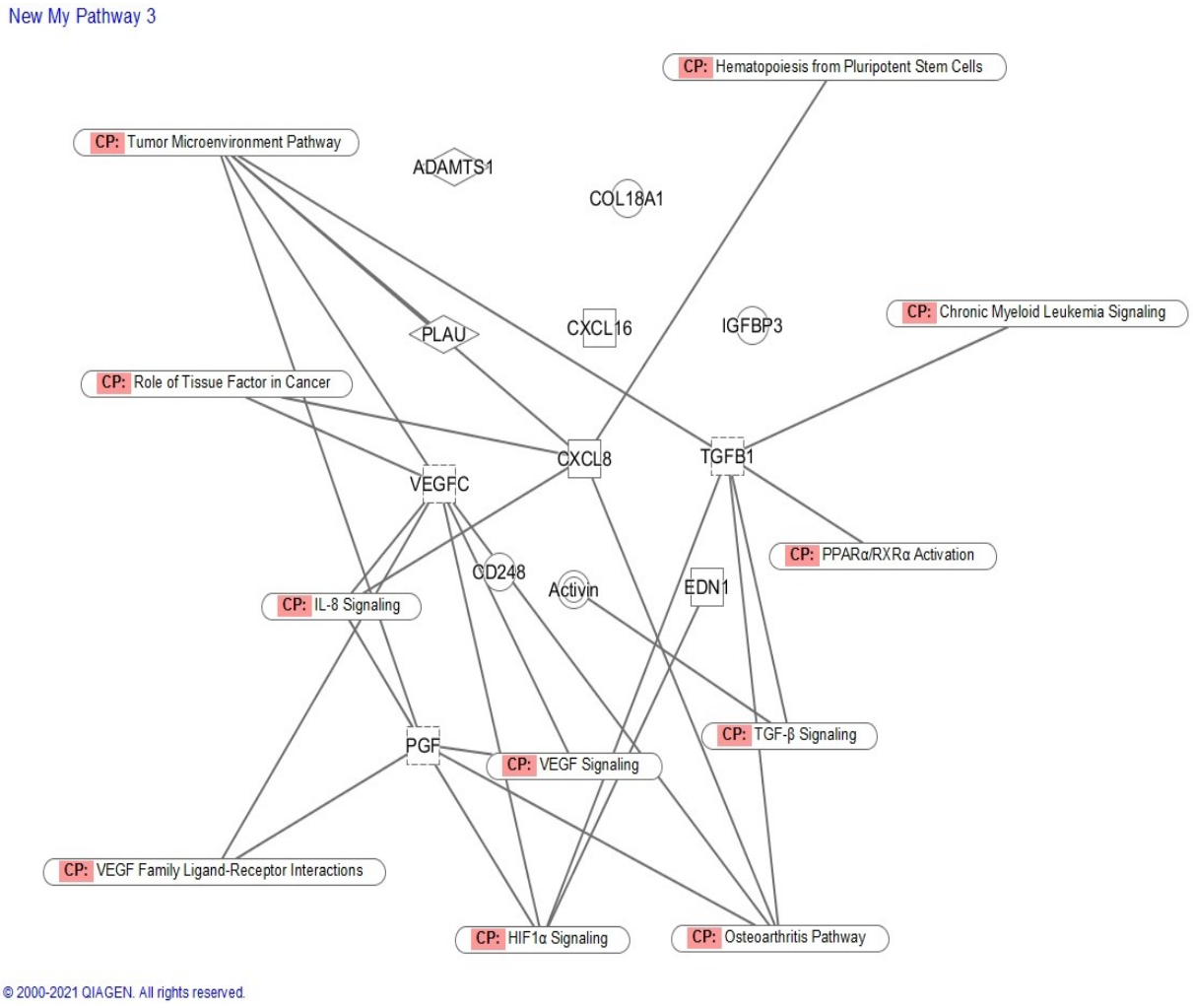

Supplementary Figure S6. Analysis of protein microarray data. Ingenuity Pathway Analysis of microarray protein profile of siCD248-treated HD-MSCs. Using the disease and function tool to determine major pathway network of the some dysregulated proteins.

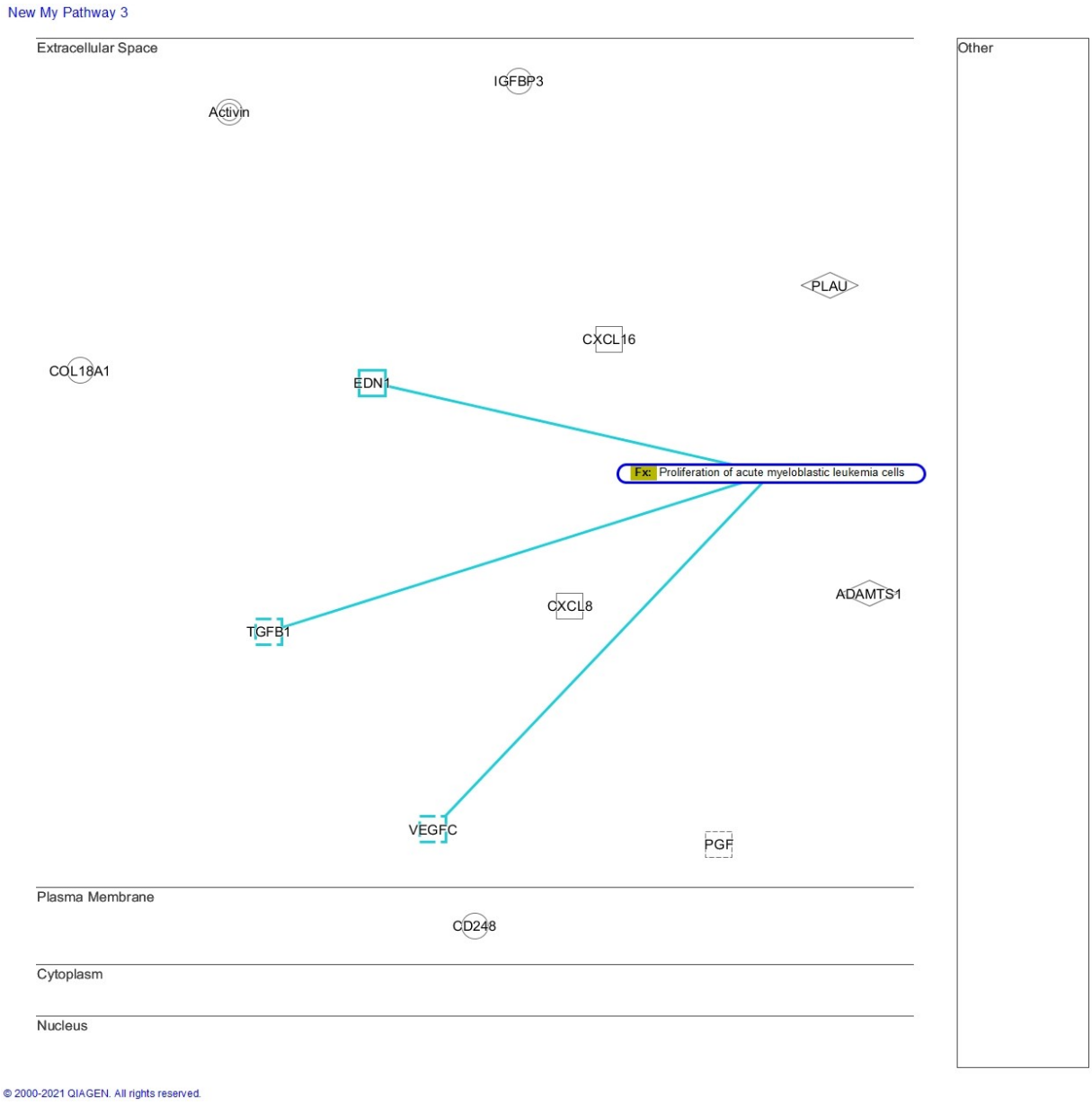

Supplementary Figure S7. Analysis of Microarray data. **Ingenuity Pathway Analysis of microarray protein profile of siCD248-treated HD-MSCs.** Using the disease and function tool to determine major pathway network of the some dysregulated proteins.

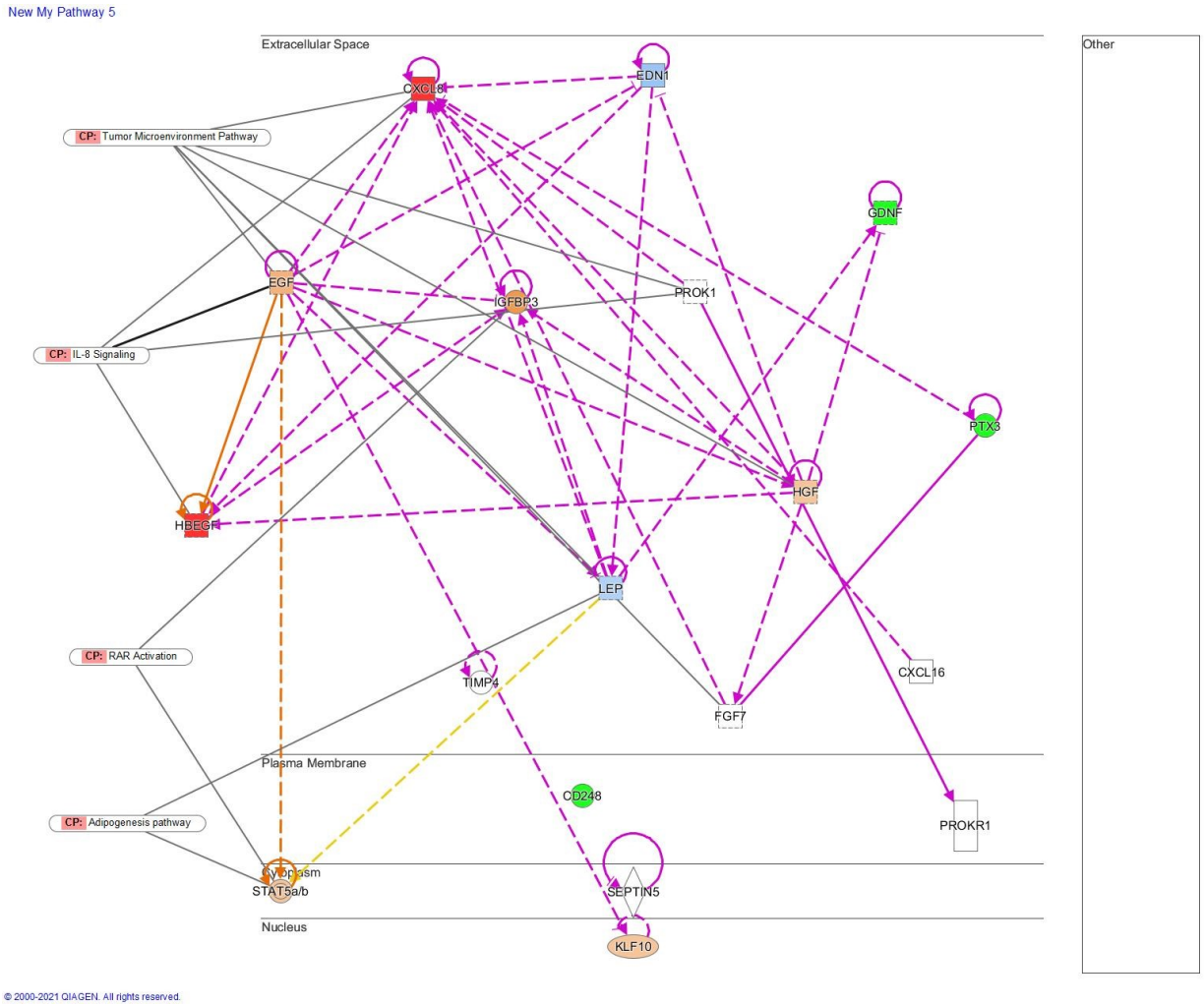

Supplementary Table S10. RT-PCR Expression data of all amplified Adipogenesis genes. Normalized expression ▲▲Cq (Relative to zero). CFX maestro data.

Expression of Adipogenesis genes			
Target	**UT-Control**	**siNeg-MSCs**	**siCD248-MSCs**
ADIG	0.98575	1.14361	1.15972
ADIPOQ	1.14311	0.6256	9.06578
ADRB2	1.14311	N/A	N/A
AGT	1.1264	1.14361	2.35601
ANGPT2	1.14311	1.07279	2.93463
AXIN1	1.14311	1.03679	1.17827
BMP2	0.57813	1.14361	1.57608
BMP7	1.14311	N/A	N/A
CDK4	1.14311	1.0098	0.86041
CDKN1B	1.14311	0.86083	0.53551
CEBPA	1.08614	1.14361	2.08099
CEBPB	1.14311	0.94714	0.84541
CEBPD	1.14311	1.05396	0.52264
CFD	1.14311	0.50259	0.44957
CREB1	1.14311	1.11308	0.30854
DDIT3	1.14311	N/A	N/A
DIO2	1.14311	0.61024	1.34775
DKK1	1.14311	1.00718	0.48185
DLK1	1.14311	1.00885	0.58102
EGR2	N/A	1.14361	8.78922
FABP4	1.14311	0.68877	0.15148
FASN	1.11225	1.14361	1.14462
FGF1	1.14311	0.75307	0.56899
FGF10	1.14311	1.03672	1.40439
FGF2	1.11867	1.14361	N/A

Supplementary Table S11. RT-PCR Expression data of all amplified Adipogenesis genes. Normalized expression ▲▲Cq (Relative to zero). CFX maestro data.

Expression of Adipogenesis genes (Continue)			
Target	**UT-Control**	**siNeg-MSCs**	**siCD248-MSCs**
FOXO1	1.14311	0.62978	1.04047
GATA2	1.14311	0.8484	0.68977
GATA3	0.86468	1.14361	0.61874
gDNA	0.67819	1.14361	N/A
HES1	1.14311	1.05904	1.14181
INSR	1.14311	0.87207	1.30773
IRS1	1.14311	0.96425	0.83036
IRS2	1.14311	0.85985	1.15175
KLF15	1.14311	1.03266	0.61441
KLF2	1.14311	1.05829	0.66599
KLF3	1.14311	1.12992	0.54416
KLF4	0.96837	1.14361	0.76894
LEP	1.14311	0.41074	0.20514
LIPE	1.14311	0.9903	0.81507
LMNA	1.14311	0.48969	0.30132
LPL	0.40054	1.14361	1.3957
LRP5	0.75017	1.14361	0.7429
MAPK14	1.14311	0.74463	0.38289
NCOA2	1.14311	0.62836	0.73064
NCOR2	1.14311	0.56838	N/A
NR0B2	1.14311	1.08095	0.5774
NR1H3	1.14311	1.00702	3.73428
NRF1	1.14311	1.0367	1.01086
PCR	1.14311	0.58833	0.05307
PPARA	1.1151	1.14361	0.45516
PPARD	1.14311	0.61391	2.01384

Supplementary Table S12. RT-PCR Expression data of all amplified Adipogenesis genes. Normalized expression ▲▲Cq (Relative to zero). CFX maestro data.

Expression of Adipogenesis genes (Continue)			
Target	**UT-Control**	**siNeg-MSCs**	**siCD248-MSCs**
PRDM16	1.14311	0.89693	0.47548
RB1	1.14311	0.90625	2.58742
RETN	1.09373	1.14361	3.09865
RQ2	1.14311	1.10172	0.73217
RT	1.14311	0.56733	0.54557
RUNX1T1	1.07198	1.14361	2.59949
RXRA	1.14311	0.76681	0.39161
SFRP1	1.14311	0.47076	0.49579
SFRP5	1.14311	0.89961	3.23047
SHH	1.14311	0.82869	0.54056
SIRT1	1.14311	0.25711	N/A
SIRT2	0.50473	0.80941	11.25715
SIRT3	0.95129	1.14361	0.28376
SLC2A4	1.14311	1.0816	2.45337
SRC	1.14311	1.09267	1.32899
SREBF1	1.14311	0.58321	0.07937
TAZ	1.14311	1.0473	2.67943
TCF7L2	1.14311	1.12879	3.2126
TSC22D3	1.14311	0.52625	0.20306
TWIST1	1.14311	0.80792	0.5653
UCP1	1.01843	1.14361	0.98026
VDR	1.14311	1.04566	1.39089
WNT1	0.72099	1.14361	1.46474
WNT3A	1.14311	0.4856	0.39683
WNT5A	1.14311	1.12491	0.73958
WNT5B	1.14311	1.05393	1.83592

Supplementary Figure S8. β-actin smeared bands in CD248 protein determination (HR AML 1-6) by Western Blot analysis.

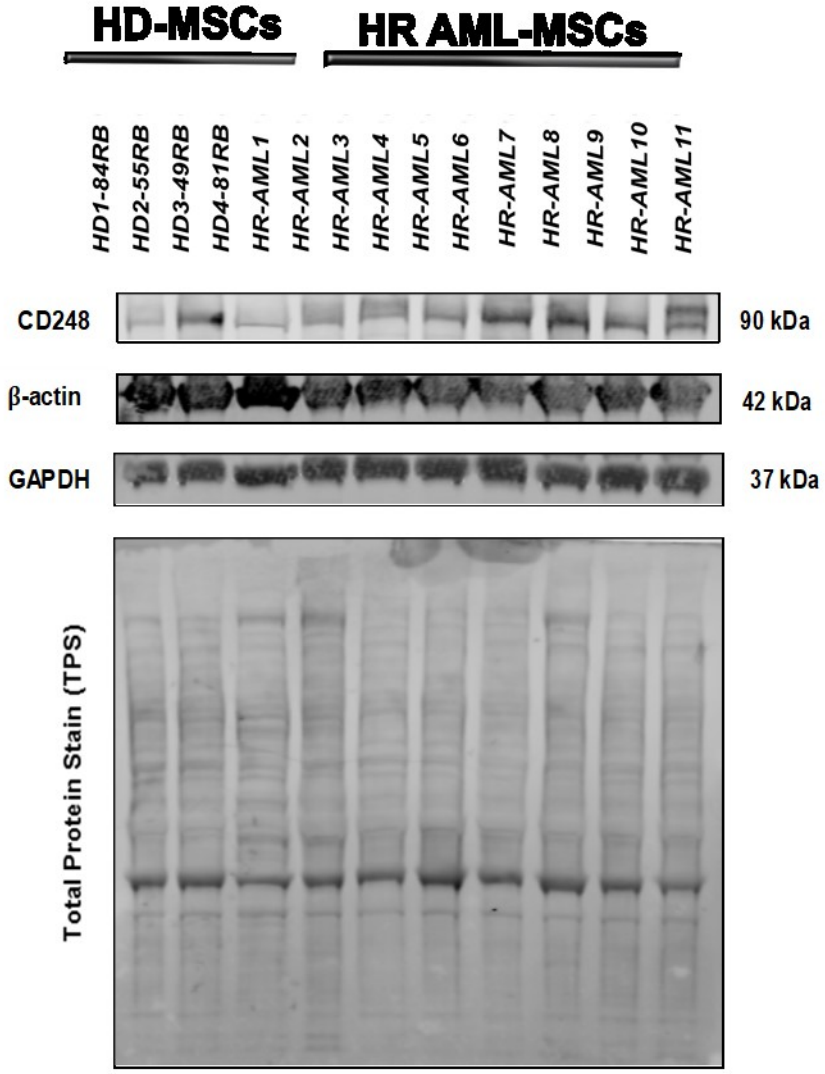

Supplementary Figure S9. β-actin smeared bands in CD248 protein determination (HR AML 7-11)

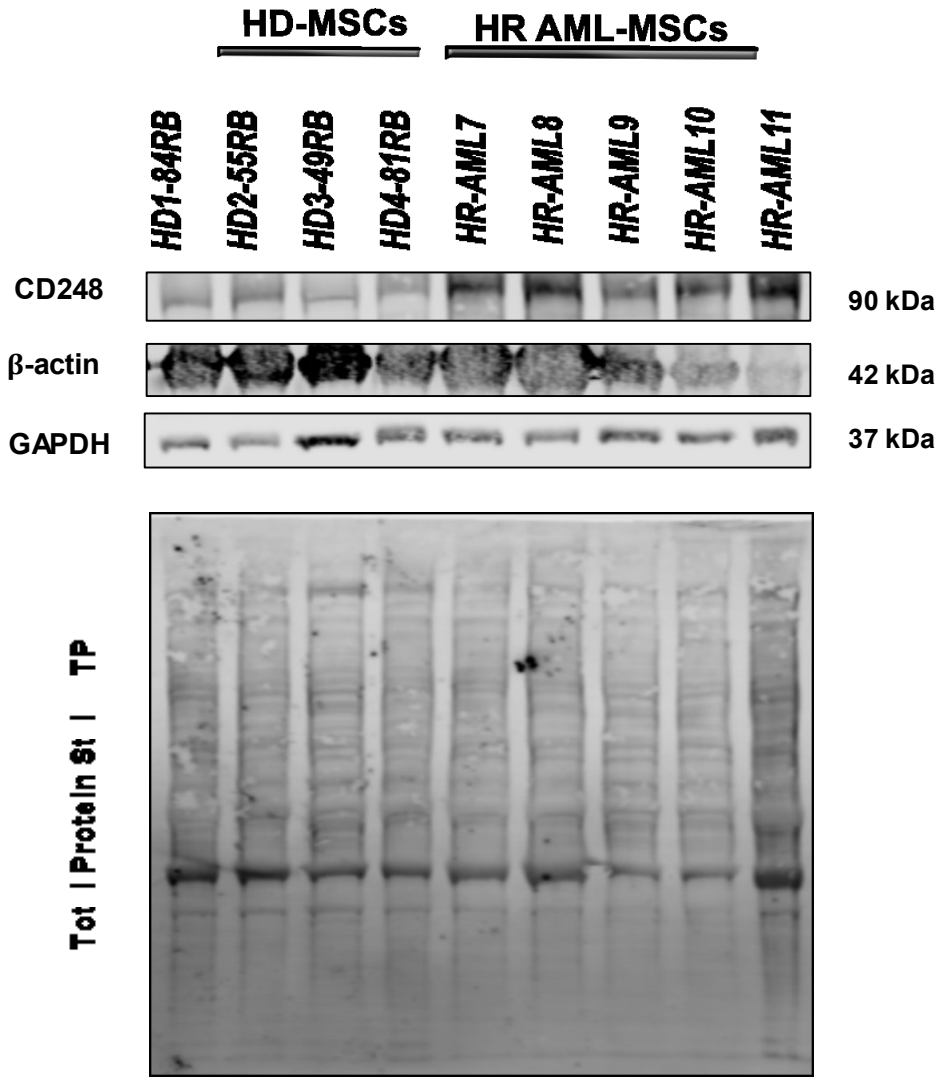

Supplementary Figure S10. CD248 knockdown 48-hour post transfection efficiency (n=3). A) and B) Incubation with TF complexes for 4 hours. C) and D) incubation with TF complexes for 24 hours. MFI and CD248+Cells.

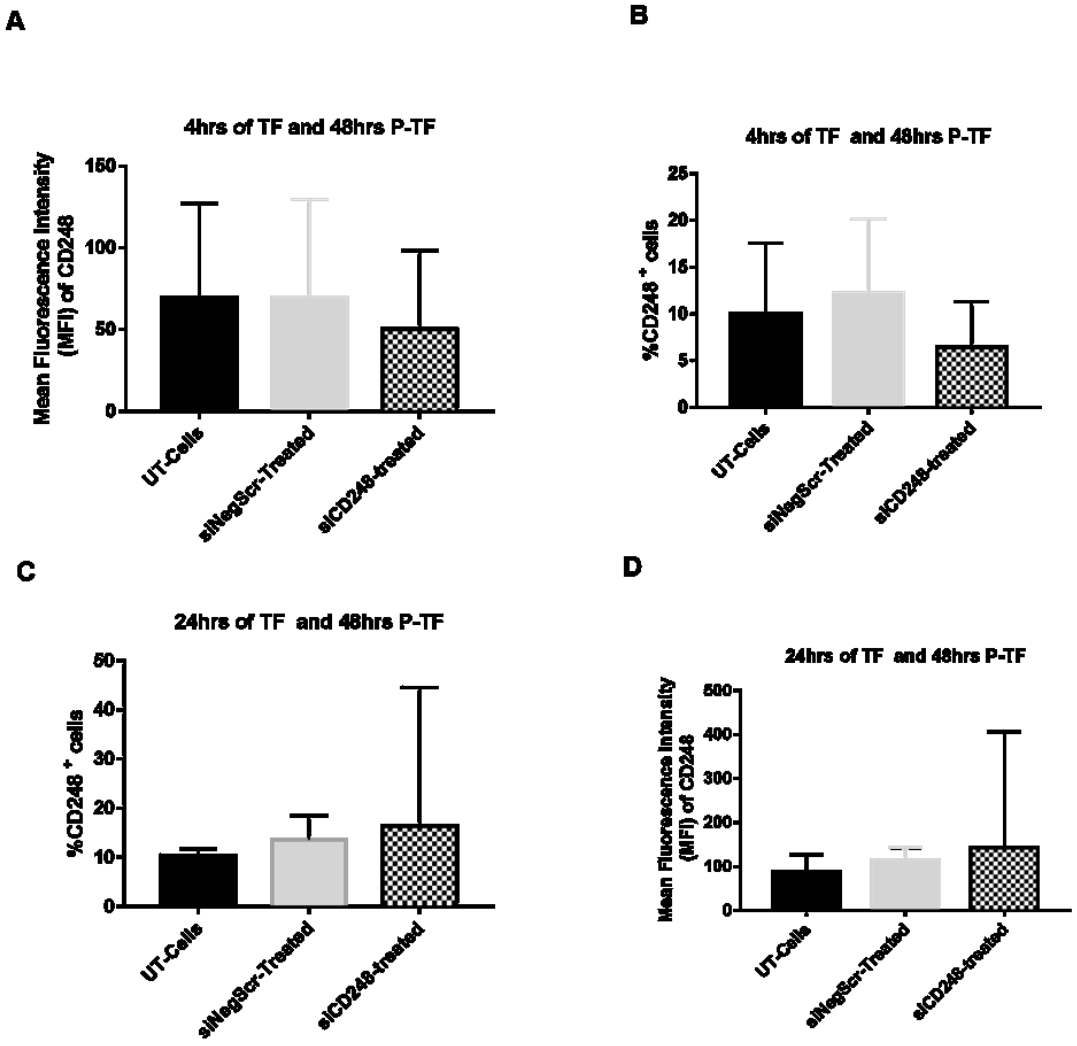

Supplementary Figure S11. CD248 Overexpression in HD-MSCs.

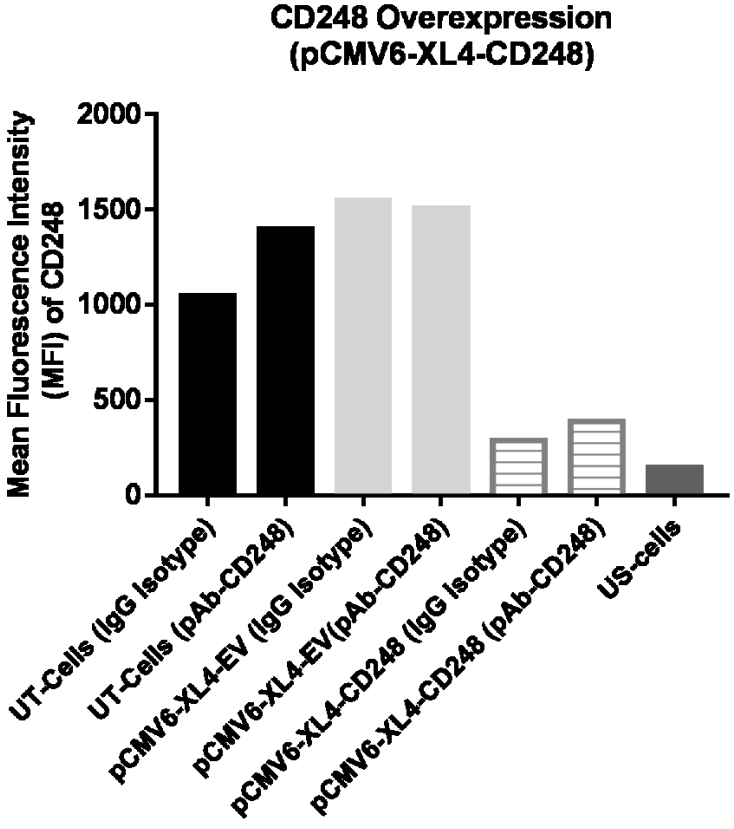

Supplementary Figure S12. CD248 predicted intracellular interactions with some of MSCs proteins through transcription factors.

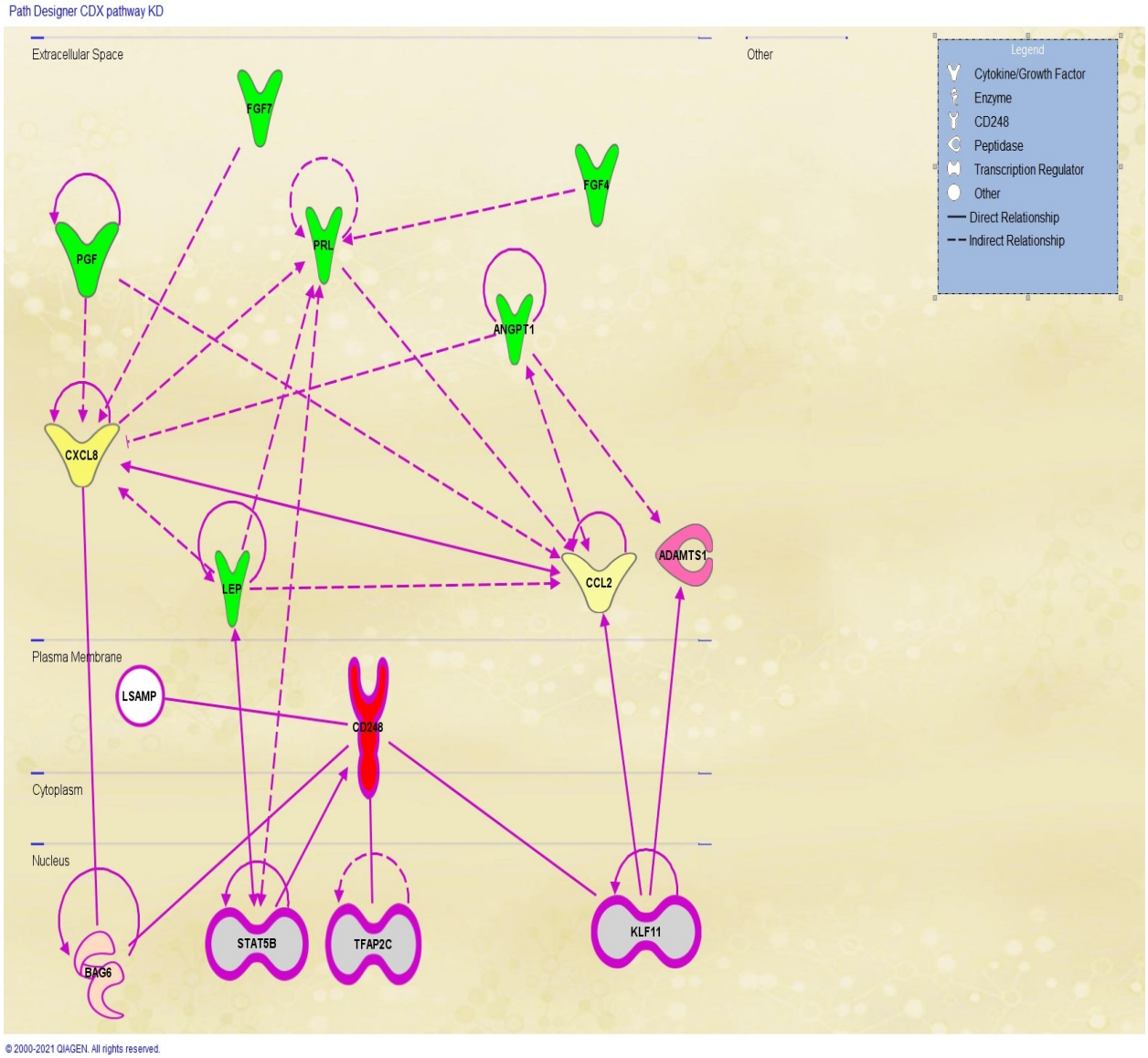

Supplementary Table S13. Antibodies titrations tested for CD248 used in flow cytometry analysis.

	Antibody Titration (2µL)	Ab Type	%CD248⁺ Cells	%Live	MFI
Sample	HD-MSCs (HD2-55RB)	CD248	12.1	ND	213
		IgG	0.2	ND	136
	HR AML-MSCs (HR-AML8)	CD248	51.3	99.9	516
		IgG	0.14	99.9	170
	Antibody Titration (5µL)	**Ab Type**	**%CD248⁺ Cells**	**%Live**	**MFI**
Sample	HD-MSCs (HD2-55RB)	CD248	10.5	ND	279
		IgG	0.44	ND	198
	HR AML-MSCs (HR-AML8)	CD248	40.2	99.9	529
		IgG	0.07	99.9	210
	Antibody Titration (10µL)	**Ab Type**	**%CD248⁺ Cells**	**%Live**	**MFI**
Sample	HR AML-MSCs (HD2-55RB)	CD248	20.7	ND	328
		IgG	0.26	ND	173
	HR AML-MSCs (HR-AML8)	CD248	37.5	99.9	578
		IgG	0.094	99.9	225

Supplementary Figure S13. Western Blot analysis of CD248 KD in HD-MSCs (n=1).

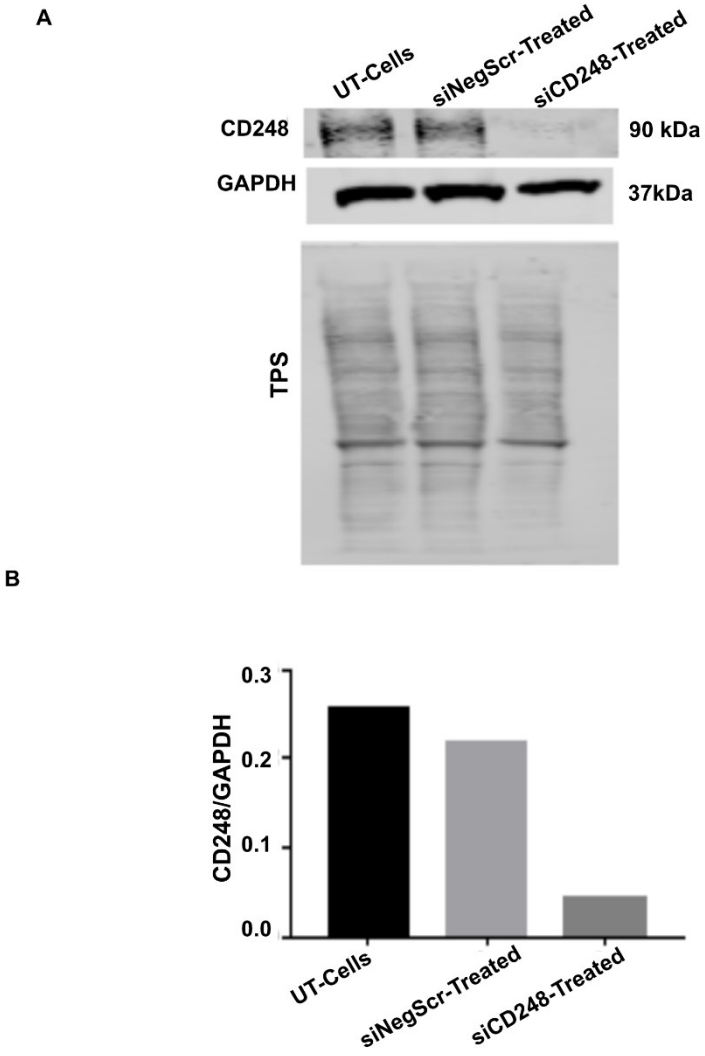

Supplementary Figure S14. CD248 gene expression and protein abundance levels in HR AML-MSCs (n=11) versus HD-MSCs (n=4).